

FINAL REPORT

ANALYSIS OF CRACKING LOCALIZATION IN CONCRETE

By

Pruettha Nanakorn

FINAL REPORT

ANALYSIS OF CRACKING LOCALIZATION IN CONCRETE

By

Pruettha Nanakorn Sirindhorn International Institute of Technology Thammasat University

วันที่ 29 ส.ค	2546
เลขทะเบียน	JU 269
	RSA GI
เลขเรียกหนังสือ	0005

Sponsored by The Thailand Research Fund

สำนักงานกองทุนสุนับสนุนการวิจัย (สกว.)

(The Thailand Research Fund may ทั้งเปลี่พลดง ละเพียงให้เก็บโลย พยั่ง presented in this report.) เลขที่ 979/17-21 ถนนพหลโยธิน แขวงสามสนใน

าหญาไท กรุงเทพฯ 10400 (7.298-0455 โทรสาร 298-0476 Home page; http://www.arf.or.th E-mail : trf-info@trf.or.th



ACKNOWLEGDEMENTS

The author wishes to express his profound gratitude and sincerest appreciation to The Thailand Research Fund for providing financial support to this study. Without the financial support from The Thailand Research Fund, it would not be possible for the author to carry out this research. The author is thankful to his graduate students, Mr. Aruz Petcherdchoo, Mr. Preecha Soparat, Mr. Konlakarn Meesomklin and Mr. Vasan Thitawat, for working with the author on this research project. Their contributions to this research project are enormous and invaluable. The author is very much indebted to Sirindhorn International Institute of Technology for all its support during this study.

ABSTRACT

Project Code:

RSA/05/2541

Project Title:

Analysis of Cracking Localization in Concrete

Investigator:

Pruettha Nanakorn, D. Eng.
Associate Professor
Civil Engineering Program
Sirindhorn International Institute of Technology
Thammasat University
PO Box 22, Thammasat-Rangsit Post Office
Pathumthani 12121, Thailand

E-mail Address:

nanakorn@siit.tu.ac.th

Project Period:

January 1, 1999 to December 31, 2001 (3 years)

In this study, an analysis method for cracking localization in quasi-brittle materials such as concrete is proposed. The proposed analysis method is an incremental analysis method and can be decomposed into two parts. The first part involves locating bifurcation points. This is done by investigating stability of equilibrium paths. For this analysis part, two specially treated smeared crack models are proposed in this study. In the two proposed smeared crack models, new discrete irreversible variables are introduced into the conventional smeared crack model in order to allow consideration of stability and bifurcation of equilibrated solutions to be done easily. The second part of the proposed analysis method involves tracing the actual equilibrium path from any bifurcation point. This is done by searching for the stable crack pattern with the minimum total potential energy. To this end, two algorithms that are the exhaustive search and genetic algorithms are used. The exhaustive search algorithm, which compares all possible solutions in order to obtain the solution with the minimum energy, can be used for problems that are not very large. For larger problems, the genetic algorithm will be more appropriate. Finally, the proposed analysis method is used to solve some cracking localization problems and the obtained results are discussed.

Keywords:

Cracking localization, Concrete, Smeared crack models, Finite element analysis, Genetic algorithms.

บทคัดย่อ

รหัสโครงการ:

RSA/05/2541

ชื่อโครงการ:

การวิเคราะห์โลคอลไลเซซันของการแตกในคอนกรีต

นักวิจัย:

ดร. พฤทธา ณ นคร รองศาสตราจารย์ สาขาวิชาวิศวกรรมโยธา สถาบันเทคโนโลยีนานาชาติสิรินธร มหาวิทยาลัยธรรมศาสตร์ ดู้ปณ. 22 โปรษณีย์ธรรมศาสตร์รังสิต ปทุมธานี 12121

E-mail Address:

nanakorn@siit.tu.ac.th

ระยะเวลาโครงการ

1 มกราคม 2542 ถึง 31 ธันวาคม 2544 (3 ปี)

การศึกษาครั้งนี้เสนอวิธีวิเคราะห์สำหรับโลคอลไลเซซันของการแตกในวัสดุกึ่งเปราะเช่นคอนกรีต วิธี วิเคราะห์ที่เสนอเป็นวิธีวิเคราะห์แบบเป็นขั้นตอนย่อย ซึ่งสามารถแบ่งออกได้เป็นสองส่วน ส่วนที่หนึ่ง เป็นส่วนที่เกี่ยวพันกับการหาจุดใบเฟอร์เคชัน โดยในการศึกษานี้ ได้มีการเสนอ smeared crack models ขึ้นมาใหม่สองแบบ ใน smeared crack models ทั้งสองแบบนี้ ได้มีการเพิ่มตัวแปรไม่ต่อ เนื่องผันกลับไม่ได้ลงใน smeared crack model แบบธรรมดา ตัวแปรไม่ต่อเนื่องผันกลับไม่ได้นี้ จะ ทำให้สามารถพิจารณาความเสถียรและไบเฟอร์เคชันของเส้นทางสมดุลย์ได้โดยง่าย ส่วนที่สองของ วิธีวิเคราะห์ที่เสนอเป็นส่วนที่เกี่ยวพันกับการหาเส้นทางสมดุลย์ที่แท้จริงจากจุดไบเฟอร์เคชัน ซึ่ง สามารถทำได้โดยการหารูปแบบรอยแตกที่เสถียรและมีพลังงานศักย์รวมด่ำสุด ในการนี้ exhaustive search algorithm และ genetic algorithm ได้ถูกนำมาใช้ exhaustive search algorithm ซึ่งเปรียบ เทียบคำตอบที่เป็นไปได้ทั้งหมดเพื่อหาคำตอบที่มีพลังงานดำสุด เป็นวิธีที่เหมาะสำหรับปัญหาที่ไม่ ใหญ่มากนัก สำหรับปัญหาที่ใหญ่ขึ้นไป genetic algorithm จะเป็นวิธีที่เหมาะสมกว่า ในที่สุด วิธี วิเคราะห์ที่เสนอได้ถูกนำไปใช้ในการวิเคราะห์ปัญหาโลคอลไลเชชันของการแตกหลายปัญหา และมี การพิจารณาผลที่ได้จากการวิเคราะห์

คำหลัก:

โลคอลไลเซชันของการแตก คอนกรีต smeared crack models การวิเคราะห์ไฟในต์อิลิเมนต์ genetic algorithms

TABLE OF CONTENTS

TI	ITLE PAGE	i
A	CKNOWLEGDEMENTS	ii
A)	BSTRACT	iii
T	HAI ABSTRACT	iv
\mathbf{T}_{A}	ABLE OF CONTENTS	V
	INTRODUCTION	1
	THE SMEARED CRACK CONCEPT	4
	STABILITY AND BIFURCATION OF EQUILIBRIUM PATHS IN	
	IRREVERSIBLE PROCESSES	7
4.	GENETIC ALGORITHMS	8
••	4.1 General	8
	4.2 Genetic Algorithms for Constrained Optimization	10
	4.3 Adaptive Penalty Function	11
	4.4 Results	18
5	OPTIMIZATION OF MATRIX STORAGES IN THE FINITE ELEMENT	
٥.	ANALYSIS BY NODE RENUMBERING	26
	5.1 Coding and GA operators	27
	5.2 Results	29
6	SMEARED CRACK MODELS FOR ANALYSIS OF CRACKING	
0.	LOCALIZATION	36
	6.1 A Smeared Crack Model with Crack Displacement Degrees of Freedom	36
	6.2 A Smeared Crack Model with A Mixed Formulation	40
7	THE EQUILIBRIUM PATH WITH THE MINIMUM TOTAL POTENTIAL	10
٠.	ENERGY	43
	7.1 Minimization of The Total Potential Energy Increment	43
	7.2 Coding and Fitness	44
	7.3 GA Operators	45
R	RESULTS	48
υ.	8.1 Uniaxial Bar Problem: Stability and Bifurcation Analysis	48
	8.2 A Four-Point Bending Problem of Plain Concrete Using Four-Noded Quadrilat	
	Elements	53
	8.3 A Four-Point Bending Problem of Steel-Fiber-Reinforced Concrete Using Four	
	Noded Quadrilateral Elements	58
9	CONCLUSIONS AND DISCUSSION	61
). REFERENCES	63
	1. RESEARCH OUTPUT	66
- 1	11.1 Publications	66
	11.2 Master's Degree Graduates	67
A	PPENDIX	68

1. INTRODUCTION

Tensile failure of quasi-brittle materials such as concrete is commonly known to start from formation of cracks, and propagation of the newly formed cracks or existing defects. After that, these cracks will localize themselves into one or a few major cracks that will subsequently lead to the final failure. This cracking localization prior to the failure plays a very important role in the fracture behavior of this kind of material. In order to capture the ultimate capacity of these materials in structures, consideration of cracking localization cannot generally be neglected. Nevertheless, consideration of cracking localization needs very expensive computations because solution methods for solving localization problems involve checking stability of many equilibrium paths. Consequently, many researchers avoid consideration of cracking localization by either allowing many cracks to grow without consideration of localization (Rots and de Borst 1987, Rots 1989, Dvorkin and Assanelli 1991, Jirasek and Zimmermann 1998, Shirai 1994) or by assuming the number of localized cracks and their positions (Shirai 1994, Carpinteri 1989). The first approach, though simple, is not realistic and can generally lead to very inaccurate results. When compared with having one or a few localized cracks, having many cracks without localization allows an incorrect amount of energy to dissipate from the domain. Thus, the obtained results will also be inaccurate. However, in some cases where the gradient of stress is very high and a stress criterion for crack initiation is used, the localized solution may be obtained from this approach (Rots and de Borst 1987, Rots 1989, Jirasek and Zimmermann 1998). Due to the large difference in magnitudes of stress between different locations, it is probable that some cracks, once initiated, will rapidly cause neighboring cracks to elastically unload. As a result, these cracks will prevail and become the localized cracks. In the analysis of localization problems in plasticity, similar behavior is also observed (Zienkiewicz, Huang and Pastor 1995). Even if the localization of cracks is obtained in this kind of problem, the localized-crack patterns may not be correct. This is because, in many cases, these patterns, which are in fact obtained without consideration of localization, are known to be sensitive to the finite element meshes employed (Jirasek and Zimmermann 1998, Zienkiewicz, Huang and Pastor 1995). The second approach, which assumes the number of localized cracks and their positions prior to the analysis, may yield reasonable results in some cases. These include cases where the number of localized cracks and their assumed positions are reasonably or undoubtedly correct, such as bending problems of concrete with long notches (Carpinteri 1989). In fact, the number of localized cracks varies during loading. In an early loading stage, it is possible to have a few localized cracks. The number of these main cracks will gradually decrease and finally only one crack will usually prevail. The speed of localization depends on the problems being solved. For very brittle problems, the localization into one crack can occur at a very early stage of loading. For ductile problems, the localization into one crack can occur at a much later loading stage. As a result, in ductile problems, a few cracks, not only one, may govern most part of the response, especially during the peak load. When the number of localized cracks is assumed prior to the analysis, in most cases, only one localized crack will be assumed from the beginning. Consequently, there is a tendency that less accurate results will be observed if the assumption of having one major crack is used in ductile problems. Another cases where the second approach may yield reasonable results are those where only one localized crack-governs the response and the required solutions, such as the ultimate load, are not much sensitive to the position of the localized crack. Nevertheless, this second approach is, overall, not appropriate for general cases since the number and locations of localized cracks may not be easily predicted or may have great effect on the required solutions.

In the analysis of cracking localization, consideration of stability and bifurcation of equilibrium states is one of the tasks to be done. Many researchers have considered the stability and bifurcation of the equilibrium states by investigating the definiteness of the stiffness matrices (Hessian matrices of energy functions) (Riks 1979, de Borst 1987, Valente 1992). When the stiffness matrix is positive-definite, the stable equilibrium is assumed. The same theory can be applied to the analysis of cracking localization. However, cracking is an irreversible process. To consider stability and bifurcation of irreversible processes, the stationary condition of the energy of the system with respect to irreversible parameters has to be examined (Nguyen 1987, Horii and Okui 1995, Brocca 1997). For this reason, the expression of the energy in terms of the irreversible parameters is required. For crack problems, the irreversible parameters can be the crack opening displacement variables in the discrete crack approach or the crack strain variables in the smeared crack approach. In the discrete crack approach, the crack opening displacement variables are usually discretized along crack paths and treated as the degrees of freedom in the analysis. The energy of the system is expressed in terms of these degrees of freedom. Constructing the Hessian matrix of the energy with respect to the crack opening displacement degrees of freedom, which are discrete, can be done easily. On the contrary, if the smeared crack approach is employed, the energy of the system will be expressed in terms of the irreversible crack strain variables, which are not discretized variables. As a result, determination of the Hessian matrix with respect to these crack strain functions is not obvious.

The aforementioned facts imply that the discrete crack approach in the finite element method may be more suitable for the analysis of cracking localization than the smeared crack approach. Nevertheless, the discrete crack approach may not perform best when there are many cracks. Usually, in the analysis of cracking localization, there will be many cracks occurring in the domain. As the number of cracks increases, the mesh topology may have to be changed to cope with new crack patterns and this leads to more degrees of freedom. On the other hand, the smeared crack approach, which is more suitable for problems with many cracks, does not provide any discrete irreversible parameters for construction of the Hessian matrices. Another disadvantage of the smeared crack approach is that, with this approach, it is necessary to define the crack-band width or the crack characteristic length. For fairly regular meshes, the characteristic length is frequently determined in an intuitive way, which is difficult to generalize in a formal manner for irregular meshes and arbitrary crack directions. However, for two-dimensional domains, this problem can be overcome. Oliver (1989) proposed a general approach for calculation of the characteristic length. In his study, a crack is modeled as a limiting case of two singular lines that coincide with the boundary of the elements covering the crack path. The expression for the characteristic length is obtained by analyzing the energy dissipated from the band bounded by these two singular lines.

If the definiteness of a stiffness matrix obtained by the conventional smeared crack models is considered (de Borst 1987), a wrong conclusion on the stability of the crack pattern may be obtained. For example, negative eigenvalues of a stiffness matrix may simply mean that the solution has already passed the critical point (Riks 1979). It must be noted that the stiffness matrix from the conventional smeared crack model is the Hessian matrix of the total potential energy of the system computed with respect to the displacement degrees of -freedom and the displacements are not purely irreversible parameters.

Investigating definiteness of Hessian matrices provides information on stability of equilibrium paths. Consequently, bifurcation points can be located. Nevertheless, tracing the actual equilibrium path from a bifurcation point needs some more efforts. Employing

Gibb's statement of the second law of thermodynamics, Nemat-Nasser (1979) pointed out that the equilibrium path that makes the total potential energy an absolute minimum will also render the elastic energy an absolute minimum and this path will also be the actual equilibrium path (Bazant and Cedolin 1991). Employing the same concept, Brocca (1997) traced the actual equilibrium path from a bifurcation point by using the Simplex method to find the path with the minimum total potential energy. In his work, Hessian matrices constructed with respect to irreversible crack opening displacement degrees of freedom are used to investigate stability and bifurcation of crack patterns.

In this study, an analysis method for cracking localization is proposed. The proposed analysis method can be categorized into two parts. The first part involves locating bifurcation points. This is done by investigating the stability of equilibrium paths. As mentioned earlier, both discrete and smeared crack approaches have drawbacks when they are used to check the stability of equilibrium paths of crack problems. To avoid the drawbacks of both approaches, in this study, two specially treated smeared crack models are proposed. In the first model, discrete nodal crack displacements are introduced to the conventional smeared crack finite element model. Crack displacements, obtained from the nodal crack displacements by interpolation, are defined in such a way that their derivatives with respect to the coordinates represent the crack strains. These new discrete irreversible crack variables will allow the consideration of stability and bifurcation of equilibrated solutions to be done easily by considering the Hessian matrix of the energy with respect to these proposed discrete variables. In the second proposed model, a mixed formulation of the finite element method that includes the discretization of the displacement and crack strain fields is developed. In this model, the energy of the system is written in terms of the discretized displacements as well as discretized crack strains. Consequently, the stability of crack patterns with respect to the discretized irreversible crack strains can be easily evaluated, and the cracking localization can be discussed.

The second part of the proposed analysis method involves tracing the actual equilibrium path from any bifurcation point. This is done by searching for the stable crack pattern with the minimum total potential energy. To this end, two algorithms that are the exhaustive search and genetic algorithms are used. The exhaustive search algorithm, which compares all possible solutions in order to obtain the solution with the minimum energy, can be used for problems that are not very large. For larger problems, the genetic algorithm will be more appropriate. Finally, the proposed analysis method is used to solve some cracking localization problems and the obtained results are discussed.

2. THE SMEARED CRACK CONCEPT

In the smeared crack concept, a cracked solid is modeled as a continuum with additional strains called crack strains. These crack strains represent the existence of cracks. The advantage of this approach is that it allows the description of cracks in terms of strains without need for special interface or cracked elements. This is at the same time the source of disadvantages as the underlying assumption of continuity conflicts with the reality of discontinuity.

The fundamental concept of the smeared crack model can be written in the incremental form as

$$\Delta \mathbf{\varepsilon} = \Delta \mathbf{\varepsilon}^o + \Delta \mathbf{\varepsilon}^{cr} \tag{1}$$

where $\Delta \varepsilon$ denotes a total strain increment which is decomposed into strain increments of an intact elastic solid part $\Delta \varepsilon^{o}$ and a cracked part $\Delta \varepsilon^{cr}$ (Rots and de Borst 1987).

The strain increment vectors in the above equation are written in the global coordinate system. It will be helpful to consider the strain increments also in a local coordinate system that aligns with the crack being considered. In two-dimensional cases, the local crack strain increment $\Delta \hat{\epsilon}^{cr}$ can be defined as

$$\Delta \hat{\boldsymbol{\varepsilon}}^{cr} = \begin{bmatrix} \Delta \hat{\boldsymbol{\varepsilon}}_{nn}^{cr} & \Delta \hat{\boldsymbol{\gamma}}_{nt}^{cr} \end{bmatrix}^T \tag{2}$$

where $\Delta \hat{\varepsilon}_{nn}^{cr}$ and $\Delta \hat{\gamma}_{nt}^{cr}$ are the normal and shear crack strain increments, respectively. The relationship between the global crack strain increment vector $\Delta \boldsymbol{\varepsilon}^{cr}$ and the local crack strain increment vector $\Delta \hat{\boldsymbol{\varepsilon}}^{cr}$ is expressed as

$$\Delta \mathbf{\varepsilon}^{cr} = \mathbf{T} \Delta \hat{\mathbf{\varepsilon}}^{cr} \tag{3}$$

where T is the transformation matrix defined as

$$\mathbf{T} = \begin{bmatrix} \cos^2 \theta & -\sin \theta \cos \theta \\ \sin^2 \theta & \sin \theta \cos \theta \\ 2\sin \theta \cos \theta & \cos^2 \theta - \sin^2 \theta \end{bmatrix}$$
(4)

where θ is the angle between the vector normal to the crack and the global x-axis as shown in Fig. 1. Similar to the local crack strain increment, in the local coordinate system, the local traction increment $\Delta \hat{\mathbf{t}}^{cr}$ across the crack is written as

$$\Delta \hat{\mathbf{t}}^{cr} = \left[\Delta \hat{t}_n^{cr} \quad \Delta \hat{s}_t^{cr} \right]^T \tag{5}$$

where $\Delta \hat{t}_n^{cr}$ and $\Delta \hat{s}_i^{cr}$ are normal and shear crack traction increments, respectively. This local traction increment is related to the local crack strain increment as

$$\Delta \hat{\mathbf{t}}^{cr} = \hat{\mathbf{D}}^{cr} \Delta \hat{\boldsymbol{\varepsilon}}^{cr} \tag{6}$$

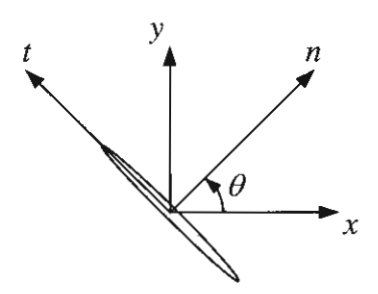


Fig. 1 Global and local coordinates

where $\hat{\mathbf{D}}^{cr}$ is the crack constitutive matrix incorporating mixed-mode properties of the crack expressed as

$$\hat{\mathbf{D}}^{cr} = \begin{bmatrix} D^{I} & 0 \\ 0 & D^{II} \end{bmatrix}. \tag{7}$$

Here, D^I and D^{II} represent the mode I and mode II crack modulus, respectively. The local traction increment $\Delta \hat{\mathbf{t}}^{cr}$ is related to the global stress increment $\Delta \boldsymbol{\sigma}$ as

$$\Delta \hat{\mathbf{t}}^{cr} = \mathbf{T}^T \Delta \mathbf{\sigma} \,. \tag{8}$$

To complete the material definition, the constitutive law for the intact solid part must also be specified, i.e.,

$$\Delta \mathbf{\sigma} = \mathbf{D}^{o} \Delta \mathbf{\varepsilon}^{o} \tag{9}$$

where \mathbf{D}^{o} is the constitutive matrix for the intact solid.

Using Eqs (1) and (3) in Eq. (9) yields

$$\Delta \mathbf{\sigma} = \mathbf{D}^{o} \Delta \mathbf{\epsilon} - \mathbf{D}^{o} \mathbf{T} \Delta \hat{\mathbf{\epsilon}}^{cr}. \tag{10}$$

Employing Eqs. (1) and (9) in Eq. (8) yields

$$\Delta \hat{\mathbf{t}}^{cr} = \mathbf{T}^T \mathbf{D}^o \left(\Delta \mathbf{\varepsilon} - \Delta \mathbf{\varepsilon}^{cr} \right) \tag{11}$$

which, by using Eq. (3), subsequently yields

$$\Delta \hat{\mathbf{t}}^{cr} = \mathbf{T}^T \mathbf{D}^o \left(\Delta \mathbf{\varepsilon} - \mathbf{T} \Delta \hat{\mathbf{\varepsilon}}^{cr} \right). \tag{12}$$

Substituting Eq. (12) into Eq. (6) gives the relationship between the local crack strain increment $\Delta \hat{\mathbf{\epsilon}}^{cr}$ and the total strain increment $\Delta \mathbf{\epsilon}$, i.e.,

$$\Delta \hat{\mathbf{\epsilon}}^{cr} = \left(\hat{\mathbf{D}}^{cr} + \mathbf{T}^T \mathbf{D}^o \mathbf{T}\right)^{-1} \mathbf{T}^T \mathbf{D}^o \Delta \mathbf{\epsilon} \,. \tag{13}$$

By substituting Eq. (13) into Eq. (10), the overall stress-strain relationship for the smeared crack material is obtained as

$$\Delta \boldsymbol{\sigma} = [\mathbf{D}^{o} - \mathbf{D}^{o} \mathbf{T} (\hat{\mathbf{D}}^{cr} + \mathbf{T}^{T} \mathbf{D}^{o} \mathbf{T})^{-1} \mathbf{T}^{T} \mathbf{D}^{o}] \Delta \boldsymbol{\varepsilon} = \overline{\mathbf{D}}^{cr} \Delta \boldsymbol{\varepsilon}$$
(14)

which is the constitutive law for the cracked material in the smeared crack model. Here, $\overline{\mathbf{D}}^{cr}$ is the constitutive matrix of the cracked material.

3. STABILITY AND BIFURCATION OF EQUILIBRIUM PATHS IN IRREVERSIBLE PROCESSES

Cracking can be thought of as an irreversible inelastic process. During cracking, the material is damaged and some of the energy is dissipated from the domain. Following Nguyen (1987) and Brocca (1997), we consider a system of a deformable body with cracks where the energy is dissipated. The total potential energy of the body can be defined as

$$\Pi(u_i, \alpha_j) = \Pi^M(u_k, \alpha_l) + \Pi^D(\alpha_m)$$
(15)

where $\Pi^M(u_k,\alpha_l)$ is the mechanical potential energy and the $\Pi^D(\alpha_m)$ is the dissipated energy. Here, u_i 's (i=1,2,...,N) represent reversible variables and α_j 's (j=1,2,...,K) represent irreversible variables. Furthermore, N and K are the number of the reversible variables and the number of the irreversible variables, respectively. In general, the irreversible variables characterize the inelastic behavior of the material. The mechanical potential energy is the sum of the strain energy and the external potential energy. The dissipated energy is the mechanical energy that is transformed into the thermal energy or other forms of energy through the irreversible process and is as a result dissipated from the system.

The fundamental solution, obtained by applying the stationary condition to Eq. (15), is written as

$$\frac{\partial \Pi}{\partial u_i} = 0, \qquad (i = 1, 2, ..., N)$$

$$\frac{\partial \Pi}{\partial \alpha_j} = 0, \qquad (j = 1, 2, ..., K).$$
(16)

By employing the equilibrated solution of Eq. (16), the reversible variables can be expressed in terms of the irreversible variables, i.e., $u_i = u_i(\alpha_j)$. Consequently, the total potential energy of the system in Eq. (15) can be expressed as a function of only the irreversible variables, i.e.,

$$\Pi^*(\alpha_i) = \Pi^{*M}(\alpha_i) + \Pi^D(\alpha_m)$$
(17)

where $\Pi^*(\alpha_l) = \Pi(u_i(\alpha_k), \alpha_j)$ and $\Pi^{*M}(\alpha_j) = \Pi^M(u_k(\alpha_m), \alpha_l)$.

The signs of the eigenvalues of the Hessian matrix $\left[\frac{\partial^2 \Pi^*}{\partial \alpha_i \partial \alpha_j}\right]$ can be used to check

the stability of the fundamental solution obtained from Eq. (16). If all the eigenvalues are positive, the fundamental solution is stable. Otherwise, the fundamental solution is unstable and the bifurcation occurs.

To apply the above concept to the numerical analysis of cracking localization, it is therefore advisable to express the total potential energy of the system being considered in terms of discrete irreversible variables so as to easily obtain the Hessian matrix.

4. GENETIC ALGORITHMS

4.1 General

In the analysis of cracking localization, after a bifurcation point is located, the actual equilibrium path must be identified. In the proposed analysis method, the identification of the actual equilibrium path is done by searching for the equilibrium path with the minimum total potential energy. Since the analysis will be performed incrementally, the equilibrium path with the minimum total potential energy increment will be the desired solution. When the size of the problem being solved is not very large, it is possible to perform an exhaustive search on all possible solutions, meaning that the total potential energy increments of all possible solutions will be evaluated and compared. This exhaustive search technique may not be appropriate for large problems where many possible solutions are available. In this case, an optimization technique can be employed. In this study, genetic algorithms (GAs) are selected as the optimization tool to be used for minimizing the total potential energy increment. The reason for selecting GAs is that this optimization technique is suitable for problems with discrete variables. Variables in the minimization problem of the total potential energy increment are discrete statuses of cracks that can be either opening or unloading. In addition, since GAs do not require the evaluation of the gradient of the function being minimized or maximized, the evaluation of the total potential energy increment is enough for the minimization process.

GAs are global probabilistic search algorithms inspired by Darwin's survival-of-the-fittest theory (Goldberg 1989). They have received considerable attention because of their versatile applications in several fields (Deb 1995, Marcelin, Trompette, and Dornberger 1995, Marcelin 1999, Goldberg 1989, Grefenstette 1986, Dawid 1999). GAs start their search from many points in search space at the same time. These starting search points are usually selected randomly. Through the consideration of fitness values of these search points, which are given based on their merit, and the randomized information exchange among the points, a new set of search points with higher merit is created. The process is then repeated until a satisfactory result is obtained. Since the technique utilizes information from many search points at the same time, there is less chance for the search to be trapped in any of the local optimal points. Another distinguishing characteristic of GAs is that the algorithms work with coding of the parameter set, not the parameters themselves. Generally, the binary code is used. Because of the discrete nature of coding, the algorithms are the perfect choice for those problems with discrete variables.

Since GAs are directly applicable only to unconstrained optimization, many researchers have proposed solutions that can eliminate this limitation. Constraints are mostly handled by using penalty functions, which penalize infeasible solutions by reducing their fitness values in proportion to their degrees of constraint violation. In all available penalty schemes, the degree of penalty can be further controlled by means of setting values of various coefficients in penalty functions (Deb 1995, Templeman 1988, Goldberg 1989, Michalewicz 1996). Most of these coefficients are treated as constants during the calculation and their values have to be specified at the beginning of the calculation (Rajeev and Krishnamoorthy 1992, Jenkins 1997, Camp, Pezeshk and Cao 1998). These coefficients usually have no clear physical meanings. Thus, it is nearly impossible to know appropriate values of the coefficients even by experience. This is because it is very hard to understand the correlation between the values of the coefficients and the characteristics of the problems being solved without physical meanings of the coefficients. Consequently, for all problems with either similar or different natures, appropriate values of the coefficients are generally obtained by trial and error. Many researchers, however, have tried to suggest different ranges of appropriate values for these coefficients, for various

types of problem. Most of these suggestions are obviously doubtful. The reason is simply that appropriate values are usually given without any reference to the units used in the problems although the coefficients may have units and appropriate values should vary with the units used. Another important concern is that these conventional penalty schemes do not adjust the strength of the penalty during the calculation, as the coefficients used are always kept constant. As a result, too weak or too strong a penalty during different phases of the evolution may occur. This will lead to inaccurate solutions. Actually, there are some penalty schemes that vary the values of the coefficients to adjust the strength of the penalty during the calculation (Rajan 1995, Rafiq and Southcombe 1998, Adeli and Cheng 1993). However, these schemes require the varying values of these coefficients to be manually specified. It therefore becomes even more difficult to judiciously select appropriate values for different phases of the calculation.

Several different ideas that are more sophisticated have been proposed to improve penalty function methods for handling constrained optimization problems (Michalewicz 1995). Powell and Skolnick (1993) re-mapped fitness values of both feasible and infeasible individuals in such a way that all feasible solutions have higher fitness than any infeasible solutions. The key concept of this approach is the assumption of the superiority of feasible solutions over infeasible ones. Unfortunately, this assumption rarely holds during the evolution since it always happens that some infeasible individuals process very good genes that can be very valuable for later generations. As a result, these infeasible individuals are more preferable during the evolution than many low fitness feasible individuals. For this reason, it is necessary to allow some infeasible individuals to have higher fitness than some feasible individuals. Le Riche, Knopf-Lenoir and Haftka (1995) proposed a segregated GA that uses two values of penalty parameters for each constraint instead of one. The population is split into two coexisting and cooperating groups, where individuals in each group are evaluated using either one of the two penalty parameters. During the evolution, the two groups interbreed. Since the two penalty parameters are different, the two groups converge in the design space along two different trajectories, which helps locate the optimal region faster. If a large value is selected for one of the penalty parameters and a small value for the other parameter, simultaneous convergence from both feasible and infeasible sides can be achieved. However, although the approach provides a new overall penalty scheme, the problem with this approach is still the way of choosing the penalty for each of the two groups.

Rasheed (1998) proposed a penalty scheme with an adaptive penalty coefficient. The scheme considers two key individuals of the population, i.e., the point that has the least sum of constraint violations and the point that has the best fitness value. These two points are compared at every certain number of generations. If both points are the same then the penalty coefficient is assumed adequate; otherwise, the penalty coefficient is increased to make the two points have equal fitness values. In addition, the penalty coefficient is reduced if at some stage the population contains no infeasible points. The inconveniences of this technique are how to choose the initial value for the penalty coefficient and how to appropriately update it. In addition, the size of the generation gap for updating the penalty coefficient must reasonably be selected. Coello (2000) proposed a technique based on the concept of co-evolution to create two populations that interact with each other in such a way thät one population evolves the penalty factors to be used by the fitness function of the main population, which is responsible for optimizing the objective function. This technique is inconvenient because the approach requires evolution of two parallel populations instead of one. Therefore, it is computationally more expensive.

Since it seems that the existing penalty techniques still endure many problems, in this study, a new adaptive penalty scheme will be proposed (see more details in

Meesomklin 2000, Nanakorn and Meesomklin 2001). The penalty function used in the scheme will be able to adjust itself automatically during the evolution in such a way that the desired degree of penalty is always obtained. The coefficient used in the proposed scheme will have a clear physical meaning that directly represents the degree of penalty employed. Therefore, for each particular problem, the appropriate value of the coefficient can be reckoned based on the appropriate degree of penalty for the problem. In addition, the coefficient in the proposed scheme will have no units. For each particular problem, if the same value of the coefficient is used, similar results can always be expected even when different units are employed in the problem. Since it is expected that similar structural optimization problems require similar degrees of penalty, with the proposed scheme, it is therefore possible to set the value of the coefficient by using experience. It must be noted that the main objective of this work is to obtain an adaptive penalty scheme that is robust and can still reproduce the same quality of results as ones obtained from GAs found in the literature, whose penalty parameters are carefully obtained for each specific problem by trial and error. In brief, the proposed scheme will be a scheme that can efficiently be used in different problems without a lot of guesswork.

4.2 Genetic Algorithms for Constrained Optimization

An optimization problem using GAs can be generally expressed as

Maximize
$$F(\mathbf{x}) = F[f(\mathbf{x})], \quad \mathbf{x} = (x_1, x_2, ..., x_N) \in \mathbf{R}^N$$
 (18)

under constraints defined as

$$g_i(\mathbf{x}) \le 0, \qquad i = 1, \dots, K$$

 $h_i(\mathbf{x}) = 0, \qquad i = 1, \dots, P.$

$$(19)$$

For structural design optimization, \mathbf{x} is an N-dimensional vector called the design vector, representing design variables of N structural components to be optimized, and $f(\mathbf{x})$ is the objective function. In addition, $g_i(\mathbf{x})$ and $h_i(\mathbf{x})$ are inequality and equality constraints, respectively. They represent constraints, which the design must satisfy, such as stress and displacement limits. Moreover, $F[f(\mathbf{x})]$ is the fitness function that is defined as a figure of merit.

It is not possible to directly utilize GAs to solve the above problem due to the presence of constraints. In GAs, constraints are usually handled by using the concept of penalty functions, which penalize infeasible solutions, i.e.,

$$F^{a}(\mathbf{x}) = F(\mathbf{x})$$
 if $\mathbf{x} \in \widetilde{\mathbf{F}}$
 $F^{a}(\mathbf{x}) = F(\mathbf{x}) - P(\mathbf{x})$ otherwise (20)

where $\tilde{\mathbf{F}}$ denotes the feasible search space. Here, $P(\mathbf{x})$ is a penalty function whose value is greater than zero. In addition, $F^a(\mathbf{x})$ represents an augmented fitness function after the penalty. Several forms of penalty functions have been proposed in the literature (Deb 1995, Marcelin, Trompette and Dornberger 1995, Goldberg 1989, Michalewicz 1996). Nevertheless, most of them can be written in the following general form, i.e.,

$$P(\mathbf{x}) = \sum_{j=1}^{K} (\lambda_G)_j [G_j(\mathbf{x})]^{\beta} + \sum_{j=1}^{P} (\lambda_H)_j [H_j(\mathbf{x})]^{\beta}$$
(21)

where

$$G_{j}(\mathbf{x}) = \max [0, g_{j}(\mathbf{x})]$$

$$H_{j}(\mathbf{x}) = \operatorname{abs}[h_{j}(\mathbf{x})].$$
(22)

Here, $G_j(\mathbf{x})$ and $H_j(\mathbf{x})$ represent the degrees of inequality and equality constraint violations, respectively. In addition, $(\lambda_G)_j$, $(\lambda_H)_j$ and β are constants. In most cases, the same value is used for all $(\lambda_G)_j$'s and $(\lambda_H)_j$'s. As for β , it is usually set to be 1 or 2. The degree of penalty can be controlled by adjusting the values of the coefficients $(\lambda_G)_j$'s and $(\lambda_H)_j$'s. These coefficients do not have physical meanings. Clearly, it is impossible to judiciously select appropriate values for them. Even though in common practice, one value is used for all $(\lambda_G)_j$'s and $(\lambda_H)_j$'s, which significantly simplifies the situation, the appropriate value of this one coefficient is still not obvious.

In the first operator in GAs, the reproduction operator, a mating pool is created by letting individuals with higher fitness values have higher chance to be selected into the mating pool. Many reasonable selection algorithms are possible. However, the most widely used technique is proportional selection. In this technique, the probability of the i^{th} individual to be selected into the mating pool is

$$p(\mathbf{x}_i) = \frac{F^a(\mathbf{x}_i)}{\sum_{i=1}^n F^a(\mathbf{x}_j)}$$
(23)

where \mathbf{x}_i represents the i^{th} individual in the population and n is the population size. Clearly, in the above equation, it is essential that all fitness values be positive. Therefore, the obtained fitness function after the penalty $F^a(\mathbf{x})$ may not be directly usable as its values may be negative. Moreover, the difference between the fitness values of the best individuals and average individuals varies generation by generation. In early generations, the difference can be very large and the best individuals become relatively too strong. As a result, premature convergence may be obtained. In later generations, the difference can be very small and average individuals become almost as strong as the best individuals. As a result, the search may become a random walk. To prevent all of these problems, an augmented fitness function is usually scaled into a specified positive range. Many fitness scaling schemes have been proposed in the literature (Kallassy and Marcelin 1997, Goldberg 1989, Grefenstette 1986, Michalewicz 1996, Rasheed 1998).

4.3 Adaptive Penalty Function

It can be easily seen that pēnalty schemes used in GAs play a very important role in the performance of GAs. This role becomes even more important when the optimal solution lies on or close to the boundary between the feasible and infeasible search spaces, which is very usual for structural design optimization. In this study, a new penalty scheme that is

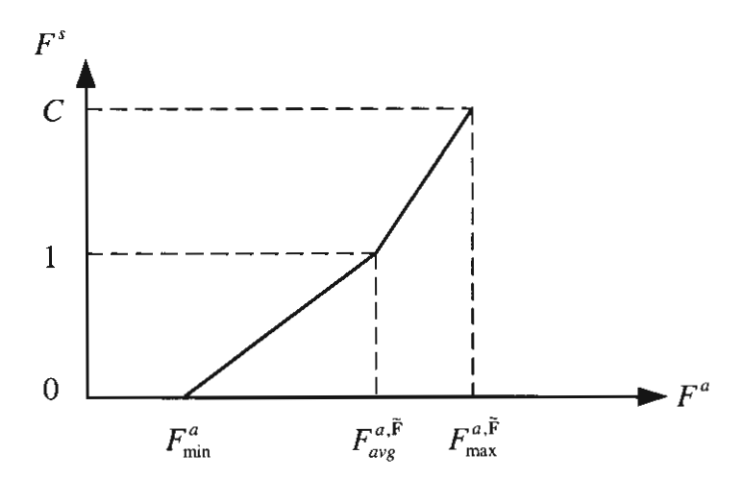


Fig. 2 Bilinear fitness scaling

free from the disadvantages of existing schemes discussed earlier is proposed. To make the scheme simple, a simple form of the penalized fitness function is employed, i.e.,

$$F_i^a = F^a(\mathbf{x}_i) = F(\mathbf{x}_i) - P(\mathbf{x}_i) = F(\mathbf{x}_i) - \lambda(t)E(\mathbf{x}_i)$$
(24)

where F_i^a represents the fitness function of the i^{th} individual after the penalty. Here, $\lambda(t)$ is a factor of an error term $E(\mathbf{x}_i)$. The factor $\lambda(t)$ varies with generation, and the generation number is denoted by t. In this study, the error term $E(\mathbf{x}_i)$ is defined as

$$E(\mathbf{x}_{i}) = \sum_{i=1}^{K} G_{j}(\mathbf{x}_{i}) + \sum_{i=1}^{P} H_{j}(\mathbf{x}_{i})$$
(25)

where $G_j(\mathbf{x}_i)$ and $H_j(\mathbf{x}_i)$ have already been defined in Eq. (22). Now, the question is what the magnitude of the factor $\lambda(t)$ should be. It is not difficult to imagine that if the factor is too small, infeasible individuals with high original fitness values may have penalized fitness values higher than the fitness value of the feasible optimal individual. If this happens, the population in subsequent generations will move toward false peaks that appear in the infeasible region. On the contrary, if the factor is too large, good characteristics in some infeasible individuals will have no chance to survive and will disappear rapidly. This may lead to premature convergence and the obtained solution can be quite wrong.

To avoid the above problems, the degree of penalty must be enough to make the feasible optimal solution have the maximum fitness value, compared with all individuals (feasible and infeasible) after the penalty. However, the penalty must not be made much stronger than that. To this end, the following condition is introduced, i.e.,

$$\ddot{F}^{a}(\mathbf{x}_{i}) \leq \phi(t) F_{avg}^{a,\tilde{\mathbf{F}}} \qquad \text{for } \forall \mathbf{x}_{i} \in \widetilde{\mathbf{U}}$$
 (26)

in which $\tilde{\mathbf{U}}$ represents the infeasible search space. Here, $F_{avg}^{a,\tilde{\mathbf{F}}}$ denotes the average fitness value of all feasible individuals in the generation and $\phi(t)$ is a factor of $F_{avg}^{a,\tilde{\mathbf{F}}}$.

The above condition sets the maximum fitness value of infeasible individuals in the generation t to be equal to $\phi(t) F_{avg}^{a,\tilde{r}}$. At this moment, it is not useful to consider the physical meaning of the coefficient $\phi(t)$ yet because the penalized fitness function will have to be scaled afterwards. Therefore, it is enough to simply say that the coefficient $\phi(t)$ is used to adjust the strength of the penalty in the generation. A way to obtain the value of this coefficient will be explained shortly.

The condition in Eq. (26) is satisfied by employing an appropriate value of the factor $\lambda(t)$ in Eq. (24). For each infeasible individual, the factor $\lambda(t)$ that makes the penalized fitness value of that infeasible individual exactly equal to $\phi(t) F_{avg}^{a, \tilde{F}}$ is computed. After that, values of the factor $\lambda(t)$ obtained from all infeasible individuals are compared and the maximum one is selected as the real $\lambda(t)$. If the maximum value is negative, zero is used instead. In short, $\lambda(t)$ can be expressed as

$$\lambda(t) = \max \left[0, \max_{\forall \mathbf{x}_i \in \tilde{\mathbf{U}}} \left[\frac{F(\mathbf{x}_i) - \phi(t) F_{avg}^{a,\tilde{\mathbf{F}}}}{E(\mathbf{x}_i)} \right] \right]. \tag{27}$$

Eq. (27) insures that Eq. (26) is satisfied.

In this study, a modified bilinear scaling technique as shown in Fig. 2 is employed for fitness scaling. The minimum scaled fitness is set to be 0 to avoid negative fitness values while the scaled fitness of the average fitness of all feasible individuals is set to be 1. Furthermore, the maximum scaled fitness that is to be obtained from the best feasible members is set to be C. Thus, the chance of the best members being selected into the mating pool is equal to C times that of the average feasible members. All together, the scaled fitness can be written as

$$F^{s}(\mathbf{x}) = \frac{C - 1}{F_{\max}^{a,\tilde{\mathbf{F}}} - F_{avg}^{a,\tilde{\mathbf{F}}}} F^{a}(\mathbf{x}) + \frac{F_{\max}^{a,\tilde{\mathbf{F}}} - CF_{avg}^{a,\tilde{\mathbf{F}}}}{F_{\max}^{a,\tilde{\mathbf{F}}} - F_{avg}^{a,\tilde{\mathbf{F}}}} \qquad \text{if } F^{a}(\mathbf{x}) \ge F_{avg}^{a,\tilde{\mathbf{F}}},$$

$$F^{s}(\mathbf{x}) = \frac{1}{F_{avg}^{a,\tilde{\mathbf{F}}} - F_{\min}^{a}} F^{a}(\mathbf{x}) + \frac{F_{\min}^{a}}{F_{\min}^{a} - F_{avg}^{a,\tilde{\mathbf{F}}}} \qquad \text{if } F^{a}(\mathbf{x}) \le F_{avg}^{a,\tilde{\mathbf{F}}},$$

$$(28)$$

where $F^s(\mathbf{x})$ denotes the scaled fitness function. In addition, F^a_{\min} denotes the minimum fitness value after the penalty while $F^{a,\tilde{\mathbf{F}}}_{\max}$ denotes the fitness value of the best feasible members. This scaled fitness function $F^s(\mathbf{x})$ will be used in Eq. (23) instead of $F^a(\mathbf{x})$.

For all generations, the chance of the best infeasible members being selected into the mating pool is set to be equal to φ times that of the average feasible members, i.e.,

$$F^{s}(\mathbf{x}_{i}) \le (\varphi \ F_{avg}^{s,\tilde{\mathbf{F}}} = \varphi)$$
 for $\forall \mathbf{x}_{i} \in \tilde{\mathbf{U}}$ (29)

where $F_{avg}^{s,\tilde{\mathbf{F}}}$ is the scaled value of the average fitness of all feasible individuals, which is equal to 1. Note that φ is constant for all generations. From the above condition, $\phi(t)$ in Eq. (26) is expressed in terms of φ as

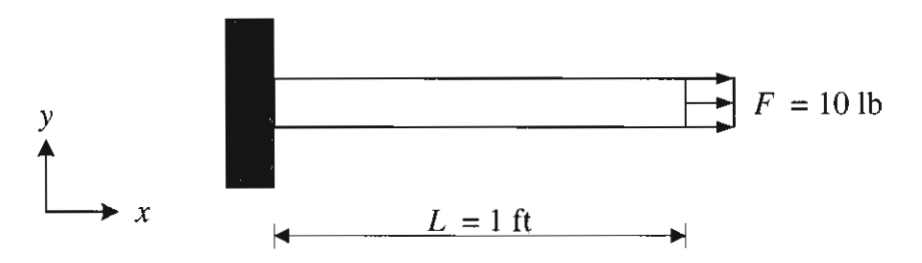


Fig. 3 Illustrative example—uniaxial problem

$$\phi(t) = \frac{CF_{avg}^{a,\tilde{\mathbf{F}}} + F_{\max}^{a,\tilde{\mathbf{F}}}(\varphi - 1) - \varphi F_{avg}^{a,\tilde{\mathbf{F}}}}{(C - 1)F_{avg}^{a,\tilde{\mathbf{F}}}} \qquad \text{for } \varphi \ge 1$$

$$\phi(t) = \frac{F_{\min}^{a} + \varphi F_{avg}^{a,\tilde{\mathbf{F}}} - \varphi F_{\min}^{a}}{F_{\max}^{a,\tilde{\mathbf{F}}}} \qquad \text{for } \varphi \le 1.$$
(30a, b)

In real calculations, the coefficient φ will be set at the beginning of the calculation. This coefficient has a very clear physical meaning, i.e., the chance to be selected into the mating pool of the best infeasible members compared with that of the average feasible members. This physical meaning is directly related to the degree of penalty. In addition, the coefficient does not have any units. Due to these reasons, it is possible to set this coefficient by using experience. After φ is set, $\phi(t)$ and, subsequently, $\lambda(t)$ can be computed. In case of $\varphi \ge 1$, $\phi(t)$ can be obtained from Eq. (30a) directly because all parameters in the equation are readily available. In this case, the parameters $F_{avg}^{a,\tilde{\mathbf{F}}}$ and $F_{max}^{a,\tilde{\mathbf{F}}}$ can be obtained directly from original fitness values of feasible individuals without any penalty consideration. On the contrary, if $\varphi < 1$, $\phi(t)$ cannot be obtained without iteration since one of the parameters, i.e., F_{\min}^a , is not readily available. Note that F_{\min}^a is the minimum fitness in the generation after the penalty and it is most likely that F_{\min}^a will belong to infeasible members. This F_{\min}^a can be obtained from Eq. (24) which, in turn, requires the value of $\phi(t)$ [see Eq. (27)]. Nevertheless, the iteration is very simple and takes almost no time to perform. To this end, the individual $\mathbf{x}_{Fa\min}$ that gives the minimum augmented fitness value is considered. Here, Eq. (24) yields

$$F_{\min}^{a} = F^{a}(\mathbf{x}_{Fa\min}) = F(\mathbf{x}_{Fa\min}) - \lambda(t)E(\mathbf{x}_{Fa\min}). \tag{31}$$

Also, consider the individual \mathbf{x}_{λ} that gives the value of $\lambda(t)$ in Eq. (27), i.e.,

$$\lambda(t) = \max \left[0, \max_{\forall \mathbf{x}_i \in \tilde{\mathbf{U}}} \left[\frac{F(\mathbf{x}_i) - \phi(t) F_{avg}^{a, \tilde{\mathbf{F}}}}{E(\mathbf{x}_i)} \right] \right] = \frac{F(\mathbf{x}_{\lambda}) - \phi(t) F_{avg}^{a, \tilde{\mathbf{F}}}}{E(\mathbf{x}_{\lambda})}.$$
(32)

Using Eq. (32) in Eq. (31) gives

$$F_{\min}^{a} = F(\mathbf{x}_{Fa\min}) - \left(\frac{F(\mathbf{x}_{\lambda}) - \phi(t)F_{avg}^{a,\tilde{\mathbf{F}}}}{E(\mathbf{x}_{\lambda})}\right) E(\mathbf{x}_{Fa\min}).$$
(33)

Substituting Eq. (33) into Eq. (30b) yields

$$\phi(t) = \frac{(\varphi - 1)E(\mathbf{x}_{Fa\min})F(\mathbf{x}_{\lambda}) + E(\mathbf{x}_{\lambda})[F(\mathbf{x}_{Fa\min}) + \varphi F_{avg}^{a,\tilde{\mathbf{F}}} - \varphi F(\mathbf{x}_{Fa\min})]}{F_{avg}^{a,\tilde{\mathbf{F}}}[E(\mathbf{x}_{\lambda}) + (\varphi - 1)E(\mathbf{x}_{Fa\min})]}.$$
 (34)

A problem is that the individuals \mathbf{x}_{λ} and $\mathbf{x}_{Fa\min}$ are not known from the beginning and iteration is required. In the first step of the iteration, it is assumed that $F_{\min}^a = F_{avg}^{a,\tilde{F}}$. By using Eq. (30b), the intermediate value of $\phi(t)$ for this step of the iteration is obtained, i.e., $\phi(t) = 1$. After that, the intermediate value of $\lambda(t)$ is obtained from Eq. (27) and at the same time the individual \mathbf{x}_{λ} can be identified. With the obtained $\lambda(t)$, the individual $\mathbf{x}_{Fa\min}$ can be subsequently identified from Eq. (24). Consequently, the value of $\phi(t)$ for the next step of the iteration is computed from Eq. (34). The process is repeated until the value of $\phi(t)$ becomes unchanging.

To be able to understand the proposed scheme better, let us consider an optimization problem of a uniaxial bar shown in Fig. 3. A uniaxial force of 10 lb is applied at the free end of the bar. Allowable stress is assumed to be 2 psi. Our task is to find the optimal area of the bar that yields minimum volume. For illustrative purpose, it is assumed that the area of the bar is a continuous variable and, as a result, the optimal solution is simply equal to 5 in². Suppose that GAs are used to obtain the solution and the fitness function is defined as

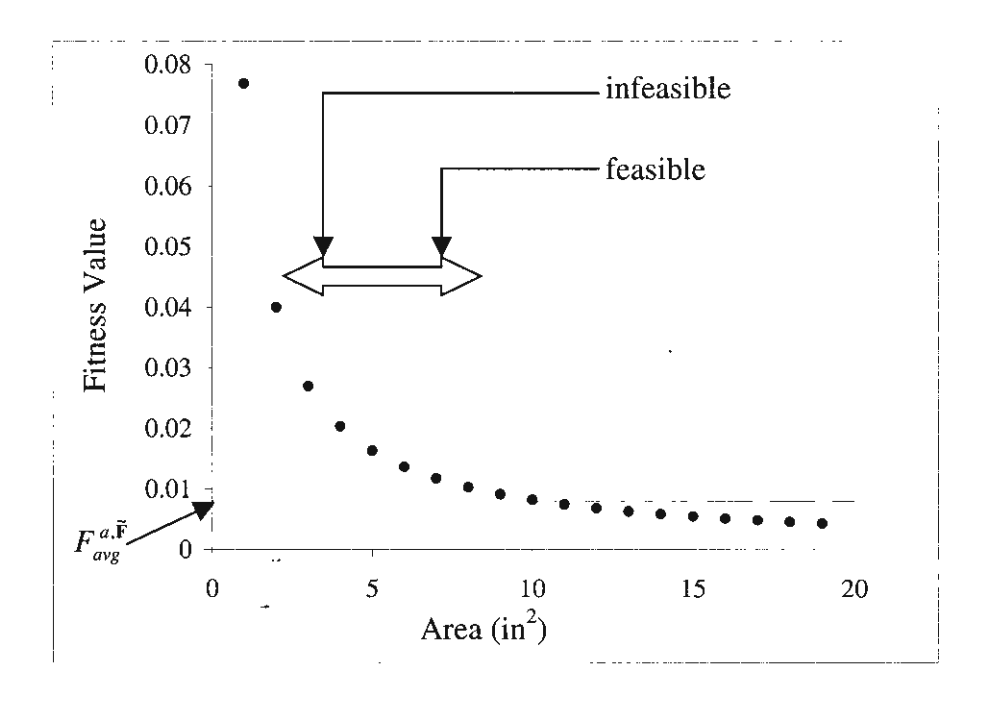


Fig. 4 Original fitness value—uniaxial problem

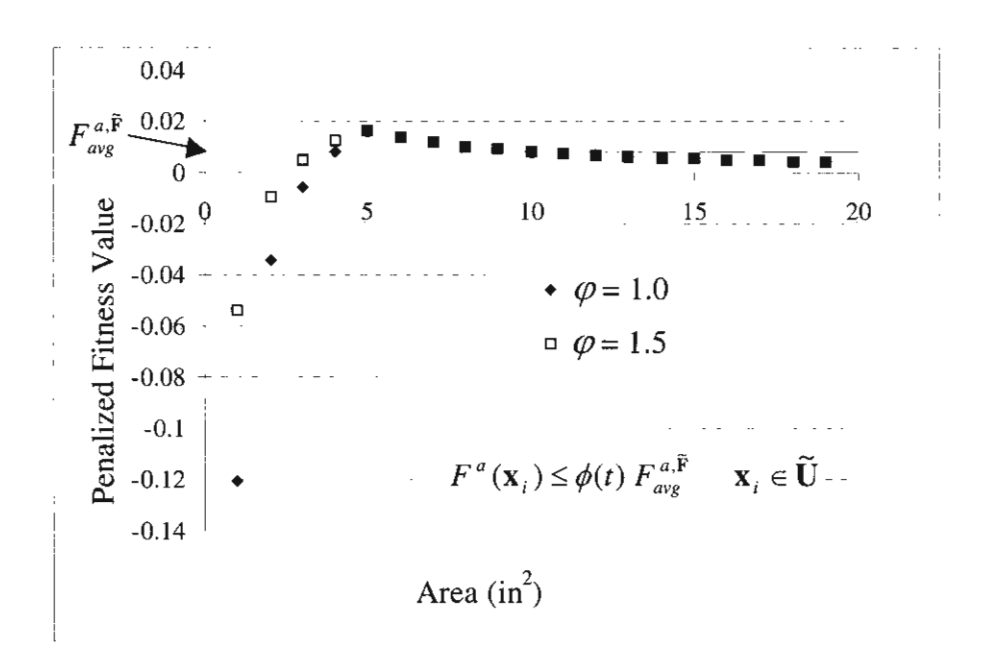


Fig. 5 Fitness value after the penalty—uniaxial problem

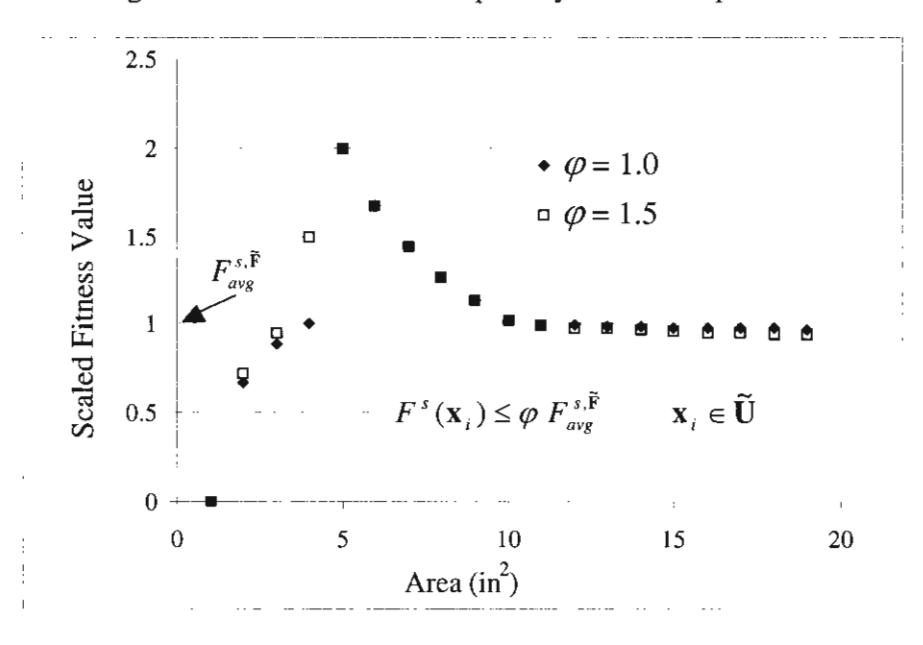


Fig. 6 Fitness value after the scaling—uniaxial problem

$$F(Area) = \frac{1}{1 + Volume (in^3)} = \frac{1}{1 + Area (in^2) \times Length (in.)}.$$
 (35)

From this fitness function, it is obvious that the smaller the area is, the larger the fitness value will be (see Fig. 4). Nevertheless, the area cannot be smaller than 5 in²; otherwise, the bar will violate the stress constraint. Therefore, fitness values of those individuals that violate the constraint have to be reduced. In this example, 19 individuals with different areas ranging from 1 to 19 in² are assumed (see Fig. 4). In the proposed penalty scheme, the average fitness of all feasible members $F_{avg}^{a,\tilde{F}}$ is calculated. If there are

any individuals that have their fitness values exactly equal to $F_{avg}^{a,\tilde{\mathbf{F}}}$, they are the average feasible members. Nevertheless, in real calculations, it does not matter whether there are any of them or not in the population since only the value of their fitness $F_{avg}^{a,\tilde{\mathbf{F}}}$ is to be used. In the proposed scheme, infeasible members are penalized in such a way that the best infeasible members have scaled fitness values equal to φ times that of the average feasible members. Fig. 6 illustratively shows scaled fitness values after the penalty and scaling when $\varphi=1.0$ and 1.5 while Fig. 5 shows fitness values just after the penalty but before the scaling. Note that, in this example, the maximum fitness is scaled to be 2.0 while the average fitness of feasible members is scaled to be 1.0. In addition, the minimum fitness is scaled to be 0. By adjusting the value of φ , the degree of penalty can be efficiently adjusted.

In fact, the purpose of the proposed scheme is to fix, throughout the calculation, the relative chance of the best infeasible members being selected into the mating pool compared with that of the average feasible members. This means that the penalty is always adjusted so that the aforementioned purpose is achieved in all generations. This guarantees that the desired degree of penalty is obtained throughout the evolution process. Consequently, the problem of too weak or too strong a penalty during different phases of the evolution is removed. Note that the relative scaled fitness values of the best feasible members and the average feasible members are set via fitness scaling (see Fig. 2). As a result, the relative chance of the best feasible members being selected into the mating pool compared with that of the best infeasible members can also be controlled. For example, when φ is set to be 1.0 in the current example, the chance of the best feasible members to be selected becomes two times that of the best infeasible members since, from the fitness scaling, the chance of the best feasible members is set to be two times that of the average feasible members.

In this study, since the fitness scaling in Fig. 2 is employed, acceptable values of φ therefore lie between 0 and C. Note that C is the scaled fitness of the best feasible individuals. Using only positive values for φ is obviously necessary because only positive scaled fitness values are acceptable. Setting φ exactly equal to zero is actually equivalent to using the death penalty scheme, which simply rejects infeasible solutions from the population. Using φ that is greater than C is in fact possible but it will mean that the best infeasible individuals will have a better chance to be selected into the mating pool than the best feasible ones. This is obviously too harsh a penalty. For this reason, the value of φ should not exceed C. For any value of φ between 0 and C, the best feasible individuals always have the maximum fitness value among all other individuals in the generation. Nevertheless, depending on the magnitude of φ , some infeasible members may have higher fitness than a certain number of feasible ones (see Fig. 6).

Actually, the key point in the development of the proposed scheme is that the user-specified penalty parameter φ is defined based on the relationship between two fitness values that are already scaled. Since scaled fitness values are directly used in the selection for the mating pool without further modification, the physical meaning of the proposed penalty parameter can be preserved. If penalty parameters are defined before the fitness scaling is performed, the fitness scaling will probably destroy the desired physical meanings of the parameters.

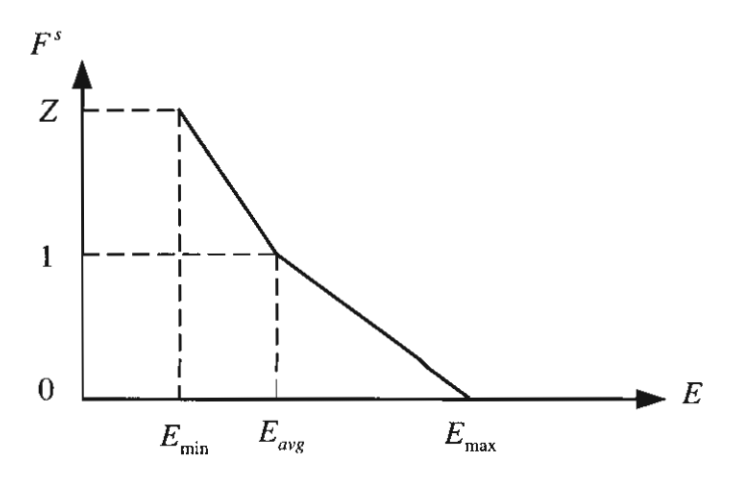


Fig. 7 Bilinear fitness scaling for the case when no feasible individual is available

Since the proposed penalty scheme requires the average fitness value over all feasible individuals, it is necessary to have at least one feasible individual in the population. In the case that there is none, the fitness values of infeasible individuals will be given based on the magnitudes of error they have. The idea is to strongly encourage the population to move toward the feasible region. Here, a bilinear scaling scheme as shown in Fig. 7 is used. Fitness is scaled in such a way that scaled fitness values of individuals with the highest error are equal to 0 and scaled fitness values of individuals with average error are equal to 1. In addition, scaled fitness values of individuals with the smallest error are set to be Z. Thus, the chance of the individuals with the smallest error being selected into the mating pool is equal to Z times that of the individuals with average error. In summary, the scaled fitness is expressed as

$$F^{s}(\mathbf{x}) = \frac{Z - 1}{E_{\min} - E_{avg}} E(\mathbf{x}) + \frac{E_{\min} - Z E_{avg}}{E_{\min} - E_{avg}} \quad \text{if } E(\mathbf{x}) \le E_{avg}$$

$$F^{s}(\mathbf{x}) = \frac{1}{E_{avg} - E_{\max}} E(\mathbf{x}) + \frac{E_{\max}}{E_{\max} - E_{avg}} \quad \text{if } E(\mathbf{x}) > E_{avg}.$$
(36)

4.4 Results

To investigate the validity and efficiency of the proposed penalty scheme, the scheme is used in design optimization of three different two-dimensional structures, i.e., a six-bar truss, a ten-bar truss, and a one-bay eight-story frame. To be able to see clearly the advantages of the proposed scheme over conventional schemes, particularly in terms of robustness, obtained results are compared with those from a selected conventional scheme. Since most conventional schemes are based on the same concept with slightly different details, comparison with one selected conventional scheme is sufficient to show advantages of the proposed scheme over conventional schemes. As already mentioned, the main objective of this study is to develop an adaptive penalty scheme that is robust and still able to reproduce the same quality of results as ones obtained from GAs found in the literature. To show this comparison of the proposed method, results are also compared with existing results in the literature.

4.4.1 Six-Bar Truss

The first problem to be considered is the six-bar truss as shown in Fig. 8. Here, only sizing optimization is considered. Thus, design variables are six sectional areas of the six

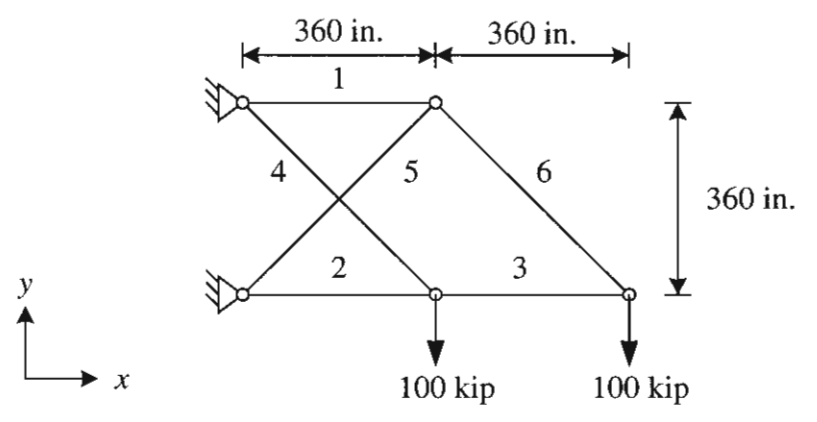


Fig. 8 Six-bar truss

members of the truss. The cross-sectional area of each member is taken from the following 32 discrete values, i.e., 1.62, 1.80, 2.38, 2.62, 2.88, 3.09, 3.13, 3.38, 3.63, 3.84, 3.87, 4.18, 4.49, 4.80, 4.97, 5.12, 5.74, 7.22, 7.97, 11.5, 13.5, 13.9, 14.2, 15.5, 16.0, 18.8, 19.9, 22.0, 22.9, 26.5, 30.0, and 33.5 in². Therefore, a five-bit string is required for each design variable. There are two types of constraint in this problem, i.e., stress and displacement constraints. Design parameters used in the problem are shown in Table 1.

For comparison, the most popular conventional penalty form is selected, i.e.,

$$F_i^a = F^a(\mathbf{x}_i) = F(\mathbf{x}_i) - P(\mathbf{x}_i) = F(\mathbf{x}_i) - \lambda E(\mathbf{x}_i)$$
(37)

where the coefficient λ is constant and the error term $E(\mathbf{x}_i)$ is the same as that defined in Eq. (25). In both proposed and conventional schemes, the fitness function $F(\mathbf{x}_i)$ is defined as

$$F(\mathbf{x}_i) = \frac{1}{1 + Weight(\mathbf{x}_i)}$$
 (38)

where two different units of weight, i.e., pound (lb) and newton (N) are used. Two units are used in order to investigate the effect of unit on the results from both schemes.

Since it is impossible to judiciously estimate an appropriate value of the coefficient λ in the conventional scheme, a wide range of values will be used. All GA parameters used in this problem can be found in Table 1. To start the calculation, an initial population is generated at random. The type of crossover operator used here is the one-point crossover (Goldberg 1989).

Fig. 9 shows results obtained from the proposed and conventional schemes. Each point in the graph represents an average weight of the best feasible designs obtained from 200 different runs. The results obtained by using newtons in Eq. (38) are converted into pounds for comparison. In the conventional scheme, the coefficient λ is varied exponentially from 0.000001 to 100 while in the proposed scheme the coefficient φ is varied from 0.25 to 1.75. Note that the value of φ should be varied between 0 to 2.0 since the maximum scaled fitness value C is set to be 2.0 (see Table 1). It can be clearly seen from the results that the proposed scheme is more robust than the conventional scheme. In the proposed scheme, changing the maximum integral particles of the proposed.

เลชที่ 979/17-21 ถนนพหลโยธิน นขวงสามเสนใน บอลพญ ไท กรุงเทพฯ 10400 ! กร.298-0455 โทรสาร 298-0476 Home page 19ttp://www.trf.or.th E-mail: trf-info@trf.or.th

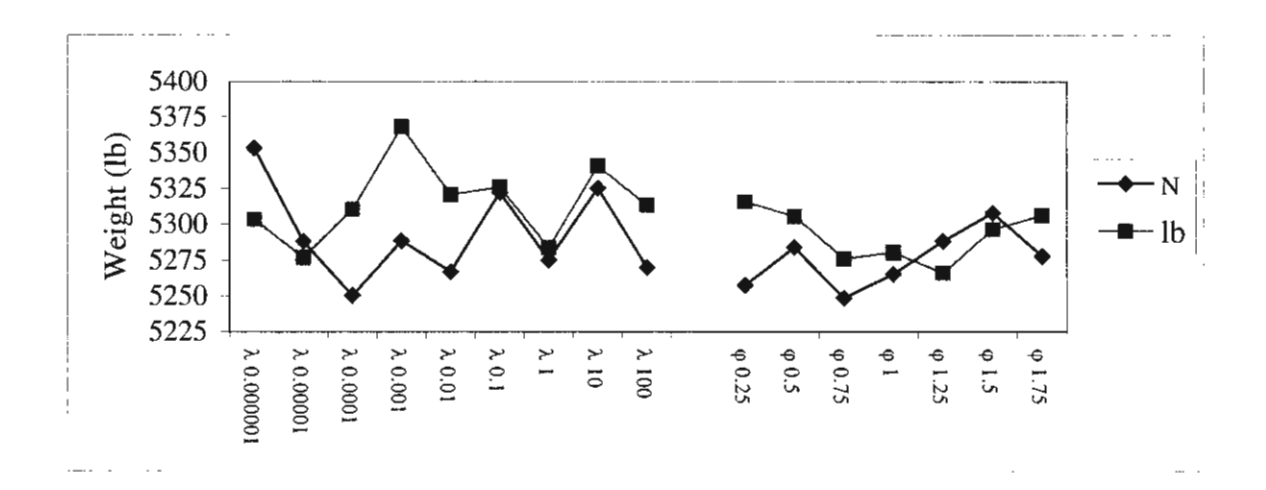


Fig. 9 Average weight of the best feasible designs obtained from 200 runs—six-bar truss

scheme, it is easier to notice a trend in the results when φ is varied. It can be reasonably said that good results are obtained with values of φ around 0.75 to 1.0. On the contrary, it is much more difficult to observe this kind of trend in the results of the conventional scheme as they are very much scattered and exhibit no recognizable pattern. Although the trend in the results of the proposed scheme can be observed, it is also important to note that, when φ is varied, the results of the proposed scheme actually vary to a much lesser degree than the results of the conventional scheme do when λ is varied. Even though it may be argued that, in this study, λ is exponentially changed while φ is linearly changed, the same difference in the way that the parameters are varied and tried is expected in the real practice. This is because, in the real practice, it will also be impossible to estimate appropriate values of the coefficient λ in the conventional scheme, so a very wide range of values must be tested. With the proposed scheme, lesser sensitivity of results to the magnitude of the parameter ensures that even when the appropriate value of φ is not clearly known, a range of values of φ may be used and reasonable results can still be obtained. This fact really confirms the robustness of the proposed scheme.

Table 1 Design and GA parameters for the six-bar truss problem

Design parameters		GA parameters	
Item	Value	Item	Value
Modulus of elasticity Weight density Allowable tensile stress Allowable compressive	10 ⁷ psi 0.1 lb/in ³ 25,000 psi 25,000 psi	Maximum number of generations Population size Crossover probability	100 70 0.8
stress Maximum y-displacement	2 in.	Mutation probability φ λ C	0.001 0.25-1.75 0.000001-100 2.0 5.0

To ensure that the proposed scheme is capable of giving results of the same quality as those GAs found in the literature, the best result obtained from the proposed scheme is also compared with the best result reported by Rajan (1995). They are exactly the same.

The details of the results are shown in Table 2. It must be noted that in this study, except for the new penalty algorithm, the rest of the algorithms are standard. This is not the case for the work by Rajan (1995), which employs more complicated GAs.

Table 2 Comparison of the results for the six-bar truss problem

Member	Size of member (in ²)		
	Proposed	Rajan (1995)	
1	30.0	30.0	
2	19.9	19.9	
3	15.5	15.5	
4	7.22	7.22	
5	22.0	22.0	
6	22.0	22.0	
Total weight (lb)	4962.1	4962.1	

4.4.2 Ten-Bar Truss

The next problem to be considered is the ten-bar truss as shown in Fig. 10. This problem is one of the benchmark problems used to test optimization methods. Also in this problem, only sizing optimization is considered. Therefore, design variables are ten sectional areas. Cross-sectional areas of members 1, 3, 4, 7, 8 and 9 are taken from the following 32 discrete values, i.e., 3.13, 3.38, 3.47, 3.55, 3.63, 3.84, 3.87, 3.88, 4.18, 4.22, 4.49, 4.59, 4.80, 4.97, 5.12, 5.74, 7.22, 7.97, 11.5, 13.5, 13.9, 14.2, 15.5, 16.0, 16.9, 18.8, 19.9, 22.0, 22.9, 26.5, 30.0, and 33.5 in². For the rest of the members, the cross-sectional areas are taken from the following 32 discrete values, i.e., 1.62, 1.80, 1.99, 2.13, 2.38, 2.62, 2.63, 2.88, 2.93, 3.09, 3.13, 3.38, 3.47, 3.55, 3.63, 3.84, 3.87, 3.88, 4.18, 4.22, 4.49, 4.59, 4.80, 4.97, 5.12, 5.74, 7.22, 7.97, 11.5, 13.5, 13.9, and 14.2 in². Similar to the previous problem, a five-bit string is required for each design variable. Design parameters and genetic parameters are shown in Table 3.

Results obtained from the proposed and conventional schemes are shown in Fig. 11. Similar to the previous problem, each point in the graph represents an average weight of the best feasible designs obtained from 200 different runs. The robustness of the proposed scheme is again obvious. The effect of the unit used on the results from the proposed scheme is noticeably less than that on the results from the conventional scheme. Moreover, the results from the proposed scheme also exhibit a rather clear tendency with respect to the value of the coefficient used while those from the conventional scheme do

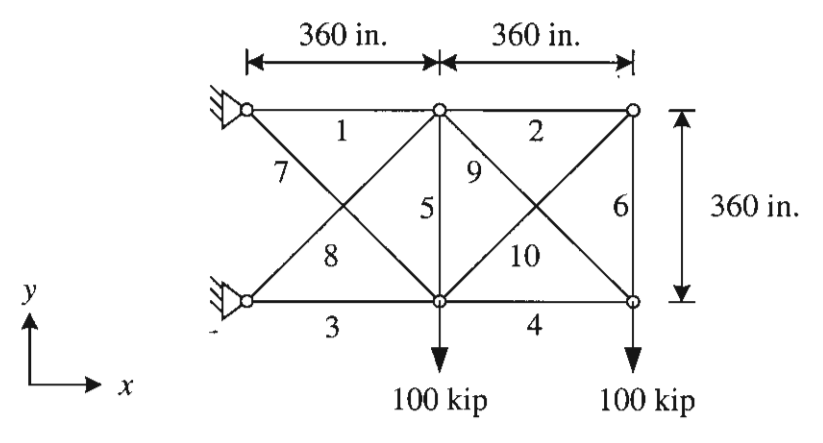


Fig. 10 Ten-bar truss

not, and are quite scattered. In the proposed scheme, it can be reasonably said that good results are obtained with values of φ around 0.5 to 0.75. Similar to the previous problem, even though the trend in the results of the proposed scheme can be observed, the results are not that much sensitive to the magnitude of the penalty parameter when compared with the conventional scheme. Consequently, a range of values of φ may be used when the appropriate value is not known. The best result obtained from the proposed scheme is also compared with the best results reported by Rajeev and Krishnamoorthy (1992), Camp et al. (1998) and Galante (1996) in Table 4. It can be seen that the result obtained from the proposed penalty scheme is relatively good although Rajeev and Krishnamoorthy (1992), Camp et al. (1998), and Galante (1996) employ more complicated GAs.

Table 3 Design and GA parameters for the ten-bar truss problem

Design parameters	3	GA parameters	
Item	Value	Item	Value
Modulus of elasticity Weight density Allowable tensile stress Allowable compressive stress Maximum x, y-displacements	10 ⁷ psi 0.1 lb/in ³ 25,000 psi 25,000 psi 2 in.	Maximum number of generations Population size Crossover probability Mutation probability φ λ C	100 40 0.8 0.001 0.25-1.75 0.000001-100 2.0 5.0

In the previous six-bar truss problem, the appropriate value of φ is around 0.75 to 1.0, which is similar to the value obtained for the ten-bar truss problem. Since the two problems are quite similar, similar values of the coefficient from the two problems are expected. In this aspect, the proposed scheme evidently outperforms the conventional scheme, which does not exhibit any obvious similarity between these two problems. Having similar appropriate values of the coefficient for similar problems allows the coefficient to be set by experience. Since the coefficient in the proposed scheme has a physical meaning, which directly corresponds to the understandable degree of penalty, the

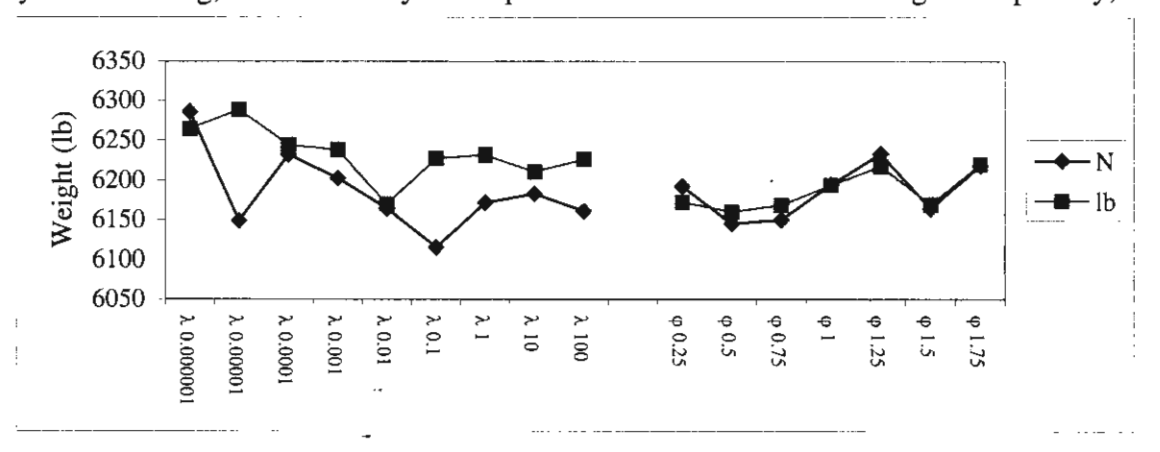


Fig. 11 Average weight of the best feasible designs obtained from 200 runs—ten-bar truss

characteristics of the problems being solved can be directly related to the appropriate degree of penalty. This kind of advantage may not be found in existing conventional schemes.

Table 4 Comparison of the results for the ten-bar truss problem

Member	Size of member (in ²)			
	Proposed	Rajeev and Camp et a		Galante (1996)
		Krishnamoorthy	(1998)	
		(1992)		
1	33.5	33.5	30.0	33.5
2	1.62	1.62	1.62	1.62
3	22.9	22.0	26.5	22.0
4	15.5	15.5	13.5	14.2
5	1.62	1.62	1.62	1.62
6	1.62	1.62	1.62	1.62
7	7.22	14.2	7.22	7.97
8	22.9	19.9	22.9	22.9
9	22.0	19.9	22.0	22.0
10	1.62	2.62	1.62	1.62
Total weight (lb)	5499.3	5613.8	5556.9	5458.3

4.4.3 One-Bay Eight-Story Frame

The last problem to be considered is the one-bay eight-story frame as shown in Fig. 12 Similar to the previous two problems, only sizing optimization is considered. The 24 members of the structure are categorized into eight groups (as indicated in Fig. 12). In this problem, 256 sections are selected from a list of 268 W-sections from the American Institute of Steel Construction Allowable Stress Design (AISC-ASD) specifications given in Burns (1995) by discarding the 12 biggest sections from the list. Thus, an eight-bit string is required for each design variable. There is only a displacement constraint in the problem that is the maximum x-displacement at the top of the structure. Design and genetic parameters are shown in Table 5.

Fig. 13 shows results obtained from the proposed and conventional schemes. In the figure, each point in the graph also represents an average weight of the best feasible designs obtained from 200 different runs. Once again, the robustness of the proposed scheme is confirmed. The effect of the unit on the results obtained from the proposed scheme is almost negligible. This conclusion is not true for the case of the conventional scheme, which exhibits large differences between the results from the two different units. In this problem, the insensitivity of the results to the value of the parameter is very apparent for the proposed scheme. On the contrary, the results from the conventional scheme show very high variation when the parameter is varied. This confirms the higher robustness of the proposed scheme over the conventional one. Although some of the averages of the best results from the conventional scheme shown in Fig. 13 may seem to be better than those from the proposed scheme, a comparison of the best result obtained from the proposed technique and results reported by Camp et al. (1998) in Table 6 shows that the proposed method is actually acceptable. In their paper, Camp et al. (1998) provide both results from their own GAs, which are not the standard GAs, and from the optimality criteria method (Khot, Venkayya, and Berke 1976).

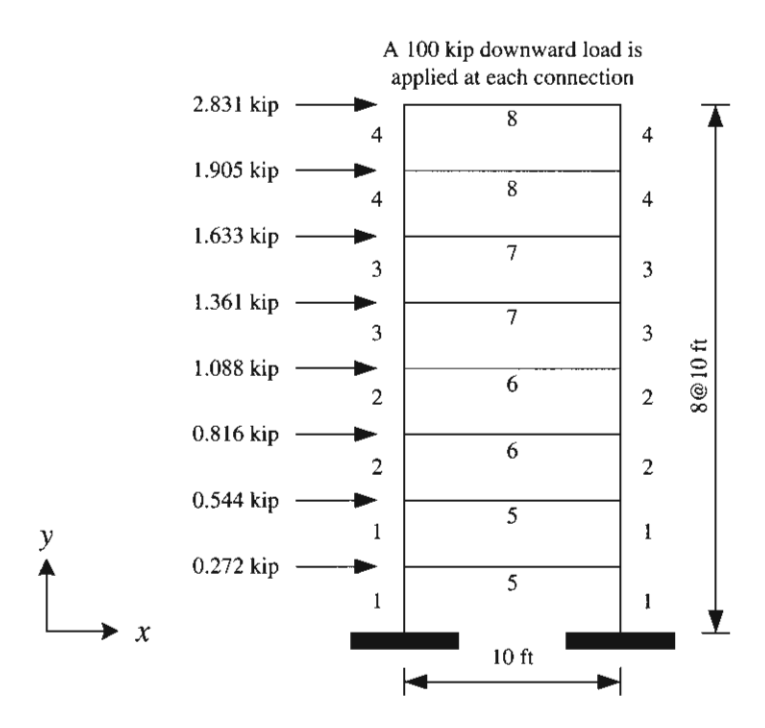


Fig. 12 One-bay eight-story frame

Table 5 Design and GA parameters for the one-bay eight-story frame problem

Design parameters		GA parameters	
Item	Value	Item	Value
Modulus of elasticity Weight density Maximum x- displacement at the top of the structure	29x10 ³ ksi 2.83x10 ⁻⁴ kip/in ³ 2 in.	Maximum number of generations Population size Crossover probability Mutation probability φ λ C	100 50 0.85 0.05 0.25-1.75 0.000001-100 2.0 5.0

Table 6 Comparison of the results for the one-bay eight-story frame problem

Group Number	Proposed	GAs	Optimality criteria
		(Camp et al. 1998)	(Camp et al. 1998)
1	W 12 x 45	W 18 x 46	W 14 x 34
2	W 14 x 34	W 16 x 31	W 10 x 39
3	W 12 x 35	W 16 x 26	W 10 x 33
4	<u>W</u> 10 x 19	W 12 x 16	W 8 x 18
5	W 18 x 35	W 18 x 35	W 21 x 68
6	W 18 x 40	W 18 x 35	W 24 x 55
7	W 16 x 36	W 18 x 35	W 21 x 50
8	W 16 x 26	W 16 x 26	W 12 x 40
Total weight (kip)	7.47	7.38	9.22

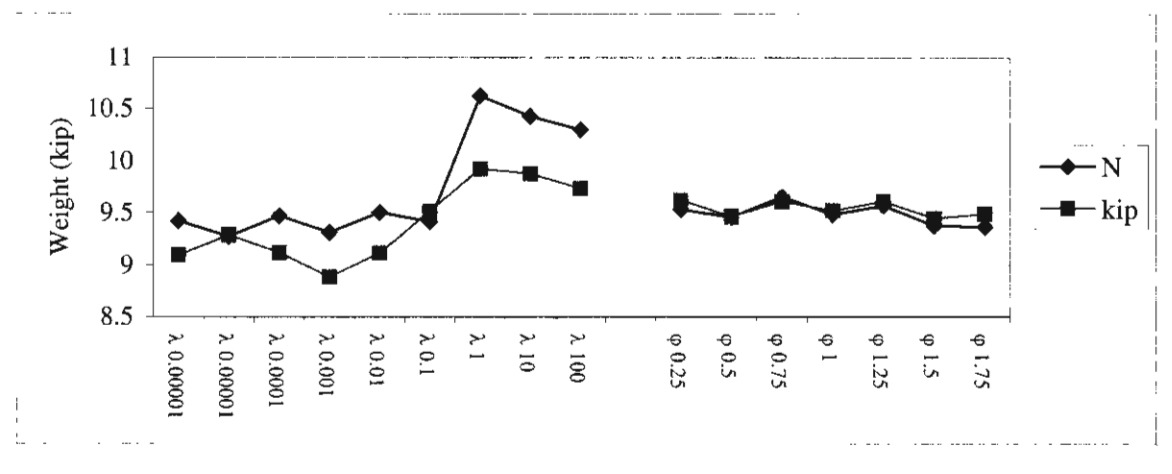


Fig. 13 Average weight of the best feasible designs obtained from 200 runs—one-bay eight-story frame

5. OPTIMIZATION OF MATRIX STORAGES IN THE FINITE ELEMENT ANALYSIS BY NODE RENUMBERING

The analysis method for cracking localization proposed in this study will involve finding a crack pattern that has the minimum total potential energy. As a result, many system stiffness equations for solutions with different crack patterns have to be formed and analyzed. Moreover, for accurate results, the finite element meshes employed will have to be rather fine in order to allow as many cracks as possible to occur. For this reason, the obtained stiffness equations will be large. This will result in both great computing memory requirement as well as long computational time. Any technique that helps lessen this problem will therefore be much helpful.

In most structural analysis problems, system stiffness matrices are generally weakly populated. This is because each row or equilibrium equation for a particular degree of freedom is only influenced by degrees of freedom associated with the often-small number of elements connecting to that degree of freedom. All other degrees of freedom for remaining unattached elements have no effect on this equilibrium equation and hence have zero or void stiffness coefficients in that row. Therefore, a sparse or profile matrix is usually used to store a system stiffness matrix. It is indicated by clustering of the nonzero stiffness coefficients about the main diagonal of the matrix (see Fig. 14). The opportunity to gain the efficiency in solving the matrix equation can be realized if all elements outside the sparseness that always retain zero value are noted. Hence, the performance of calculation can be improved by modifications that avoid the storage and manipulation of the useless zeros outside the clustering.

Element stiffness matrices are assembled to form a system stiffness matrix according to the degrees of freedom of the elements, which are commonly assigned by the node numbers. Actually, the numbering sequence of the nodes has no influence on the result, but it influences the computational time and the requirement of storage space of the system stiffness matrix. If the nodes are numbered in an appropriate sequence, the coefficients in the system stiffness matrix are arranged close to the diagonal of the matrix. Thereafter, the profile matrix can store fewer components and certainly use lower computational time. In this section, a method to optimize the storage of system stiffness matrices by node renumbering is proposed (see more details in Thitawat 2001). The objective of the method is to find a node numbering sequence that requires the minimum storage area by having most of the coefficients of the system stiffness matrix close to the diagonal of the matrix. The optimization technique employed is the genetic algorithm (GA). The genetic algorithm is selected because of its ability to perform global searches and its suitability for problems with discrete variables.

One of the famous optimization problems that have been solved by GAs is the traveling salesman problem. The goal of this problem is to find the shortest route that

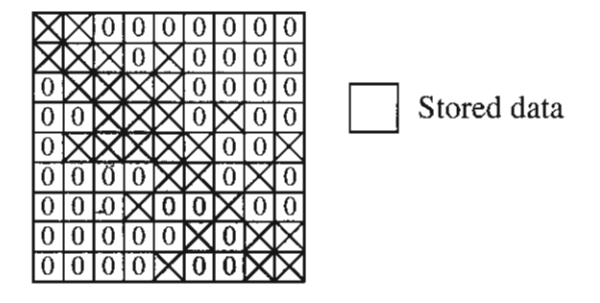
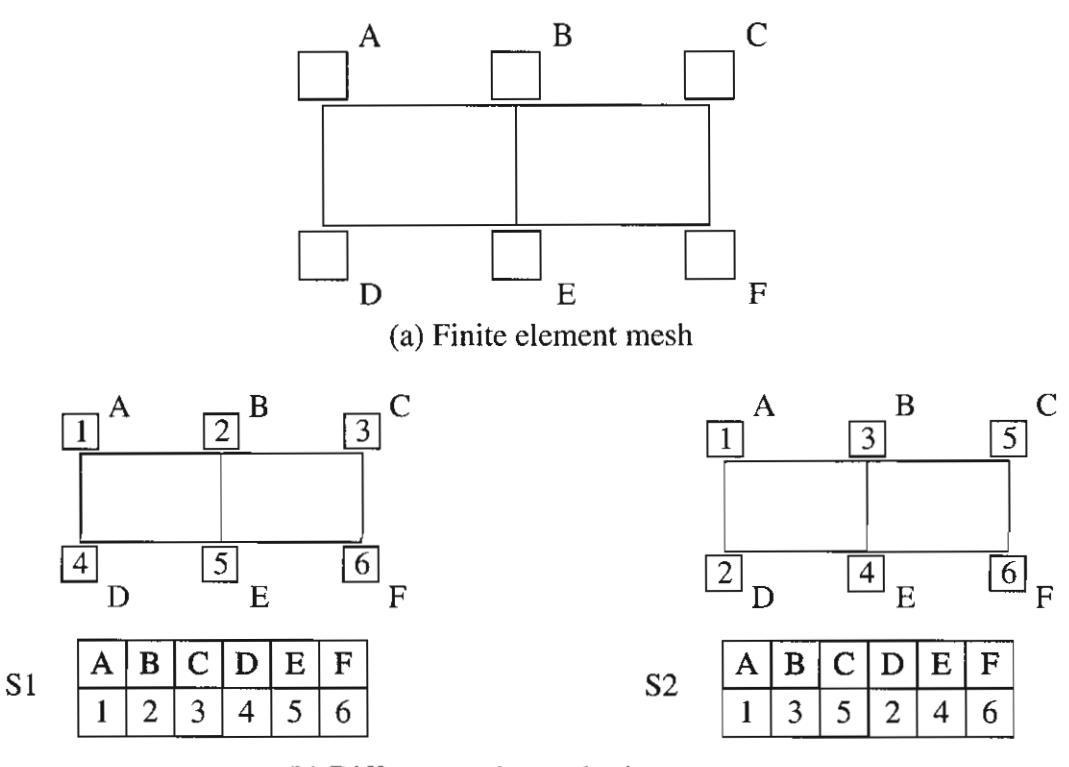


Fig. 14 Storage of a profile symmetric matrix



(b) Different node numbering sequences

Fig. 15 Analogy between the node numbering and traveling salesman problems

passes all prescribed cities for a salesman to visit. In other words, the goal is to find the best sequence of cities to visit. The usual constraint of the problem is that the salesman can visit each city only once. In the optimization of the stiffness matrix storage, numbering of nodes is considered. Since each node number cannot be repeated in a finite element mesh, different numbering sequences of nodes can be considered as different sequences of cities in the traveling salesman problem. If each node number is thought of as a city name, then the problem can be considered as the traveling salesman problem. In order to illustrate this idea, consider a finite element mesh shown in Fig. 15. Assume that the name of the first city that the salesman visits is placed in the A box and the second city is in the B box and so on. The different node numbering sequences S1 and S2 indicate the different order of cities to visit (see Fig. 15b). In S1, the sequence of cities is 1, 2, 3, 4, 5, and 6 while, in S2, the sequence is 1, 3, 5, 2, 4, and 6. These two sequences will lead to different storages of the matrix.

From the above similarity, the minimization of the stiffness matrix storage in this study will be based on GAs for the traveling salesman problem. Here, the simple genetic algorithm will be used. The details of the method are described as follows.

5.1 Coding and GA operators

5.1.1 Coding

In usual coding for GAs, binary strings are often used. Nevertheless, for the traveling salesman problem, strings of city names can be directly used. For example, consider two meshes for a one-dimensional bar shown in Fig. 16. The genotypes that represent the two different numbering sequences in the figure are simply the strings of the node sequences. Coding node numbering sequences this way is to make certain that it is possible to find appropriate crossover and mutation operators that will not result in repeated node numbers in the mesh.

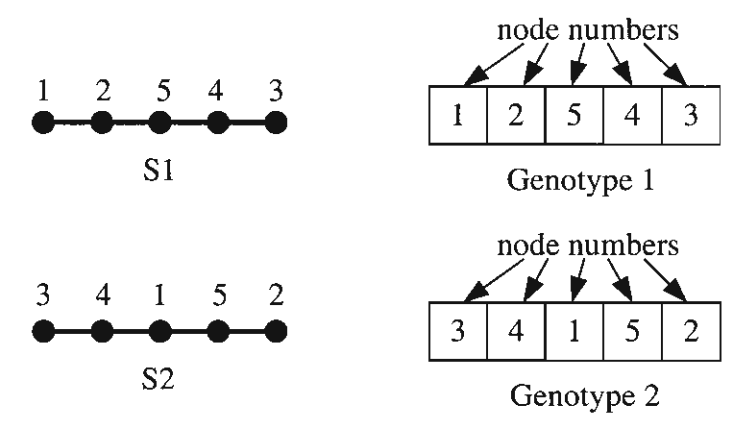


Fig. 16 Coding for different node numbering sequences

5.1.2 Crossover operator

The function of the crossover operator is to create new genotypes (children strings) by exchanging the data (bits) between the existing genotypes (parent strings). The traditional crossover algorithm, which is a crossover of binary-coded strings, cannot be applied to integer-coded strings used in this problem because it might cause repetition or loss of some node numbers. Thus, a different type of crossover algorithm must be used to avoid such problems.

Usually, the crossover operator needs two parent strings and returns two children strings as the outputs. The crossover operator used here also needs two parent strings and gives two children strings. Nevertheless, this algorithm is divided into two parts, i.e., the first part for the first children string and the second one for the second children string. It begins with random selection of the crossing site (see Fig. 17a). Next, the node numbers in the parent string P2 that appear on the left side of the crossing site in the parent string P1 are removed from P2 (see Fig. 17b). Then, the remaining bits in P2 are moved to the right by keeping the order of the node numbers (see Fig. 17c). Finally, all bits on the right side of the crossing site in P1 are replaced by all remaining bits on the right side of the crossing site in P2 (see Fig. 17d) and the children string C1 is obtained. In order to create the second children string C2, the same procedure can be perfomed. The difference is only that, at the

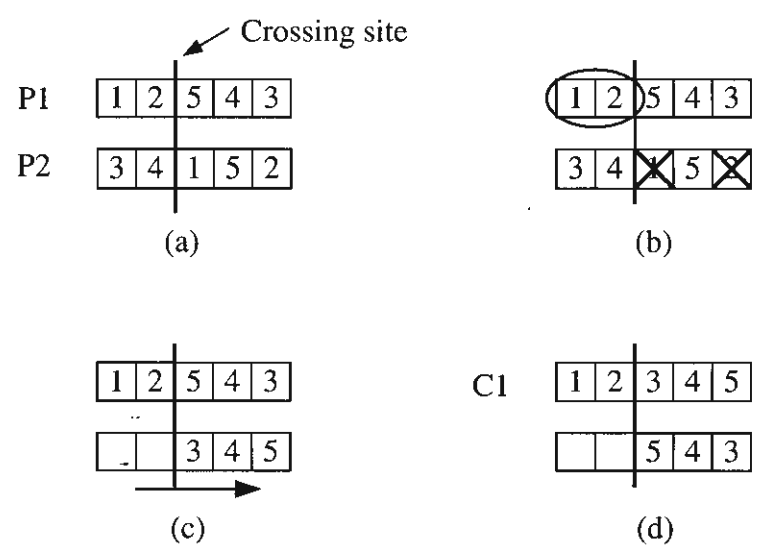


Fig. 17 Schematic diagram of the crossover operator



Fig. 18 Schematic diagram of the mutation operator

beginning, bits on the left side of P2 instead of P1 are kept unchanged.

5.1.3 Mutation operator

The mutation operator is another operator to create new genotypes. The difference from the crossover operator is that the crossover operator needs another genotype to exchange the data while the mutation operator manipulates the data within itself. Certainly, the traditional mutation operator cannot be used for this problem since repetition of node numbers will definitely result. The new algorithm begins by selecting two exchange bits at random and subsequently swapping the node numbers of the two bits (see Fig. 18).

5.2 Results

In order to illustrate the advantages of the proposed method in the optimization of the stiffness matrix storage, the following example problems are considered, i.e.,

5.2.1 Example problem 1

In this example, a finite element mesh consisting of 8 eight-noded elements and 37 nodes shown in Fig. 19 is considered (Gajewski and Lompies 1996). The total number of all possible numbering sequences is $37!=1.376x10^{43}$. The mesh's original numbering sequence is shown also in Fig. 19 (Gajewski and Lompies 1996). The system stiffness matrix of the original mesh is shown Fig. 20. Since the matrix is symmetric, only components in the shaded area will have to be stored. The original numbering sequence requires storage of 449 coefficients.

The objective function in this optimization problem is the number of the coefficients that have to be stored in the profile matrix. The fitness function $F(\mathbf{x})$ is defined as

$$F(\mathbf{x}) = \frac{1}{1 + N(\mathbf{x})} \tag{39}$$

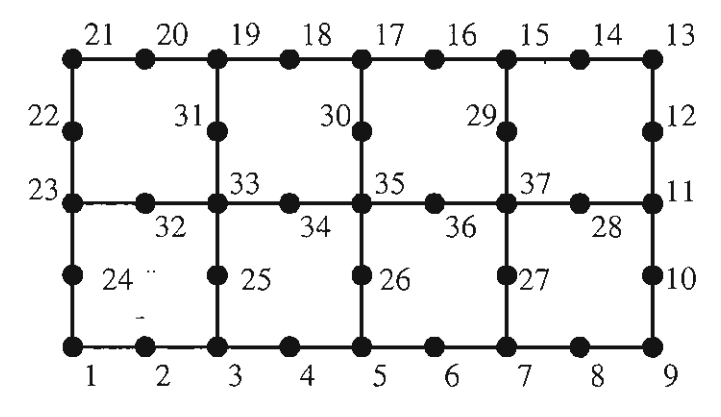


Fig. 19 Example problem 1—configuration

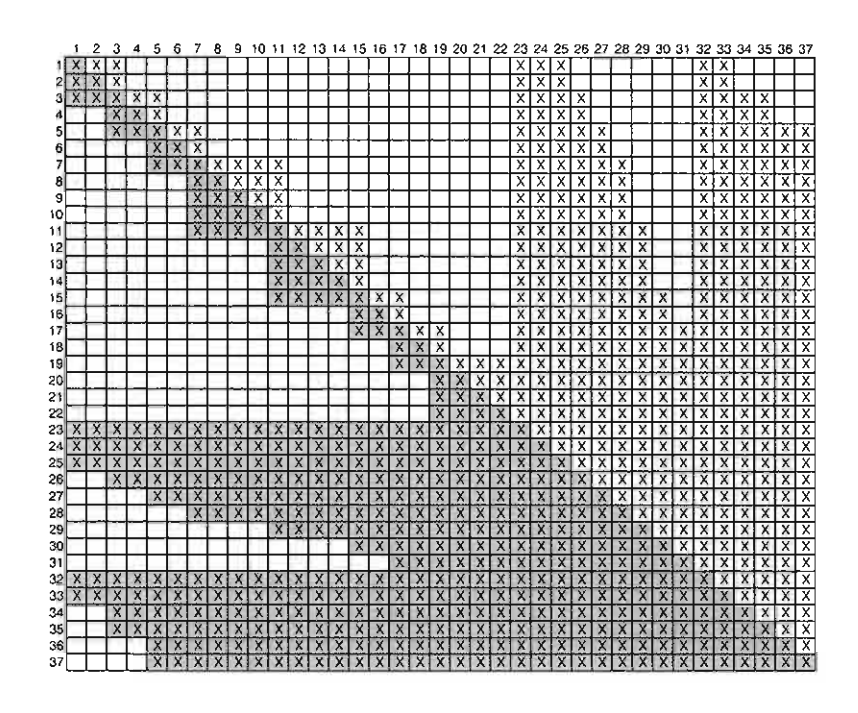


Fig. 20 Stiffness matrix of the original mesh

where x represents the genotype while $N(\mathbf{x})$ denotes the objective function, which is the number of the coefficients to be stored. In the GA calculation, the maximum number of generation is set to 5,000. The population size is set to 100. The algorithm is executed with the probability of crossover p_c and the probability of mutation p_m equal to 0.8 and 0.05, respectively. The population of the first generation is selected at random.

Fig. 21 is a plot between the average value of the required storage size in each generation and the generation number. Note that the average storage size of each generation is calculated from the storage sizes of all individuals in the generation. In addition, the storage size is the number of the coefficients that have to be stored. It can be seen from the graph that the convergence is actually obtained very quickly and 5,000 generations are actually not necessary.

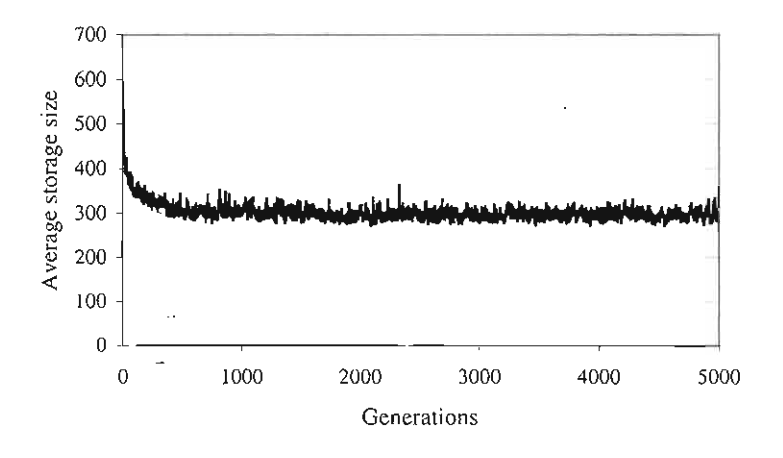


Fig. 21 Convergence of the average storage size

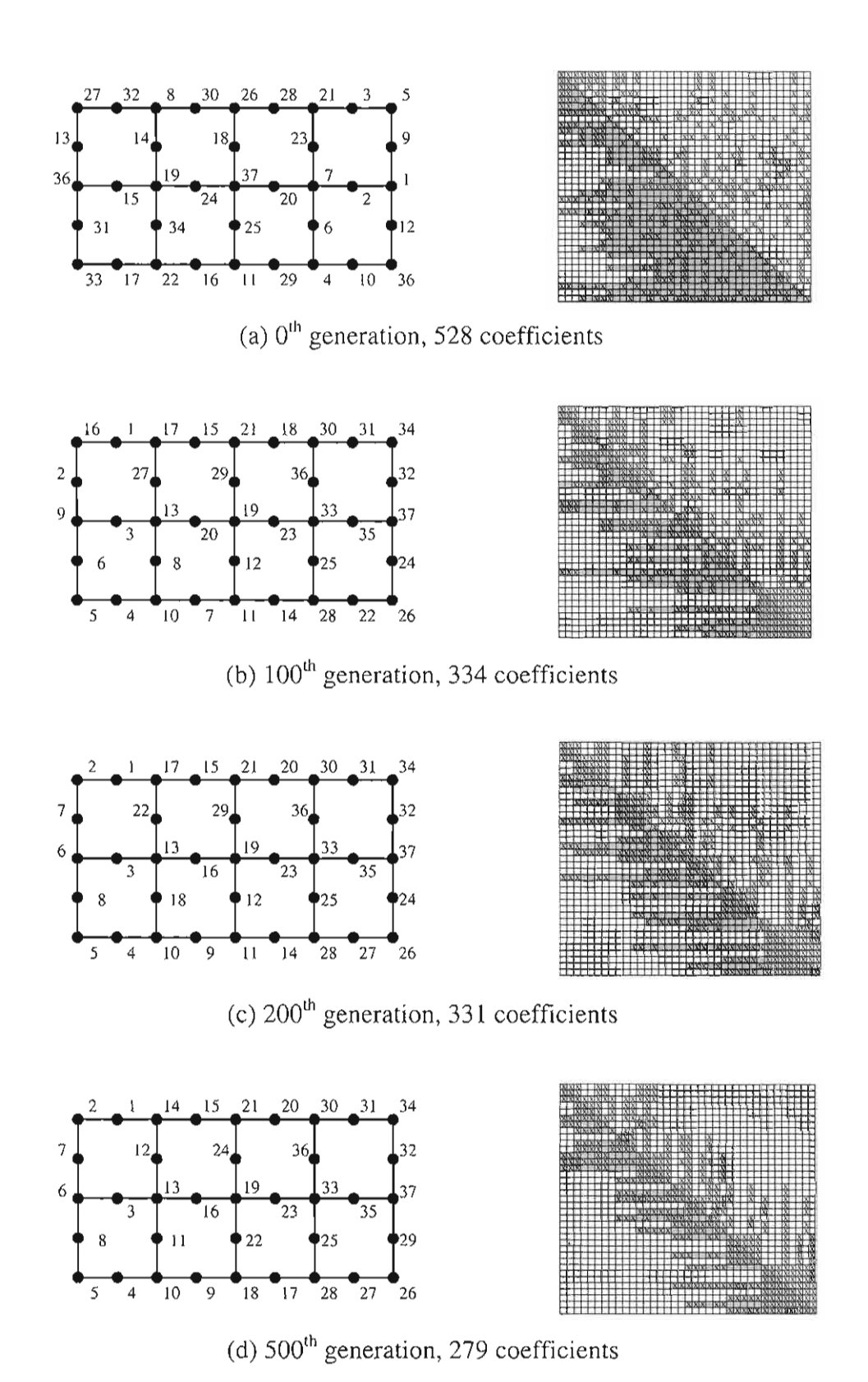
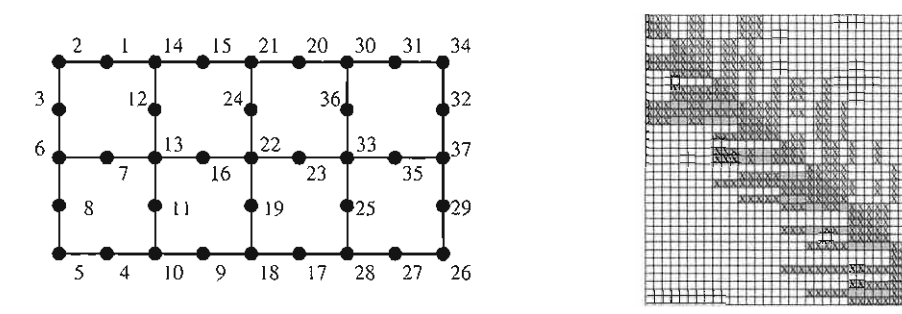


Fig. 22(a) The best solutions obtained up to different numbers of generations

Fig. 22 shows the best solutions obtained up to different numbers of generations. Note that the best solution obtained up to a certain generation is the best solution obtained so far and it may or may not be the best solution of the last generation. From Fig. 22, it can be seen that the required storage size drops dramatically in the early generations.



(e) 1500th generation, 271 coefficients

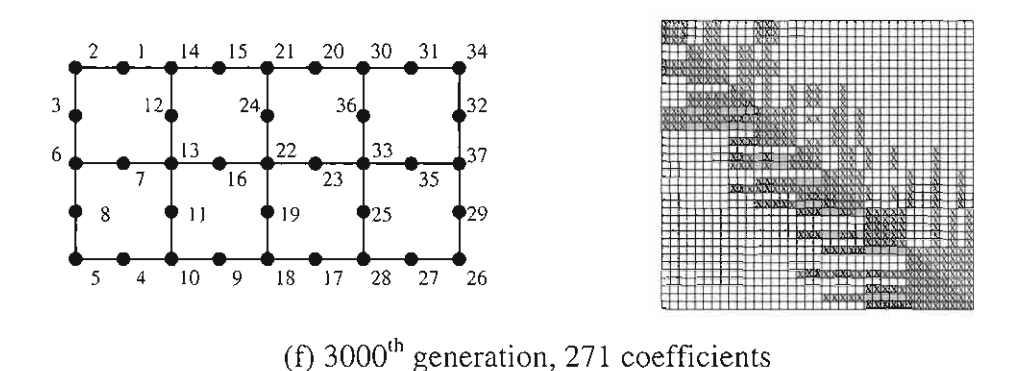


Fig. 22(b) The best solutions obtained up to different numbers of generations

Moreover, from the profiles of the matrix in different generations, it is clear that in the early generations the matrix still stores many zeros. After many generations, non-zero coefficients are moved closer to the diagonal of the matrix which results in less required storage.

Fig. 23 compares the profile of the stiffness matrix obtained by the proposed method with the one obtained by Gajewski and Lompies (1996). The profile from the

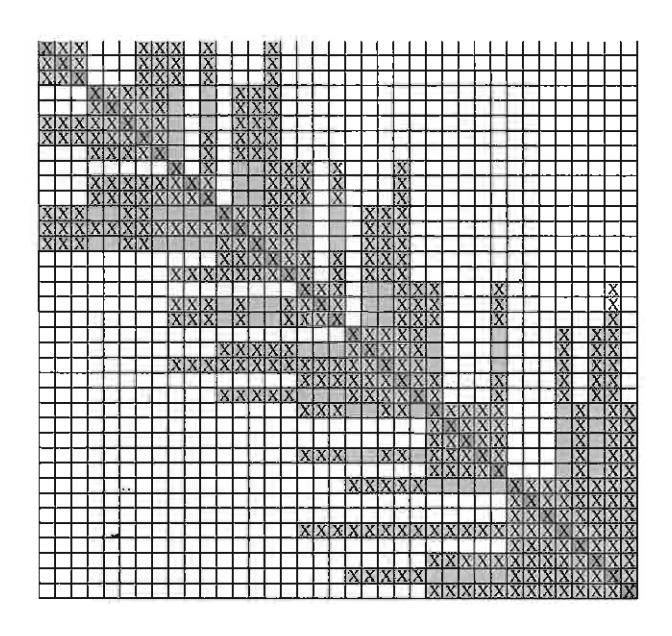


Fig. 23 Results of the example problem 1 from the proposed method (lower triangular) and Gajewski and Lompies (1996) (upper triangular)

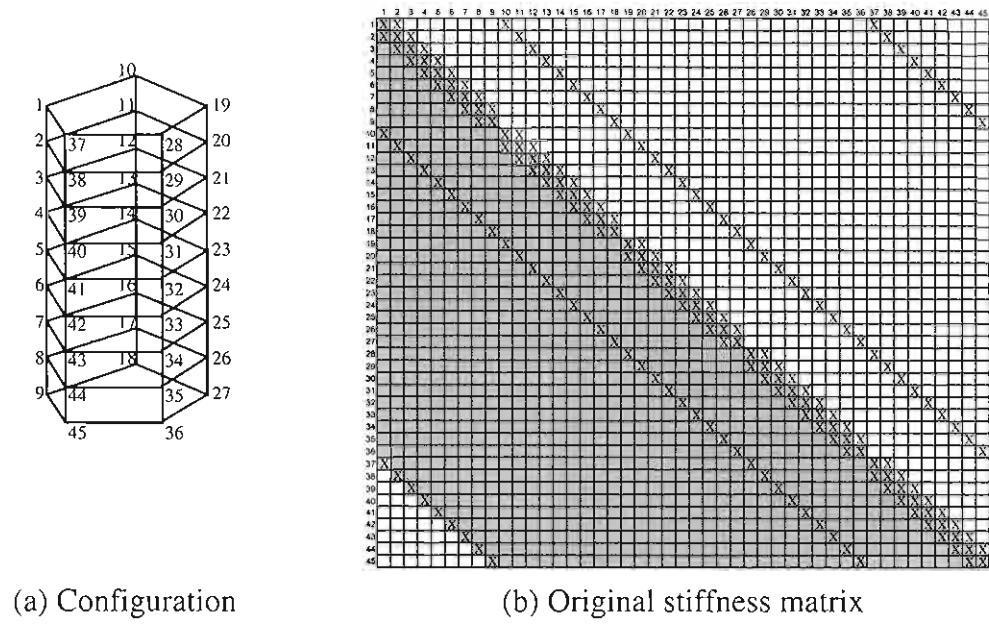


Fig. 24 Example problem 2

proposed method is shown in the lower triangular part of the matrix while the one from Gajewski and Lompies (1996) is shown in the upper triangular part. Gajewski and Lompies proposed object-oriented implementation of bandwidth, profile and wavefront reduction algorithms based on an algorithm published by Sloan (1986). Their work yields a matrix with storage requirement of 270 coefficients while the proposed method yields a matrix with storage requirement of 271 coefficients. These two solutions are comparable. It must be noted that Sloan's concept is complicated and its implementation is more difficult than the implementation of the proposed method based on GAs.

5.2.2 Example problem 2

The second problem is a finite element mesh of a space truss shown in Fig. 24 (Collins 1973). The mesh consists of 85 two-noded line elements and 45 nodes. The total number of

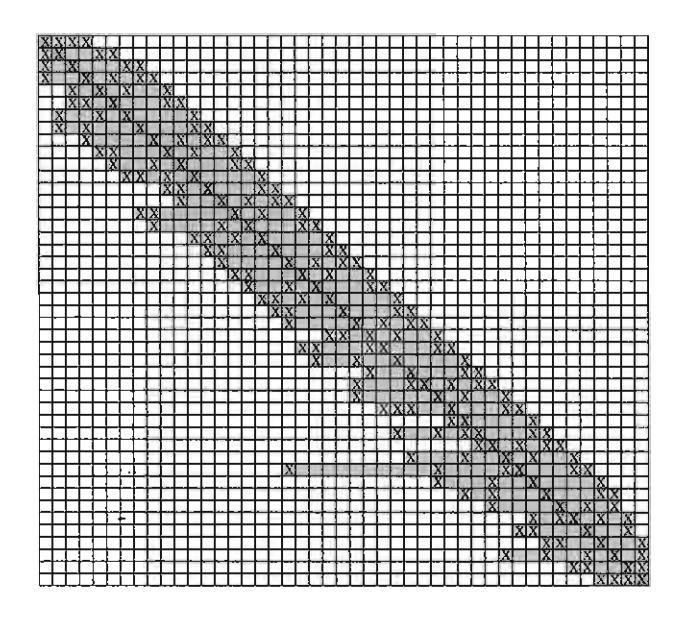


Fig. 25 Results of the example problem 2 from the proposed method (lower triangular) and Collins (1973) (upper triangular)

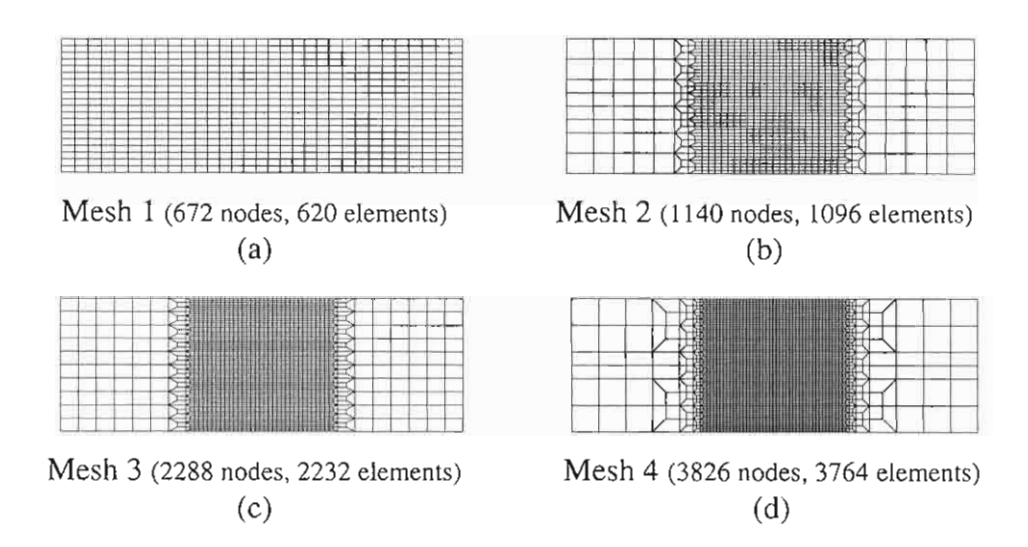


Fig. 26 Example problem 3—configuration

all possible numbering sequences is $45!=1.196x10^{56}$. Fig. 24 also shows the mesh's original numbering sequence and its corresponding stiffness matrix (Collins 1973). The original numbering sequence requires storage of 620 coefficients.

The GA parameters used in this problem are the same as those of the previous problem. Fig. 25 compares the profile of the stiffness matrix obtained by the proposed method with the one obtained by Collins (1973). The profile from the proposed method is shown in the lower triangular part of the matrix while the result from Collins is shown in the upper triangular part. Both methods yield a matrix with storage requirement of 249 coefficients. However, the profiles from both methods are different.

5.2.3 Example problem 3

This example represents finite element meshes shown in Fig. 26. They are meshes prepared for a mesh-convergence test for the analysis of a four-point bending beam. The cracking localization analysis of the four-point bending test will be performed in this study. Here, there are four meshes with 672, 1140, 2288 and 3826 nodes and the numbers of all possible numbering sequences are 9.101x10¹⁶⁰⁹, 5.051x10²⁹⁹¹, 7.054x10⁶⁶⁹⁴ and 1.452x10¹²⁰⁴⁸, respectively. All meshes use only the four-noded quadrilateral elements. It is clear that the difficulty in optimizing the matrix storage requirement is directly proportional to the size of the problem.

Since various sizes of search space are being considered, different GA parameters are used for different meshes as shown in Table 7. These parameters are heuristically set. It is obvious that the problem with the largest search space is the most difficult one (Mesh 4). As a result, for Mesh 4, the population size is set to be larger than the other meshes and higher probability of mutation is also used. This is to allow higher degree of exploration

Table 7 GA parameters for the example problem 3

Item	Value			
	Mesh 1	Mesh 2	Mesh 3	Mesh 4
Maximum number of generations	10,000	10,000	10,000	10,000
Population size	100	100	100	300
Crossover probability	0.85	0.85	0.85	0.85
Mutation probability	0.05	0.05	0.05	0.1

Table 8 Comparison between storage requirements with and without optimization

Mesh	Storag	Reduction (%)	
	Original numbering	Optimized numbering	
1	24,831	14,962	39.7%
2	63,561	47,020	26.0%
3	186,878	144,891	22.5%
4	370,249	309,950	16.3%

into the search space since the search space is very large.

When the four meshes are first created, the numbering sequences obtained during the creation of the meshes are designated as the original numbering sequences and the results of the optimization will be compared with these original numbering sequences. In this problem, the initial population is first created at random. After that, two members in the population are randomly selected and then replaced by the original numbering sequence and the reverse sequence of the original sequence. This additional procedure has to be added because the search space is very large and the randomized initial population may be much worse than the original numbering sequence. Therefore, it is logical to add the original sequence and its reverse sequence to the initial population to possibly improve the quality of the genes in the initial population.

Table 8 shows the storage sizes of the obtained results compared with the storage sizes of the original numbering sequences. It can be seen that the required storage sizes decrease significantly after the optimization especially when the size of the problem is small. For larger problems, the optimization naturally becomes more difficult and less reduction in the storage size is observed.

6. SMEARED CRACK MODELS FOR ANALYSIS OF CRACKING LOCALIZATION

6.1 A Smeared Crack Model with Crack Displacement Degrees of Freedom

In order to discuss the cracking localization, the concept of stability and bifurcation of equilibrium paths explained previously is followed. To begin with, the total potential energy increment for the domain of interest V is considered, i.e., (see more details in Petcherdchoo 1999)

$$\Delta \Pi = \left[\frac{1}{2} \int_{V} \Delta \mathbf{\epsilon}^{\sigma^{T}} \Delta \mathbf{\sigma} dV - \int_{V} \Delta \mathbf{u}^{T} \Delta \mathbf{f} dV - \int_{S} \Delta \mathbf{u}^{T} \Delta \mathbf{t} dS \right] + \left[\frac{1}{2} \int_{V} \Delta \hat{\mathbf{\epsilon}}^{cr^{T}} \Delta \hat{\mathbf{t}}^{cr} dV \right]$$
(40)

where the first and second pairs of the brackets represent the mechanical potential energy increment and the dissipated energy increment, respectively. Here, Δt and Δf denote the surface traction increment vector and the body force increment vector, respectively. In addition, Δu denotes the total displacement increment vector.

The expression of the total potential energy increment in Eq. (40) is actually the same as the conventional expression used for the conventional smeared crack finite element analysis, which is written as

$$\Delta \Pi = \frac{1}{2} \int_{V} \Delta \mathbf{\epsilon}^{T} \overline{\mathbf{D}}^{cr} \Delta \mathbf{\epsilon} dV - \int_{V} \Delta \mathbf{u}^{T} \Delta \mathbf{f} dS - \int_{V} \Delta \mathbf{u}^{T} \Delta \mathbf{t} dV.$$
 (41)

To show that Eqs. (40) and (41) are in fact the same, Eqs. (6) and (9) are substituted into Eq. (40) to obtain

$$\Delta \Pi = \Delta \Pi^{M} + \Delta \Pi^{D}$$

$$= \left[\frac{1}{2} \int_{V} \Delta \boldsymbol{\epsilon}^{\sigma^{T}} \mathbf{D}^{\sigma} \Delta \boldsymbol{\epsilon}^{\sigma} dV - \int_{V} \Delta \mathbf{u}^{T} \Delta \mathbf{f} dV - \int_{S} \Delta \mathbf{u}^{T} \Delta \mathbf{t} dS \right] + \left[\frac{1}{2} \int_{V} \Delta \hat{\boldsymbol{\epsilon}}^{cr^{T}} \hat{\mathbf{D}}^{cr} \Delta \hat{\boldsymbol{\epsilon}}^{cr} dV \right].$$
(42)

By substituting Eq. (1) into Eq. (42), the equation becomes

$$\Delta \Pi = \frac{1}{2} \left[\int_{V} \Delta \mathbf{\epsilon}^{T} \mathbf{D}^{o} \Delta \mathbf{\epsilon} dV - \int_{V} \Delta \mathbf{\epsilon}^{T} \mathbf{D}^{o} \Delta \mathbf{\epsilon}^{cr} dV - \int_{V} \Delta \mathbf{\epsilon}^{cr^{T}} \mathbf{D}^{o} \Delta \mathbf{\epsilon} dV \right]$$

$$+ \int_{V} \Delta \mathbf{\epsilon}^{cr^{T}} \mathbf{D}^{o} \Delta \mathbf{\epsilon}^{cr} dV + \int_{V} \Delta \hat{\mathbf{\epsilon}}^{cr^{T}} \hat{\mathbf{D}}^{cr} \Delta \hat{\mathbf{\epsilon}}^{cr} dV$$

$$- \int_{S} \Delta \mathbf{u}^{T} \Delta \mathbf{f} dS - \int_{V} \Delta \mathbf{u}^{T} \Delta \mathbf{t} dV.$$

$$(43)$$

Transforming the global crack strain increment $\Delta \varepsilon^{cr}$ to the local crack strain increment $\Delta \hat{\varepsilon}^{cr}$ by applying Eq. (3) to Eq. (43), we get

$$\Delta\Pi = \frac{1}{2} \left[\int_{V} \Delta \mathbf{\epsilon}^{T} \mathbf{D}^{o} \Delta \mathbf{\epsilon} dV - \int_{V} \Delta \mathbf{\epsilon}^{T} \mathbf{D}^{o} \mathbf{T} \Delta \hat{\mathbf{\epsilon}}^{cr} dV - \int_{V} \Delta \hat{\mathbf{\epsilon}}^{cr} \mathbf{T}^{T} \mathbf{D}^{o} \Delta \mathbf{\epsilon} dV \right]$$

$$+ \int_{V} \Delta \hat{\mathbf{\epsilon}}^{cr} \left(\hat{\mathbf{D}}^{cr} + \mathbf{T}^{T} \mathbf{D}^{o} \mathbf{T} \right) \Delta \hat{\mathbf{\epsilon}}^{cr} dV$$

$$- \int_{S} \Delta \mathbf{u}^{T} \Delta \mathbf{f} dS - \int_{V} \Delta \mathbf{u}^{T} \Delta \mathbf{f} dV.$$

$$(44)$$

Applying Eq. (13) to Eq. (44) yields

$$\Delta \Pi = \frac{1}{2} \int_{V} \Delta \mathbf{\epsilon}^{T} \left(\mathbf{D}^{o} - \mathbf{D}^{o} \mathbf{T} \left(\hat{\mathbf{D}}^{cr} + \mathbf{T}^{T} \mathbf{D}^{o} \mathbf{T} \right)^{-1} \mathbf{T}^{T} \mathbf{D}^{o} \right) \Delta \mathbf{\epsilon} dV - \int_{S} \Delta \mathbf{u}^{T} \Delta \mathbf{f} dS - \int_{V} \Delta \mathbf{u}^{T} \Delta \mathbf{t} dV.$$
 (45)

From Eq. (14), the total potential energy increment expressed above becomes

$$\Delta \Pi = \frac{1}{2} \int_{V} \Delta \mathbf{\epsilon}^{T} \overline{\mathbf{D}}^{cr} \Delta \mathbf{\epsilon} dV - \int_{V} \Delta \mathbf{u}^{T} \Delta \mathbf{f} dS - \int_{V} \Delta \mathbf{u}^{T} \Delta \mathbf{t} dV$$

$$= \frac{1}{2} \int_{V} \Delta \mathbf{\epsilon}^{T} \Delta \mathbf{\sigma} dV - \int_{V} \Delta \mathbf{u}^{T} \Delta \mathbf{f} dS - \int_{V} \Delta \mathbf{u}^{T} \Delta \mathbf{t} dV$$

$$(46)$$

which is the same equation as Eq. (41). Therefore, Eq. (40) is the same as Eq. (41). From Eqs. (1), (6), (9) and (40) and the inverse relationship of Eq. (3), i.e.,

$$\Delta \hat{\mathbf{\epsilon}}^{cr} = \hat{\mathbf{T}} \Delta \mathbf{\epsilon}^{cr} \tag{47}$$

where

$$\hat{\mathbf{T}} = \begin{bmatrix} \cos^2 \theta & -2\sin\theta\cos\theta \\ \sin^2 \theta & 2\sin\theta\cos\theta \\ \sin\theta\cos\theta & \cos^2 \theta - \sin^2 \theta \end{bmatrix}^T, \tag{48}$$

we obtain

$$\Delta\Pi = \left[\frac{1}{2} \int_{V} (\Delta \mathbf{\epsilon} - \Delta \mathbf{\epsilon}^{cr})^{T} \mathbf{D}^{o} (\Delta \mathbf{\epsilon} - \Delta \mathbf{\epsilon}^{cr})^{T} dV - \int_{V} \Delta \mathbf{u}^{T} \Delta \mathbf{f} dV - \int_{S} \Delta \mathbf{u}^{T} \Delta \mathbf{t} dS \right] + \left[\frac{1}{2} \int_{V} \Delta \mathbf{\epsilon}^{cr} \mathbf{D}^{cr} \Delta \mathbf{\epsilon}^{cr} dV \right]$$
(49)

where

$$\mathbf{D}^{cr} = \hat{\mathbf{T}}^T \hat{\mathbf{D}}^{cr} \hat{\mathbf{T}} . \tag{50}$$

At this point, we introduce an intact-solid displacement increment vector $\Delta \mathbf{u}^o$ and a crack displacement increment vector $\Delta \mathbf{u}^{cr}$ defined as

$$\Delta \mathbf{u} = \Delta \mathbf{u}^o + \Delta \mathbf{u}^{cr} \tag{51}$$

where the strain increments computed from Δu , Δu^{σ} and Δu^{cr} are $\Delta \epsilon$, $\Delta \epsilon^{\sigma}$ and $\Delta \epsilon^{cr}$, respectively.

Consider the i^{th} element in the finite element analysis. The element is assumed to be a cracked element. The three displacement increments above can be interpolated from nodal quantities, i.e.,

$$\Delta^{i}\mathbf{u} = \mathbf{N}\Delta^{i}\mathbf{U},$$

$$\Delta^{i}\mathbf{u}^{o} = \mathbf{N}\Delta^{i}\mathbf{U}^{o},$$

$$\Delta^{i}\mathbf{u}^{cr} = \mathbf{N}\Delta^{i}\mathbf{U}^{cr}$$
(52)

in which $\Delta^i \mathbf{U}$, $\Delta^i \mathbf{U}^o$ and $\Delta^i \mathbf{U}^{cr}$ are the nodal quantities of $\Delta \mathbf{u}$, $\Delta \mathbf{u}^o$ and $\Delta \mathbf{u}^{cr}$, respectively and $\Delta^i \mathbf{U} = \Delta^i \mathbf{U}^o + \Delta^i \mathbf{U}^{cr}$. Here, \mathbf{N} is the shape function matrix. Note that the superscript i for the i^{th} element is used in the equations because the nodal crack displacement increments of the same node for different elements can be different. This is natural because, in the smeared crack approach, cracking in each element is completely independent of each other. Therefore, the continuity of the crack displacement increment between elements is not required and must not be enforced. On the contrary, the total displacement increment $\Delta \mathbf{u}$ must be continuous across elements. Therefore, the superscript i representing the element number is not actually necessary for the nodal values of the total displacement increment. Similar to the crack displacement increment, the displacement increment related to the strain increment of the uncracked solid $\Delta^i \mathbf{u}^o$ is not continuous across elements' boundaries; therefore, the superscript i is required.

Computing strains from Eq. (52), we obtain Eq. (1), i.e.,

$$\Delta^{i} \mathbf{\varepsilon} = \Delta^{i} \mathbf{\varepsilon}^{o} + \Delta^{i} \mathbf{\varepsilon}^{cr} \tag{53}$$

where

$$\Delta^{i} \mathbf{\varepsilon} = \mathbf{B} \Delta^{i} \mathbf{U},$$

$$\Delta^{i} \mathbf{\varepsilon}^{o} = \mathbf{B} \Delta^{i} \mathbf{U}^{o},$$

$$\Delta^{i} \mathbf{\varepsilon}^{cr} = \mathbf{B} \Delta^{i} \mathbf{U}^{cr}.$$
(54)

Substituting Eq. (54) into Eq. (49) for the i^{th} element gives

$$\Delta\Pi = \frac{1}{2}\Delta^{i}\mathbf{U}^{T}\int_{V}\mathbf{B}^{T}\mathbf{D}^{o}\mathbf{B}dV\Delta^{i}\mathbf{U} - \frac{1}{2}\Delta^{i}\mathbf{U}^{T}\int_{V}\mathbf{B}^{T}\mathbf{D}^{o}\mathbf{B}dV\Delta^{i}\mathbf{U}^{cr}$$

$$-\frac{1}{2}\Delta^{i}\mathbf{U}^{cr}\int_{V}\mathbf{B}^{T}\mathbf{D}^{o}\mathbf{B}dV\Delta^{i}\mathbf{U} + \frac{1}{2}\Delta^{i}\mathbf{U}^{cr}\int_{V}\mathbf{B}^{T}\mathbf{D}^{o}\mathbf{B}dV\Delta^{i}\mathbf{U}^{cr}$$

$$+\frac{1}{2}\Delta^{i}\mathbf{U}^{cr}\int_{V}\mathbf{B}^{T}\mathbf{D}^{cr}\mathbf{B}dV\Delta^{i}\mathbf{U}^{cr} - \Delta^{i}\mathbf{U}^{T}\int_{V}\mathbf{N}^{T}\Delta\mathbf{f}dV - \Delta^{i}\mathbf{U}^{T}\int_{S}\mathbf{N}^{T}\Delta\mathbf{t}dS.$$
(55)

Next, we apply the stationary condition $\delta(\Delta\Pi) = 0$, and assume that both \mathbf{D}^o and \mathbf{D}^{cr} are symmetric. Since $\delta(\Delta\mathbf{U}^T)$ and $\delta(\Delta^i\mathbf{U}^{cr^T})$ are arbitrary, the element stiffness equation for the i^{th} element is obtained as

$$\begin{bmatrix} \int_{V} \mathbf{B}^{T} \mathbf{D}^{o} \mathbf{B} dV & -\int_{V} \mathbf{B}^{T} \mathbf{D}^{o} \mathbf{B} dV \\ -\int_{V} \mathbf{B}^{T} \mathbf{D}^{o} \mathbf{B} dV & \int_{V} \mathbf{B}^{T} \mathbf{D}^{o} \mathbf{B} dV + \int_{V} \mathbf{B}^{T} \mathbf{D}^{c'} \mathbf{B} dV \end{bmatrix} \begin{bmatrix} \Delta^{i} \mathbf{U} \\ \Delta^{i} \mathbf{U}^{cr} \end{bmatrix} = \begin{bmatrix} \int_{V} \mathbf{N}^{T} \Delta \mathbf{f} dV + \int_{S} \mathbf{N}^{T} \Delta \mathbf{f} dS \\ \mathbf{0} \end{bmatrix} .$$
(56)

After assembling all elements and applying prescribed displacements and forces, the system stiffness equation is obtained as

$$\begin{bmatrix} \mathbf{K}_{11} & \mathbf{K}_{12} \\ \mathbf{K}_{21} & \mathbf{K}_{22} \end{bmatrix} \begin{bmatrix} \Delta \mathbf{U} \\ \Delta \mathbf{U}^{cr} \end{bmatrix} = \begin{bmatrix} \Delta \mathbf{R}_{1} \\ \Delta \mathbf{R}_{2} \end{bmatrix}. \tag{57}$$

The static condensation is then used to remove the nodal total displacement increment from the obtained system matrix equation. Consequently, the equation can be written in the following form, i.e.,

$$\mathbf{K}^{cr} \Delta \mathbf{U}^{cr} = \Delta \mathbf{R}^{cr} \tag{58}$$

where \mathbf{K}^{cr} and $\Delta \mathbf{R}^{cr}$ are defined as

$$\mathbf{K}^{cr} = \mathbf{K}_{22} - \mathbf{K}_{21} \mathbf{K}_{11}^{-1} \mathbf{K}_{12},$$

$$\Delta \mathbf{R}^{cr} = \Delta \mathbf{R}_2 - \mathbf{K}_{21} \mathbf{K}_{11}^{-1} \Delta \mathbf{R}_1.$$
(59)

In consideration of the stability of equilibrium paths, the eigenvalue analysis of \mathbf{K}^{cr} can be performed. However, it must be noted that Eq. (58) is a singular equation because $\Delta \mathbf{U}^{cr}$ contains rigid-body crack displacement increments. For example, for two-dimensional cases, they are two rigid translations and one rigid rotation. These rigid-body crack displacement increments will result in zero eigenvalues of the stiffness \mathbf{K}^{cr} . When the numerical eigenvalue analysis is performed on the stiffness matrix, we may not obtain zero eigenvalues for these rigid-body crack displacements but very small numbers, instead. Therefore, the results will be indistinguishable from those modes with real small non-zero eigenvalues. To avoid this confusion, constraints to remove these rigid-body modes from all elements must be applied to the equation. In this study, the following constraints are employed for two-dimensional problems at the center of each element without loss of generality, i.e.,

$$\Delta u^{cr}(\xi = 0, \eta = 0) = 0$$

$$\Delta v^{cr}(\xi = 0, \eta = 0) = 0$$

$$\frac{\partial v^{cr}(\xi = 0, \eta = 0)}{\partial x} = 0$$
(60)

where the global x-y and natural $\xi-\eta$ coordinate systems are used in the equation. Here, Δu^{cr} and Δv^{cr} are the incremental crack displacements in x- and y-directions, respectively.

Constraining the rigid-body crack displacement increments can be done in this fashion because the magnitudes of the crack displacement increments are not important. The important things are the crack strain increments. As long as the values of the crack strain increments are not constrained, the generality is not lost.

Eq. (58), after applying the constraints, can be expressed as

$$\tilde{\mathbf{K}}^{cr} \Delta \tilde{\mathbf{U}}^{cr} = \Delta \tilde{\mathbf{R}}^{cr}. \tag{61}$$

The stability condition is obtained by checking the eigenvalues of $\tilde{\mathbf{K}}^{cr}$. If all the eigenvalues are positive, the equilibrium path is stable with respect to the current crack pattern and there is no bifurcation. On the contrary, if some of the eigenvalues are negative, the equilibrium path is not stable with respect to the current crack pattern. This means that bifurcation has occurred and the actual equilibrium path must be found. Note that this proposed scheme is only used for stability analysis of crack patterns, not for obtaining the displacement solution. The displacement solution will be obtained from the original smeared crack model where the basic unknowns are the nodal displacement increments.

6.2 A Smeared Crack Model with A Mixed Formulation

The technique of introducing the new crack displacement increment variable into the smeared crack finite element analysis shown in the previous section provides a way to obtain the Hessian matrix of the total potential energy increment in Eq. (49) with respect to the irreversible parameter. Nevertheless, the procedure still leaves some room for further development. For example, the crack displacement increment used does not have a very clear physical meaning. Moreover, constraints have to be introduced to prevent the rigid-body crack displacements in all crack elements. The implementation of these constraints can be troublesome in some cases.

Introduction of discrete irreversible parameters into the smeared crack model can be done in another different way by using a mixed finite element formulation that discretizes not only the displacement field but also the crack strain field (see more details in Soparat 2000 and Thitawat 2001). To begin with, consider the i^{th} element in the finite element analysis. The displacement increment $\Delta \mathbf{u}$ and the local crack strain increment $\Delta \hat{\mathbf{e}}^{cr}$ are discretized as

$$\Delta \mathbf{u} = \mathbf{N} \Delta^i \mathbf{U}, \tag{62}$$

$$\Delta \hat{\mathbf{\varepsilon}}^{cr} = \mathbf{N}^{cr} \Delta^i \hat{\mathbf{E}}^{cr} \tag{63}$$

where N and N^{cr} represent the shape function matrices for the displacement increment and the local crack strain increment, respectively. In addition, $\Delta^i \mathbf{U}$ and $\Delta^i \hat{\mathbf{E}}^{cr}$ represent the nodal displacement increment and the nodal local crack strain increment, respectively. Note that the local crack strain increments are not continuous across elements and the nodal local crack strain increments of the same node for different elements can be different. One example is a problem with one cracked element surrounded by uncracked elements (see Fig. 27). In the cracked element including its boundary, non-zero crack strain increments can be expected. However, in the surrounding uncracked elements, the crack

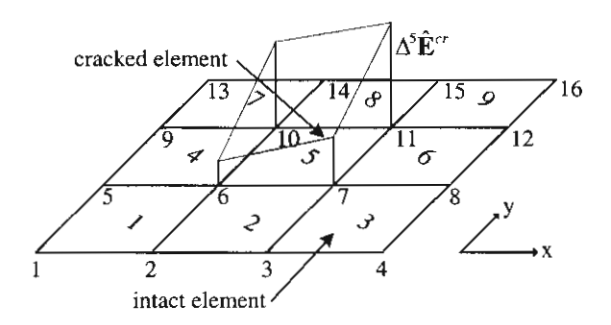


Fig. 27 A problem with one cracked element surrounded by intact elastic elements

strain increments are expected to be zero because there is no crack in those elements. On the contrary, the total displacement increments must be continuous across all the elements.

From Eqs. (3), (62) and (63), the total strain increment and the global crack strain increment are expressed as

$$\Delta \mathbf{\varepsilon} = \mathbf{B} \Delta^i \mathbf{U} \,, \tag{64}$$

$$\Delta \mathbf{\varepsilon}^{cr} = \mathbf{T} \mathbf{N}^{cr} \Delta^{i} \hat{\mathbf{E}}^{cr}. \tag{65}$$

From Eqs. (43), (62), (63), (64) and (65), the total potential energy increment can be expressed as

$$\Delta\Pi = \frac{1}{2} \int_{V} \Delta^{i} \mathbf{U}^{T} \mathbf{B}^{T} \mathbf{D}^{o} \mathbf{B} \Delta^{i} \mathbf{U} dV - \frac{1}{2} \int_{V} \Delta^{i} \mathbf{U}^{T} \mathbf{B}^{T} \mathbf{D}^{o} \mathbf{T} \mathbf{N}^{cr} \Delta^{i} \hat{\mathbf{E}}^{cr} dV$$

$$- \frac{1}{2} \int_{V} \Delta^{i} \hat{\mathbf{E}}^{cr} \mathbf{N}^{cr} \mathbf{T}^{T} \mathbf{D}^{o} \mathbf{B} \Delta^{i} \mathbf{U} dV + \frac{1}{2} \int_{V} \Delta^{i} \hat{\mathbf{E}}^{cr} \mathbf{N}^{cr} \mathbf{T}^{T} \mathbf{D}^{o} \mathbf{T} \mathbf{N}^{cr} \Delta^{i} \hat{\mathbf{E}}^{cr} dV$$

$$+ \frac{1}{2} \int_{V} \Delta^{i} \hat{\mathbf{E}}^{cr} \mathbf{N}^{cr} \hat{\mathbf{D}}^{cr} \mathbf{N}^{cr} \Delta^{i} \hat{\mathbf{E}}^{cr} dV - \int_{V} \Delta^{i} \mathbf{U}^{T} \mathbf{N}^{T} \Delta \mathbf{f} dV - \int_{S} \Delta^{i} \mathbf{U}^{T} \mathbf{N}^{T} \Delta \mathbf{t} dS.$$

$$(66)$$

Applying the stationary condition $\delta(\Delta\Pi)=0$, the element stiffness equation for the i^{th} element is obtained as

$$\begin{bmatrix} \mathbf{k}_{11} & \mathbf{k}_{12} \\ \mathbf{k}_{21} & \mathbf{k}_{22} \end{bmatrix} \begin{bmatrix} \mathbf{\Delta}^{i} \mathbf{U} \\ \mathbf{\Delta}^{i} \hat{\mathbf{E}}^{cr} \end{bmatrix} = \begin{bmatrix} \Delta \mathbf{r} \\ 0 \end{bmatrix}$$
 (67)

where

$$\mathbf{k}_{11} = \int_{V} \mathbf{B}^{T} \mathbf{D}^{o} \mathbf{B} dV,$$

$$\mathbf{k}_{12} = -\int_{V} \mathbf{B}^{T} \mathbf{D}^{o} \mathbf{T} \mathbf{N}^{cr} dV,$$

$$\mathbf{k}_{21} = -\int_{V} \mathbf{N}^{cr} \mathbf{T}^{T} \mathbf{D}^{o} \mathbf{B} dV,$$

$$\mathbf{k}_{22} = \int_{V} \mathbf{N}^{cr} \left(\hat{\mathbf{D}}^{cr} + \mathbf{T}^{T} \mathbf{D}^{o} \mathbf{T} \right) \mathbf{N}^{cr} dV,$$

$$\Delta \mathbf{r} = \int_{V} \mathbf{N}^{T} \Delta \mathbf{f} dV + \int_{S} \mathbf{N}^{T} \Delta \mathbf{f} dS.$$

After assembling all element stiffness equations and applying prescribed displacements and forces, the system stiffness equation is arranged as

$$\begin{bmatrix} \mathbf{K}_{11} & \mathbf{K}_{12} \\ \mathbf{K}_{21} & \mathbf{K}_{22} \end{bmatrix} \begin{bmatrix} \Delta \mathbf{U} \\ \Delta \hat{\mathbf{E}}^{cr} \end{bmatrix} = \begin{bmatrix} \Delta \mathbf{R}_1 \\ \Delta \mathbf{R}_2 \end{bmatrix}$$
(68)

where ΔU and $\Delta \hat{E}^{cr}$ are the nodal displacement increment and the nodal local crack strain increment of the system, respectively.

The static condensation is then used to remove the nodal displacement increment from the obtained system matrix equation. Consequently, the equation can be written in the following form, i.e.,

$$\mathbf{K}^{cr}\Delta\hat{\mathbf{E}}^{cr} = \Delta\mathbf{R}^{cr} \tag{69}$$

where \mathbf{K}^{cr} and $\Delta \mathbf{R}^{cr}$ are defined as

$$\mathbf{K}^{cr} = \mathbf{K}_{22} - \mathbf{K}_{21} \mathbf{K}_{11}^{-1} \mathbf{K}_{12}, \tag{70}$$

$$\Delta \mathbf{R}^{cr} = \Delta \mathbf{R}_2 - \mathbf{K}_{21} \mathbf{K}_{11}^{-1} \Delta \mathbf{R}_1. \tag{71}$$

In the consideration of stability of crack patterns, the eigenvalue analysis of \mathbf{K}^{cr} is performed. If all the eigenvalues are positive, then it means that the stationary solution in Eq. (69) is stable with respect to the current crack pattern. Otherwise, the stationary solution is unstable and bifurcation occurs. Similar to the case of the previous scheme, this proposed scheme is only used for stability analysis of crack patterns, not for obtaining the displacement solution. The displacement solution will be obtained from the original smeared crack model where the basic unknowns are the nodal displacement increments.

7. THE EQUILIBRIUM PATH WITH THE MINIMUM TOTAL POTENTIAL ENERGY

When the equilibrium path reaches a bifurcation point, a fan of many possible equilibrium paths emanates from the bifurcation point. In fact, if instability occurs in the real system, the actual equilibrium path is the path that contains the minimum total potential energy (Bazant and Cedolin 1991) or the minimum elastic strain energy (Nemat-Nasser 1979). These two conditions are actually the same (Nemat-Nasser 1979), given that one defines the total potential energy in the usual way. In this study, the minimum total potential energy criterion is employed. However, since the analysis is performed incrementally, and the total potential energy is written in the incremental form [see Eq. (40)], the stable path with the minimum total potential energy increment is the desired solution path.

In order to obtain the solution path with the minimum total potential energy increment, energy increments of all possible equilibrium paths, which depend on their crack patterns, can be compared. This approach of comparing all possible solutions is essentially an exhaustive search. The algorithm for this search approach is simple and straightforward. Nevertheless, it is obvious that the technique is expensive and suitable only for small problems where the complete search is still possible. In the case of larger problems where many cracks occur in the domain and, as a result, many crack patterns are possible, the exhaustive search may not be practical and it is advisable to employ an appropriate optimization technique to find the minimum energy path. In this study, the GA (Goldberg 1989) is used for this purpose because this optimization technique is suitable for problems with discrete variables. Variables in the minimization problem of the total potential energy increment are discrete statuses of cracks that can be either opening or unloading. Since GAs do not require the evaluation of the gradient of the function being minimized or maximized, the evaluation of the total potential energy increment is enough for the minimization process.

7.1 Minimization of The Total Potential Energy Increment

The analysis of cracking localization in this study is in the form of piecewise-linear incremental steps. Each step is ended when a new cracked element is initiated by the stress criterion or when the incremental crack constitutive law of one of the existing cracked elements needs to be updated. The incremental constitutive law of a crack needs to be updated when the slope of its tension-softening curve changes or when the crack switches from loading to unloading or vice versa. During each incremental step, the behavior of the system is actually linear. As an example, Fig. 28 schematically illustrates a four-point bending test and its load-deformation curve. At the end of the first incremental step (point a), cracks are initiated. Because of the initiated cracks, the stiffness of the beam is changed (path ab). If the equilibrium path ab is stable, the analysis is continued with the second incremental step along the path ab. As mentioned earlier, the path ab ends at point b either because, at the point b, a new cracked element is initiated or the incremental crack constitutive law of one of the existing cracks needs to be updated. Assume that the analysis is continued until point c where the current crack pattern yields an unstable equilibrium path (path cd' in Fig. 28). This means that the point c is a bifurcation point and the actual equilibrium must be found. For better understanding, it is further assumed that there are five possible equilibrium paths at the bifurcation point c (see Fig. 28). The total potential energy increments of all possible paths are then compared in order to obtain the path with the minimum total potential energy increment, which is the actual equilibrium path. In order to compare the energy of the paths, all paths must be executed under the same controlled parameter. For this problem, the controlled displacement increment $\Delta \overline{u}$ can be used as the controlled parameter. For small problems, the exhaustive search algorithm can

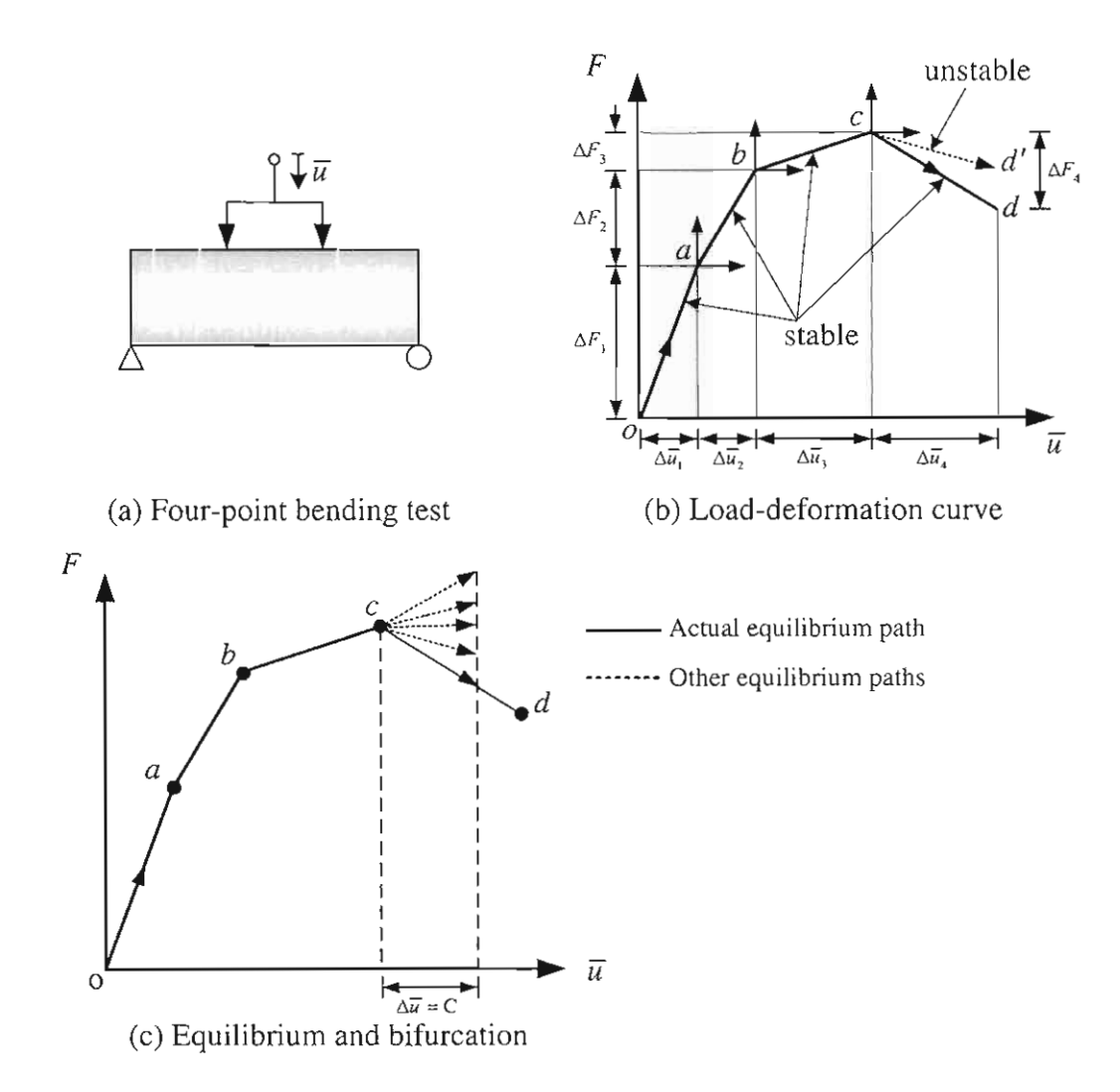


Fig. 28 Four-point bending test and its load-deformation curve

be used but, for larger problems, the GA will be more suitable. Since the optimization problem being solved in this study is the minimization of the total potential energy increment, the objective function $f(\mathbf{x})$ for the GA is the total potential energy increment itself, i.e.,

$$f(\mathbf{x}) = \Delta \Pi(\mathbf{x}) \tag{72}$$

where x is the variable representing crack patterns.

7.2 Coding and Fitness

In general, GAs do not directly work with the parameters themselves. The algorithms start with coding of the parameter set. For coding, binary strings are most popular and convenient. Each point in search space, often called "individual" in the GA terminology, is represented by a single string of number 0's and 1's. The optimization problem of this study is to minimize the total potential energy increment. The total potential energy increment to be minimized is a function of crack patterns. Therefore, each crack pattern will be coded as a binary string. The idea of the coding is to have each bit in a binary string represent the status of one particular crack. If the value of the bit is one (1), it indicates that its corresponding crack is opening. If the value of the bit is zero (0), the corresponding

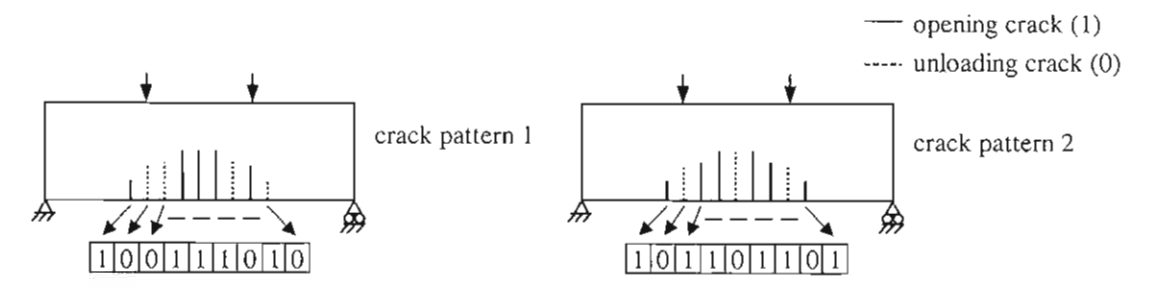


Fig. 29 Examples of coding of crack patterns

crack is unloading. Fig. 29 shows examples of the coding of two different crack patterns. The number of bits used in the string is equal to the number of the existing crack paths.

In GAs, the reproduction operator defines a process in which individuals are selected for mating based on their fitness values relative to that of the population. Fitness is defined as a figure of merit. Individuals with higher fitness values have higher probabilities of being selected for mating and subsequent genetic actions. Consequently, highly fit individuals live and reproduce, and less fit individuals die. In this study, a crack pattern that results in a smaller total potential energy increment will be given a higher fitness value. To this end, the following equation for the fitness $F(\mathbf{x})$ is employed, i.e.,

$$F(\mathbf{x}) = \frac{1}{1 + k\Delta\Pi(\mathbf{x})} \tag{73}$$

where k is a user-defined constant. In this study, k equal to $\frac{1}{100}$ is used in all problems.

7.3 GA Operators

In this study, the simple GA is employed. As mentioned earlier, the algorithm is composed of three different operators, i.e., reproduction, crossover and mutation operators. In the first operator in GAs, the reproduction operator, a mating pool is created by letting individuals with higher fitness values have higher chance to be selected into the mating pool. In this study, the proportional selection algorithm [see Eq. (23)] is employed. In the crossover operator, new strings are created by exchanging information among strings. Many

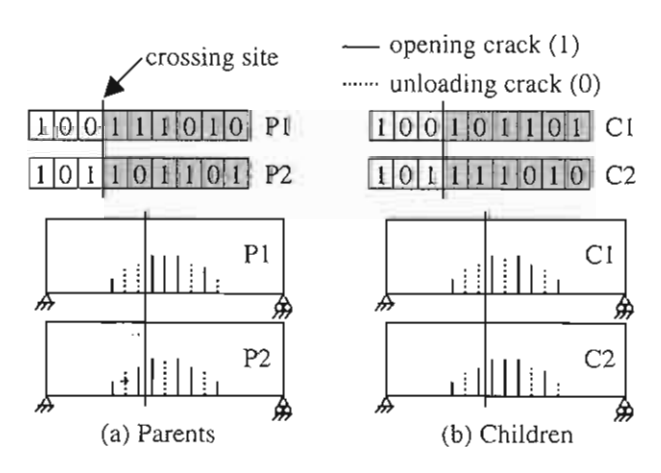


Fig. 30 One-point crossover

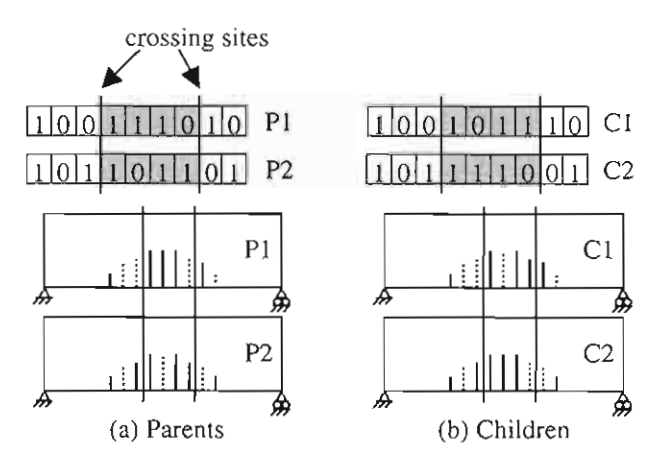


Fig. 31 Two-point crossover

crossover operators exist in the literature (Goldberg 1989). Generally, two strings are selected at random as a crossover pair and some portions of the two strings are exchanged. The two strings participating in the crossover are known as parent strings and the resulting strings are known as children strings. In this study, three types of crossover operator are employed, i.e., one-point, two-point and uniform crossover operators.

Fig. 30 shows an example of the one-point crossover. In this study, the one-point crossover is performed by randomly selecting a crossing site along the parent strings and by exchanging all bits on the right side of the selected crossing site. In the case of the two-point crossover, two crossing sites are randomly selected and all the bits between the two crossing sites of the two parent strings are exchanged as shown in Fig. 31. For the uniform crossover, the number of bits to be crossed over and their positions are randomly determined. Fig. 32 shows an example of this type of crossover in this study. It is clear that the crossover operator may yield better or worse children strings. To be able to adjust the degree of the uncertainty of the crossover phase, it is not necessary to use all individuals in the mating pool in the operator. This is done by adjusting the probability that a crossover is performed (crossover probability).

The last genetic algorithm operator is the mutation operator. Fig. 33 shows an example of the mutation operator employed in this study. The mutation operator changes 1 to 0 and vice versa at a randomly chosen bit. The operator is used sparingly with a small

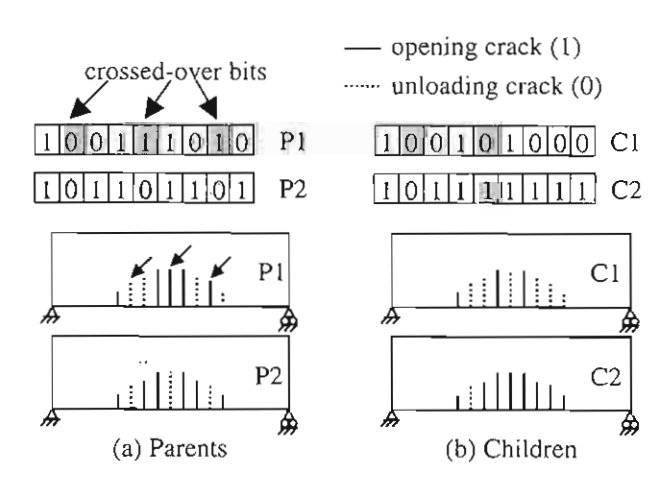


Fig. 32 Uniform crossover

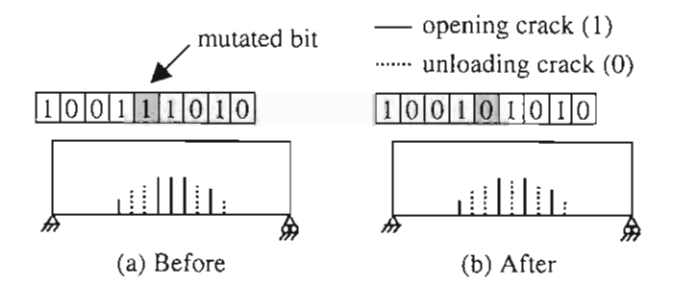


Fig. 33 Mutation

probability (mutation probability).

8. RESULTS

In the analysis procedure proposed in this study, the specimen under consideration is analyzed by using the conventional smeared crack model. A crack is initiated when the maximum principal tensile stress reaches the tensile strength of the material. The orientation of the initiated crack is specified by the direction of the maximum principal tensile stress. Thereafter the crack follows the tension-softening curve, which is treated as one of the material properties. The tension-softening curve is the relationship between the tensile stress transferred across the crack surfaces and the crack opening displacement. Note that, in this study, shear retention of cracks is assumed negligible. As mentioned earlier, the analysis is done incrementally. In each step, the stability of the obtained crack pattern will be investigated by performing eigenvalue analysis of the matrix $\tilde{\mathbf{K}}^{cr}$ or \mathbf{K}^{cr} obtained from one of the proposed smeared crack finite element formulations. If the crack pattern is found to be stable, the analysis is continued to the next step. However, if the crack pattern is unstable, the search for the crack pattern with the minimum total potential energy increment must be performed. Here, if the number of possible crack patterns is not very large, the exhaustive search can be employed; otherwise, the GA may be used, instead. It must be noted that, if the GA or another optimization technique is used, the obtained crack pattern may have a near-minimum total potential energy increment, not the true minimum one for the finite element discretization currently being used. In order to compare total potential energy increments of different crack patterns, the energy for cases with different crack patterns must be evaluated under the same controlled parameter. In all examples in this study, the controlled displacement is used. After the crack pattern with the minimum or near-minimum total potential energy increment is obtained, the analysis is carried on to the next step. The same process is then repeated and the actual equilibrium path can be traced.

Here, three problems will be solved. The proposed smeared crack model with crack displacement degrees of freedom will be used in the first example problem only while the smeared crack model with a mixed finite element formulation will be used in all example problems. This is because the second proposed model is actually more efficient than the first proposed model. More example problems can be found in Petcherdchoo (1999), Soparat (2000) and Thitawat (2001).

8.1 Uniaxial Bar Problem: Stability and Bifurcation Analysis

In order to illustrate the advantage of the proposed smeared crack finite element models in the analysis of cracking localization, a simple one-dimensional uniaxial problem shown in Fig. 34 is considered. As shown in Fig. 34, the bar has one fixed support at one end. At the other end, the controlled displacement \bar{u} is applied. The length of the bar is 2L and the area is A. The material is assumed elastic with Young's modulus equal to E. The bar is discretized into two elements, each of which has the length of L. Each element can accommodate one crack. The characteristic length or crack-band width of each crack, in this case, is equal to the length of the element. The conventional linear shape function is used for the displacement interpolation. Note that, in this example, only stability and bifurcation analysis will be performed.

It is assumed that there is no crack at the beginning. The controlled displacement is then increased until the stress of the bar reaches the tensile strength f_t . By the strength criterion, both elements are cracked. The cracks follow the constitutive law for cracks. For opening cracks, a linear relationship between the transmitted tensile stress and the crack opening displacement (COD) with the slope $\frac{\Delta \sigma}{\Delta \text{COD}}$ equal to H is assumed. For unloading

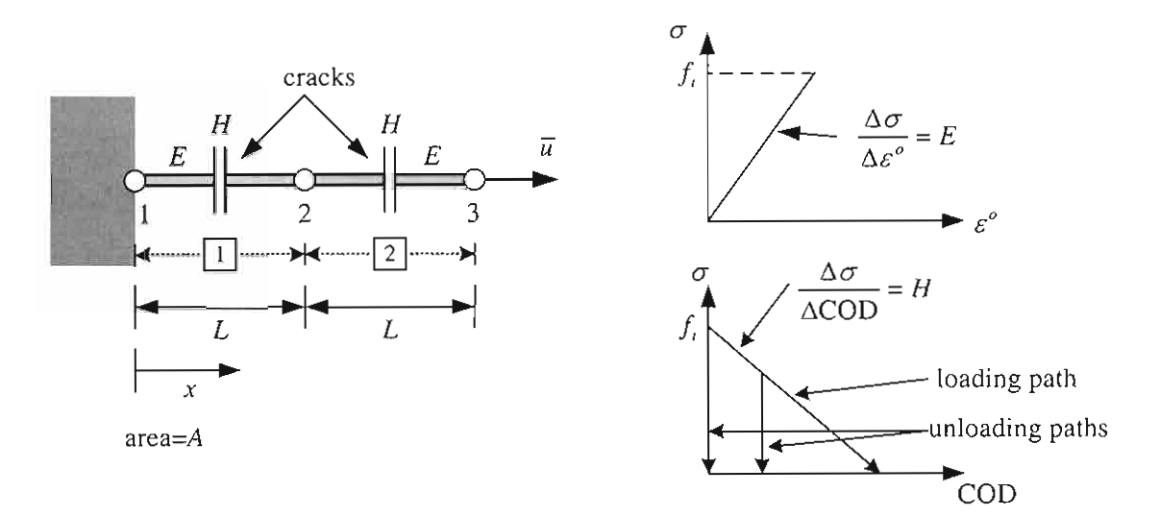


Fig. 34 Uniaxial problem using two 1-D bar elements

cracks, a vertical unloading path with a constant COD equal to the existing COD is applied (see Fig. 34).

The proposed smeared crack model with crack displacement degrees of freedom is employed first. Consider an incremental step after the initiation of the cracks. Assembling all element stiffness equations given by Eq. (56), we can write the system stiffness equation. After applying the prescribed boundary conditions, we obtain

$$\frac{A}{L} \begin{bmatrix}
2E & E & -E & -E & E \\
E & E + \tilde{H} & -(E + \tilde{H}) & 0 & 0 \\
-E & -(E + \tilde{H}) & E + \tilde{H} & 0 & 0 \\
-E & 0 & 0 & E + \tilde{H} & -(E + \tilde{H}) \\
E & 0 & 0 & -(E + \tilde{H}) & E + \tilde{H}
\end{bmatrix} \begin{bmatrix}
\Delta U_2 \\
\Delta^l U_1^{cr} \\
\Delta^l U_2^{cr} \\
\Delta^l U_2^{cr} \\
\Delta^l U_2^{cr} \\
\Delta^l U_2^{cr} \\
\Delta^l U_3^{cr}
\end{bmatrix} = \frac{A}{L} \begin{bmatrix}
E \Delta \bar{u} \\
0 \\
0 \\
-E \Delta \bar{u} \\
E \Delta \bar{u}
\end{bmatrix} \tag{74}$$

where $\tilde{H} = \frac{\Delta \sigma}{\Delta \varepsilon^{cr}} = HL^* = HL$. Here, L^* represents the characteristic length of the crack and is equal to L. In addition, ΔU_i represents the nodal displacement increment of the node i. Moreover, $\Delta^i U_j^{cr}$ represents the nodal crack displacement increment of the node j and, at the same time, of the element i.

Using the static condensation to remove ΔU_2 yields.

$$\frac{A}{L} \begin{bmatrix}
\frac{E+2\widetilde{H}}{2} & -\frac{E+2\widetilde{H}}{2} & \frac{E}{2} & -\frac{E}{2} \\
-\frac{E+2\widetilde{H}}{2} & \frac{E+2\widetilde{H}}{2} & -\frac{E}{2} & \frac{E}{2} \\
\frac{E}{2} & -\frac{E}{2} & \frac{E+2\widetilde{H}}{2} & -\frac{E+2\widetilde{H}}{2} \\
-\frac{E}{2} & \frac{E}{2} & -\frac{E+2\widetilde{H}}{2} & \frac{E+2\widetilde{H}}{2}
\end{bmatrix} \begin{bmatrix}
\Delta^{1}U_{1}^{cr} \\
\Delta^{1}U_{2}^{cr} \\
\Delta^{2}U_{2}^{cr} \\
\Delta^{2}U_{3}^{cr}
\end{bmatrix} = \frac{A}{L} \begin{bmatrix}
-\frac{E\Delta\overline{u}}{2} \\
\frac{E\Delta\overline{u}}{2} \\
-\frac{E\Delta\overline{u}}{2} \\
\frac{E\Delta\overline{u}}{2}
\end{bmatrix}. (75)$$

The above equation is singular due to the rigid-body crack displacement increments in the two elements. For one-dimensional problems, the crack displacement increment at the center of each element is set to zero, i.e.,

$$\Delta^{l} u^{cr}(\xi = 0) = \frac{1}{2} (\Delta^{l} U_{1}^{cr} + \Delta^{l} U_{2}^{cr}) = 0,
\Delta^{2} u^{cr}(\xi = 0) = \frac{1}{2} (\Delta^{2} U_{2}^{cr} + \Delta^{2} U_{3}^{cr}) = 0,$$
(76)

which leads to

$$\frac{A}{L} \begin{bmatrix} 2(E+2\tilde{H}) & 2E \\ 2E & 2(E+2\tilde{H}) \end{bmatrix} \begin{bmatrix} \Delta^{1}U_{1}^{cr} \\ \Delta^{2}U_{1}^{cr} \end{bmatrix} = \frac{A}{L} \begin{bmatrix} -E\Delta\overline{u} \\ -E\Delta\overline{u} \end{bmatrix}.$$
 (77)

Note that, in applying the constraints to Eq. (75), not only the row but also the column operations must be performed to the stiffness matrix so as to obtain the symmetric matrix in Eq. (77). Actually, the constraints may be directly applied to each element before assembling the element stiffness equations.

The eigenvalues of the obtained stiffness matrix are $\frac{4A\widetilde{H}}{L}$ and $\frac{4A(E+\widetilde{H})}{L}$. Both eigenvalues are positive only when $\widetilde{H}>0$. This means that the crack pattern having two cracks opening at the same time is unstable unless hardening behavior occurs at the cracks. In reality, cracks will exhibit softening behavior. As a result, the two cracks cannot continue to open at the same time.

If we assume that the crack in the element 2 undergoes the elastic unloading, this crack will follow the vertical unloading path shown in Fig. 34. Note from the figure that the unloading path for the crack in the element 2 has the COD equal to zero. This is because, at the current state, the cracks in both elements are just initiated and the CODs are still exactly equal to zero. Note also that an incremental step after the initiation of the cracks is being considered. With the crack in the element 2 unloading, the system stiffness equation will contain only one cracked element. Employing the same process of applying the prescribed boundary conditions and using the static condensation for this case, we obtain

$$\frac{A}{L} \left[2(E + 2\widetilde{H}) \right] \left\{ \Delta^{1} U_{1}^{cr} \right\} = \frac{A}{L} \left\{ -E \Delta \overline{u} \right\}$$
 (78)

The eigenvalue of the stiffness matrix is $\frac{2A(E+2\tilde{H})}{L}$ which is positive when $\tilde{H} > -\frac{E}{2}$.

Assuming that the crack in the element 1 undergoes the elastic unloading will yield the same conclusion.

In summary, immediately after the two elements are cracked due to the strength criterion employed, the equilibrium path with two opening cracks is unstable and bifurcation occurs unless both cracks exhibit hardening behavior, i.e., when $\tilde{H} > 0$. In reality, cracks will exhibit softening behavior. Therefore, the two cracks cannot continue to open at the same time. If one of the cracks undergoes the elastic unloading, the stable

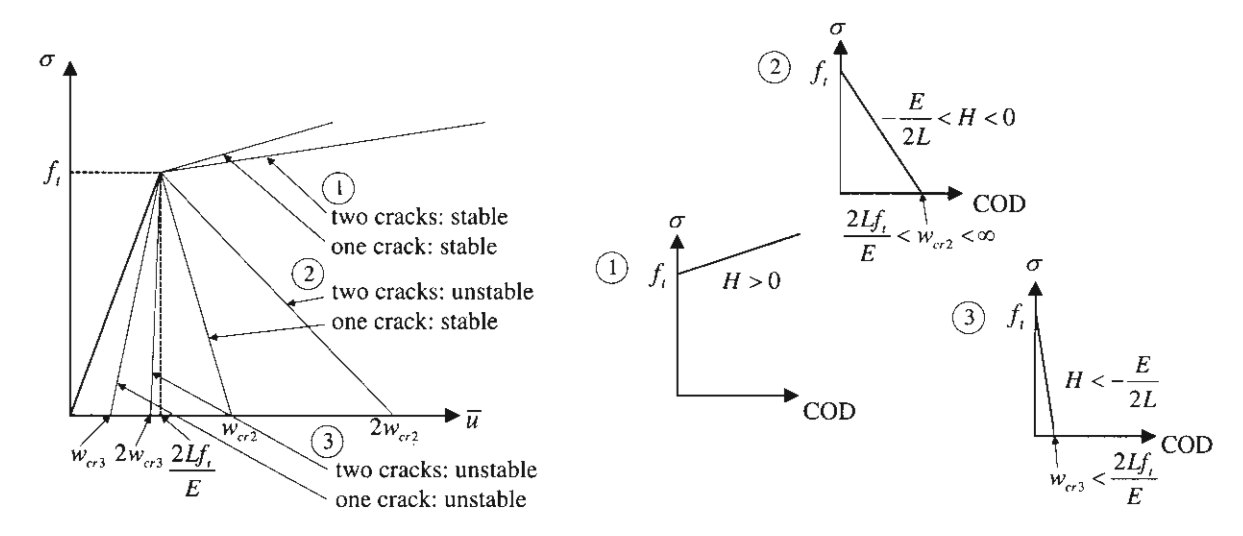


Fig. 35 Responses of the uniaxial problem using two 1-D bar elements

equilibrium path can be observed as long as $\widetilde{H} > -\frac{E}{2}$. In the case of $\widetilde{H} < -\frac{E}{2}$, even the equilibrium path with one opening crack is not stable. Fig. 35 shows the responses for all possible cases. For this uniaxial problem, the responses obtained from the finite element analysis are exact since the linear shape function used in each element can exactly represent the exact displacement solutions. Note that the exact solutions mean the solutions that are obtained exactly from the equilibrium although they may not be stable. From Fig.

35, it can be seen that, when there is one opening crack and $\tilde{H} < -\frac{E}{2}$, the obtained responses are the responses with snapback behavior. Under displacement-controlled loading, the snapback responses are always unstable.

Next, the second proposed smeared crack model, which is the model derived with a mixed finite element formulation, will be used to solve the same problem. The conventional linear shape function is used for both the displacement and local crack strain interpolations. Again, consider an incremental step after the initiation of the cracks. Assembling all element stiffness equations given by Eq. (67), we write the system stiffness equation as

$$A \begin{bmatrix} \frac{E}{L} & -\frac{E}{L} & 0 & \frac{E}{2} & \frac{E}{2} & 0 & 0 \\ -\frac{E}{L} & \frac{2E}{L} & -\frac{E}{L} & -\frac{E}{2} & -\frac{E}{2} & \frac{E}{2} & \frac{E}{2} \\ 0 & -\frac{E}{L} & \frac{E}{L} & 0 & 0 & -\frac{E}{2} & -\frac{E}{2} \\ \frac{E}{2} & -\frac{E}{2} & 0 & \frac{(E+\tilde{H})L}{3} & \frac{(E+\tilde{H})L}{6} & 0 & 0 \\ \frac{E}{2} & -\frac{E}{2} & 0 & \frac{(E+\tilde{H})L}{3} & \frac{(E+\tilde{H})L}{3} & 0 & 0 \\ 0 & \frac{E}{2} & -\frac{E}{2} & 0 & 0 & \frac{(E+\tilde{H})L}{3} & \frac{(E+\tilde{H})L}{3} & \frac{(E+\tilde{H})L}{3} \\ 0 & \frac{E+\tilde{H})L}{3} & \frac{(E+\tilde{H})L}{3} & \frac{(E+\tilde{H})L}{3} \end{bmatrix} \begin{bmatrix} \Delta U_1 \\ \Delta U_2 \\ \Delta U_3 \\ \Delta^1 \hat{E}_1^{cr} \\ \Delta^1 \hat{E}_2^{cr} \\ \Delta^2 \hat{E}_2^{cr} \\ \Delta^2 \hat{E}_3^{cr} \end{bmatrix} = \begin{bmatrix} \Delta R_1 \\ \Delta R_2 \\ \Delta R_3 \\ 0 \\ 0 \\ 0 \\ 0 \end{bmatrix}. (79)$$

Here, ΔU_i and ΔR_i represent the nodal displacement increment and the nodal force increment of the node i, respectively. Moreover, $\Delta^i \hat{E}^{cr}_j$ represents the nodal local crack strain increment of the node j and, at the same time, of the element i.

Since ΔU_1 , ΔU_3 and ΔR_2 are prescribed, the equation can be reduced into

$$A = \begin{bmatrix} \frac{2E}{L} & -\frac{E}{2} & -\frac{E}{2} & \frac{E}{2} & \frac{E}{2} \\ -\frac{E}{2} & \frac{(E+\tilde{H})L}{3} & (E+\tilde{H})L & 0 & 0 \\ -\frac{E}{2} & \frac{(E+\tilde{H})L}{6} & \frac{(E+\tilde{H})L}{3} & 0 & 0 \\ \frac{E}{2} & 0 & 0 & \frac{(E+\tilde{H})L}{3} & \frac{(E+\tilde{H})L}{6} & \frac{(E+\tilde{H})L}{6} \\ \frac{E}{2} & 0 & 0 & \frac{(E+\tilde{H})L}{6} & \frac{(E+\tilde{H})L}{3} \end{bmatrix} = AE \begin{cases} \frac{\Delta \overline{u}}{L} \\ \frac{\Delta \overline{u}}{L} \\ 0 \\ 0 \\ \frac{\Delta \overline{u}}{2} \\ \frac{\Delta \overline{u}}{2} \end{cases}. (80)$$

Using the static condensation to remove ΔU_2 yields

$$\frac{AL}{24} \begin{bmatrix} \left(5E + 8\tilde{H}\right) & \left(E + 4\tilde{H}\right) & 3E & 3E \\ \left(E + 4\tilde{H}\right) & \left(5E + 8\tilde{H}\right) & 3E & 3E \\ 3E & 3E & \left(5E + 8\tilde{H}\right) & \left(E + 4\tilde{H}\right) \\ 3E & 3E & \left(E + 4\tilde{H}\right) & \left(5E + 8\tilde{H}\right) \end{bmatrix} \begin{bmatrix} \Delta^{1} \hat{E}_{1}^{cr} \\ \Delta^{1} \hat{E}_{2}^{cr} \\ \Delta^{2} \hat{E}_{2}^{cr} \end{bmatrix} = \frac{A}{4} \begin{bmatrix} E\Delta \overline{u} \\ E\Delta \overline{u} \\ E\Delta \overline{u} \end{bmatrix}. \tag{81}$$

The eigenvalues of the obtained stiffness matrix are $\frac{A\widetilde{H}L}{2}$, $\frac{A(E+\widetilde{H})L}{6}$, $\frac{A(E+\widetilde{H})L}{6}$ and $\frac{A(E+\widetilde{H})L}{2}$. All eigenvalues will be positive only when $\widetilde{H}>0$. This means that the crack pattern having two cracks opening at the same time is unstable unless hardening behavior occurs at the cracks $(\widetilde{H}>0)$. This result is the same as the one obtained from the smeared crack model with crack displacement degrees of freedom. Again, if we assume that the crack in the element 2 undergoes the elastic unloading, the system stiffness equation will contain only one crack element, i.e.,

$$\begin{bmatrix}
\frac{E}{L} & -\frac{E}{L} & 0 & \frac{E}{2} & \frac{E}{2} \\
-\frac{E}{L} & \frac{2E}{L} & -\frac{E}{L} & -\frac{E}{2} & -\frac{E}{2} \\
0 & -\frac{E}{L} & \frac{E}{L} & 0 & 0 \\
\frac{E}{2} & -\frac{E}{2} & 0 & \frac{(E+\tilde{H})L}{3} & \frac{(E+\tilde{H})L}{6} \\
\frac{E}{2} & -\frac{E}{2} & 0 & \frac{(E+\tilde{H})L}{6} & \frac{(E+\tilde{H})L}{3}
\end{bmatrix}
\begin{bmatrix}
\Delta U_{1} \\
\Delta U_{2} \\
\Delta U_{3} \\
\Delta^{1}\hat{E}_{1}^{cr} \\
\Delta^{1}\hat{E}_{2}^{cr}
\end{bmatrix} = \begin{bmatrix}
\Delta R_{1} \\
\Delta R_{2} \\
\Delta R_{3} \\
0 \\
0
\end{bmatrix}$$
(82)

Employing the same process of applying the prescribed boundary conditions and using the static condensation, we obtain

$$\frac{AL}{24} \begin{bmatrix} (5E+8\tilde{H}) & (E+4\tilde{H}) \\ (E+4\tilde{H}) & (5E+8\tilde{H}) \end{bmatrix} \begin{bmatrix} \Delta^1 \hat{E}_1^{cr} \\ \Delta^1 \hat{E}_2^{cr} \end{bmatrix} = \frac{A}{4} \begin{bmatrix} E\Delta \overline{u} \\ E\Delta \overline{u} \end{bmatrix}. \tag{83}$$

The eigenvalues of the stiffness matrix are $\frac{A(E+\tilde{H})L}{6}$ and $\frac{A(E+2\tilde{H})L}{4}$. Both will

be positive at the same time only when $\tilde{H} > -\frac{E}{2}$. Assuming that the crack in the element 1

undergoes the elastic unloading will yield the same result. Once again, the same conclusion as the one obtained from the smeared crack model with crack displacement degrees of freedom is obtained.

It can be seen from the results that both proposed modified smeared crack models allow the consideration of cracking localization to be done even when the smeared crack approach is used. Note that there is no intention to use the stiffness equations obtained from the proposed methods in the analysis to obtain the unknown displacements. For that purpose, the original smeared crack approach is much more appropriate and will be used. The proposed schemes are used only for the investigation of stability of crack patterns. It can be also seen from the results of both proposed smeared crack models that the second model that uses a mixed finite element formulation may be considered as a more efficient model than the first proposed model that uses crack displacement degrees of freedom. This is because the second model is simpler, more straightforward and does not need any implementation of constraint equations for rigid-body modes. Therefore, for subsequent examples, the second proposed model will be employed.

8.2 A Four-Point Bending Problem of Plain Concrete Using Four-Noded Quadrilateral Elements

Here, the classical four-point bending test of a plain concrete beam shown in Fig. 36 is investigated. This problem is selected because, under the test configuration, the axial stress at the bottom fiber of the beam in the middle span will be rather uniform. This will subsequently result in many cracks distributed uniformly along the bottom of the beam in the middle span. These cracks will, at the beginning, grow but finally only major cracks will continue to grow while the others stop growing and start to unload. Having many cracks before localization makes the localization analysis rather difficult.

The dimensions of the specimen are 300×100×100 mm. Controlled displacements are applied at the top of the beam, 100 mm from both ends. Young's modulus and Poisson's ratio used are 27.5 GPa and 0.2, respectively. Unit weight of the material is 2,300 kg/m³. The tension-softening curve used is shown in Fig. 36b. In the analysis, four-noded quadrilateral elements are employed. The conventional bilinear shape function is used for the displacement and local crack strain interpolations. The finite element mesh used in this analysis consists of 2,232 elements and 2,288 nodes (see Fig. 37). Note that each element can accommodate one crack.

Initiation of a crack and determination of its angle in each element are based on the value of the maximum principal tensile stress and its direction. When a crack grows across elements, it develops its path. For this problem, it can be reasonably assumed that all crack paths are straight. To simplify the problem, cracks will be allowed to occur only on prespecified paths. The problem is solved both with and without the specimen's self-weight. When the self-weight is neglected, the problem is solved with various numbers of

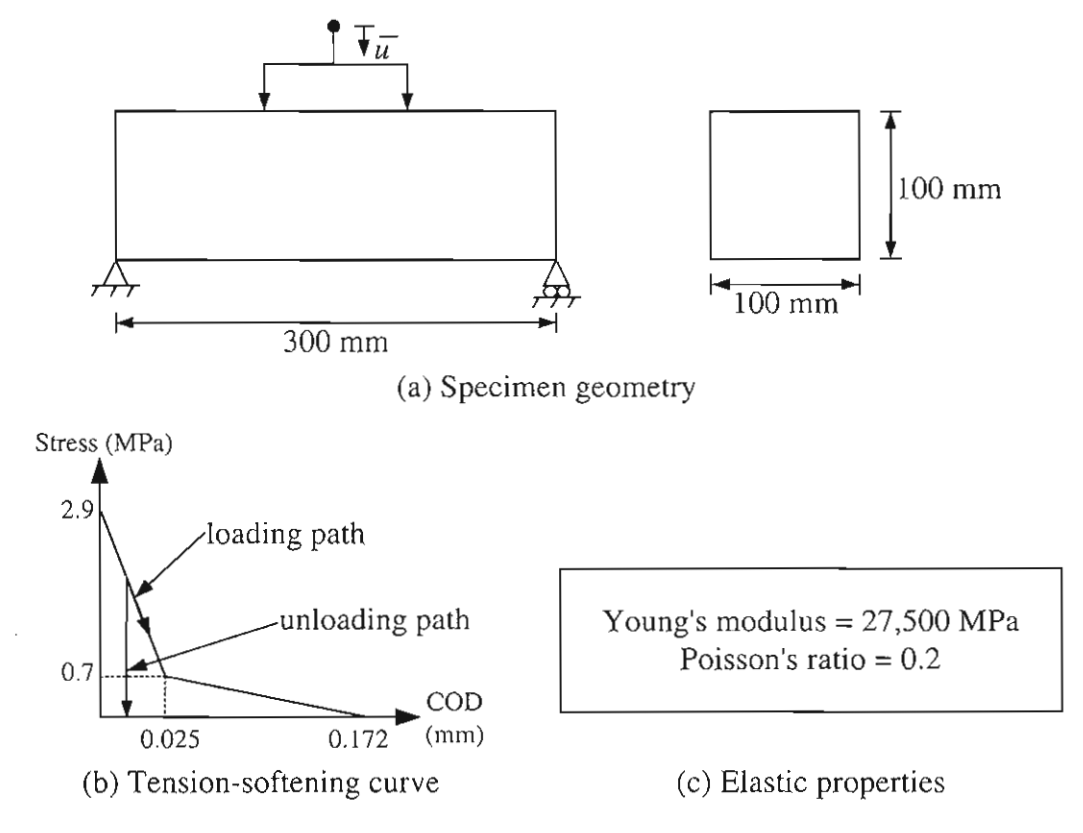


Fig. 36 Four-point bending problem of a plain concrete beam

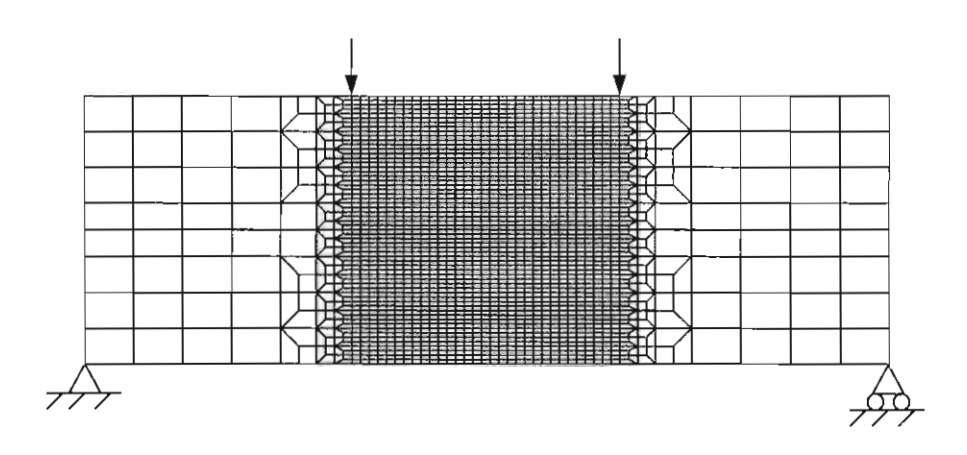


Fig. 37 Finite element mesh for the four-point bending problem

allowable crack paths as shown in Fig. 38, and, in all of these cases with different allowable crack paths, the equilibrium path with the minimum total potential energy increment is traced by employing the exhaustive search. In addition, only for the case with 31 allowable crack paths, the GA is also employed for the search. When the self-weight is considered, the analysis is done only for the case with 31 allowable crack paths, and the equilibrium path with the minimum total potential energy increment is traced by employing both exhaustive search and GA. GA parameters used in the analysis are shown in Table 9. Note that, in those cases where the GA is used for the search, the GA will be used only when there are more than 10 cracks occurring in the specimen since the advantages of the GA are not significant if the search space is not large.

Fig. 39a shows load-controlled displacement responses for all of the calculations mentioned above. Moreover, it also includes the case with 31 allowable crack paths when

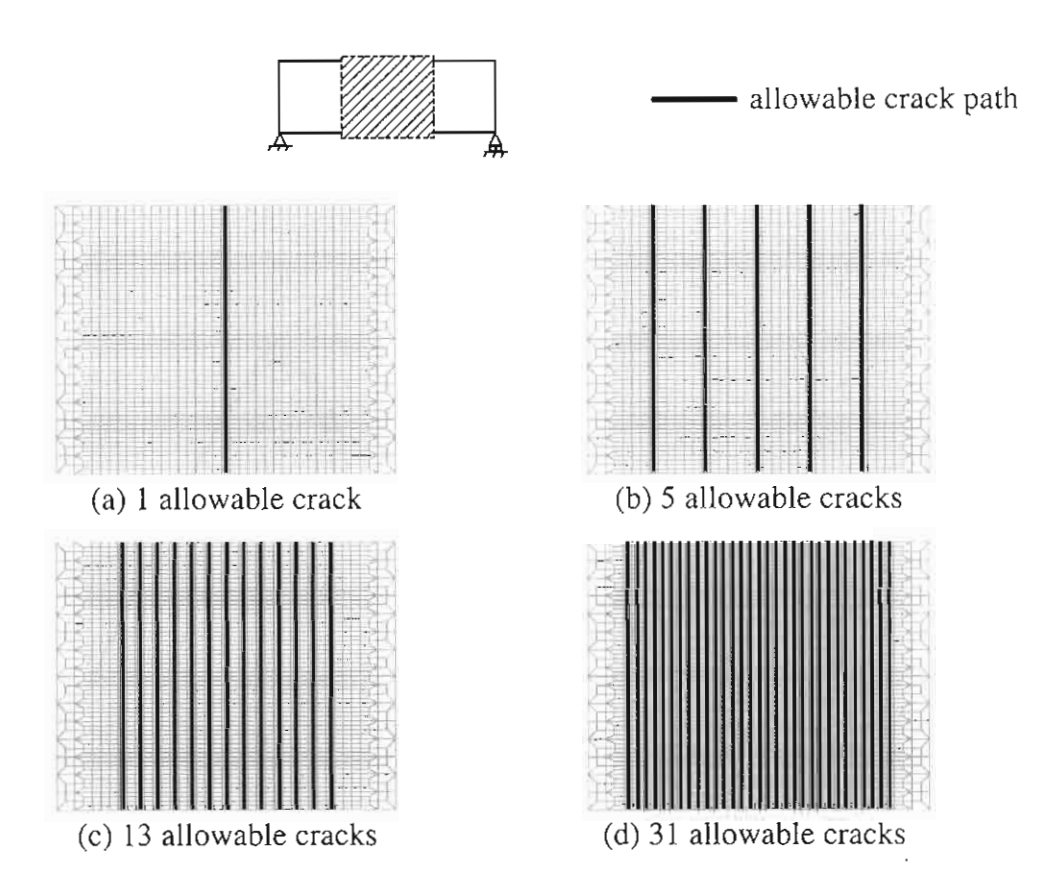


Fig. 38 Allowable crack paths for the four-point bending test of a plain concrete beam

Table 9 GA parameters

Population size	40
Number of generations	40
Crossover probability	0.80
Mutation probability	0.05

the cracking localization is not considered. This additional case is performed without the self-weight and it will allow the importance of the localization analysis to be observed. Fig. 39b shows crack patterns obtained from these different cases at the loading points indicated by black circular markers on every response curve. At these loading points, the main cracks in all cases reach the length of 90 percent of the beam depth. For the case with 31 allowable crack paths with the localization consideration (the cases D and E), it can be seen that the results obtained from the exhaustive search and the GA are exactly the same. Therefore, it is shown that GAs can be used instead of the exhaustive search. It must be noted that the time used by the exhaustive search is very much longer than that used by the GA.

For the cases B, C, and D where no self-weight is assumed, it can be seen that the obtained results, both crack patterns and response curves, are not much different. Therefore, for this problem, having only five allowable crack paths that are distributed properly is actually sufficient for obtaining the converged solution. Since it can be observed from the crack patterns of the cases B, C, and D that there are actually two long cracks in the beam, it may be understood that the response is actually governed by the two main localized cracks which are not localized into one crack until at a much later loading

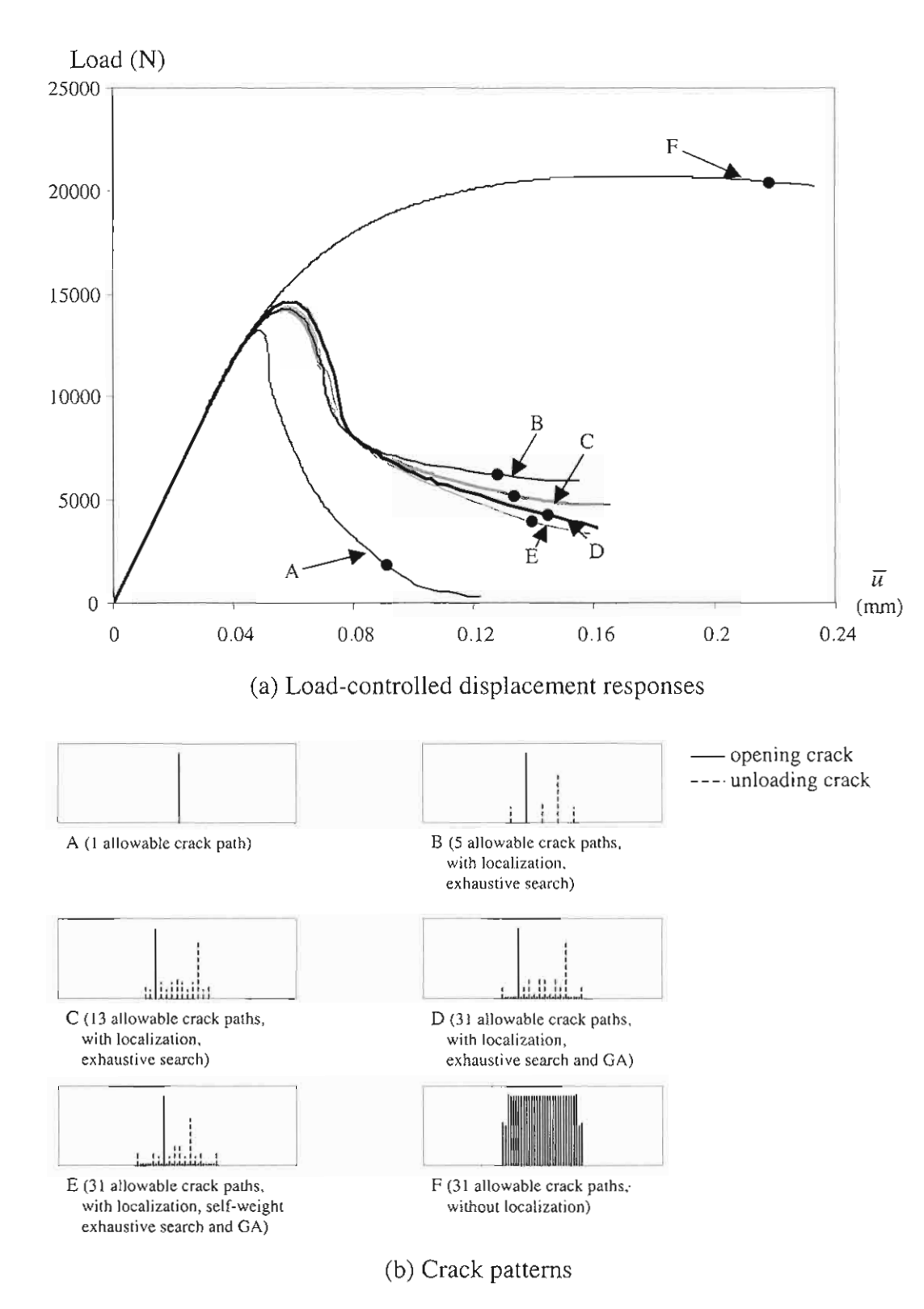


Fig. 39 Load-controlled displacement responses and crack patterns

stage. Also from the response curves, it is seen that the results of the case A, which assumes one localized crack at the center of the span from the beginning, and the case F, which does not consider the localization, are very much different from those of the cases B, C, and D which properly consider the localization.

Finally, from a comparison of the results of the cases D (without self-weight) and E

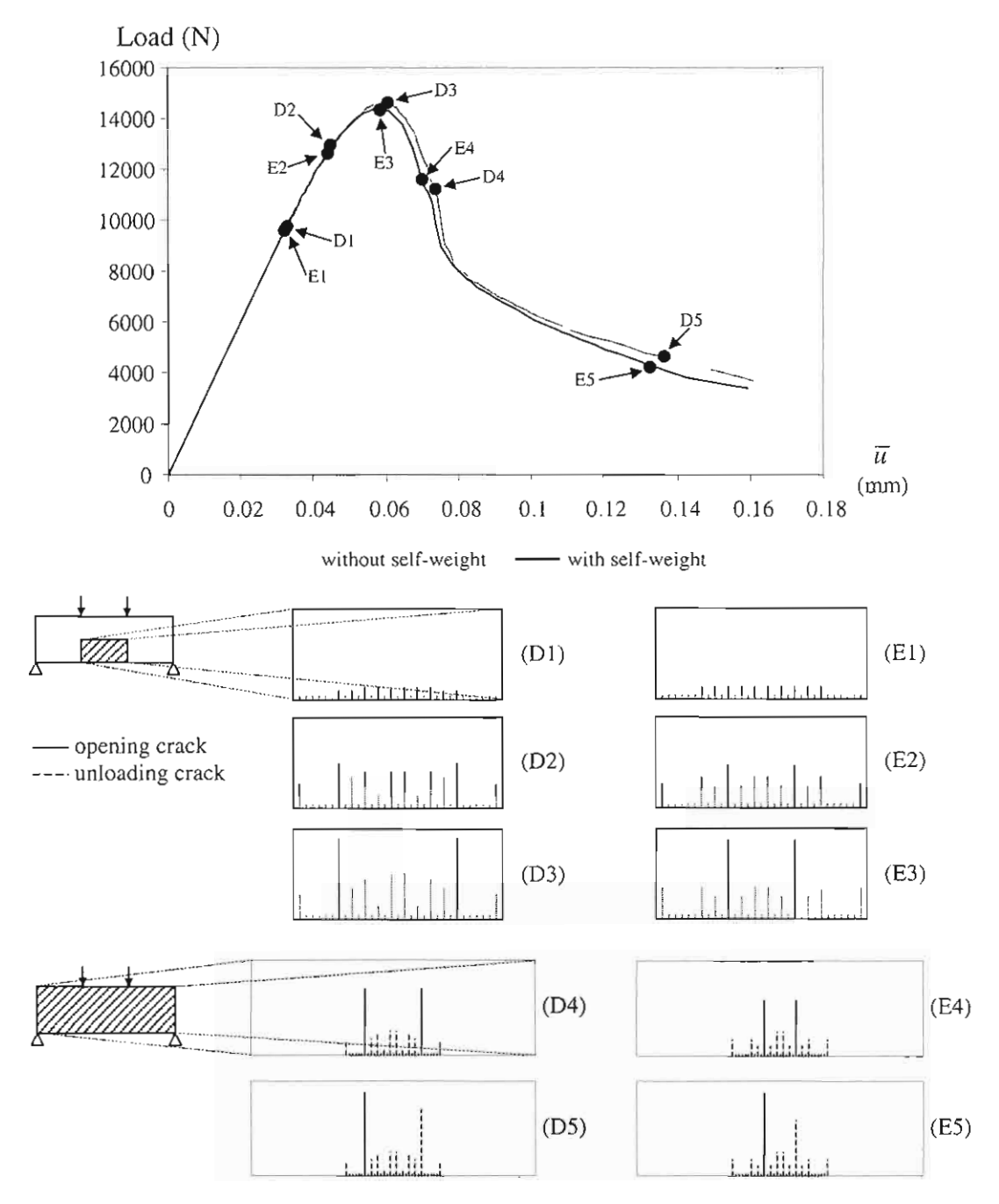


Fig. 40 Crack patterns of the specimen with 31 allowable crack paths

(with self-weight), it can be seen that the load-displacement responses of both cases are very similar. Therefore, for this particular problem, neglecting the self-weight does not have a significant effect. Nevertheless, it can also be observed from the obtained crack patterns that the two main cracks are closer to each other when the self-weight is considered. This is to be expected since the self-weight makes the stress higher at locations closer to the center of the spän. Fig. 40 shows the crack patterns of the cases D and E at different loading stages. The figure clearly shows the process of localization. At the beginning there are many cracks initiated along the bottom surface of the beam. These cracks initially grow but are gradually localized into a few cracks later.

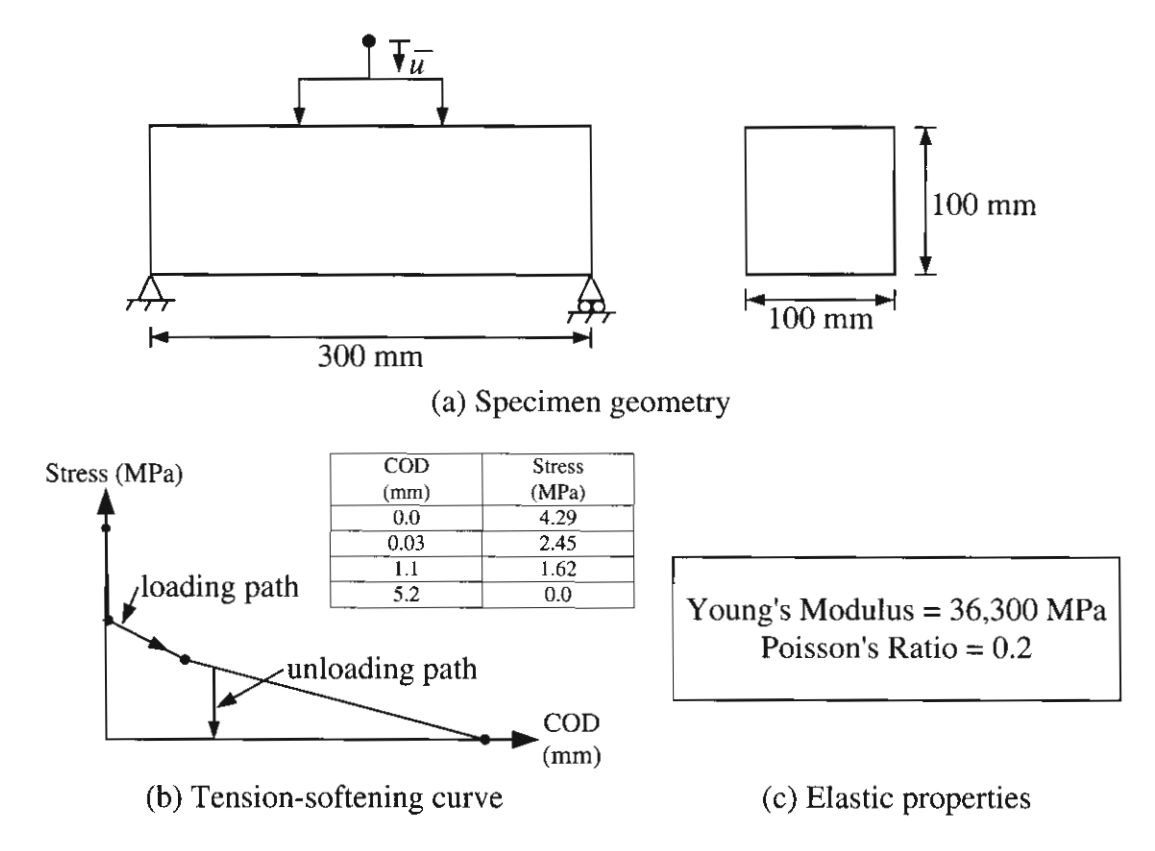


Fig. 41 Four-point bending problem of a steel-fiber-reinforced concrete beam

8.3 A Four-Point Bending Problem of Steel-Fiber-Reinforced Concrete Using Four-Noded Quadrilateral Elements

The test in this problem is the same as the previous one but the material used is changed from plain concrete to steel-fiber-reinforced concrete (SFRC). Different responses from those responses of the previous example are to be expected because steel-fiber-reinforced concrete has much larger fracture energy than plain concrete due to the presence of its steel fibers. The steel fibers in steel-fiber-reinforced concrete help transmit the bridging stresses across cracks in addition to the stress transmission by aggregates. The fibers will make the stress transmission possible even when the crack opening displacement becomes large. This fact is automatically incorporated into the calculation by means of the tension-softening curve. The tension-softening curve of steel-fiber-reinforced concrete will have a longer tail and larger area under the curve than the curve for plain concrete. The area under a tension-softening curve represents the fracture energy of the material.

The dimensions of the specimen and its boundary conditions are the same as those of the previous example. Young's modulus and Poisson's ratio used are 36.3 GPa and 0.2, respectively. Unit weight of the material is 2,500 kg/m³. The tension-softening curve used is shown in Fig. 41b. The finite element mesh in Fig. 37 is also used in this problem. For this problem, it is still assumed that all crack paths are straight and cracks are allowed to occur only on pre-specified paths. The allowable paths are shown in Fig. 42. When the case with one allowable crack path is considered, it implies that the cracking localization is not properly considered. For the case with 31 allowable crack paths, the equilibrium path with the minimum total potential energy increment is traced by employing both the exhaustive search and GA. Note that, similar to the previous problem, the genetic algorithm will be used only when there are more than 10 cracks occurring in the specimen.

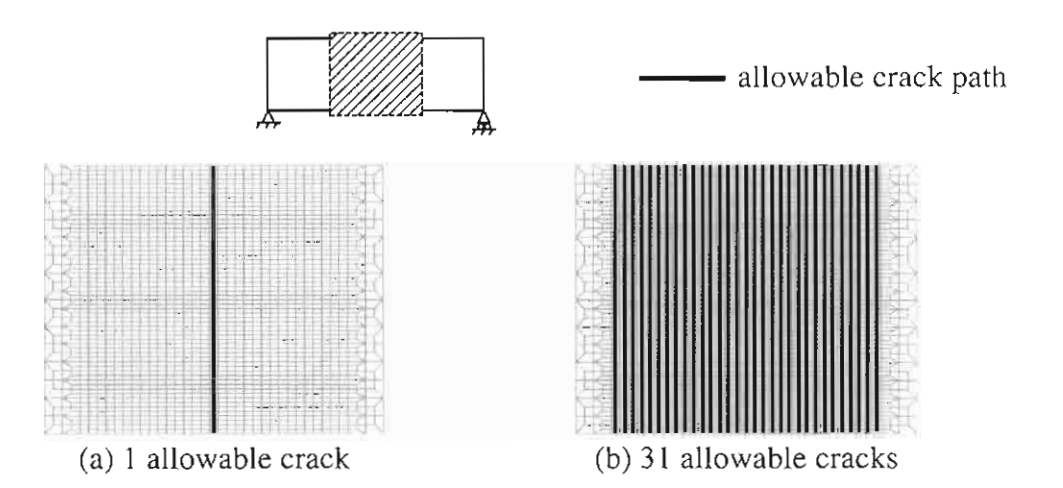
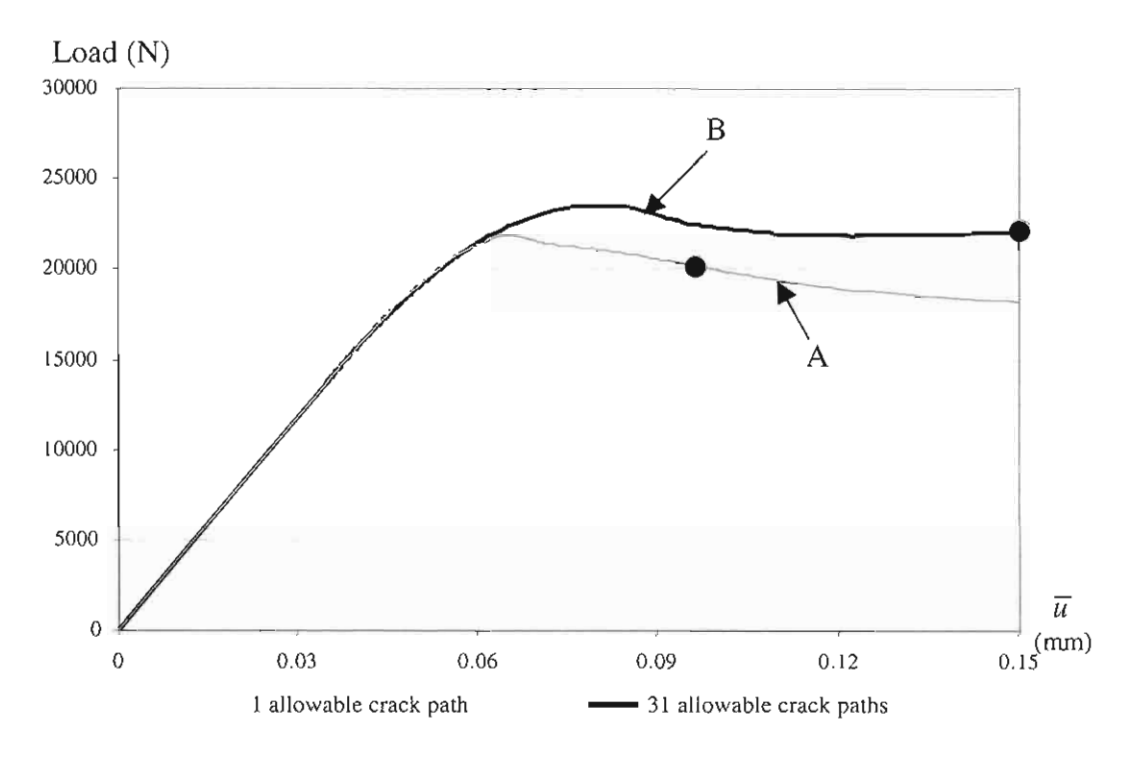


Fig. 42 Allowable crack paths for the four-point bending test of an SFRC beam

GA parameters used in the analysis are shown in Table 9. For both cases, the problem is solved with the specimen's self-weight

Fig. 43a shows load-controlled displacement responses of the two cases in Fig. 42. In Fig. 43, the case A represents the case when one crack is assumed from the beginning (see Fig. 42a). In addition, the case B represents the case when 31 crack paths are allowed (see Fig. 42b). Crack patterns obtained from both cases are shown in Fig. 43b. The corresponding loading points are indicated by black circular markers on the response curves. At these loading points, the lengths of the main cracks in both cases reach 80 percent of the beam depth. In this problem, the analyses of the two cases are stopped early when the compressive stresses in the ligaments become high and the nonlinear material behavior in compression can no longer be neglected. Since the nonlinear material behavior in compression is not included in this study, the analyses have to be discontinued.

From the obtained response curves, it can be seen that the post-peak response obtained with proper localization consideration is quite different from the one with pre-assumed crack at the center of the span. Assuming one crack from the beginning results in more brittle behavior. This is natural since having one crack from the beginning implies that the cracks are forced to localize themselves into one crack from the beginning. From the crack patterns, it is clear that there are two major cracks in the case with the consideration of cracking localization. These two cracks are expected to be localized into one crack if the loading continues. Therefore, if only one crack is assumed from the beginning, it is obvious that the analysis done in such a fashion will not be able to capture this behavior.



(a) Load-controlled displacement responses

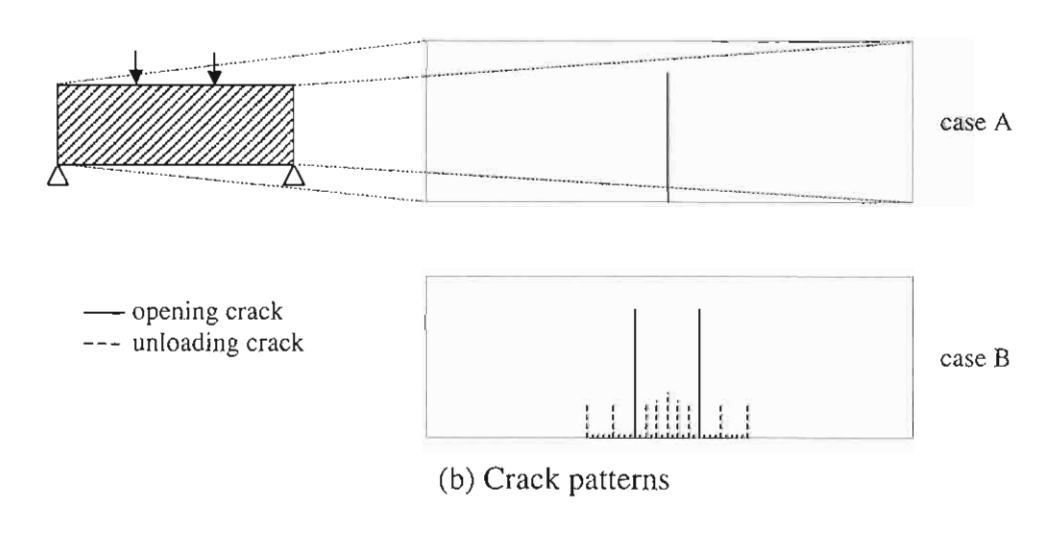


Fig. 43 Load-controlled displacement responses and crack patterns

9. CONCLUSIONS AND DISCUSSION

In this study, an analysis method for cracking localization in quasi-brittle materials such as concrete is presented. The proposed analysis method is an incremental analysis method and it is composed of two key processes. The first key process involves locating bifurcation points and the second one involves tracing the actual equilibrium path at any bifurcation point. For the first process, two specially treated smeared crack finite element models are proposed. In the first model, nodal crack displacement degrees of freedom are introduced into the conventional smeared crack finite element model in order to allow the stability and bifurcation analysis of crack patterns to be performed easily. The newly introduced nodal crack displacement degrees of freedom will serve as discrete irreversible variables in the stability analysis of crack patterns. The second model also employs the same basic idea of introducing discrete irreversible variables into the original smeared crack finite element model. Nevertheless, the implementation of the idea is rather different from the first model. In the second model, the smeared crack model is formulated by using a mixed finite element formulation, which discretizes not only the displacement field but also the crack strain field. This results in a smeared crack finite element model with local crack strain degrees of freedom. These local crack strain degrees of freedom serve as discrete irreversible variables that are essential to the stability analysis of crack patterns. The reason why the smeared crack model is selected as a base model for the development of these two proposed model is that the smeared crack approach is suitable for problems with many cracks, compared with the discrete crack approach. However, the stability analysis of crack patterns cannot be performed easily with the conventional smeared crack finite element analysis since the irreversible parameter in the model—the crack strain—is not discrete, but continuous. The two proposed treatments of the smeared crack finite element model overcome this drawback. By comparing both proposed models, it is found that the second model is more efficient than the first model. This is because the second model is simpler, more straightforward and does not require difficult implementation. By using the stability analysis of crack patterns, it is then possible to identify when the current crack pattern becomes unstable. When that happens, it means that a bifurcation point is reached. At the bifurcation point, a fan of many equilibrium paths can be observed. Each equilibrium path represents an equilibrium path for each different crack pattern.

The second key process traces the actual equilibrium path from a bifurcation point incrementally by finding the path with the minimum total potential energy increment. The search for the minimum total potential energy increment is done by employing both the exhaustive and GA search algorithms, depending on the size of the problem being solved. If the size of the problem is small, the exhaustive search, which directly compares the total potential energy increments of all possible crack patterns, is possible. In this case, the crack pattern with the minimum total potential energy increment obtained from the search is numerically exact with respect to the discretization being used. However, when the size of the problem becomes large and there are subsequently many possible crack patterns to be investigated, performing the exhaustive search becomes impossible and the GA is employed instead. From the obtained results in this study, it is found that GAs can be efficiently used for this search.

The major problems used to validate the proposed analysis method in this study include the uniaxial problem of plain concrete as well as the four-point bending problems of plain concrete and steel-fiber-reinforced concrete. The results obtained from the uniaxial problem clearly illustrate the importance of the analysis of cracking localization. The results actually explain why only one localized crack, not many cracks, should appear in the uniaxial test of a homogeneous material. It is seen from the results that the solution

with multiple opening cracks is actually unstable and, therefore, cannot be the actual solution. The results obtained from the four-point bending problem of plain concrete show that the true localized solution is very much different from the solution obtained by assuming one localized crack at the center of the span. Furthermore, the true localized solution is also very much different from the solution obtained without the localization consideration. It is also found that there are two major localized cracks that are not localized into one crack until at a much later loading stage. The behavior of the beam is therefore governed by these two cracks. This clearly illustrates that assuming only one localized crack from the beginning will lead to erroneous results. Finally, it is found that, for the four-point bending test of plain concrete, neglecting the self-weight does not have significant effect on the obtained results. With self-weight or without self-weight, there are two main localized cracks. Although these two cracks are slightly closer when the selfweight is considered, the difference between the obtained responses from both cases are negligible. The results for the steel-fiber-reinforced concrete beam also exhibit rather large difference between the solution with the localization consideration and the solution that assumes one localized crack at the center of the span from the beginning. Similar to the case of plain concrete, it is also found that there are two major localized cracks. These two cracks are expected to finally localize themselves into one crack at a later loading stage. However, since the nonlinear behavior of the material in compression is not considered in this study, the analysis has to be stopped before the localization into one crack happens.

One of the difficulties that can be expected during the analysis of cracking localization using the smeared crack finite element model is how to maintain the continuity of crack paths in the case of very curved cracks. In the concept of the smeared crack finite element analysis, cracks are allowed to occur in all elements independently. In fact, the path of any crack is not rigorously defined since there is no predefined link between cracks in different elements even when these elements are adjacent to each other. In this aspect, the discrete crack finite element analysis is considered superior since it is possible and actually common, in the discrete crack finite element analysis, to enforce the continuity of crack paths via the continuity of crack opening displacement degrees of freedom. However, as mentioned earlier, the discrete crack approach may not perform best when there are many cracks. One of the possibilities to avoid these problems is to use a new class of methods called meshless methods. These methods use a concept of interpolation that is different from the finite element method. The interpolation is no longer performed within an element enclosing the point of interest but it is done rather within a pre-specified space around the point. As a result, there is no element necessary and only nodes are required. If the meshless methods are used in the analysis of crack problems, it may be possible to easily maintain the continuity of crack paths even when the smeared crack concept is employed. Since there is no element in the meshless methods, it should be possible to implement the smeared crack model in such a way that a band of a smeared crack can continuously propagate virtually everywhere in the domain. Consequently, the continuity of crack paths can be maintained.

10. REFERENCES

- o Adeli H, Cheng N. Integrated genetic algorithm for optimization of space structures. Journal of Aerospace Engineering 1993;6(4):315-328.
- o Bazant ZP, Cedolin L. Stability of structures: elastic, inelastic, fracture, and damage theories. New York: Oxford University Press; 1991.
- o Brocca M. Analysis of cracking localization and crack growth based on thermomechanical theory of localization (master's degree thesis). Tokyo: The University of Tokyo; 1997.
- o Burns T. Structural steel design—LRFD. New York: Delmar Publishers; 1995.
- o Camp C, Pezeshk S, Cao G. Optimized design of two-dimensional structures using a genetic algorithm. Journal of Structural Engineering 1998;124(5):551-559.
- o Carpinteri A. Softening and snap-back instability in cohesive solids. International Journal for Numerical Methods in Engineering 1989;28:1521-1537.
- o Coello CAC. Use of a self-adaptive penalty approach for engineering optimization problems. Computers in Industry 2000;41:113-127.
- o Collins RJ. Bandwidth reduction by automatic renumbering. International Journal for Numerical Methods in Engineering 1973;6:345-356.
- o Dawid H. Adaptive learning by genetic algorithms: analytical results and applications to economic models. New York: Springer; 1999.
- o de Borst R. Computation of post-bifurcation and post-failure behavior of strain-softening solids. Computers and Structures 1987;25(2):211-224.
- o Deb K. Optimization for engineering design: algorithms and examples. New Delhi: Prentice-Hall; 1995.
- Dvorkin EN, Assanelli AP. 2D finite elements with displacement interpolated embedded localization lines: the analysis of fracture in frictional materials. Computer Methods in Applied Mechanics and Engineering 1991;90:829-844.
- Gajewski RR, Lompies P. Object-oriented implementation of bandwidth, profile and wavefront reduction algorithms. In: Topping BHV, editor. Advances in computational structures technology. Edinburgh: Civil-Comp Press; 1996:115-119.
- o Galante M. Genetic algorithms as an approach to optimize real-world trusses. International Journal for Numerical Methods in Engineering 1996;39:361-382.
- o Goldberg DE. Genetic algorithms in search, optimization, and machine learning. Reading, Massachusetts: Addison-Wesley; 1989.
- o Grefenstette JJ. Optimization of control parameters for genetic algorithms. IEEE Transactions on Systems, Man, and Cybernetics 1986;SMC-16(1):122-128.
- Horii H, Okui Y. Thermomechanics and micromechanics-based continuum theory for localization phenomena. In: Baker G, Karihaloo BL, editors. Fracture of brittle, disordered materials: concrete, rock, and ceramics. London: E&FN Spon; 1995:391-405.
- o Jenkins WM. On the application of natural algorithms to structural design optimization. Engineering Structures 1997;19(4):302-308.
- o Jirasek M, Zimmermann T. Rotating crack model with transition to scalar damage. Journal of Engineering Mechanics 1998;124(3):277-284.
- o Kallassy A, Marcelin JL. Optimization of stiffened plates by genetic search. Structural Optimization 1997;13:134-141.
- o Khot NS, Venkayya VB, Berke L. Optimum structural design with stability constraints. International Journal for Numerical Methods in Engineering 1976;10:1097-1114.
- o Le Riche RG, Knopf-Lenoir C, Haftka RT. A segregated genetic algorithm for constrained structural optimization. In: Eshelman LJ, editor. Proceedings of the sixth

- international conference on genetic algorithms. San Francisco: Morgan Kaufmann; 1995:558-565.
- o Marcelin JL, Trompette P, Dornberger, R. Optimization of composite beam structures using a genetic algorithm. Structural Optimization 1995;9:236-244.
- o Marcelin JL. Evolutionary optimisation of mechanical structures: towards an integrated optimisation. Engineering with Computers 1999;15:326-333.
- o Meesomklin K. A novel penalty scheme in genetic algorithms for structural design optimization (master's degree thesis). Pathumthani, Thailand: Sirindhorn International Institute of Technology, Thammasat University; 2000.
- Michalewicz Z. Genetic algorithms + data structures = evolution programs. New York: Springer; 1996.
- Michalewicz Z. Genetic algorithms, numerical optimization, and constraints. In: Eshelman LJ, editor. Proceedings of the sixth international conference on genetic algorithms. San Francisco: Morgan Kaufmann; 1995:151-158.
- o Nanakorn P, Meesomklin K. An adaptive penalty function in genetic algorithms for structural design optimization. Computers and Structures 2001;79(29-30):2527-2539.
- Nemat-Nasser S. The second law of thermodynamics and noncollinear crack growth. In: Proceedings of the third ASCE/EMD specialty conference. Texas, Austin: The University of Texas at Austin; 1979:449-452.
- o Nguyen QS. Bifurcation and post-bifurcation analysis in plasticity and brittle fracture. Journal of the Mechanics and Physics of Solids 1987;35(3):303-324.
- o Oliver J. A consistent characteristic length for smeared cracking models. International Journal for Numerical Methods in Engineering 1989;28:461-474.
- Petcherdchoo A. Analysis of cracking localization in quasi-brittle materials using the smeared crack approach (master's degree thesis). Pathumthani, Thailand: Sirindhorn International Institute of Technology, Thammasat University; 1999.
- o Powell D, Skolnick MM. Using genetic algorithms in engineering design optimization with non-linear constraints. In: Forrest S, editor. Proceedings of the fifth international conference on genetic algorithms. San Mateo: Morgan Kaufmann; 1993:424-431.
- o Rafiq MY, Southcombe C. Genetic algorithms in optimal design and detailing of reinforced concrete biaxial columns supported by a declarative approach for capacity checking. Computers and Structures 1998;69:443-457.
- o Rajan SD. Sizing, shape, and topology design optimization of trusses using genetic algorithm. Journal of Structural Engineering 1995;121(10):1480-1487.
- o Rajeev S, Krishnamoorthy CS. Discrete optimization of structures using genetic algorithms. Journal of Structural Engineering 1992;118(5):1233-1249.
- o Rasheed KM. GADO: a genetic algorithm for continuous design optimization (doctoral dissertation). New Brunswick, New Jersey: The State University of New Jersey; 1998.
- o Riks E. An incremental approach to the solution of snapping and buckling problems. Int. J. Solids Structures 1979;15:529-551.
- o Rots JG, de Borst R. Analysis of mixed-mode fracture in concrete. Journal of Engineering Mechanics 1987;113(11):1739-1758.
- o Rots JG. Stress rotation and stress locking in smeared analysis of separation. In: Fracture toughness and fracture energy: test methods for concrete and rock. Rotterdam: Balkema; 1989:367-382.
- o Shirai N. JCI round robin analysis of size effect in concrete structures. In: Size effect in concrete structures. London: E&FN Spon; 1994:295-322.
- o Sloan SW. An algorithm for profile and wavefront reduction of sparse matrices. International Journal for Numerical Methods in Engineering 1986;23:239-251.

- o Soparat P. A mixed finite element formulation for analysis of cracking localization in quasi-brittle materials (master's degree thesis). Pathumthani, Thailand: Sirindhorn International Institute of Technology, Thammasat University; 2000.
- o Templeman AB. Discrete optimum structural design. Computers and Structures 1988;30(3):511-518.
- Thitawat V. Stability and bifurcation analysis of crack patterns in quasi-brittle materials (master's degree thesis). Pathumthani, Thailand: Sirindhorn International Institute of Technology, Thammasat University; 2001.
- o Valente S. Bifurcation phenomena in cohesive crack propagation. Computers and Structures 1992;44(1/2):55-62.
- o Zienkiewicz OC, Huang M, Pastor M. Localization problems in plasticity using finite elements with adaptive remeshing. International Journal for Numerical and Analytical Methods in Geomechanics 1995,19:127-148.

11. RESEARCH OUTPUT

11.1 Publications

11.1.1 International journals

 Nanakorn P, Meesomklin K. An adaptive penalty function in genetic algorithms for structural design optimization. Computers and Structures 2001;79(29-30):2527-2539.

11.1.2 Regional journals

 Nanakorn P, Meesomklin K. A novel penalty scheme in genetic algorithms for structural design optimization. ASEAN Journal on Science and Technology for Development 2000;17(2):17-30.

11.1.3 National journals

- o Nanakorn P, Petcherdchoo A, Kittiwattanchai N. Analysis of cracking localization using the smeared crack approach. Research and Development Journal of the Engineering Institute of Thailand, The Engineering Institute of Thailand under H.M. the King's Patronage 2000;11(4):1-9.
- Nanakorn P, Soparat P. Finite element analysis of cracking localization: the smeared crack approach with a mixed formulation. Thammasat International Journal of Science and Technology 2000;5(3):28-39.
- o Nanakorn P, Thitawat V. Cracking localization analysis using a specially treated smeared crack finite element model with energy consideration. Research and Development Journal of the Engineering Institute of Thailand, The Engineering Institute of Thailand under H.M. the King's Patronage 2001;12(3):11-20

11.1.4 International conferences

- Nanakorn P, Petcherdchoo A. Analysis of cracking localization using the smeared crack approach. In: International association for bridge and structural engineering (IABSE) report, volume 80. Phuket: IABSE; 1999:241-246.
- o Petcherdchoo A, Nanakorn P, Kittiwattanachai N. A smeared crack finite element for analysis of cracking localization. In: Choi CK, Schnobrich WC, editors. Proceedings of the first international conference on advances in structural engineering and mechanics, volume 1. Taejon: Techo-Press; 1999:399-404.
- Nanakorn P, Meesomklin K. An adaptive penalty function in genetic algorithms for structural design optimization. In: European congress on computational methods in applied sciences and engineering: ECCOMAS 2000. Barcelona: European Community of Computational Methods and Applied Sciences; 2000.
- Nanakorn P, Soparat P. A mixed finite element formulation for analysis of cracking localization in quasi-brittle materials. In: European congress on computational methods in applied sciences and engineering: ECCOMAS 2000. Barcelona: European Community of Computational Methods and Applied Sciences; 2000.
- Nanakorn P, Thitawat V. Analysis of cracking localization by the smeared crack approach: the four-point bending problem. In: Proceedings of the eight East Asia-Pacific conference on structural engineering and construction. Singapore: Nanyang Technological University; 2001.

11.1.5 National conferences

- Nanakorn P, Meesomklin K. Adaptive penalty functions in genetic algorithms for structural design optimization. In: Proceedings of the sixth national convention on civil engineering. The Engineering Institute of Thailand under H.M. the King's Patronage; 2000:(STR-7)-(STR-18). (Invited Paper)
- o Nanakorn P, Soparat P. A mixed finite element formulation for analysis of cracking localization in quasi-brittle materials, In: Proceedings of the sixth national

convention on civil engineering. The Engineering Institute of Thailand under H.M. the King's Patronage; 2000:(STR-31)-(STR-36).

11.2 Master's Degree Graduates

o Mr. Aruz Petcherdchoo

Degree: Master of Engineering (Civil Engineering)

Year of graduation: 1999

Thesis title: Analysis of Cracking Localization in Quasi-Brittle Materials Using The

Smeared Crack Approach

o Mr. Preecha Soparat

Degree: Master of Engineering (Civil Engineering)

Year of graduation: 2000

Thesis title: A Mixed Finite Element Formulation for Analysis of Cracking

Localization in Quasi-Brittle Materials

o Mr. Konlakarn Meesomklin

Degree: Master of Engineering (Civil Engineering)

Year of graduation: 2000

Thesis title: A Novel Penalty Scheme in Genetic Algorithms for Structural Design

Optimization

o Mr. Vasan Thitawat

Degree: Master of Engineering (Civil Engineering)

Year of graduation: 2001

Thesis title: Stability and Bifurcation Analysis of Crack Patterns in Quasi-Brittle

Materials

Reprints of Publication	APPEI ns in Internatio	nd National Journ	nals
 -			



Computers and Structures 79 (2001) 2527-2539

Computers & Structures

www.elsevier.com/locate/compstruc

An adaptive penalty function in genetic algorithms for structural design optimization

Pruettha Nanakorn*, Konlakarn Meesomklin

Civil Engineering Program, Sirindhorn International Institute of Technology, Thammasat University, P.O. Box 22, Thammasat-Rangsit Post Office, Pathumthani 12121, Thailand Received 4 July 2000; accepted 23 July 2001

Abstract

In genetic algorithms, constraints are mostly handled by using the concept of penalty functions, which penalize infeasible solutions by reducing their fitness values in proportion to the degrees of constraint violation. In most penalty schemes, some coefficients or constants have to be specified at the beginning of the calculation. Since these coefficients usually have no clear physical meanings, it is nearly impossible to estimate appropriate values of these coefficients even by experience. Moreover, most schemes employ constant coefficients throughout the entire calculation. This may result in too weak or too strong a penalty during different phases of the evolution. In this study, a new penalty scheme that is free from the aforementioned disadvantages is developed. The proposed penalty function will be able to adjust itself during the evolution in such a way that the desired degree of penalty is always obtained. The coefficient used in the proposed scheme will have a clear physical meaning. Thus, it will not be difficult to set the value of the coefficient by using experience. © 2001 Elsevier Science Ltd. All rights reserved.

Keywords: Genetic algorithms; Optimization; Structural design; Adaptive penalty function; Constrained optimization; Truss and frame structures

1. Introduction

When designing structures, engineers have to consider not only the load-carrying capacity of the structures but also the cost to construct them. Material cost is one of the major costs in construction. Designs that use a smaller amount of materials are therefore preferable, given that the construction methods do not become too expensive or impractical. To achieve this goal, optimization techniques have been employed in structural design [1–5]. There are many conventional optimization methods [6,7], each of which may work well for some specific problems. To select appropriate optimization methods for structural design, it is necessary to under-

GAs are global probabilistic search algorithms inspired by Darwin's survival-of-the-fittest theory [15].

E-mail address: nanakorn@siit.tu.ac.th (P. Nanakorn).

0045-7949/01/\$ - see front matter © 2001 Elsevier Science Ltd. All rights reserved. PII: \$0045-7949(01)00137-7

stand characteristics of this kind of optimization problem. The first important characteristic of structural design optimization is that, in structural design optimization, the solution sought is the global optimal solution. Moreover, in structural design, design variables are generally discrete variables. Finally, structural design optimization always contains constraints. These three major characteristics suggest that genetic algorithms (GAs) can be the choice. This is simply because this optimization technique is generally suitable for problems with discrete variables. Moreover, it searches for the global optimal point. Though GAs cannot be directly applied to problems with constraints, small modification can be used to incorporate constraints. Due to these facts, the technique is gaining popularity among researchers in the field of structural design optimization

^{*}Corresponding author. Tel.: +66-2-986-9009x1906; fax: +66-2-986-9009x1900.

They have received considerable attention because of their versatile applications in several fields [6,8,14-17]. GAs start their search from many points in search space at the same time. These starting search points are usually selected randomly. Through the consideration of fitness values of these search points, which are given based on their merit, and the randomized information exchange among the points, a new set of search points with higher merit is created. The process is then repeated until a satisfactory result is obtained. Since the technique utilizes information from many search points at the same time, there is less chance for the search to be trapped in any of the local optimal points. Another distinguishing characteristic of GAs is that the algorithms work with coding of the parameter set, not the parameters themselves. Generally, the binary code is used. Because of the discrete nature of coding, the algorithms are the perfect choice for those problems with discrete variables.

Since GAs are directly applicable only to unconstrained optimization, many researchers have proposed solutions that can eliminate this limitation. Constraints are mostly handled by using penalty functions, which penalize infeasible solutions by reducing their fitness values in proportion to their degrees of constraint violation. In all available penalty schemes, the degree of penalty can be further controlled by means of setting values of various coefficients in penalty functions [6,8, 15,18]. Most of these coefficients are treated as constants during the calculation and their values have to be specified at the beginning of the calculation [19-21]. These coefficients usually have no clear physical meanings. Thus, it is nearly impossible to know appropriate values of the coefficients even by experience. This is because it is very hard to understand the correlation between the values of the coefficients and the characteristics of the problems being solved without physical meanings of the coefficients. Consequently, for all problems with either similar or different natures, appropriate values of the coefficients are generally obtained by trial and error. Many researchers, however, have tried to suggest different ranges of appropriate values for these coefficients, for various types of problem. Most of these suggestions are obviously doubtful. The reason is simply that appropriate values are usually given without any reference to the units used in the problems although the coefficients may have units and appropriate values should vary with the units used. Another important concern is that these conventional penalty schemes do not adjust the strength of the penalty during the calculation, as the coefficients used are always kept constant. As a result, too weak or too strong a penalty during different phases of the evolution may occur. This will lead to inaccurate solutions. Actually, there are some penalty schemes that vary the values of the coefficients to adjust the strength of the penalty during the calculation [9,12,22]. However, these schemes

require the varying values of these coefficients to be manually specified. It therefore becomes even more difficult to judiciously select appropriate values for different phases of the calculation.

Several different ideas that are more sophisticated have been proposed to improve penalty function methods for handling constrained optimization problems [23]. Powell and Skolnick [24] re-mapped fitness values of both feasible and infeasible individuals in such a way that all feasible solutions have higher fitness than any infeasible solutions. The key concept of this approach is the assumption of the superiority of feasible solutions over infeasible ones. Unfortunately, this assumption rarely holds during the evolution since it always happens that some infeasible individuals process very good genes that can be very valuable for later generations. As a result, these infeasible individuals are more preferable during the evolution than many low fitness feasible individuals. For this reason, it is necessary to allow some infeasible individuals to have higher fitness than some feasible individuals. Le Riche et al. [25] proposed a segregated GA that uses two values of penalty parameters for each constraint instead of one. The population is split into two coexisting and cooperating groups, where individuals in each group are evaluated using either one of the two penalty parameters. During the evolution, the two groups interbreed. Since the two penalty parameters are different, the two groups converge in the design space along two different trajectories, which helps locate the optimal region faster. If a large value is selected for one of the penalty parameters and a small value for the other parameter, simultaneous convergence from both feasible and infeasible sides can be achieved. However, although the approach provides a new overall penalty scheme, the problem with this approach is still the way of choosing the penalty for each of the two groups.

Rasheed [26] proposed a penalty scheme with an adaptive penalty coefficient. The scheme considers two key individuals of the population, i.e., the point that has the least sum of constraint violations and the point that has the best fitness value. These two points are compared at every certain number of generations. If both points are the same then the penalty coefficient is assumed adequate; otherwise, the penalty coefficient is increased to make the two points have equal fitness values. In addition, the penalty coefficient is reduced if at some stage the population contains no infeasible points. The inconveniences of this technique are how to choose the initial value for the penalty coefficient and how to appropriately update it. In addition, the size of the generation gap for updating the penalty coefficient must reasonably be setected. Coello [27] proposed a technique based on the concept of co-evolution to create two populations that interact with each other in such a way that one population evolves the penalty factors to be used by the fitness

function of the main population, which is responsible for optimizing the objective function. This technique is inconvenient because the approach requires evolution of two parallel populations instead of one. Therefore, it is computationally more expensive.

In this study, a new adaptive penalty scheme is proposed. The penalty function used in the scheme will be able to adjust itself automatically during the evolution in such a way that the desired degree of penalty is always obtained. The coefficient used in the proposed scheme will have a clear physical meaning that directly represents the degree of penalty employed. Therefore, for each particular problem, the appropriate value of the coefficient can be reckoned based on the appropriate degree of penalty for the problem. In addition, the coefficient in the proposed scheme will have no units. For each particular problem, if the same value of the coefficient is used, similar results can always be expected even when different units are employed in the problem. Since it is expected that similar structural optimization problems require similar degrees of penalty, with the proposed scheme, it is therefore possible to set the value of the coefficient by using experience. It must be noted that the main objective of this work is to obtain an adaptive penalty scheme that is robust and can still reproduce the same quality of results as ones obtained from GAs found in the literature, whose penalty parameters are carefully obtained for each specific problem by trial and error. In brief, the proposed scheme will be a scheme that can efficiently be used in different problems without a lot of guesswork.

2. Genetic algorithms for constrained optimization

An optimization problem using GAs can be generally expressed as

Maximize

$$F(\mathbf{x}) = F[f(\mathbf{x})], \ \mathbf{x} = (x_1, x_2, \dots, x_N) \in \mathbf{R}^N,$$
 (1)

under constraints defined as

$$g_i(\mathbf{x}) \leq 0, \quad i = 1, \dots, K,$$

 $h_i(\mathbf{x}) = 0, \quad i = 1, \dots, P.$ (2)

For structural design optimization, x is an N-dimensional vector called the design vector, representing design variables of N structural components to be optimized, and f(x) is the objective function. In addition, $g_i(x)$ and $h_i(x)$ are inequality and equality constraints, respectively. They represent constraints, which the design must satisfy, such as stress and displacement limits. Moreover, F[f(x)] is the fitness function that is defined as a figure of merit.

It is not possible to directly utilize GAs to solve the above problem due to the presence of constraints. In GAs, constraints are usually handled by using the concept of penalty functions, which penalize infeasible solutions, i.e.,

$$F^{u}(\mathbf{x}) = F(\mathbf{x})$$
 if $\mathbf{x} \in \widetilde{\mathbf{F}}$,
 $F^{u}(\mathbf{x}) = F(\mathbf{x}) - P(\mathbf{x})$ otherwise, (3)

where $\tilde{\mathbf{F}}$ denotes the feasible search space. Here, $P(\mathbf{x})$ is a penalty function whose value is greater than zero. In addition, $F^{a}(\mathbf{x})$ represents an augmented fitness function after the penalty. Several forms of penalty functions have been proposed in the literature [6,8,15,18]. Nevertheless, most of them can be written in the following general form, i.e.,

$$P(\mathbf{x}) = \sum_{i=1}^{K} (\lambda_G)_j [G_i(\mathbf{x})]^{\beta} + \sum_{i=1}^{P} (\lambda_H)_j [H_j(\mathbf{x})]^{\beta}, \tag{4}$$

where

$$G_i(\mathbf{x}) = \max[0, g_i(\mathbf{x})].$$

$$H_i(\mathbf{x}) = \operatorname{abs}[h_i(\mathbf{x})].$$
(5)

Here, $G_j(\mathbf{x})$ and $H_j(\mathbf{x})$ represent the degrees of inequality and equality constraint violations, respectively. In addition, $(\lambda_G)_i$, $(\lambda_H)_j$ and β are constants. In most cases, the same value is used for all $(\lambda_G)_i$'s and $(\lambda_H)_j$'s. As for β , it is usually set to be 1 or 2. The degree of penalty can be controlled by adjusting the values of the coefficients $(\lambda_G)_j$'s and $(\lambda_H)_j$'s. These coefficients do not have physical meanings. Clearly, it is impossible to judiciously select appropriate values for them. Even though in common practice, one value is used for all $(\lambda_G)_j$'s and $(\lambda_H)_j$'s, which significantly simplifies the situation, the appropriate value of this one coefficient is still not obvious.

In the first operator in GAs, the reproduction operator, a mating pool is created by letting individuals with higher fitness values have higher chance to be selected into the mating pool. Many reasonable selection algorithms are possible. However, the most widely used technique is proportional selection. In this technique, the probability of the *i*th individual to be selected into the mating pool is

$$p(\mathbf{x}_t) = \frac{F^{\mathbf{d}}(\mathbf{x}_t)}{\sum_{j=1}^{n} F^{\mathbf{d}}(\mathbf{x}_j)}.$$
 (6)

where \mathbf{x}_i represents the *i*th individual in the population and *n* is the population size. Clearly, in the above equation, it is essential that all fitness values be positive. Therefore, the obtained fitness function after the penalty $F^a(\mathbf{x})$ may not be directly usable as its values may be negative. Moreover, the difference between the fitness values of the best individuals and average individuals

varies generation by generation. In early generations, the difference can be very large and the best individuals become relatively too strong. As a result, premature convergence may be obtained. In later generations, the difference can be very small and average individuals become almost as strong as the best individuals. As a result, the search may become a random walk. To prevent all of these problems, an augmented fitness function is usually scaled into a specified positive range. Many fitness scaling schemes have been proposed in the literature [11,15,16,18,28].

3. Adaptive penalty function

It can be easily seen that penalty schemes used in GAs play a very important role in the performance of GAs. This role becomes even more important when the optimal solution lies on or close to the boundary between the feasible and infeasible search spaces, which is very usual for structural design optimization. In this study, a new penalty scheme that is free from the disadvantages of existing schemes discussed earlier is proposed. To make the scheme simple, a simple form of the penalized fitness function is employed, i.e.,

$$F_i^{\mathbf{a}} = F^{\mathbf{a}}(\mathbf{x}_i) = F(\mathbf{x}_i) - P(\mathbf{x}_i) = F(\mathbf{x}_i) - \lambda(t)E(\mathbf{x}_i), \tag{7}$$

where F_i^a represents the fitness function of the *i*th individual after the penalty. Here, $\lambda(t)$ is a factor of an error term $E(\mathbf{x}_i)$. The factor $\lambda(t)$ varies with generation, and the generation number is denoted by t. In this study, the error term $E(\mathbf{x}_i)$ is defined as

$$E(\mathbf{x}_i) = \sum_{j=1}^{K} G_j(\mathbf{x}_i) + \sum_{j=1}^{P} H_j(\mathbf{x}_i),$$
 (8)

where $G_j(\mathbf{x}_i)$ and $H_j(\mathbf{x}_i)$ have already been defined in Eq. (5).

Now, the question is what the magnitude of the factor $\lambda(t)$ should be. It is not difficult to imagine that if the factor is too small, infeasible individuals with high original fitness values may have penalized fitness values higher than the fitness value of the feasible optimal individual. If this happens, the population in subsequent generations will move toward false peaks that appear in the infeasible region. On the contrary, if the factor is too large, good characteristics in some infeasible individuals will have no chance to survive and will disappear rapidly. This may lead to premature convergence and the obtained solution can be quite wrong.

To avoid the above problems, the degree of penalty must be enough to make the feasible optimal solution have the maximum fitness value, compared with all individuals (feasible and infeasible) after the penalty. However, the penalty must not be made much stronger than that. To this end, the following condition is introduced, i.e.,

$$F^{a}(\mathbf{x}_{i}) \leq \phi(t)F_{\text{avg}}^{a,F} \quad \text{for } \forall \mathbf{x}_{i} \in \widetilde{\mathbf{U}}$$
 (9)

in which $\widetilde{\mathbf{U}}$ represents the infeasible search space. Here, $F_{\mathrm{avg}}^{\mathbf{a},\mathbf{\hat{F}}}$ denotes the average fitness value of all feasible individuals in the generation and $\phi(t)$ is a factor of $F_{\mathrm{avg}}^{\mathbf{a},\mathbf{\hat{F}}}$.

The above condition sets the maximum fitness value of infeasible individuals in the generation t to be equal to $\phi(t)F_{\text{arg}}^{a,f}$. At this moment, it is not useful to consider the physical meaning of the coefficient $\phi(t)$ yet because the penalized fitness function will have to be scaled afterwards. Therefore, it is enough to simply say that the coefficient $\phi(t)$ is used to adjust the strength of the penalty in the generation. A way to obtain the value of this coefficient will be explained shortly.

The condition in Eq. (9) is satisfied by employing an appropriate value of the factor $\lambda(t)$ in Eq. (7). For each infeasible individual, the factor $\lambda(t)$ that makes the penalized fitness value of that infeasible individual exactly equal to $\phi(t)F_{\text{avg}}^{\text{a.f.}}$ is computed. After that, values of the factor $\lambda(t)$ obtained from all infeasible individuals are compared and the maximum one is selected as the real $\lambda(t)$. If the maximum value is negative, zero is used instead. In short, $\lambda(t)$ can be expressed as

$$\lambda(t) = \max\left(0, \max_{\forall \mathbf{x}_i \in \hat{\mathbf{U}}} \left[\frac{F(\mathbf{x}_i) - \phi(t) F_{\mathsf{avg}}^{\mathsf{a.f.}}}{E(\mathbf{x}_i)} \right] \right). \tag{10}$$

Eq. (10) insures that Eq. (9) is satisfied.

In this study, a modified bilinear scaling technique as shown in Fig. 1 is employed for fitness scaling. The minimum scaled fitness is set to be 0 to avoid negative fitness values while the scaled fitness of the average fitness of all feasible individuals is set to be 1. Furthermore, the maximum scaled fitness that is to be obtained from the best feasible members is set to be C. Thus, the chance of the best members being selected into the mating pool is equal to C times that of the average feasible members. All together, the scaled fitness can be written as

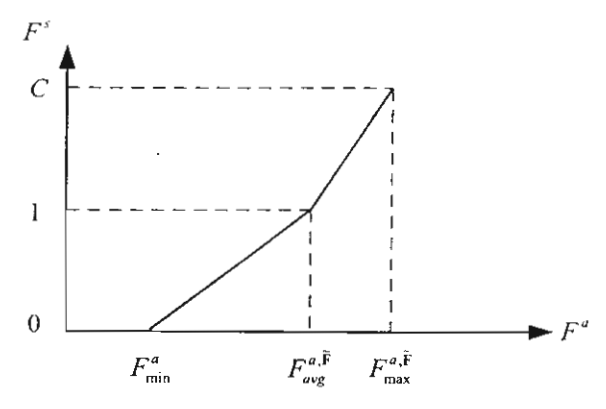


Fig. 1. Bilinear fitness scaling.

$$F^{s}(\mathbf{x}) = \frac{C - 1}{F_{\text{max}}^{a,\hat{\mathbf{F}}} - F_{\text{avg}}^{a,\hat{\mathbf{F}}}} F^{a}(\mathbf{x}) + \frac{F_{\text{max}}^{a,\hat{\mathbf{F}}} - CF_{\text{avg}}^{a,\hat{\mathbf{F}}}}{F_{\text{max}}^{a,\hat{\mathbf{F}}} - F_{\text{avg}}^{a,\hat{\mathbf{F}}}}$$
if $F^{s}(\mathbf{x}) \ge F_{\text{avg}}^{a,\hat{\mathbf{F}}}$,
$$F^{s}(\mathbf{x}) = \frac{1}{F_{\text{avg}}^{a,\hat{\mathbf{F}}} - F_{\text{min}}^{a}} F^{a}(\mathbf{x}) + \frac{F_{\text{min}}^{a}}{F_{\text{min}}^{a} - F_{\text{avg}}^{a,\hat{\mathbf{F}}}}$$
if $F^{a}(\mathbf{x}) \le F_{\text{avg}}^{a,\hat{\mathbf{F}}}$,
$$(11)$$

where $F^s(\mathbf{x})$ denotes the scaled fitness function. In addition, F^a_{\min} denotes the minimum fitness value after the penalty while $F^{a,\dot{x}}_{\max}$ denotes the fitness value of the best feasible members. This scaled fitness function $F^s(\mathbf{x})$ will be used in Eq. (6) instead of $F^a(\mathbf{x})$.

For all generations, the chance of the best infeasible members being selected into the mating pool is set to be equal to φ times that of the average feasible members, i.e.,

$$F^{s}(\mathbf{x}_{i}) \leq (\varphi F_{avg}^{s,\dot{\mathbf{F}}} = \varphi) \quad \text{for } \forall \mathbf{x}_{i} \in \widetilde{\mathbf{U}},$$
 (12)

where $F_{\text{avg}}^{\text{s.f.}}$ is the scaled value of the average fitness of all feasible individuals, which is equal to 1. Note that φ is constant for all generations. From the above condition, $\phi(t)$ in Eq. (9) is expressed in terms of φ as

$$\phi(t) = \frac{CF_{\text{avg}}^{\hat{\mathbf{a}},\hat{\mathbf{F}}} + F_{\text{max}}^{\hat{\mathbf{a}},\hat{\mathbf{F}}}(\varphi - 1) - \varphi F_{\text{avg}}^{\hat{\mathbf{a}},\hat{\mathbf{F}}}}{(C - 1)F_{\text{avg}}^{\hat{\mathbf{a}},\hat{\mathbf{F}}}} \quad \text{for } \varphi \ge 1, \quad (13a)$$

$$\phi(t) = \frac{F_{\min}^a + \varphi F_{\text{avg}}^{a,F} - \varphi F_{\min}^a}{F_{\text{avg}}^{a,F}} \quad \text{for } \varphi \leqslant 1.$$
 (13b)

In real calculations, the coefficient φ will be set at the beginning of the calculation. This coefficient has a very clear physical meaning, i.e., the chance to be selected into the mating pool of the best infeasible members compared with that of the average feasible members. This physical meaning is directly related to the degree of penalty. In addition, the coefficient does not have any units. Due to these reasons, it is possible to set this coefficient by using experience. After φ is set, $\varphi(t)$ and, subsequently, $\lambda(t)$ can be computed. In case of $\varphi \ge 1$, $\phi(t)$ can be obtained from Eq. (13a) directly because all parameters in the equation are readily available. In this case, the parameters $F_{\text{avg}}^{a,F}$ and $F_{\text{max}}^{a,F}$ can be obtained directly from original fitness values of feasible individuals without any penalty consideration. On the contrary, if $\varphi < 1$, $\phi(t)$ cannot be obtained without iteration since one of the parameters, i.e., F_{\min}^{u} , is not readily available. Note that F_{\min}^a is the minimum fitness in the generation after the penalty and it is most likely that F_{\min}^a will belong to infeasible members. This F_{\min}^a can be obtained from Eq. (7) which, in turn, requires the value of $\phi(t)$ (see Eq. (10)). Nevertheless, the iteration is very simple and takes almost no time to perform. To

this end, the individual $x_{F_{inlin}^a}$ that gives the minimum augmented fitness value is considered. Here, Eq. (7) yields

$$F_{\min}^{a} = F^{a}\left(\mathbf{x}_{F_{\min}^{a}}\right) = F\left(\mathbf{x}_{F_{\min}^{a}}\right) - \lambda(t)\mathcal{E}\left(\mathbf{x}_{F_{\min}^{a}}\right). \tag{14}$$

Also, consider the individual x_{λ} that gives the value of $\lambda(t)$ in Eq. (10), i.e.,

$$\lambda(t) = \max\left(0, \max_{\forall \mathbf{x}_i \in \hat{\mathbf{U}}} \left[\frac{F(\mathbf{x}_i) - \phi(t) F_{avg}^{a, \hat{\mathbf{F}}}}{E(\mathbf{x}_i)} \right] \right) \\
= \frac{F(\mathbf{x}_{\lambda}) - \phi(t) F_{avg}^{a, \hat{\mathbf{F}}}}{E(\mathbf{x}_i)}.$$
(15)

Using Eq. (15) in Eq. (14) gives

$$F_{\min}^{a} = F\left(\mathbf{x}_{F_{\min}^{a}}\right) - \left(\frac{F(\mathbf{x}_{\lambda}) - \phi(t)F_{\text{avg}}^{a,F}}{E(\mathbf{x}_{\lambda})}\right)E\left(\mathbf{x}_{F_{\min}^{a}}\right). \tag{16}$$

Substituting Eq. (16) into Eq. (13b) yields

$$\phi(t) = \left\{ (\varphi - 1) \mathcal{E} \left(\mathbf{x}_{F_{\min}^a} \right) F(\mathbf{x}_{\lambda}) + \mathcal{E}(\mathbf{x}_{\lambda}) \left[F \left(\mathbf{x}_{F_{\min}^a} \right) + \varphi F_{\text{avg}}^{a, \hat{F}} - \varphi F \left(\mathbf{x}_{F_{\min}^a} \right) \right] \right\} / \left\{ F_{\text{avg}}^{a, \hat{F}} \left[\mathcal{E}(\mathbf{x}_{\lambda}) + (\varphi - 1) \mathcal{E} \left(\mathbf{x}_{F_{\min}^a} \right) \right] \right\}.$$

$$(17)$$

A problem is that the individuals \mathbf{x}_{λ} and $\mathbf{x}_{F_{\min}^a}$ are not known from the beginning and iteration is required. In the first step of the iteration, it is assumed that $F_{\min}^a = F_{\text{avg}}^{a,F}$. By using Eq. (13b), the intermediate value of $\phi(t)$ for this step of the iteration is obtained, i.e., $\phi(t) = 1$. After that, the intermediate value of $\lambda(t)$ is obtained from Eq. (10) and at the same time the individual \mathbf{x}_{λ} can be identified. With the obtained $\lambda(t)$, the individual $\mathbf{x}_{F_{\min}^a}$ can be subsequently identified from Eq. (7). Consequently, the value of $\phi(t)$ for the next step of the iteration is computed from Eq. (17). The process is repeated until the value of $\phi(t)$ becomes unchanging.

To be able to understand the proposed scheme better, let us consider an optimization problem of a uniaxial bar shown in Fig. 2. A uniaxial force of 10 lb is applied at the free end of the bar. Allowable stress is assumed to be 2 psi. Our task is to find the optimal area of the bar that yields minimum volume. For illustrative purpose, it is



Fig. 2. Illustrative example-uniaxial problem.

assumed that the area of the bar is a continuous variable and, as a result, the optimal solution is simply equal to 5 in.² Suppose that GAs are used to obtain the solution and the fitness function is defined as

$$F \text{ (Area)} = \frac{1}{1 + \text{Volume (in.}^3)}$$

$$= \frac{1}{1 + \text{Area (in.}^2) \times \text{Length (in.)}}.$$
(18)

From this fitness function, it is obvious that the smaller the area is, the larger the fitness value will be (see Fig. 3). Nevertheless, the area cannot be smaller than 5 in.2; otherwise, the bar will violate the stress constraint. Therefore, fitness values of those individuals that violate the constraint have to be reduced. In this example, 19 individuals with different areas ranging from 1 to 19 in.² are assumed (see Fig. 3). In the proposed penalty scheme, the average fitness of all feasible members $F_{avo}^{a,\hat{\mathbf{f}}}$ is calculated. If there are any individuals that have their fitness values exactly equal to $F_{avg}^{a,\hat{F}}$, they are the average feasible members. Nevertheless, in real calculations, it does not matter whether there are any of them or not in the population since only the value of their fitness $F_{\text{avg}}^{\text{a.F}}$ is to be used. In the proposed scheme, infeasible members are penalized in such a way that the best infeasible members have scaled fitness values equal to φ times that of the average feasible members. Fig. 5 illustratively shows scaled fitness values after the penalty and scaling when $\varphi = 1.0$ and 1.5 while Fig. 4 shows fitness values just after the penalty but before the scaling. Note that, in this example, the maximum fitness is scaled to be 2.0 while the average fitness of feasible members is scaled to be 1.0. In addition, the minimum fitness is scaled to be 0. By adjusting the value of φ , the degree of penalty can be efficiently adjusted.

In fact, the purpose of the proposed scheme is to fix, throughout the calculation, the relative chance of the

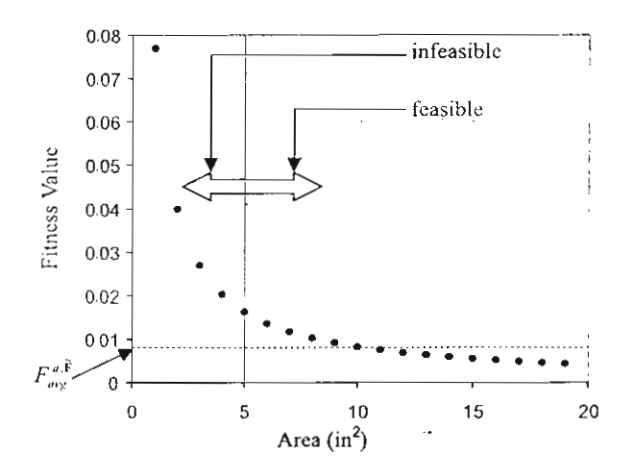


Fig. 3. Original fitness value—uniaxial problem.

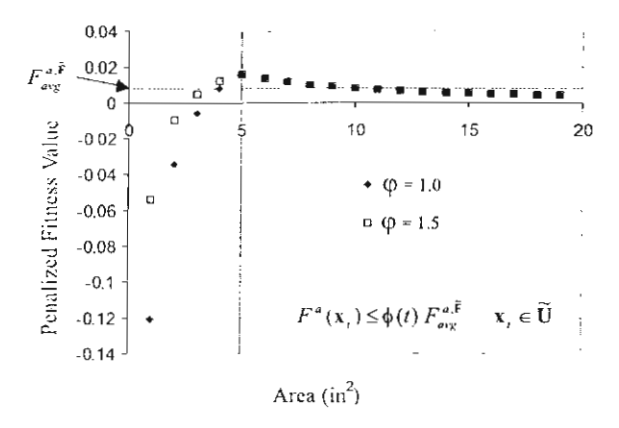


Fig. 4. Fitness value after the penalty—uniaxial problem.

best infeasible members being selected into the mating pool compared with that of the average feasible members. This means that the penalty is always adjusted so that the aforementioned purpose is achieved in all generations. This guarantees that the desired degree of penalty is obtained throughout the evolution process. Consequently, the problem of too weak or too strong a penalty during different phases of the evolution is removed. Note that the relative scaled fitness values of the best feasible members and the average feasible members are set via fitness scaling (see Fig. 1). As a result, the relative chance of the best feasible members being selected into the mating pool compared with that of the best infeasible members can also be controlled. For example, when φ is set to be 1.0 in the current example, the chance of the best feasible members to be selected becomes two times that of the best infeasible members since, from the fitness scaling, the chance of the best feasible members is set to be two times that of the average feasible members.

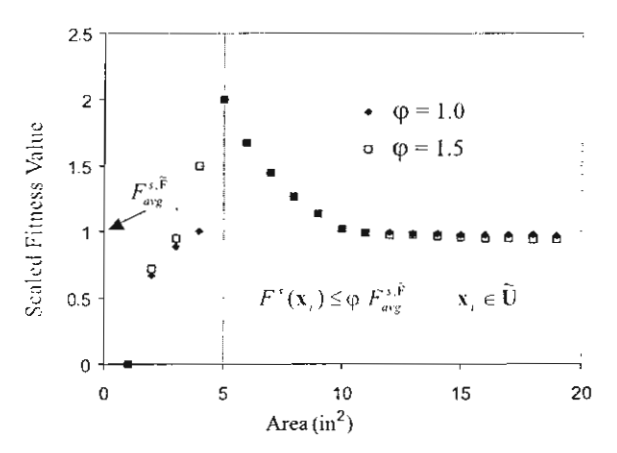


Fig. 5. Fitness value after the scaling—uniaxial problem.

In this study, since the fitness scaling in Fig. 1 is employed, acceptable values of φ therefore lie between 0 and C. Note that C is the scaled fitness of the best feasible individuals. Using only positive values for φ is obviously necessary because only positive scaled fitness values are acceptable. Setting φ exactly equal to zero is actually equivalent to using the death penalty scheme, which simply rejects infeasible solutions from the population. Using φ that is greater than C is in fact possible but it will mean that the best infeasible individuals will have a better chance to be selected into the mating pool than the best feasible ones. This is obviously too harsh a penalty. For this reason, the value of φ should not exceed C. For any value of φ between 0 and C, the best feasible individuals always have the maximum fitness value among all other individuals in the generation. Nevertheless, depending on the magnitude of φ , some infeasible members may have higher fitness than a certain number of feasible ones (see Fig. 5).

Actually, the key point in the development of the proposed scheme is that the user-specified penalty parameter φ is defined based on the relationship between two fitness values that are already scaled. Since scaled fitness values are directly used in the selection for the mating pool without further modification, the physical meaning of the proposed penalty parameter can be preserved. If penalty parameters are defined before the fitness scaling is performed, the fitness scaling will probably destroy the desired physical meanings of the parameters.

Since the proposed penalty scheme requires the average fitness value over all feasible individuals, it is necessary to have at least one feasible individual in the population. In the case that there is none, the fitness values of infeasible individuals will be given based on the magnitudes of error they have. The idea is to strongly encourage the population to move toward the feasible region. Here, a bilinear scaling scheme as shown in Fig. 6 is used. Fitness is scaled in such a way that scaled fitness values of individuals with the highest error are equal to 0 and scaled fitness values of individuals with average error are equal to 1. In addition, scaled fitness

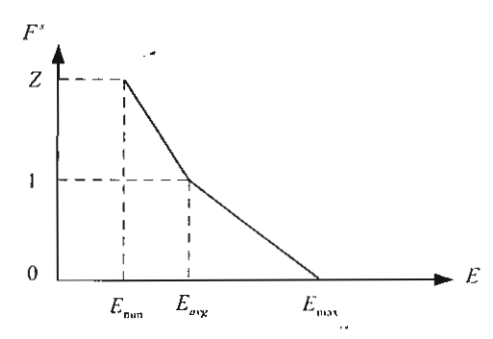


Fig. 6. Bilinear fitness scaling for the case when no feasible individual is available.

values of individuals with the smallest error are set to be Z. Thus, the chance of the individuals with the smallest error being selected into the mating pool is equal to Z times that of the individuals with average error. In summary, the scaled fitness is expressed as

$$F^{s}(\mathbf{x}) = \frac{Z - 1}{E_{\min} - E_{\text{avg}}} E(\mathbf{x}) + \frac{E_{\min} - ZE_{\text{avg}}}{E_{\min} - E_{\text{avg}}} \quad \text{if } E(\mathbf{x}) \leqslant E_{\text{avg}};$$

$$F^{s}(\mathbf{x}) = \frac{1}{E_{\text{avg}} - E_{\text{indx}}} E(\mathbf{x}) + \frac{E_{\max}}{E_{\max} - E_{\text{avg}}} \quad \text{if } E(\mathbf{x}) > E_{\text{avg}}.$$
(19)

4. Results

To investigate the validity and efficiency of the proposed penalty scheme, the scheme is used in design optimization of three different two-dimensional structures, i.e., a six-bar truss, a ten-bar truss, and a one-bay eightstory frame. To be able to see clearly the advantages of the proposed scheme over conventional schemes, particularly in terms of robustness, obtained results are compared with those from a selected conventional scheme. Since most conventional schemes are based on the same concept with slightly different details, comparison with one selected conventional scheme is sufficient to show advantages of the proposed scheme over conventional schemes. As already mentioned, the main objective of this study is to develop an adaptive penalty scheme that is robust and still able to reproduce the same quality of results as ones obtained from GAs found in the literature. To show this comparison of the proposed method, results are also compared with existing results in the literature.

4.1. Six-bar truss

The first problem to be considered is the six-bar truss as shown in Fig. 7. Here, only sizing optimization is considered. Thus, design variables are six sectional areas of the six members of the truss. The cross-sectional area of each member is taken from the following 32 discrete values, i.e., 1.62, 1.80, 2.38, 2.62, 2.88, 3.09, 3.13, 3.38, 3.63, 3.84, 3.87, 4.18, 4.49, 4.80, 4.97, 5.12, 5.74, 7.22, 7.97, 11.5, 13.5, 13.9, 14.2, 15.5, 16.0, 18.8, 19.9, 22.0, 22.9, 26.5, 30.0, and 33.5 in.² Therefore, a five-bit string is required for each design variable. There are two types of constraint in this problem, i.e., stress and displacement constraints. Design parameters used in the problem are shown in Table 1.

For comparison, the most popular conventional penalty form is selected, i.e.,

$$F_i^a = F^a(\mathbf{x}_i) = F(\mathbf{x}_i) - P(\mathbf{x}_i) = F(\mathbf{x}_i) - \lambda E(\mathbf{x}_i). \tag{20}$$

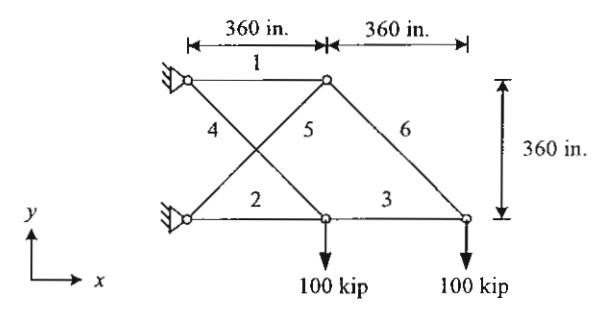


Fig. 7. Six-bar truss.

where the coefficient λ is constant and the error term $E(\mathbf{x}_i)$ is the same as that defined in Eq. (8). In both proposed and conventional schemes, the fitness function $F(\mathbf{x}_i)$ is defined as

$$F(\mathbf{x}_i) = \frac{1}{1 + \text{Weight}(\mathbf{x}_i)},\tag{21}$$

where two different units of weight, i.e., pound (lb) and newton (N) are used. Two units are used in order to investigate the effect of unit on the results from both schemes.

Since it is impossible to judiciously estimate an appropriate value of the coefficient λ in the conventional scheme, a wide range of values will be used. All GA parameters used in this problem can be found in Table 1. To start the calculation, an initial population is generated at random. The type of crossover operator used here is the one-point crossover [15].

Table 1
Design and GA parameters for the six-bar truss problem

Design parameters		GA parameters	
Item	Value	Item	Value
Modulus of elasticity	10 ⁷ psi	Maximum number of generations	100
Weight density	0.1 lb/in.3		
Allowable ten- sile stress	25,000 psi	Population size	70
Allowable compressive stress	25,000 psi	Crossover probability	0.8
		Mutation probability	0.001
Maximum y- displacement	2 in.	φ	0.25-1.75
-		λ	0.000001 - 100
		C	2.0
		Z .	5.0

Fig. 8 shows results obtained from the proposed and conventional schemes. Each point in the graph represents an average weight of the best feasible designs obtained from 200 different runs. The results obtained by using newtons in Eq. (21) are converted into pounds for comparison. In the conventional scheme, the coefficient λ is varied exponentially from 0.000001 to 100 while in the proposed scheme the coefficient φ is varied from 0.25 to 1.75. Note that the value of φ should be varied between 0 to 2.0 since the maximum scaled fitness value C is set to be 2.0 (see Table 1). It can be clearly seen from the results that the proposed scheme is more robust than the conventional scheme. In the proposed scheme, changing the unit has little effect on the results while in the conventional scheme the effect is much more noticeable. Moreover, in the proposed scheme, it is easier to notice a trend in the results when φ is varied. It can be reasonably said that good results are obtained with values of φ around 0.75–1.0. On the contrary, it is much more difficult to observe this kind of trend in the results of the conventional scheme as they are very much scattered and exhibit no recognizable pattern. Although the trend in the results of the proposed scheme can be observed, it is also important to note that, when φ is varied, the results of the proposed scheme actually vary to a much lesser degree than the results of the conventional scheme do when λ is varied. Even though it may be argued that, in this study, λ is exponentially changed while φ is linearly changed, the same difference in the way that the parameters are varied and tried is expected in the real practice. This is because, in the real practice, it will also be impossible to estimate appropriate values of the coefficient λ in the conventional scheme, so a very wide range of values must be tested. With the proposed scheme, lesser sensitivity of results to the magnitude of the parameter ensures that even when the appropriate value of φ is not clearly known, a range of values of φ may be used and reasonable results can still be obtained. This fact really confirms the robustness of the proposed scheme.

To ensure that the proposed scheme is capable of giving results of the same quality as those GAs found in the literature, the best result obtained from the proposed scheme is also compared with the best result reported by Rajan [9]. They are exactly the same. The details of the results are shown in Table 2. It must be noted that in this study, except for the new penalty algorithm, the rest of the algorithms are standard. This is not the case for the work by Rajan [9], which employs more complicated GAs.

4.2. Ten-bar truss

The next problem to be considered is the ten-bar truss as shown in Fig. 9. This problem is one of the

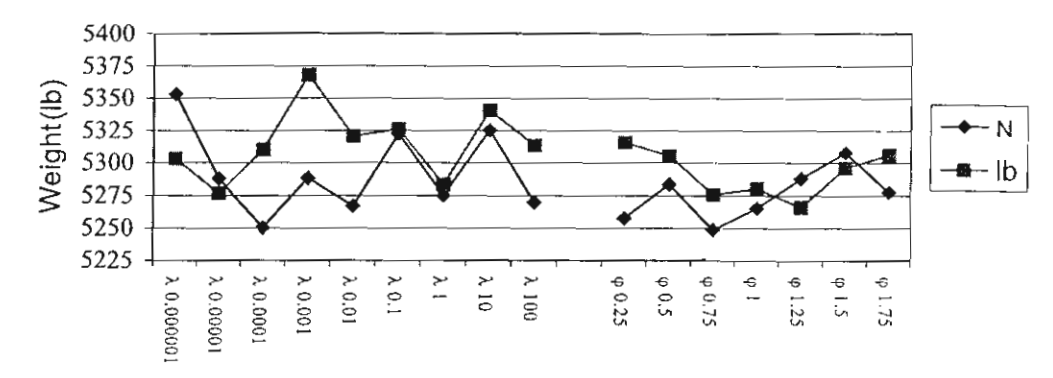


Fig. 8. Average weight of the best feasible designs obtained from 200 runs—six-bar truss.

Table 2 Comparison of the results for the six-bar truss problem

Member	Size of member (in.2)			
	Proposed	Ref. [9]]	
1	30.0	30.0		
2	19.9	19.9		
3	15.5	15.5		
4	7.22	7.22		
5	22.0	22.0		
6	22.0	22.0		
Total weight (lb)	4962.1	4962.1		

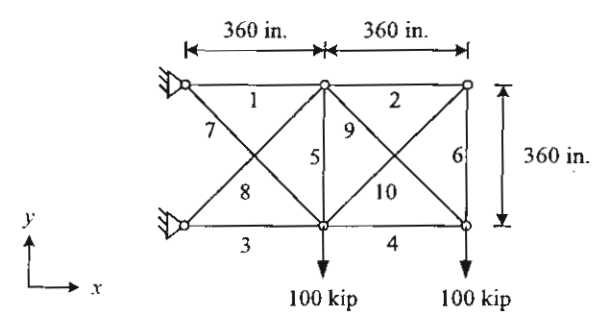


Fig. 9. Ten-bar truss.

benchmark problems used to test optimization methods. Also in this problem, only sizing optimization is considered. Therefore, design variables are ten sectional areas. Cross-sectional areas of members 1, 3, 4, 7, 8 and 9 are taken from the following 32 discrete values, i.e., 3.13, 3.38, 3.47, 3.55, 3.63, 3.84, 3.87, 3.88, 4.18, 4.22, 4.49, 4.59, 4.80, 4.97, 5.12, 5.74, 7.22, 7.97, 11.5, 13.5, 13.9, 14.2, 15.5, 16.0, 16.9, 18.8, 19.9, 22.0, 22.9, 26.5, 30.0, and 33.5 in.² For the rest of the members, the cross-sectional areas are taken from the following 32 discrete values, i.e., 1.62, 1.80, 1.99, 2.13, 2.38, 2.62, 2.63, 2.88, 2.93, 3.09, 3.13, 3.38, 3:47, 3.55, 3.63, 3.84,

Table 3

Design and GA parameters for the ten-bar truss problem

Design parameters		GA parame	ters
ltem	Value	Item	Value
Modulus of elasticity	10 ⁷ psi	Maximum number of	100
Weight density	0.1 lb/in. ³	genera- tions	
Allowable ten- sile stress	25,000 psi	Population size	40
Allowable com- pressive stress	25,000 psi	Crossover probability	0.8
Maximum x, y displacements	2 in.	Mutation probability	0.001
		φ	0.25 - 1.75
		į.	0.000001-100
		C	2.0
		Z	5.0

3.87, 3.88, 4.18, 4.22, 4.49, 4.59, 4.80, 4.97, 5.12, 5.74, 7.22, 7.97, 11.5, 13.5, 13.9, and 14.2 in.² Similar to the previous problem, a five-bit string is required for each design variable. Design parameters and genetic parameters are shown in Table 3.

Results obtained from the proposed and conventional schemes are shown in Fig. 10. Similar to the previous problem, each point in the graph represents an average weight of the best feasible designs obtained from 200 different runs. The robustness of the proposed scheme is again obvious. The effect of the unit used on the results from the proposed scheme is noticeably less than that on the results from the conventional scheme. Moreover, the results from the proposed scheme also exhibit a rather clear tendency with respect to the value of the coefficient used while those from the conventional scheme do not, and are quite scattered. In the proposed scheme, it can be reasonably said that good results are obtained with values of φ around 0.5–0.75. Similar to the previous problem, even though the trend in the

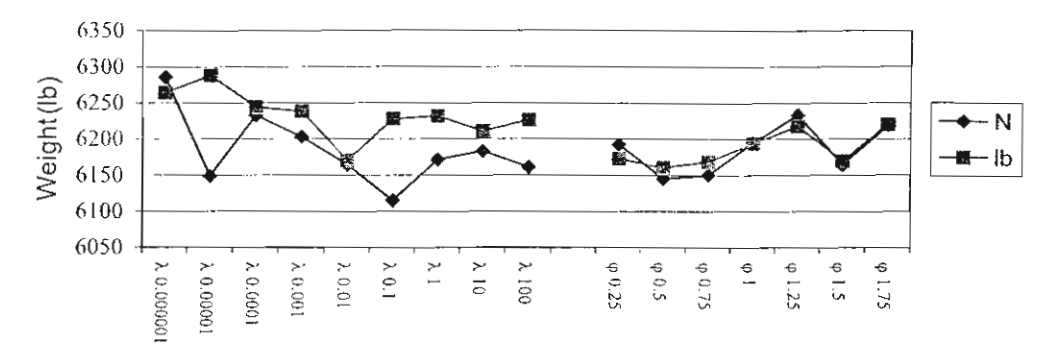


Fig. 10. Average weight of the best feasible designs obtained from 200 runs—ten-bar truss.

Table 4
Comparison of the results for the ten-bar truss problem

Member	Size of me	mber (in.	2))			
	Proposed	Ref. [19]	Ref. [21]	Ref. [29]			
1	33.5	33.5	30.0	33.5			
2	1.62	1.62	1.62	1.62			
3	22.9	22.0	26.5	22.0			
4	15.5	15.5	13.5	14.2			
5	1.62	1.62	1.62	1.62			
6	1.62	1.62	1.62	1.62			
7	7.22	14.2	7.22	7.97			
8	22.9	19.9	22.9	22.9			
9	22.0	19.9	22.0	22.0			
10	1.62	2.62	1.62	1.62			
Total weight (lb)	5499.3	5613.8	5556.9	5458.3			

results of the proposed scheme can be observed, the results are not that much sensitive to the magnitude of the penalty parameter when compared with the conventional scheme. Consequently, a range of values of φ may be used when the appropriate value is not known. The best result obtained from the proposed scheme is also compared with the best results reported by Rajeev and Krishnamoorthy [19], Camp et al. [21], and Galante [29] in Table 4. It can be seen that the result obtained from the proposed penalty scheme is relatively good although Rajeev and Krishnamoorthy [19], Camp et al. [21], and Galante [29] employ more complicated GAs.

In the previous six-bar truss problem, the appropriate value of φ is around 0.75-1.0, which is similar to the value obtained for the ten-bar truss problem. Since the two problems are quite similar, similar values of the coefficient from the two problems are expected. In this aspect, the proposed scheme evidently outperforms the conventional scheme, which does not exhibit any obvious similarity between these two problems. Having similar

appropriate values of the coefficient for similar problems allows the coefficient to be set by experience. Since the coefficient in the proposed scheme has a physical meaning, which directly corresponds to the understandable degree of penalty, the characteristics of the problems being solved can be directly related to the appropriate degree of penalty. This kind of advantage may not be found in existing conventional schemes.

4.3. One-bay eight-story frame

The last problem to be considered is the one-bay eight-story frame as shown in Fig. 11. Similar to the previous two problems, only sizing optimization is considered. The 24 members of the structure are categorized

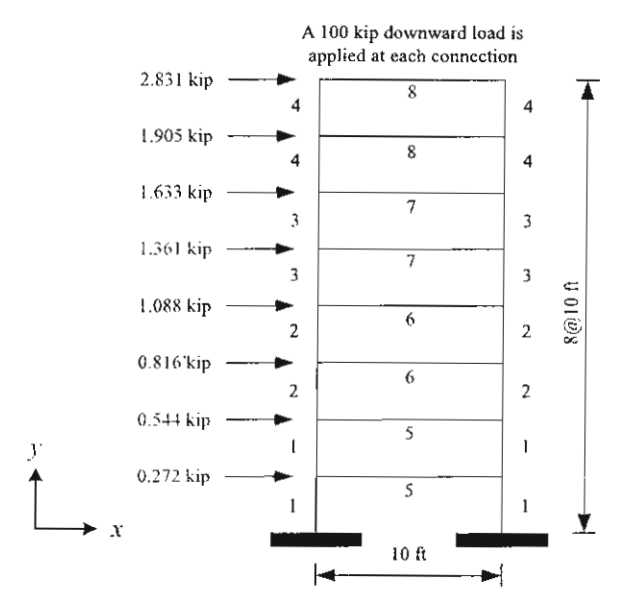


Fig. 11. One-bay eight-story frame.

Table 5
Design and GA parameters for the one-bay eight-story frame problem

Design parameters		GA parameters		
Item	Value	Item	Value	
Modulus of elasticity	29 × 10³ ksi	Maximum number of generations	100	
Weight density	2.83×10^{-4} kip/in. ³			
Maximum x- displacement at the top of	2 in.	Population size	50	
the structure		Crossover probability	0.85	
		Mutation probability	0.05	
		φ	0.25 - 1.75	
		À	0.000001-100	
		C	2.0	
		Z	5.0	

into eight groups (as indicated in Fig. 11). In this problem, 256 sections are selected from a list of 268 W-sections from the American Institute of Steel Construction Allowable Stress Design (AISC-ASD) specifications given in Ref. [30] by discarding the 12 biggest sections from the list. Thus, an eight-bit string is required for each design variable. There is only a displacement constraint in the problem that is the maximum x-displacement at the top of the structure. Design and genetic parameters are shown in Table 5.

Fig. 12 shows results obtained from the proposed and conventional schemes. In the figure, each point in the graph also represents an average weight of the best feasible designs obtained from 200 different runs. Once

Table 6
Comparison of the results for the one-bay eight-story frame problem

Group number	Proposed	GAs [21]	Optimality criteria [21
1	W 12 × 45	W 18 × 46	W 14 × 34
2	$W 14 \times 34$	W 16×31	W 10 × 39
3	$W 12 \times 35$	W 16×26	W 10×33
4	W 10×19	W 12×16	W 8 × 18
5	$W 18 \times 35$	W 18×35	W 21 × 68
6	$W.18 \times 40$	W 18×35	W 24 × 55
7	W 16×36	W 18×35	W 21 × 50
8	W 16×26	W 16×26	W 12×40
Total weight (kip)	7.47	7.38	9.22

again, the robustness of the proposed scheme is confirmed. The effect of the unit on the results obtained from the proposed scheme is almost negligible. This conclusion is not true for the case of the conventional scheme, which exhibits large differences between the results from the two different units. In this problem, the insensitivity of the results to the value of the parameter is very apparent for the proposed scheme. On the contrary, the results from the conventional scheme show very high variation when the parameter is varied. This confirms the higher robustness of the proposed scheme over the conventional one. Although some of the averages of the best results from the conventional scheme shown in Fig. 12 may seem to be better than those from the proposed scheme, a comparison of the best result obtained from the proposed technique and results reported by Camp et al. [21] in Table 6 shows that the proposed method is actually acceptable. In their paper, Camp et al. [21] provide both results from their own GAs, which are not the standard GAs, and from the optimality criteria method [31].

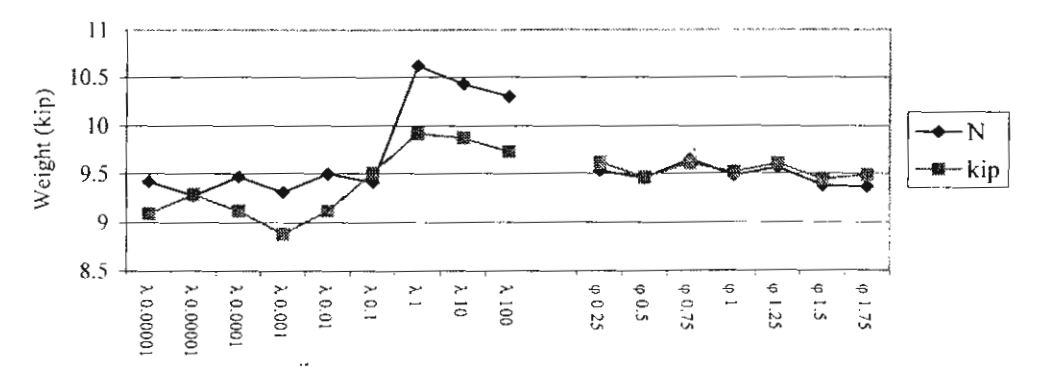


Fig. 12. Average weight of the best feasible designs obtained from 200 runs-one-bay eight-story frame.

5. Conclusion

This paper presents a new adaptive penalty scheme in GAs for structural design optimization. Existing penalty schemes generally require the values of some coefficients to be specified at the beginning of the calculation and these coefficients usually have no clear physical meanings. Consequently, it is very difficult to select appropriate values of these coefficients even by experience. Moreover, most existing schemes employ constant coefficients throughout the entire calculation. This may result in too weak or too strong a penalty during different phases of the evolution. To avoid these drawbacks, a new penalty scheme is proposed. The main concept of the proposed scheme is to fix, throughout all generations, the chance to be selected into the mating pool of the best infeasible members compared with that of the average feasible members. The parameter that has to be set is the ratio between the fitness value of the best infeasible members and the fitness value of the average feasible members. This ratio has a very clear physical meaning. Therefore, it can be set easily, based on experience of different types of problem. In addition, under this concept, the penalty is always adjusted so that the desired degree of penalty is achieved in all generations.

The proposed scheme is tested by using three optimization problems of truss and frame structures. Comparisons with a representative conventional scheme clearly show the advantages of the proposed method. From the results, it can be seen that the proposed scheme is very robust. The results from the proposed scheme do not significantly depend on the units used. In addition, for some problems, it will be possible to observe trends in the results of the proposed scheme when the magnitude of the coefficient is varied. Moreover, it can be expected that, if similar problems are considered, appropriate values of the coefficient will be similar. All these characteristics encourage setting the value of the coefficient by experience. It is also observed that the results of the proposed scheme do not exhibit high fluctuation when the penalty coefficient is varied. As a result, even when appropriate values of the coefficient are not clearly known, a range of values may be used and reasonable results can still be obtained. Finally, comparisons with results from the literature also show that the proposed penalty scheme yields relatively good results although, except for the new penalty algorithm, the proposed technique employs very standard GAs.

Acknowledgements

The authors are grateful to the Thailand Research Fund (TRF) for providing financial support for this study.

References

- [1] Qian L, Zhong W, Sui Y, Zhang J. Efficient optimum design of structures-program DDDU. Comput Meth Appl Mech Eng 1982;30:209-24.
- [2] Templeman AB. Discrete optimum structural design. Comput Struct 1988;30(3):511-8.
- [3] Hall SK, Cameron GE, Grierson DE. Least-weight design of steel frameworks accounting for P-Δ effects. J Struct Eng 1989;115(6):1463-75.
- [4] Adeli H, Park HS. A neural dynamics model for structural optimization-theory. Comput Struct 1995;57(3):383– 90.
- [5] Tzan S, Pantelides CP. Annealing strategy for optimal structural design. J Struct Eng 1996;122(7):815–27.
- [6] Deb K. Optimization for engineering design: algorithms and examples. New Delhi: Prentice-Hall: 1995.
- [7] Rao SS. Engineering optimization. New York: Wiley; 1996.
- [8] Marcelin JL, Trompette P, Dornberger R. Optimization of composite beam structures using a genetic algorithm. Struct Optimiz 1995;9:236-44.
- [9] Rajan SD. Sizing, shape, and topology design optimization of trusses using genetic algorithm. J Struct Eng 1995;121(10):1480-7.
- [10] Ramasamy JV, Rajasekaran S. Artificial neural network and genetic algorithm for the design optimization of industrial roofs—a comparison. Comput Struct 1996;58(4):747-55.
- [11] Kallassy A, Marcelin JL. Optimization of stiffened plates by genetic search. Struct Optimiz 1997;13:134–41.
- [12] Rafiq MY, Southcombe C. Genetic algorithms in optimal design and detailing of reinforced concrete biaxial columns supported by a declarative approach for capacity checking. Comput Struct 1998:69:443-57.
- [13] Shrestha SM, Ghaboussi J. Evolution of optimum structural shapes using genetic algorithm. J Struct Eng 1998; 124(11):1331-8.
- [14] Marcelin JL. Evolutionary optimisation of mechanical structures: towards an integrated optimisation. Eng Comput 1999;15:326-33.
- [15] Goldberg DE. Genetic algorithms in search, optimization, and machine learning. Reading, Massachusetts: Addison-Wesley; 1989.
- [16] Grefenstette JJ. Optimization of control parameters for genetic algorithms. IEEE Trans Syst. Man. Cybernet 1986;SMC-16(1):122-8.
- [17] Dawid H. Adaptive learning by genetic algorithms: analytical results and applications to economic models. New York: Springer; 1999.
- [18] Michalewicz Z. Genetic algorithms + data structures = evolution programs. New York: Springer; 1996.
- [19] Rajeev S. Krishnamoorthy CS. Discrete optimization of structures using genetic algorithms. J Struct Eng 1992;118(5):1233-49.
- [20] Jenkins WM. On the application of natural algorithms to structural design optimization. Eng Struct 1997;19(4):302– 8.
- [21] Camp C, Pezeshk S. Cao G. Optimized design of twodimensional structures using a genetic algorithm. J Struct Eng 1998;124(5):551-9.

- [22] Adeli H, Cheng N. Integrated genetic algorithm for optimization of space structures. J Aerosp Eng 1993; 6(4):315-28.
- [23] Michalewicz Z. Genetic algorithms, numerical optimization, and constraints. In: Eshelman LJ, editor. Proceedings of the sixth international conference on genetic algorithms. San Francisco: Morgan Kaufmann; 1995.
- [24] Powell D, Skolnick MM. Using genetic algorithms in engineering design optimization with non-linear constraints. In: Forrest S, editor. Proceedings of the fifth international conference on genetic algorithms. San Mateo: Morgan Kaufmann; 1993.
- [25] Le Riche RG, Knopf-Lenoir C, Haftka RT. A segregated genetic algorithm for constrained structural optimization. In: Eshelman LJ, editor. Proceedings of the sixth international conference on genetic algorithms. San Francisco: Morgan Kaufmann; 1995.

- [26] Rasheed K.M. GADO: a genetic algorithm for continuous design optimization (doctoral dissertation). New Brunswick, New Jersey: The State University of New Jersey; 1998.
- [27] Coello CAC. Use of a self-adaptive penalty approach for engineering optimization problems. Comput Industry 2000;41:113-27.
- [28] Rajeev S, Krishnamoorthy CS. Genetic algorithms-based methodologies for design optimization of trusses. J Struct Eng 1997;123(3):350-8.
- [29] Galante M. Genetic algorithms as an approach to optimize real-world trusses. Int J Numer Meth Eng 1996;39:361–82.
- [30] Burns T. Structural steel design—LRFD. New York: Delmar; 1995.
- [31] Khot NS, Venkayya VB, Berke L. Optimum structural design with stability constraints. Int J Numer Meth Eng 1976;10:1097-114.

A NOVEL PENALTY SCHEME IN GENETIC ALGORITHMS FOR STRUCTURAL DESIGN OPTIMIZATION

Pruettha Nanakorn and Konlakarn Meesomklin

Sirindhorn International Institute of Technology, Thammasat University, Thailand

ABSTRACT

In genetic algorithms, constraints are mostly handled by using the concept of penalty functions, which penalize infeasible solutions by reducing their fitness values in proportion to the degrees of constraint violation. In most of the available penalty schemes, some coefficients or constants have to be specified at the beginning of the calculation. Since these coefficients usually have no clear physical meanings, it is nearly impossible to estimate the appropriate values of these coefficients even by experience. Moreover, most of the schemes employ constant coefficients throughout the entire calculation. This may result in too weak or too strong a penalty during different phases of the evolution. In this study, a new penalty scheme that is free from the aforementioned disadvantages is developed. The proposed penalty function will be able to adjust itself during the evolution in such a way that the desired degree of the penalty is always obtained. The coefficient used in the proposed scheme will have a clear physical meaning. Thus, it will not be difficult to set the value of the coefficient by using experience.

1. INTRODUCTION

It is commonly known that Genetic Algorithms (GAs) are directly applicable only to unconstrained optimization. Nevertheless, many researchers have proposed solutions that can eliminate this limitation. Constraints are mostly handled by using the concept of penalty functions, which penalize infeasible solutions by reducing their fitness values in proportion to their degrees of constraint violation. In all available penalty schemes, the degree of the penalty can be further controlled by means of setting values of various coefficients in the penalty functions^{1,2,3}. Most of these coefficients are treated as constants during the calculation and their values have to be specified at the beginning of the calculation^{4.5,6}. These coefficients usually have no clear physical meanings. Thus, it is nearly impossible to know the appropriate values of the coefficients even by experience. This is because it is very hard to understand the correlation between the values of the coefficients and the characteristics of the problems without physical meanings of the coefficients. Consequently, for all problems with either similar or different natures, the appropriate values of the coefficients are generally obtained by trial and error. Many researchers, however, have tried to suggest different ranges of appropriate values for these coefficients, for various types of problem. Most of these suggestions are obviously doubtful. The reason is simply

that the appropriate values are usually given without any reference to the units used in the problems although the coefficients may have units and the appropriate values should vary with the units used. Another important concern is that these conventional penalty schemes do not usually adjust the strength of the penalty during the calculation, as the coefficients used are always kept constant. As a result, too weak or too strong penalty during different phases of the evolution may occur. This may lead to inaccurate solutions. Actually, there are some penalty schemes that vary the values of the coefficients to adjust the strength of the penalty during the calculation^{7,8,9}. However, this kind of scheme usually requires the varying values of these coefficients to be manually specified. It, therefore, becomes even more difficult to judiciously select appropriate values for different phases of the calculation.

Keeping these facts in mind, we develop a new penalty scheme that is free from the above disadvantages in this study. The proposed penalty function will be able to adjust itself during the evolution in such a way that the desired degree of the penalty is always obtained. The coefficient used in the proposed scheme will have a clear physical meaning and it will have no unit. Thus, it will not be difficult to set the value of the coefficient by experience.

2. GENETIC ALGORITHMS FOR CONSTRAINED OPTIMIZATION

In GAs, an optimization problem can be generally written as

$$F(x) = F[f(x)] \tag{1}$$

under constraints defined as

$$g_i(x) \le 0, \quad i = 1, ..., K,$$

 $h_i(x) = 0, \quad i = 1, ..., P$
(2)

For the structural design optimization, x is an N-dimensional vector called the design vector, representing design variables of N structural components to be optimized and f(x) is the objective function. In addition, $g_i(x)$ and $h_i(x)$ are inequality and equality constraints, respectively. They represent constraints, which the design must satisfy, such as stress and displacement limits. Finally, F(x) is the fitness function which is defined as a figure of merit¹⁰.

It is not possible to directly utilize GAs to solve the above problem due to the presence of the constraints. In GAs, constraints are mostly handled by using the concept of penalty functions, which penalize infeasible solutions, i.e.,

$$F^{a}(x) = F(x) \qquad x \in \tilde{F}$$

$$F^{a}(x) = F(x) - P(x)$$
(3)

where \tilde{F} denotes the feasible search space. Here, P(x) is a penalty function whose value is greater than zero. In addition, $F^a(x)$ represents the augmented fitness function after

the penalty. Several forms of penalty functions have been proposed in the literature^{11,12,13}. Nevertheless, most of them can be written in the following general form, i.e.,

$$P(x) = \sum_{j=1}^{k} (\lambda_G)_j [G_j(x)]^{\beta} + \sum_{j=1}^{p} (\lambda_H)_j [H_j(x)]^{\beta}$$
(4)

where

$$G_{j}(x) = \max \left[0, g_{j}(x)\right]$$

$$H_{j}(x) = \operatorname{abs}\left[h_{j}(x)\right]$$
(5)

Here, $G_j(x)$ and $H_j(x)$ represent the degrees of the inequality and equality constraint violations, respectively. In addition, $(\lambda_G)_j$, $(\lambda_H)_j$ and β are constants. In most cases, the same value is used for all $(\lambda_G)_j$'s and $(\lambda_H)_j$'s. As for β , it is usually set to be 1 or 2.

In the first operator in GAs, the reproduction operator, a mating pool is created by letting individuals with higher fitness values have higher chance to be selected into the mating pool. Many reasonable selection algorithms are possible. However, the most widely used technique is the proportional selection. In this technique, the probability of the with individual to be selected into the mating pool is

$$p(x_i) = \frac{F^a(x_i)}{\sum_{i=1}^n F^a(x_i)}$$
(6)

where x_i represents the i^{th} individual in the population and n is the population size. Clearly, in the above equation, it is essential that all fitness values must be positive. Therefore, the obtained fitness function after the penalty $F^a(x)$ may not be directly usable as its values may be negative. Moreover, the difference between the fitness values of the best feasible individuals and the average individuals varies generation by generation. In early generations, the difference can be very large and the best individuals become relatively too strong. As a result, the premature convergence may be obtained. In later generations, the difference can be very small and the average individuals become almost as strong as the best individuals. As a result, the search may become a random walk. To prevent all of these problems, the augmented fitness function is usually scaled into a specified positive range.

The penalty schemes used in GAs play a very important role in the performance of GAs. This role becomes even more important when the optimal solution lies on or close to the boundary between feasible and infeasible search spaces, which is very usual for the structural design optimization. In this study, we propose a new penalty scheme. The aim of the development is to create a scheme that is free from the disadvantages of the existing schemes, mentioned earlier.

19

3. ADAPTIVE PENALTY FUNCTION

To make the scheme simple, we employ a simple form of the penalized fitness function, i.e.,

$$F_i^a = F^a(x_i) = F(x_i) - P(x_i) = F(x_i) - \lambda(t)E(x_i)$$
(7)

where F_i^a represents the fitness function of the i^{th} individual after the penalty. Here, $\lambda(t)$ is a factor multiplied to $E(x_i)$ that is an error term. The factor $\lambda(t)$ varies with generation and the generation number is denoted by t. In this study, the error term $E(x_i)$ is defined as

$$E(x_i) = \sum_{j=1}^{K} G_j(x_i) + \sum_{j=1}^{P} H_j(x_i)$$
 (8)

where $G_i(x_i)$ and $H_i(x_i)$ have already been defined in Eq. (5).

Now, the question is what the magnitude of the factor $\lambda(t)$ should be. It is not difficult to imagine that if the factor is too small, infeasible individuals with high original fitness values may have penalized fitness values higher than the fitness value of the feasible optimal individual being searched. If this happens, the population in subsequent generations will move toward the false peaks that appear in the infeasible region. On the contrary, if $\lambda(t)$ is too large, good characteristics in some infeasible individuals will have no chance to survive and will disappear rapidly. This may lead to premature convergence and the obtained solution can be quite wrong.

To avoid the above problems, the degree of the penalty must be enough to make the feasible optimal solution have the maximum fitness value, compared with all individuals (feasible and infeasible) after the penalty. However, the penalty must not be made too much stronger than that. To this end, we introduce the following condition, i.e.,

$$F^{a}(x_{i}) \le \phi \quad F_{avg}^{a,\tilde{F}} \quad \text{for } \forall x_{i} \in \tilde{U}$$
 (9)

in which \tilde{U} represents the infeasible search space. Here, $F_{avg}^{a,\tilde{F}}$ denotes the average fitness value of all feasible individuals in the generation and ϕ is a constant.

The above condition sets the maximum fitness value of the infeasible individuals in the generation to be at most equal to ϕ $F_{avg}^{a,\bar{F}}$, but not more than that. At this moment, it is not useful to consider the physical meaning of the constant ϕ yet because the penalized fitness function will have to be scaled afterwards. Therefore, it is enough to simply say that the factor ϕ is used to adjust the strength of the penalty. A way to obtain the value of this constant will be explained shortly. To satisfy the condition in Eq. (9), we calculate the factor $\lambda(t)$ by computing, for each infeasible individual, the factor $\lambda(t)$ that makes the penalized fitness value of that infeasible individual exactly equal to ϕ $F_{avg}^{a,\bar{F}}$. After that, the values of the factor obtained from all infeasible individuals are compared and the

maximum one is selected as $\lambda(t)$. If the maximum value is negative, zero is used instead. In short, we can express $\lambda(t)$ as

$$\lambda(t) = \max \left[0, \max_{\forall x_i \in \hat{\mathbf{U}}} \left[\frac{F^a(x_i) - \phi \ F_{avg}^{a, \bar{F}}}{E(x_i)} \right] \right]$$
 (10)

Eq. (10) insures that Eq. (9) is satisfied.

In this study, we employ a modified bilinear scaling technique shown in Figure 1. The minimum scaled fitness is set to zero to avoid negative fitness values while the scaled

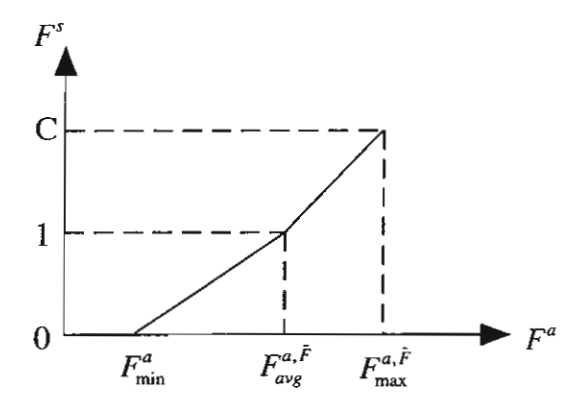


Figure 1: Bilinear fitness scaling.

fitness of the average fitness of all feasible individuals $F_{avg}^{a,\tilde{F}}$ is set to one. Furthermore, the maximum scaled fitness that is to be obtained from the best feasible members is set to C. Thus, the chance of the best feasible members being selected into the mating pool is equal to C times that of the average feasible members. All together, we have

$$F^{s}(x) = \frac{C - 1}{F_{\max}^{a,\tilde{F}} - F_{avg}^{a,\tilde{F}}} F^{a}(x) + \frac{F_{\max}^{a,\tilde{F}} - CF_{avg}^{a,\tilde{F}}}{F_{\max}^{a,\tilde{F}} - F_{avg}^{a,\tilde{F}}} \quad \text{if } F^{a}(x) \ge F_{avg}^{a,\tilde{F}}$$

$$F^{s}(x) = \frac{1}{F_{avg}^{a,\tilde{F}} - F_{\min}^{a}} F^{a}(x) + \frac{F_{\min}^{a}}{F_{\min}^{a} - F_{avg}^{a,\tilde{F}}} \quad \text{if } F^{a}(x) \le F_{avg}^{a,\tilde{F}}$$

$$(11)$$

where $F^s(x)$ denotes the scaled fitness function. In addition, F^a_{\min} denotes the minimum fitness value after the penalty while $F^{a,\bar{F}}_{\max}$ denotes the fitness value of the best feasible members. This scaled fitness function $F^s(x)$ will be used in Eq. (6) instead of $F^a(x)$.

21

For all generations, we set the chance of the best infeasible members being selected into the mating pool to be equal to φ times that of the average feasible members, i.e.,

$$F^{s}(x_{i}) \le (\varphi F_{avg}^{s,\tilde{F}} = \varphi)$$
 for $\forall x_{i} \in \tilde{U}$ (12)

where $F_{avg}^{s,\bar{F}}$ is the scaled value of the average fitness of all feasible individuals which is equal to 1. From the above condition, we can express ϕ in Eq. (9) in terms of φ as

$$\phi = \frac{CF_{avg}^{a,\tilde{F}} + F_{\max}^{a,\tilde{F}}(\varphi - 1) - \varphi F_{avg}^{a,\tilde{F}}}{(C - 1)F_{avg}^{a,\tilde{F}}} \quad \text{for } \varphi \ge 1$$

$$\phi = \frac{F_{\min}^{a} + \varphi F_{avg}^{a,\tilde{F}} - \varphi F_{\min}^{a}}{F_{avg}^{a,\tilde{F}}} \quad \text{for } \varphi \le 1$$
(13a, b)

In the real calculation, the coefficient φ will be set at the beginning of the calculation. This coefficient has a very clear physical meaning, i.e., the chance to be selected into the mating pool of the best infeasible members compared with that of the average feasible members. In addition, the coefficient does not have any unit. Due to these reasons, it is possible to set this coefficient by using experience. Knowing φ , we can compute φ and, subsequently, the factor $\lambda(t)$. In case of $\varphi \ge 1$, φ can be obtained from Eq. (13a) directly because all parameters in the equation are readily available. In this case, the parameters $F_{avg}^{a,\bar{F}}$ and $F_{max}^{a,\bar{F}}$ can be obtained directly from the original fitness values of the feasible individuals without any penalty consideration. On the contrary, if $\varphi < 1$, φ cannot be obtained without iteration since one of the parameters, i.e., F_{min}^a , is not readily available. Note that F_{min}^a is the minimum fitness in the generation after the penalty and it is most likely that F_{min}^a will belong to the infeasible members. This F_{min}^a can be obtained from Eq. (7), which, in turn, requires the value of φ [see Eq. (10)]. Nevertheless, the required iteration is very simple and takes almost no time to perform.

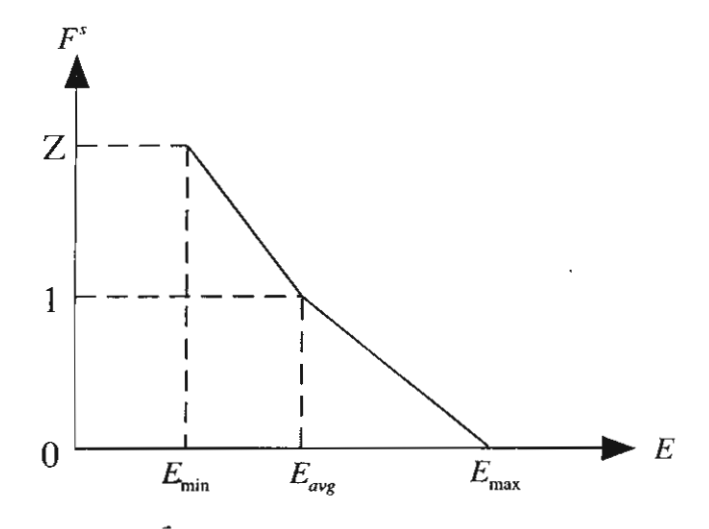


Figure 2: Bilinear fitness scaling for cases where no feasible individual is available.

In short, the purpose of the scheme is to fix, throughout the calculation, the relative chance of the best infeasible members being selected into the mating pool compared with that of the average feasible members. This means that the penalty is always adjusted so that the aforementioned purpose is achieved in all generations. This guarantees that the desired degree of the penalty is obtained throughout the evolution. Consequently, the problem of too weak or too strong penalty during different phases of the evolution is removed.

Since the proposed penalty scheme requires the average fitness value over all feasible individuals, it is necessary to have at least one feasible individual in the population. In the case that there is none, the fitness values of the infeasible individuals will be given based on the magnitudes of the error they have. The idea is to strongly encourage the population to move toward the feasible region. Here, a bilinear scaling scheme shown in Figure 2 is used. The fitness is scaled in such a way that the scaled fitness values of the individuals with the highest error are equal to zero and the scaled fitness values of the individuals with the average error are equal to one. In addition, the scaled fitness values of the individuals with the smallest error being selected into the mating pool is equal to Z times that of the individuals with the average error. In summary, we have

$$F^{s}(x) = \frac{Z - 1}{E_{\min} - E_{avg}} E(x) + \frac{E_{\min} - ZE_{avg}}{E_{\min} - E_{avg}} \quad \text{if } E(x) \le E_{avg}$$

$$F^{s}(x) = \frac{1}{E_{avg} - E_{\max}} E(x) + \frac{E_{\max}}{E_{\max} - E_{avg}} \quad \text{if } E(x) > E_{avg}$$
(14)

4. RESULTS

To investigate the validity and efficiency of the proposed penalty scheme, the scheme is used in the design optimization of two different structures, i.e., six-bar and ten-bar trusses. To be able to see clearly the advantages of the proposed scheme over the conventional schemes, the obtained results are compared with those from a selected conventional scheme. Since most of the conventional schemes are based on the same concept with slightly different details, comparison with one selected conventional scheme is sufficient to show the advantages of the proposed scheme over the conventional schemes. Finally, the results are also compared with the existing results in the literature.

4.1. Six-Bar Truss

The first problem to be considered is the six-bar truss shown in Figure 3. Here, we consider only the sizing optimization. Thus, the design variables are six sectional areas of the six members of the truss. The cross-sectional area of each member is taken from the following 32 discrete values, i.e., 1.62, 1.80, 2.38, 2.62, 2.88, 3.09, 3.13, 3.38, 3.63, 3.87, 4.18, 4.49, 4.80, 4.97, 5.12, 5.74, 7.22, 7.97, 11.5, 13.5, 13.9, 14.2, 15.5, 16.0, 18.8, 19.9, 22.0, 22.9, 26.5, 30.0, and 33.5 in². Therefore, a five-bit string is required for each design variable. There are two types of constraint in this problem, i.e., the stress and displacement constraints. The design parameters used in the problem are shown in Table 1.

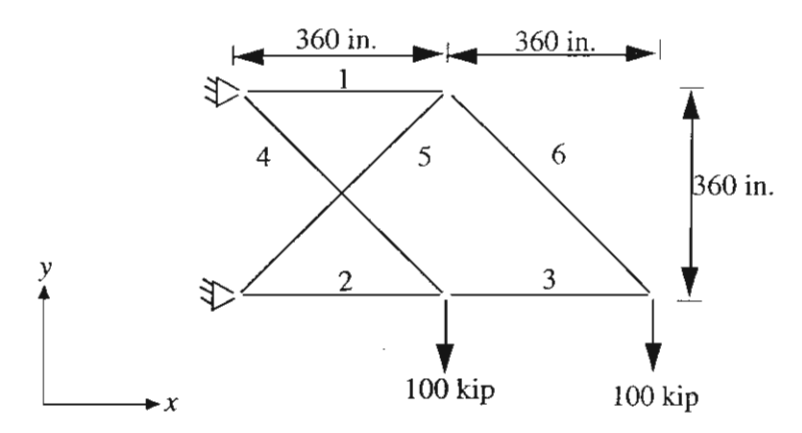


Figure 3: Six-bar truss.

For comparison, the most popular conventional penalty scheme is also used to solve the problem. The conventional form is expressed as

$$F_i^a = F^a(x_i) = F(x_i) - P(x_i) = F(x_i) - \lambda E(x_i)$$
(15)

where the coefficient λ is constant and the error term $E(x_i)$ is the same as that defined in Eq. (8). In both proposed and conventional schemes, the fitness function $F(x_i)$ is defined as

$$F(x_i) = \frac{1}{1 + Weight(x_i)} \tag{16}$$

where two different units of weight, i.e., pound (lb) and newton (N) are used. Two units are used in order to investigate the effect of unit on the results from both schemes. Since it is impossible to judiciously estimate the appropriate value of the coefficient λ in the conventional scheme, a wide range of vaslues will be used. All GA parameters used can be found in Table 1. To start the calculation, the initial population is generated at random. The type of crossover operator used here is the one-point crossover¹.

Figure 4 shows the results obtained from the proposed and conventional schemes. Each point in the graph represents an average weight of the best feasible designs obtained from 200 different runs. The results obtained by using newtons in Eq. (16) are converted into pounds for comparison. In the conventional scheme, the coefficient λ is varied

Table 1: Design and GA parameters for the six-bar truss problem.
--

Design parameters		GA parameters		
Item	Item Value		Value	
Modulus of elasticity	10 ⁷ psi	Maximum number of generations	100	
Weight density	0.1 lb/in ³			
Allowable tensile stress	25,000 psi	Population size	70	
Allowable compressive stress	25,000 psi	Crossover probability	0.8	
Maximum y-displacement	2 in.	Mutation probability φ γ C Z	0.001 0.25 - 1.75 0.000001 -100 2 5	

Table 2: Comparison of the results for the six-bar truss problem.

Item	Proposed	Rajan [8]
Area 1 (in²)	30.0	30.0
Area 2	19.9	19.9
Area 3	15.5	15.5
Area 4	7.22	7.22
Area 5	22.0	22.0
Area 6	22.0	22.0
Total Weight (lb)	4962.1	4962.1

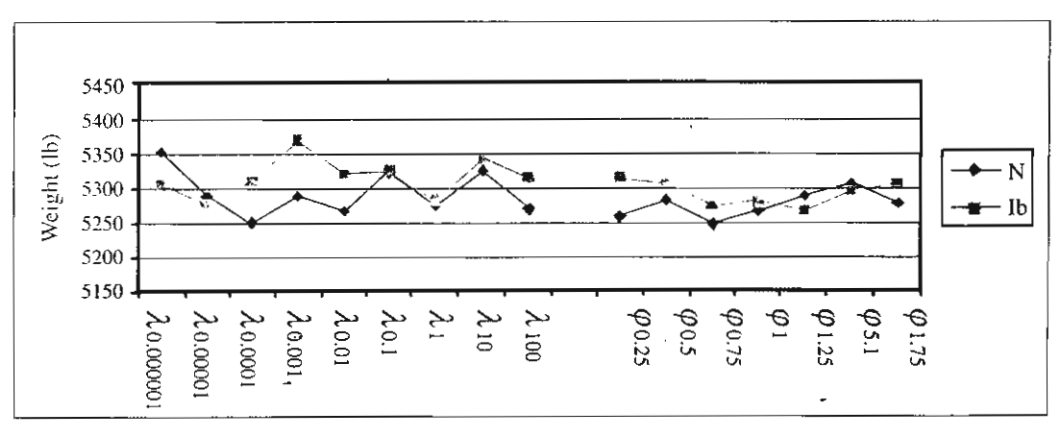


Figure 4: Average weight of the best feasible designs obtained from 200 runs — six-bar truss.

exponentially from 0.000001 to 100 while in the proposed scheme the coefficient is varied from 0.25 to 1.75. Note that the value of φ should be varied between 0 to 2.0 since the maximum scaled fitness value C is set to be 2.0 (see Table 1). It can be clearly seen from the results that the proposed scheme is more robust than the conventional scheme. In the proposed scheme, changing the unit has little effect on the results while in the conventional scheme the effect is much more noticeable. Moreover, in the proposed scheme, it is easier to notice the trend of the results when φ is varied. It can be reasonably said that good results are obtained with the value of φ around 0.75. On the contrary, in the conventional scheme, this kind of trend is not very obvious, considering both results obtained with newtons and pounds. Nevertheless, we may say that good results are obtained with the value of λ around 0.0001.

The best result obtained from the proposed scheme is also compared with the best result reported by Rajan⁸. They are exactly the same. The details of the result are shown in Table 2. It must be noted that in this study, except for the new penalty algorithm, the rest of the algorithms are standard. This is not the case for the work by Rajan⁸, which employs more complicated GAs.

4.2 Ten-Bar Truss

The next problem to be considered is the ten-bar truss shown in Figure 5. This problem is one of the benchmark problems used to test optimization methods. In this problem, we also consider only the sizing optimization. Therefore, the design variables are ten sectional areas. The cross-sectional areas of members 1, 3, 4, 7, 8 and 9 are taken from the following 32 discrete values, i.e., 3.13, 3.38, 3.47, 3.55, 3.63, 3.84, 3.87, 3.88, 4.18, 4.22, 4.49, 4.59, 4.80, 4.97, 5.12, 5.74, 7.22, 7.97, 11.5, 13.5, 13.9, 14.2, 15.5, 16.0, 16.9, 18.8, 19.9, 22.0, 22.9, 26.5, 30.0, and 33.5 in². For the rest of the members, the cross-sectional areas are taken from the following 32 discrete values, i.e., 1.62, 1.80, 1.99, 2.13, 2.38, 2.62, 2.63, 2.88, 2.93, 3.09, 3.13, 3.38, 3.47, 3.55, 3.63, 3.84, 3.87, 3.88, 4.18, 4.22, 4.49, 4.59, 4.80, 4.97, 5.12, 5.74, 7.22, 7.97, 11.5, 13.5, 13.9, and 14.2 in². Similar to the previous problem,

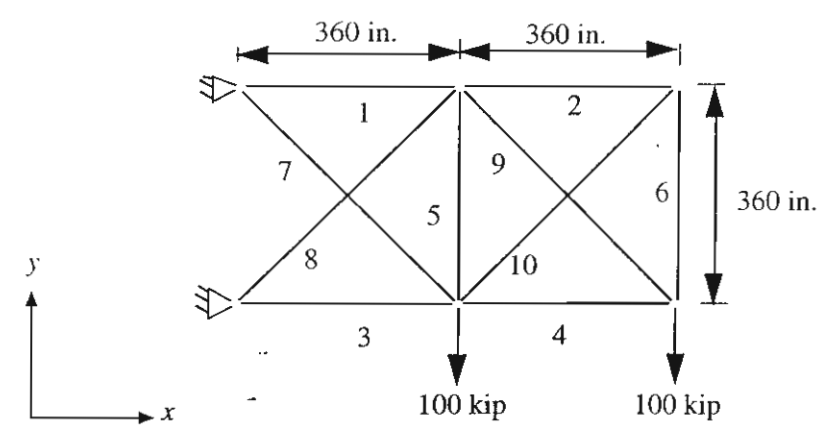


Figure 5: Ten-bar truss.

Design parameters		GA parameters		
Item	Value	Item	Value	
Modulus of elasticity	10 ⁷ psi	Maximum number of generations	100	
Weight density	0.1 lb/in ³			
Allowable tensile stress	25,000 psi	Population size	40	
Allowable compressive stress	25,000 psi	Crossover probability	0.8	
Maximum x, y-displacement	2 in.	Mutation probability φ γ C	0.001 0.25 - 1.75 0.000001 -100 2 5	

Table 3: Design and GA parameters for the ten-bar truss problem.

a five-bit string is required for each design variable. The design parameters and genetic parameters are shown in Table 3.

The results obtained from the proposed and conventional schemes are shown in Figure 6. Similar to the previous problem, each point in the graph represents an average weight of the best feasible designs obtained from 200 different runs. The robustness of the proposed scheme is again obvious. The effect of the unit used on the results from the proposed scheme is noticeably less than that on the results from the conventional scheme. Moreover, the results from the proposed scheme also exhibit clear tendency with respect to the value of the coefficient used while those from the conventional scheme do not. In the proposed

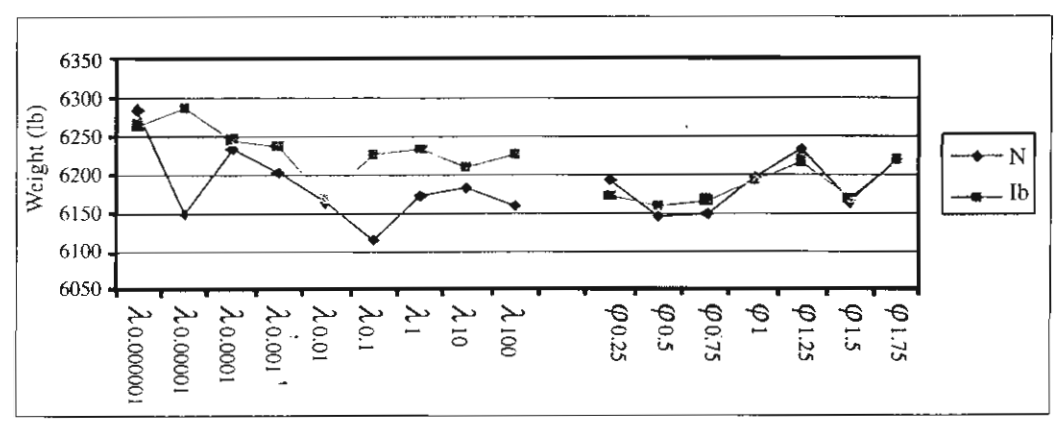


Figure 6: Average weight of the best feasible designs obtained from 200 runs — ten-bar truss.

7.97

22.9

22.0

1.62

5,458.3

7.22

22.9

22.0

1.62

5,556.9

Area 7

Area 8

Area 9

Area 10

Total Weight (lb)

Item	Proposed	Rajeev and Krishnamoorthy [e beginning of the calculation ⁴]	Camp et al. [,6]	Galante [Error! Reference source not found.]
Area 1 (in²)	33.5	33.5	30.0	33.5
Area 2	1.62	1.62	1.62	1.62
Area 3	22.9	22.0	26.5	22.0
Area 4	15.5	15.5	13.5	14.2
Area 5	1.62	1.62	1.62	1.62
Area 6	1.62	1.62	1.62	1.62

14.2

19.9

19.9

2.62

5,613.8

7.22

22.9

22.0

1.62

5,499.3

Table 4: Comparison of the results for the ten-bar truss problem.

scheme, it can be said that good results are obtained with the value of φ around 0.5. In the conventional scheme, although it is not very obvious, we may barely say that good results are obtained with the value of λ around 0.1.

The best result obtained from the proposed scheme is also compared with the best results reported by Rajeev and Krishnamoorthy⁴, Camp et al.⁶, and Galante¹⁰ in Table 4. It can be seen that the result obtained from the proposed penalty scheme is relatively very good although Rajeev and Krishnamoorthy⁴, Camp et al.⁶, and Galante¹⁰ employ more complicated GAs.

In the previous problem, the appropriate value of φ is around 0.75 and the appropriate value of λ is around 0.0001. Since the two problems are quite similar, similar values of the coefficients from the two problems are expected. In this aspect, the proposed scheme evidently outperforms the conventional scheme. Having similar appropriate values of the coefficient for similar problems allows the coefficient to be set by experience. Since the coefficient in the proposed scheme has a physical meaning, which directly corresponds to the understandable degree of the penalty, the characteristics of the problems being solved can be directly related to the appropriate degree of the penalty. This kind of advantage cannot be found in the conventional schemes.

5. CONCLUSION

This paper presents a new adaptive penalty scheme in GAs for structural design optimization. The existing penalty schemes generally require the values of some coefficients to be specified at the beginning of the calculation and these coefficients usually have no clear physical meanings. Consequently, it is very difficult to select the appropriate values of these coefficients even by experience. Moreover, most of the existing schemes employ constant coefficients throughout the entire calculation. This may result in too weak or too strong penalty during different phases of the evolution. To avoid these drawbacks, a new penalty scheme is proposed. The main concept of the proposed scheme is to fix, throughout all generations, the chance to be selected into the mating pool of the best infeasible members compared with that of the average feasible members. The parameter that has to be set is the ratio between the fitness value of the best infeasible members and the fitness value of the average feasible members. This ratio has a very clear physical meaning. Therefore, it can be set easily, based on experience of different types of problem. In addition, under this concept, the penalty is always adjusted so that the desired degree of the penalty is achieved in all generations.

The proposed scheme is tested by using two optimization problems of truss structures. The comparisons with a representative conventional scheme clearly show the advantages of the proposed method. From the results, it can be seen that the proposed scheme is robust and the required parameter can be obtained by experience. In addition, the comparisons with the results from the literature also show that the proposed penalty scheme yields relatively good results although, except for the new penalty algorithm, the proposed technique employs very standard GAs.

6. ACKNOWLEDGEMENTS

The authors are grateful to the Thailand Research Fund (TRF) for providing the financial support to this study.

7. REFERENCES

- 1. Goldberg, D. E. 1989. Genetic Algorithms in Search, Optimization, and Machine Learning. Addison-Wesley. Reading. Massachusetts.
- 2. Deb, K. 1995. Optimization for Engineering Design. Prentice-Hall. Englewood Cliffs. N.J.
- 3. Michalewicz, Z. 1996. *Genetic Algorithms + Data Structures = Evolution Programs*. Springer. New York.
- 4. Rajeev, S. and Krishnamoorthy, C. S. 1992. Discrete optimization of structures using genetic algorithms. *Journal of Structural Engineering*. 118(5):1233-1249.
- 5. Jenkins, W. M. 1997. On the application of natural algorithms to structural design optimization. *Engineering Structures*. 19(4):302-308.

- 6. Camp, C., Pezeshk, S. and Cao, G. 1998. Optimized design of two-dimensional structures using a genetic algorithm. *Journal of Structural Engineering*. 124(5):551-559.
- 7. Adeli, H. and Cheng, N. 1993. Integrated genetic algorithm for optimization of space structures. *Journal of Aerospace Engineering*. 6(4):315-328.
- 8. Rajan, S. D. 1995. Sizing, shape, and topology design optimization of trusses using genetic algorithm. *Journal of Structural Engineering*. 121(10):1480-1487.
- 9. Rafiq, M. Y. and Southcombe, C. 1998. Genetic algorithms in optimal design and detailing of reinforced concrete biaxial columns supported by a declarative approach for capacity checking. *Computers and Structures*. 69:443-457.
- 10. Galante, M. 1996. Genetic algorithms as an approach to optimize real-world trusses. *International Journal for Numerical Methods in Engineering*. 39:361-382.

Analysis of Cracking Localization Using the Smeared Crack Approach

Pruettha Nanakorn, Aruz Petcherdchoo Sirindhorn International Institute of Technology Thammasat University, Pathumthani 12121, Thailand Phone (66-2) 986-9103~8 Ext. 1906 Fax (66-2) 986-9113 E-mail: nanakorn@siit.tu.ac.th

and
Nuttapol Kittiwattanchai
Asian Institute of Technology
Pathumthani 12120, Thailand
Phone (66-2) 516-0110~40

Fax (66-2) 516-2126

Abstract

In consideration of cracking localization, it is more suitable to have an energy expression written in terms of discrete irreversible variables, which will allow the variations of the energy with respect to the irreversible variables to be considered easily. This implies that the discrete crack approach should be more appropriate for this kind of analysis than the smeared crack approach. However, the discrete crack approach may not be the best choice for problems with many cracks, which unavoidable for the analysis of the cracking localization. To avoid the drawbacks in both approaches, a special treatment on the smeared crack approach to allow the consideration of the cracking localization is developed. To this end, discrete irreversible variables related to crack strains are introduced, and the cracking localization is investigated, based on these discrete irreversible variables. The results obtained show promising capability of the method in analyzing problems with the cracking localization.

1. Introduction

Cracking localization prior to the failure plays a very important role in the fracture behavior of quasi-brittle materials, such as concrete. In order to capture-the real ultimate capacity of such materials in structures, consideration of the cracking localization

cannot generally be neglected. However, the analysis of the cracking localization is very expensive. Because of this reason, many researchers avoid the consideration of the cracking localization. This can be done by either allowing many cracks to open or grow without the consideration of the localization [1, 2, 3, 4, 5] or assuming the locations of the localized cracks [5, 6]. The first approach is not realistic and can lead to very inaccurate results. When compared with having one or a few localized cracks, having many cracks without localization allows different amounts of energy to dissipate from the domain. Thus, the obtained results will be different as well. Only in some cases where the stress gradients of the problems are very large and the stress criteria for crack initiation are used, can the localized solution possibly be obtained from this approach [1, 2, 4]. When the stress gradient is very high, it is numerically possible that major cracks will finally prevail and the other cracks will undergo the elastic unloading. The second approach, which assumes the locations of the localized cracks prior to the analysis, may also possibly yield reasonable results in some cases. These include cases where the assumed locations of the localized cracks are reasonably correct, such as bending problems of concrete beams with long notches [6]. The others are cases where the required solutions, such as the ultimate loads, are not sensitive to the locations of the localized cracks [5]. Nevertheless, this second approach is not appropriate for general

cases since the locations of the localized cracks may not be easily predicted or the required solution may be sensitive to the locations of the cracks.

analysis of the In the cracking localization, consideration of stability and bifurcation of equilibrium states is one of the tasks to be done. Many researchers have considered the stability and bifurcation of the by investigating eauilibrium states definiteness of the stiffness matrices (Hessian Matrices) [7, 8, 9]. When the matrix is positive-definite, the equilibrium is stable. The same theory can be applied to the analysis of the cracking localization. Nevertheless, consider the stability and bifurcation irreversible processes such as cracking, the stationary condition of the energy of the system with respect to irreversible parameters has to be examined [10, 11, 12]. This requires expression of the energy in terms of the irreversible parameters. For crack problems, the irreversible parameters can be the crack opening displacement variables in the discrete crack approach or the crack strain variables in the smeared crack approach. In the discrete approach, the crack opening crack displacement variables are usually discretized along crack paths and treated as the degrees of freedom in the analysis. The energy of the system is expressed in terms of these degrees of freedom. Computing the first and second variations of the energy with respect to the crack opening displacement degrees of freedom can be done easily. The stability bifurcation of the equilibrated solutions can be considered by employing just the ordinary calculus [12]. On the contrary, if the smeared crack approach is employed, the energy of the system will be expressed in terms of the irreversible crack strain variables, which are not discretized variables. These crack strain variables are functions of position. To compute the first and second variations of the energy with respect to these crack strain functions, complex mathematics involving the calculus of variations must be employed.

This fact implies that the discrete crack approach in the finite element method may be

more suitable for the cracking localization analysis than the smeared crack approach. Nevertheless, the discrete crack approach may not perform best when there are many cracks. In this aspect, the smeared crack approach is more appropriate.

To avoid the drawbacks in both methods, in this study, a special treatment on the smeared crack finite element analysis is proposed. The proposed treatment will make it possible to consider the cracking localization by using the smeared crack models. In the proposed method, discrete irreversible variables related to the crack strains are introduced in the smeared crack models. These discrete variables will allow the consideration of the stability and bifurcation of the equilibrated solution to be done by considering the variations of the energy with respect to the proposed discrete variables. The proposed scheme will not be used to obtain the stiffness equation that is used to obtain the equilibrium paths. The original smeared crack models will be still used for that purpose. The proposed method will be used only for the investigation of the stability and bifurcation.

2. Cracking Localization

Consider a system of a deformable body with cracks where the energy is dissipated. Following Nguyen [10] and Brocca [12], we define the total energy of the body as

$$\Pi(u_i,\alpha_j) = \Pi^M(u_k,\alpha_l) + \Pi^D(\alpha_m) \qquad (1)$$

where $\Pi^M(u_k,\alpha_l)$ is the mechanical potential energy and $\Pi^D(\alpha_m)$ is the dissipated energy. The arguments of the functions, u_i (i=1,...,N) and α_i (i=1,...,K), represent the reversible variables and irreversible variables, respectively. Here, N is the number of the reversible variables and K is the number of the irreversible variables.

Applying the stationary conditions to Eq. (1), we have

$$\frac{\partial \Pi}{\partial u_i} = 0 \qquad i = 1, ..., N, \tag{2a}$$

$$\frac{\partial \Pi}{\partial u_i} = 0 \qquad i = 1, ..., N, \qquad (2a)$$

$$\frac{\partial \Pi}{\partial \alpha_j} = 0 \qquad j = 1, ..., K. \qquad (2b)$$

From Eq. (2), the equilibrated solution can be obtained. Employing the obtained solution, we can express the reversible parameters in terms of the irreversible parameters, i.e., $u_i = u_i(\alpha_i)$. Therefore, we can express the total energy in Eq. (1) as a function of only the irreversible parameters, i.e.,

$$\Pi^{\bullet}(\alpha_{t}) = \Pi^{\bullet M}(\alpha_{i}) + \Pi^{D}(\alpha_{m})$$
 (3)

where
$$\Pi^*(\alpha_l) = \Pi(u_i(\alpha_k), \alpha_j)$$
 and $\Pi^{*M}(\alpha_l) = \Pi^M(u_k(\alpha_m), \alpha_l)$.

The signs of the eigenvalues of the Hessian Matrix $\left[\frac{\partial^2 \Pi^*}{\partial \alpha_i \partial \alpha_i}\right]$ are used to check

the stability of the equilibrated solution obtained from Eq. (2). If all the eigenvalues are positive, the equilibrated solution is stable and there is no bifurcation. Otherwise, the solution is unstable and the bifurcation, which leads to the localization, occurs.

3. Smeared Crack Finite Element Analysis for Cracking Localization

The fundamental scheme of the smeared crack models is the decomposition of the total strain increment $\Delta \epsilon$ into a strain increment of the intact solid between the cracks $\Delta \epsilon^{o}$ and the crack strain increment $\Delta \epsilon^{cr}$, i.e., [1, 13, 14]

$$\Delta \epsilon = \Delta \epsilon^o + \Delta \epsilon^{cr}. \tag{4}$$

The strain increment vectors in the above equation are in the global coordinate system. It will be helpful to consider the strain increments also in a local coordinate system, which aligns with the crack. Based on the local coordinate system, a local crack strain increment vector in two-dimensional cases is written as

$$\Delta \hat{\epsilon}^{cr} = \left(\Delta \hat{\varepsilon}_{nn}^{cr} \quad \Delta \hat{\gamma}_{nt}^{cr} \right)^{T} \tag{5}$$

where $\Delta \hat{\varepsilon}^{cr}_{nn}$ and $\Delta \hat{\gamma}^{cr}_{nt}$ are the mode I normal crack strain increment and the mode II shear crack strain increment, respectively. The relationship between the global crack strain increment $\Delta \epsilon^{cr}$ and the local crack strain increment $\Delta \hat{\epsilon}^{cr}$ is written as

$$\Delta \epsilon^{cr} = \mathbf{T} \Delta \hat{\epsilon}^{cr} \tag{6}$$

where T is the transformation matrix between the global and local coordinate systems defined

$$\mathbf{T} = \begin{bmatrix} \cos^2 \theta & -\sin \theta \cos \theta \\ \sin^2 \theta & \sin \theta \cos \theta \\ 2\sin \theta \cos \theta & \cos^2 \theta - \sin^2 \theta \end{bmatrix}$$
(7)

where θ is the angle between the normal of the crack and the global x-axis. In the local coordinate system, we consider the local traction increment across the crack, i.e.,

$$\Delta \hat{\mathbf{t}}^{cr} = \begin{pmatrix} \Delta \hat{t}_{n}^{cr} & \Delta \hat{t}_{i}^{cr} \end{pmatrix}^{T} \tag{8}$$

where $\Delta \hat{t}_n^{cr}$ denotes the mode I normal traction increment and $\Delta \hat{t}_{i}^{cr}$ denotes the mode II shear traction increment. By using the transformation matrix T, the relationship between the traction increment $\Delta \hat{\mathbf{t}}^{cr}$ and the global stress increment $\Delta \sigma$ is expressed as

$$\Delta \hat{\mathbf{t}}^{cr} = \mathbf{T}^T \Delta \boldsymbol{\sigma} . \tag{9}$$

The constitutive models for the material between the cracks and for the smeared cracks must be specified. For the material between the cracks, we have

$$\Delta \sigma = \mathbf{D}^{o} \Delta \epsilon^{o} \tag{10}$$

where D^{o} is the constitutive matrix for the material between the cracks. For the cracks, we have the local traction-crack strain relationship, i.e.,

$$\Delta \hat{\mathbf{t}}^{cr} = \hat{\mathbf{D}}^{cr} \Delta \hat{\boldsymbol{\epsilon}}^{cr} \tag{11}$$

where $\hat{\mathbf{D}}^{cr}$ is the crack constitutive matrix incorporating mixed-mode properties of the cracks.

By using Eqs. (4)-(11), the incremental stress-strain relationship for the cracked material is obtained as

$$\Delta \sigma = \left(\mathbf{D}^{o} - \mathbf{D}^{o} \mathbf{T} \left[\hat{\mathbf{D}}^{cr} + \mathbf{T}^{T} \mathbf{D}^{o} \mathbf{T} \right]^{-1} \mathbf{T}^{T} \mathbf{D}^{o} \right) \Delta \epsilon . (12)$$

In order to discuss the cracking localization, we follow the concept of the localization explained in the previous section. To begin with, we consider the total energy increment for the domain of interest V, i.e.,

$$\Delta \Pi = \left[\frac{1}{2} \int_{V} \Delta \epsilon^{\sigma^{T}} \Delta \sigma dV - \int_{V} \Delta \mathbf{u}^{T} \Delta \mathbf{f} dV - \int_{S} \Delta \mathbf{u}^{T} \Delta \mathbf{f} dS \right]$$

$$+ \left[\frac{1}{2} \int_{V} \Delta \hat{\epsilon}^{cr^{T}} \Delta \hat{\mathbf{f}}^{cr} dV \right]$$
(13)

where the first and second pairs of the brackets represent the mechanical potential energy increment and the dissipated energy increment, respectively [10, 12]. Here, Δt and Δf denote the surface traction increment vector and the body force increment vector, respectively. In addition, Δu denotes the total displacement increment vector.

From Eqs. (4), (10), (11), and (13) and the inverse relationship of Eq. (6), i.e.,

$$\Delta \hat{\epsilon}^{cr} = \hat{\mathbf{T}} \Delta \epsilon^{cr} \tag{14}$$

where

$$\hat{\mathbf{T}} = \begin{bmatrix} \cos^2 \theta & -2\sin\theta \cos\theta \\ \sin^2 \theta & 2\sin\theta \cos\theta \\ \sin\theta \cos\theta & \cos^2 \theta - \sin^2 \theta \end{bmatrix}^T, \quad (15)$$

we obtain

$$\Delta\Pi = \left[\frac{1}{2} \int_{V} (\Delta \epsilon - \Delta \epsilon^{cr})^{T} \mathbf{D}^{o} (\Delta \epsilon - \Delta \epsilon^{cr})^{T} dV - \int_{V} \Delta \mathbf{u}^{T} \Delta \mathbf{f} dV - \int_{S} \Delta \mathbf{u}^{T} \Delta \mathbf{t} dS\right]$$

$$+ \left[\frac{1}{2} \int_{V} \Delta \epsilon^{cr} \mathbf{D}^{cr} \Delta \epsilon^{cr} dV\right]$$
(16)

in which

$$\mathbf{D}^{cr} = \hat{\mathbf{T}}^T \hat{\mathbf{D}}^{cr} \hat{\mathbf{T}} . \tag{17}$$

Here, we introduce a crack displacement increment vector $\Delta \mathbf{u}^{cr}$ defined as

$$\Delta \mathbf{u} = \Delta \mathbf{u}^o + \Delta \mathbf{u}^{cr} \tag{18}$$

where the strain increments computed from $\Delta \mathbf{u}$, $\Delta \mathbf{u}^o$ and $\Delta \mathbf{u}^{cr}$ are $\Delta \epsilon$, $\Delta \epsilon^o$ and $\Delta \epsilon^{cr}$, respectively.

Consider the ith element in the finite element analysis. The element is assumed to be a cracked element. Interpolate these three displacement increments from nodal quantities, i.e.,

$$\Delta^{i}\mathbf{u} = \mathbf{N}\Delta^{i}\mathbf{U}, \quad \Delta^{i}\mathbf{u}^{o} = \mathbf{N}\Delta^{i}\mathbf{U}^{o}, \Delta^{i}\mathbf{u}^{cr} = \mathbf{N}\Delta^{i}\mathbf{U}^{cr}, \quad \Delta^{i}\mathbf{U} = \Delta^{i}\mathbf{U}^{o} + \Delta^{i}\mathbf{U}^{cr}$$
(19)

in which $\Delta^i \mathbf{U}$, $\Delta^i \mathbf{U}^o$ and $\Delta^i \mathbf{U}^{cr}$ are the nodal quantities of $\Delta \mathbf{u}$, $\Delta \mathbf{u}^o$ and $\Delta \mathbf{u}^{cr}$, respectively. Here, \mathbf{N} is the shape function matrix. Note that the superscript i for the i^{th} element is used in the equations because the nodal crack displacement increments of the same node for different elements can be different. This is natural because, in the smeared crack approach, cracking in each element is completely

independent of each other. Therefore, the continuity of the crack displacement increment between elements is not required and must not be enforced. On the contrary, the total displacement increment must Δu continuous across elements. Therefore, the superscript i representing the element number is not actually necessary for the nodal values of the total displacement increment. Similar to the displacement increment, crack displacement increment related to the strain increment of the uncracked solid $\Delta' \mathbf{u}^o$ is not continuous across elements' boundaries: therefore, the superscript *i* is required.

Computing strains from Eq. (18), we obtain Eq. (4), i.e.,

$$\Delta^{i} \epsilon = \Delta^{i} \epsilon^{o} + \Delta^{i} \epsilon^{cr} \tag{20}$$

where

$$\Delta^{i} \epsilon = \mathbf{B} \Delta^{i} \mathbf{U} \,, \tag{21a}$$

$$\Delta^{i} \epsilon^{o} = \mathbf{B} \Delta^{i} \mathbf{U}^{o} \,, \tag{21b}$$

$$\Delta^{i} \epsilon^{cr} = \mathbf{B} \Delta^{i} \mathbf{U}^{cr} \,. \tag{21c}$$

Substituting Eq. (21) into Eq. (16) for the i^{th} element gives

$$\Delta \Pi = \frac{1}{2} \Delta \mathbf{U}^{T} \int_{\nu} \mathbf{B}^{T} \mathbf{D}^{o} \mathbf{B} dV \Delta \mathbf{U}$$

$$-\frac{1}{2} \Delta \mathbf{U}^{T} \int_{\nu} \mathbf{B}^{T} \mathbf{D}^{o} \mathbf{B} dV \Delta^{i} \mathbf{U}^{cr}$$

$$-\frac{1}{2} \Delta^{i} \mathbf{U}^{cr}^{T} \int_{\nu} \mathbf{B}^{T} \mathbf{D}^{o} \mathbf{B} dV \Delta \mathbf{U}$$

$$+\frac{1}{2} \Delta^{i} \mathbf{U}^{cr}^{T} \int_{\nu} \mathbf{B}^{T} \mathbf{D}^{o} \mathbf{B} dV \Delta^{i} \mathbf{U}^{cr}$$

$$+\frac{1}{2} \Delta^{i} \mathbf{U}^{cr}^{T} \int_{\nu} \mathbf{B}^{T} \mathbf{D}^{cr} \mathbf{B} dV \Delta^{i} \mathbf{U}^{cr}$$

$$-\Delta \mathbf{U}^{T} \int_{\nu} \mathbf{N}^{T} \Delta \mathbf{f} dV - \Delta \mathbf{U}^{T} \int_{c} \mathbf{N}^{T} \Delta \mathbf{t} dS.$$
(22)

Next, we apply the stationary condition $\delta(\Delta\Pi) = 0$, and assume that both \mathbf{D}^{o} and \mathbf{D}^{cr} are symmetric. Since $\delta(\Delta\mathbf{U}^{T})$ and $\delta(\Delta^{i}\mathbf{U}^{cr^{T}})$

are arbitrary, we obtain the element stiffness equation for the i^{th} element, i.e.,

$$\begin{bmatrix}
\int_{V} \mathbf{B}^{T} \mathbf{D}^{o} \mathbf{B} dV & -\int_{V} \mathbf{B}^{T} \mathbf{D}^{o} \mathbf{B} dV \\
-\int_{V} \mathbf{B}^{T} \mathbf{D}^{o} \mathbf{B} dV & \int_{V} \mathbf{B}^{T} \mathbf{D}^{o} \mathbf{B} dV + \int_{V} \mathbf{B}^{T} \mathbf{D}^{cr} \mathbf{B} dV
\end{bmatrix} \begin{bmatrix} \Delta \mathbf{U} \\ \Delta^{i} \mathbf{U}^{cr} \end{bmatrix} \\
= \begin{cases}
\int_{V} \mathbf{N}^{T} \Delta \mathbf{f} dV + \int_{S} \mathbf{N}^{T} \Delta \mathbf{t} dS \\
\mathbf{0}
\end{bmatrix}.$$
(23)

After assembling all elements and applying prescribed displacements and forces, we arrange the global stiffness equation as

$$\begin{bmatrix} \mathbf{K}_{11} & \mathbf{K}_{12} \\ \mathbf{K}_{21} & \mathbf{K}_{22} \end{bmatrix} \begin{bmatrix} \Delta \mathbf{U} \\ \Delta \mathbf{U}^{cr} \end{bmatrix} = \begin{bmatrix} \Delta \mathbf{R}_{1} \\ \Delta \mathbf{R}_{2} \end{bmatrix}. \quad (24)$$

The static condensation is used to remove the nodal total displacement increment from the obtained global matrix equation. Therefore, the equation can be written in the following form, i.e.,

$$\mathbf{K}^{cr} \Delta \mathbf{U}^{cr} = \Delta \mathbf{R}^{cr}. \tag{25}$$

It must be noted that Eq. (25) is a singular equation because ΔU^{cr} contains the rigid-body crack displacement increments, i.e., for two-dimensional cases, two rigid translations and one rigid rotation. These three rigid-body crack displacement increments can be found in all cracked elements. To avoid them, constraints to remove them from all elements must be applied to the equation. In this study, the following constraints are employed at the center of each element without loss of generality, i.e.,

$$\Delta u^{cr}(\xi = 0, \eta = 0) = 0$$

$$\Delta v^{cr}(\xi = 0, \eta = 0) = 0$$

$$\frac{\partial v^{cr}(\xi = 0, \eta = 0)}{\partial x} = 0$$
(26)

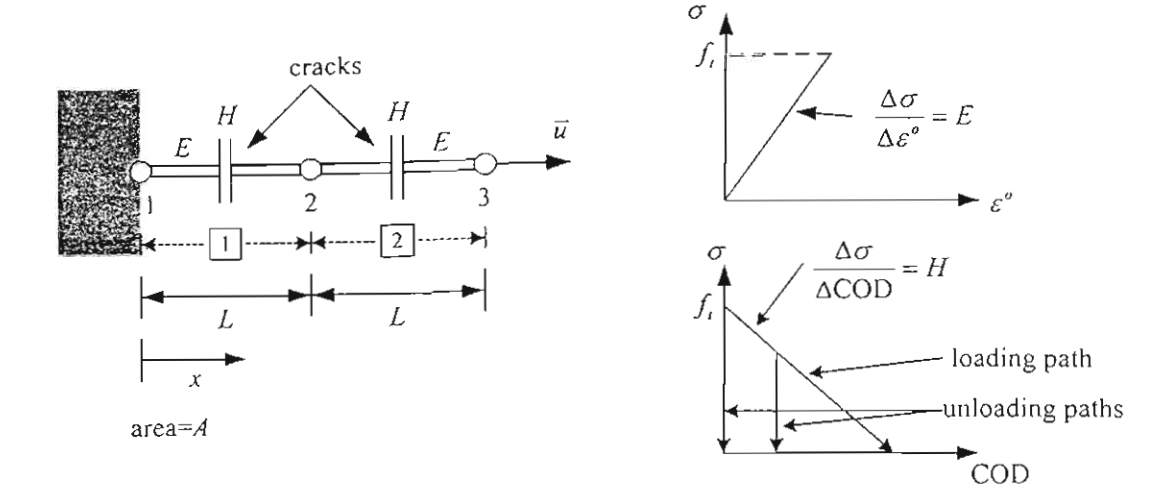


Fig. 1 Uniaxial problem using two 1-D bar elements

where the global x-y and natural $\xi-\eta$ coordinate systems are used in the equation. Here, Δu^{cr} and Δv^{cr} are the incremental crack displacements in x- and y-directions, respectively.

Eq. (25), after applying the constraints, can be expressed as

$$\hat{\mathbf{K}}^{cr} \Delta \hat{\mathbf{U}}^{cr} = \Delta \hat{\mathbf{R}}^{cr} \,. \tag{27}$$

The stability condition is obtained by checking the eigenvalues of $\hat{\mathbf{K}}^{cr}$. If all the eigenvalues are positive, it means that the equilibrium path is stable with respect to the current crack pattern and there is no bifurcation. On the contrary, if some of the eigenvalues are negative, the equilibrium path is not stable with respect to the current crack pattern and a stable crack pattern must be found.

4. Results and Discussion

In order to illustrate the advantage of the method in the analysis of the cracking localization, a simple one-dimensional uniaxial problem shown in Fig. 1 is considered. Application of the proposed method to problems in two- and three-dimensional domains is just straightforward. Nevertheless, two- and three-dimensional problems are not used here because illustrative analytical results

cannot be easily obtained from them. As shown in Fig. 1, the bar has one fixed support at one end. At the other end, controlled displacement \overline{u} is applied. The length of the bar is 2L and the area is A. The material is assumed to be elastic with Young's modulus equal to E. The bar is discretized into two elements, each of which has the length of L. Each element can accommodate one crack. The characteristic length or crack band width of each crack, in this case, is equal to the length of the element. The conventional linear shape function is used for the displacement interpolation.

It is assumed that there is no crack at the beginning. The controlled displacement is then increased until the stress of the bar reaches the tensile strength f_i . By the strength criterion, both elements are cracked. The cracks follow the constitutive law for cracks. For opening cracks, a linear relationship between the transmitted tensile stress and the crack opening

displacement (COD) with the slope $\frac{\Delta \sigma}{\Delta \text{COD}}$ equal to H is assumed. For unloading cracks, a vertical unloading path with a constant COD equal to the existing COD is applied (see Fig. 1).

Consider an incremental step after the initiation of the cracks. Assembling all element stiffness equations given by Eq. (23), we can write the global stiffness equation. After

applying the prescribed boundary conditions, we obtain

$$\begin{split} & \underbrace{\frac{A}{L}} \begin{bmatrix} 2E & E & -E & -E & E \\ E & E + \widetilde{H} & -(E + \widetilde{H}) & 0 & 0 \\ -E & -(E + \widetilde{H}) & E + \widetilde{H} & 0 & 0 \\ -E & 0 & 0 & E + \widetilde{H} & -(E + \widetilde{H}) \\ E & 0 & 0 & -(E + \widetilde{H}) & E + \widetilde{H} \end{bmatrix} \begin{bmatrix} \Delta U_2 \\ \Delta^t U_1'' \\ \Delta^t U_2'' \\ \Delta^t U_2'' \\ \Delta^t U_2'' \end{bmatrix} \\ & = \underbrace{\frac{A}{L}} \begin{bmatrix} E \Delta \widetilde{u} \\ 0 \\ 0 \\ -E \Delta \widetilde{u} \\ E \Delta \widetilde{u} \end{bmatrix} \end{split}$$

where $\widetilde{H} = HL$. Here, ΔU_i represents the nodal displacement increment of the node i. Moreover, $\Delta^i U_j^{cr}$ represents the nodal crack displacement increment of the node j and, at the same time, of the element i.

Using the static condensation to remove ΔU_2 , we get

$$\frac{A}{L} \begin{bmatrix}
\frac{E+2\widetilde{H}}{2} & -\frac{E+2\widetilde{H}}{2} & \frac{E}{2} & -\frac{E}{2} \\
-\frac{E+2\widetilde{H}}{2} & \frac{E+2\widetilde{H}}{2} & -\frac{E}{2} & \frac{E}{2} \\
\frac{E}{2} & -\frac{E}{2} & \frac{E+2\widetilde{H}}{2} & -\frac{E+2\widetilde{H}}{2} \\
-\frac{E}{2} & \frac{E}{2} & -\frac{E+2\widetilde{H}}{2} & \frac{E+2\widetilde{H}}{2}
\end{bmatrix} \begin{bmatrix}
\Delta^{1}U_{1}^{\alpha} \\
\Delta^{1}U_{2}^{\alpha} \\
\Delta^{2}U_{2}^{\alpha} \\
\Delta^{2}U_{3}^{\alpha}
\end{bmatrix}$$

$$= \frac{A}{L} \begin{bmatrix}
-\frac{E\Delta\overline{u}}{2} \\
\frac{E\Delta\overline{u}}{2} \\
\frac{E\Delta\overline{u}}{2}
\end{bmatrix}$$

$$= \frac{A}{L} \begin{bmatrix}
-\frac{E\Delta\overline{u}}{2} \\
\frac{E\Delta\overline{u}}{2} \\
\frac{E\Delta\overline{u}}{2}
\end{bmatrix}$$
(29)

The above equation is singular due to the rigid-body crack displacement increments in the two elements. For one-dimensional problems, the crack displacement increment at the center of each element is set to zero, i.e.,

$$\Delta^{1}u^{cr}(\xi=0) = \frac{1}{2}(\Delta^{1}U_{1}^{cr} + \Delta^{1}U_{2}^{cr}) = 0,$$

$$\Delta^{2}u^{cr}(\xi=0) = \frac{1}{2}(\Delta^{2}U_{2}^{cr} + \Delta^{2}U_{3}^{cr}) = 0,$$
(30)

which leads to

(28)

$$\frac{A}{L} \begin{bmatrix} 2(E+2\widetilde{H}) & 2E \\ 2E & 2(E+2\widetilde{H}) \end{bmatrix} \begin{bmatrix} \Delta^{1}U_{1}^{cr} \\ \Delta^{2}U_{1}^{cr} \end{bmatrix} \\
= \frac{A}{L} \begin{cases} -E\Delta\overline{u} \\ -E\Delta\overline{u} \end{cases}.$$
(31)

Note that, in applying the constraints to Eq. (29), not only the row but also the column operations must be performed to the stiffness matrix so as to obtain the symmetric matrix in Eq. (31). Actually, the constraints may be directly applied to each element before assembling the element stiffness equations.

The eigenvalues of the obtained stiffness

matrix are
$$\frac{4A\widetilde{H}}{L}$$
 and $\frac{4A(E+\widetilde{H})}{L}$. Both

eigenvalues are positive only when $\widetilde{H}>0$. This means that the crack pattern having two cracks opening at the same time is unstable unless hardening behavior occurs at the cracks.

If we assume that the crack in the element 2 undergoes the elastic unloading, the global stiffness equation will contain only one cracked element. Employing the same process of applying the prescribed boundary conditions and using the static condensation for this case, we obtain

$$\frac{A}{L} \left[2(E + 2\widetilde{H}) \right] \left\{ \Delta^{\mathsf{I}} U_{\mathsf{I}}^{\mathsf{cr}} \right\} = \frac{A}{L} \left\{ -E \Delta \overline{u} \right\} \quad (32)$$

The eigenvalue of the stiffness matrix is $\frac{2A(E+2\widetilde{H})}{L}$ which is positive when $\widetilde{H} > -\frac{E}{2}$.

Assuming that the crack in the element l undergoes the elastic unloading will yield the same conclusion.

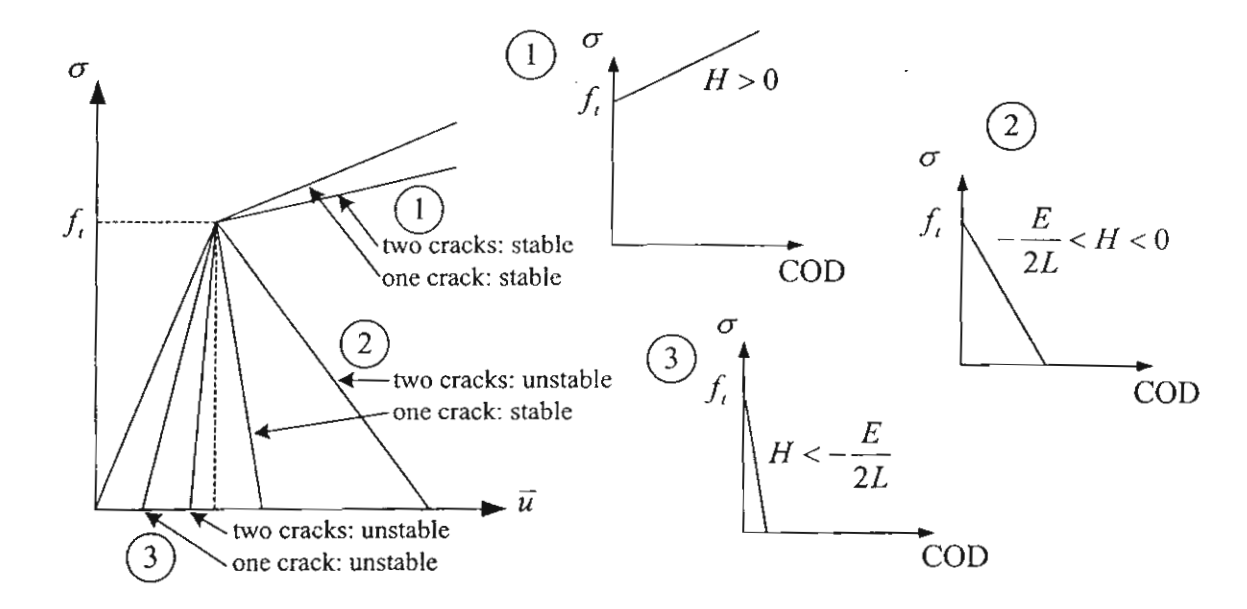


Fig. 2 Responses of the uniaxial problem using two 1-D bar elements

In summary, immediately after the two elements are cracked due to the strength criterion employed, the equilibrium path is unstable and bifurcation occurs unless both cracks exhibit hardening behavior, i.e., when $\tilde{H} > 0$. In reality, cracks will exhibit softening behavior. Therefore, the two cracks cannot continue to open at the same time. If one of the cracks undergoes the elastic unloading, the stable equilibrium path can be observed as long as $\widetilde{H} > -\frac{E}{2}$. As shown in Fig. 2, which summarizes all the possible results, the cases where $\widetilde{H} < -\frac{E}{2}$ represent the responses with snapback behavior. Under the displacement control, the snapback responses are always unstable.

It can be seen from the results that the proposed method allows the consideration of the cracking localization to be done even when the smeared crack approach is used. As mentioned before, there is no intention to use the stiffness equation obtained from the proposed method in the analysis to obtain the unknown displacements. For that purpose, the original smeared crack approach is much more appropriate and will be used. The proposed

scheme is used only for the investigation of the stability of the crack patterns.

The reason that the smeared crack approach is selected for the analysis of the localization is that the analysis of this kind involves problems with many cracks. To permit the investigation of the stability of the crack patterns with the smeared crack models. discrete irreversible the variables introduced to the models. As it is seen from the derivation and the results, the introduced irreversible variables, which are the crack displacement variables, allow the energy of the system to be expressed as a function of the discrete irreversible variables. Therefore, the stationary condition of the energy with respect to these discrete irreversible variables can be done easily. Consequently, we can use the smeared crack models both for computing the unknown displacements and for checking the stability of the crack patterns.

Nevertheless, there are still many more problems, related to the analysis of the cracking localization, to be solved. For complex localization problems, such as the four-point bending problem, there are chances that there will be many stable crack patterns occurring at the same time. Because of the complicated crack patterns, it is not easy to single out the correct solutions. The complete

and efficient analysis methods still have to be developed.

5. Acknowledgements

The authors would like to express their sincere gratitude to the Thailand Research Fund for supporting this research.

References

- [1] J. G. Rots and R. de Borst, "Analysis of Mixed-Mode Fracture in Concrete", Journal of Engineering Mechanics, Vol. 113, No. 11, 1987, pp. 1739-1758.
- [2] J. G. Rots, "Stress Rotation and Stress Locking in Smeared Analysis of Separation", Fracture Toughness and Fracture Energy: Test Methods for Concrete and Rock (Eds: H. Mihashi, H. Takahashi and F. Wittmann), Rotterdam, Balkema, 1989, pp. 367-382.
- [3] E. N. Dvorkin and A. P. Assanelli, "2D Finite Elements with Displacement Interpolated Embedded Localization Lines: The Analysis of Fracture in Frictional Materials", Computer Methods in Applied Mechanics and Engineering, Vol. 90, 1991, pp. 829-844.
- [4] M. Jirasek and T. Zimmermann, "Rotating Crack Model with Transition to Scalar Damage", Journal of Engineering Mechanics, 1998, Vol. 124, No. 3, pp. 277-284.
- [5] N. Shirai, "JCI Round Robin Analysis of Size Effect in Concrete Structures", Size Effect in Concrete Structures (Eds: H. Mihashi, H. Okamura and Z. P. Bazant), London, E&FN Spon, 1994, pp. 295-322.
- [6] A. Carpinteri, "Softening and Snap-Back Instability in Cohesive Solids" International Journal for Numerical

- Methods in Engineering, 1989, Vol. 28, pp. 1521-1537.
- [7] E. Riks, "An Incremental Approach to the Solution of Snapping and Buckling Problems", International Journal of Solids Structures, 1979, Vol. 15, pp. 529-551.
- [8] R. de Borst, "Computation of Post-Bifurcation and Post-Failure Behavior of Strain-Softening Solids", Computers and Structures, 1987, Vol. 25, No. 2, pp. 211-224.
- [9] S. Valente, "Bifurcation Phenomena in Cohesive Crack Propagation", Computers and Structures, 1992, Vol. 44, No. 1/2, pp. 55-62.
- [10] Q. S. Nguyen, "Bifurcation and Post-Bifurcation Analysis in Plasticity and Brittle Fracture", Journal of the Mechanics and Physics of Solids, 1987, Vol. 35, No. 3, pp. 303-324.
- [11] H. Horii, "Micromechanics and Localization in Concrete and Rock", Fracture and Damage of Concrete and Rock (Ed: H. P. Rossmanith), London, E&FN Spon, 1993, pp. 54-65.
- [12] M. Brocca, Analysis of Cracking Localization and Crack Growth Based on Thermomechanical Theory of Localization (Master's Degree Thesis), Tokyo, University of Tokyo, 1997.
- [13] Z. P. Bazant and B. H. Oh, "Crack Band Theory for Fracture of Concrete", Materiaux et Constructions, 1983, Vol. 16, No. 93, pp. 155-177.
- [14] S. P. Shah, S. E. Swartz and C. Ouyang, Fracture Mechanics of Concrete: Applications of Fracture Mechanics to Concrete, Rock, and Other Quasi-Brittle Materials, New York, John Wiley & Sons, 1995.

problems of concrete beams with long notches [6]. The others are cases where the required solutions, such as the ultimate loads, are not sensitive to the locations of the localized cracks [5]. However, this second approach is not appropriate for general cases since the locations of the localized cracks may not be easily predicted or the required solutions may be sensitive to the locations of the cracks.

In the analysis of the cracking which involves irreversible localization, processes, consideration of stability and bifurcation of equilibrium states with respect to irreversible parameters is one of the tasks to be done. Many researchers have considered the stability and bifurcation of the equilibrium states by investigating the definiteness of the stiffness matrices (Hessian Matrices) [7, 8, 9]. When the matrix is positive-definite, the equilibrium is stable. The same theory can be applied to the analysis of the cracking localization. However, cracking is an irreversible process. To consider stability and bifurcation of irreversible processes, the stationary condition of the energy of the system with respect to irreversible parameters has to be investigated [10, 11, 12]. For this reason, the expression of the energy in terms of the irreversible parameters is required. For crack problems, the irreversible parameters can be the discrete irreversible crack opening displacements in the discrete crack approach or the irreversible crack strains in the smeared crack approach. In the discrete crack approach, the crack opening displacements are usually discretized along crack paths and treated as the degrees of freedom in the analysis. The energy of the system can be expressed in terms of these degrees of freedom. Computing the first and second variations of the energy with respect to these discrete crack opening displacements can be done easily by employing ordinary calculus [12]. In the smeared crack approach, the energy is expressed in terms of irreversible crack strains, which are functions of position and are generally not discretized. To compute the first and second variations of the energy with respect to these crack strains, a complex mathematics involving the calculus of variations must be employed. This fact implies that the discrete crack approach in the finite element method may be more suitable for the cracking localization analysis than the smeared crack_approach.

However, the discrete crack approach

may not be the best choice for problems with many cracks. In the cracking localization analysis, there will be many cracks appearing in the domain. Having many cracks in the domain leads to many degrees of freedom. Furthermore. as the number of cracks increases, the mesh topology of the problem may have to be changed significantly to cope with the new crack patterns. In addition, the singularity problem of the system stiffness equation may also arise. These problems can be mostly avoided if the smeared crack approach is employed. In the smeared crack models, no increase in the number of the degrees of freedom or change in the mesh topology is required during the propagation of cracks. Although the smeared crack models may also face the singularity problem of the system in case of softening materials, the problem is less serious than that of the discrete crack models.

To avoid the drawbacks in both approaches, in this study, discrete irreversible variables are introduced in the smeared crack models. To this end, a mixed formulation of the finite element method that includes the discretization of the displacement and crack strain fields is proposed. The energy of the system is written in terms of the discretized displacements and crack strains. Consequently, the stability of crack patterns with respect to the discretized irreversible crack strains can be easily evaluated, and the cracking localization can be discussed.

In this paper, the derivation of the proposed mixed formulation is shown. After that, the validity of the proposed technique is checked by solving a benchmark uniaxial problem using one- and two-dimensional elements. The obtained results show promising capability of the method for the analysis of the cracking localization.

2. Mixed Finite Element Formulation for Analysis of Cracking Localization

The fundamental scheme of the smeared crack models [1, 13, 14] is the decomposition of the total strain increment $\Delta\epsilon$ into the strain increments of an intact solid part $\Delta\epsilon''$ and a cracked part $\Delta\epsilon''$, i.e.,

$$\Delta \varepsilon = \Delta \varepsilon^{o} + \Delta \varepsilon^{cr}. \tag{1}$$

displacement and local crack strain increments. For the i^{th} element in the finite element analysis, we have

$$\Delta \mathbf{u} = \mathbf{N} \Delta' \mathbf{U} \tag{10a}$$

$$\Delta \hat{\mathbf{\epsilon}}^{cr} = \mathbf{N}^{cr} \Delta' \hat{\mathbf{E}}^{cr} \tag{10b}$$

where N and N^{cr} represent the shape function matrices for the displacement and local crack strain increments, respectively. In addition, $\Delta'U$ and $\Delta'\hat{\mathbf{E}}^{cr}$ represent the nodal displacement and nodal local crack strain increment vectors, respectively.

Note that the local crack strain increments are not continuous across elements and the nodal local crack strain increments of the same node for different elements can be different. The continuity of the local crack strain increments between elements is not required and must not be enforced. One example is a problem with one cracked element surrounded by uncracked elements. In the cracked element including its boundary, non-zero crack strain increments (see Fig. 1) can be expected. However, in the surrounding uncracked elements, the crack strain increments are expected to be zero because there is no crack in those elements. On the contrary, the total displacement increments must be continuous across the elements.

By substituting Eq. (1) into Eq. (9), the total energy increment for the i^{th} element is rewritten as

$$\Delta \Pi = \frac{1}{2} \int_{V} (\Delta \varepsilon - \Delta \varepsilon^{cr})^{T} \mathbf{D}^{o} (\Delta \varepsilon - \Delta \varepsilon^{cr}) dV$$

$$+ \frac{1}{2} \int_{V} \Delta \hat{\varepsilon}^{cr} \hat{\mathbf{D}}^{cr} \Delta \hat{\varepsilon}^{cr} dV$$

$$- \int_{V} \Delta \mathbf{u}^{T} \Delta \mathbf{f} dV - \int_{S} \Delta \mathbf{u}^{T} \Delta \mathbf{t} dS.$$
(11)

From Eq. (10a), we write the total strain increment in terms of the nodal displacement increment, i.e.,

$$\Delta \varepsilon = \mathbf{B} \Delta^i \mathbf{U} . \tag{12}$$

Substituting Eq. (10b) into Eq. (3) yields

$$\Delta \varepsilon^{cr} = \mathbf{T} \mathbf{N}^{cr} \Delta^{i} \hat{\mathbf{E}}^{cr}. \tag{13}$$

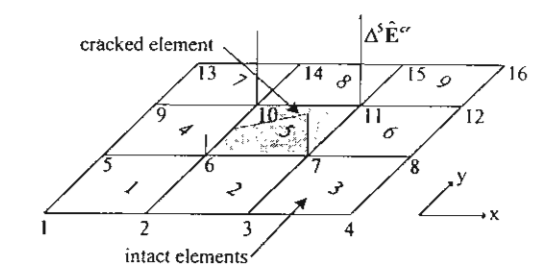


Fig. 1 A problem with one cracked element surrounded by uncracked elements

Substituting Eqs. (12) and (13) into Eq. (11), we get

$$\Delta\Pi = \frac{1}{2} \int_{\nu} \Delta' \mathbf{U}^{T} \mathbf{B}^{T} \mathbf{D}^{\alpha} \mathbf{B} \Delta' \mathbf{U} dV$$

$$- \frac{1}{2} \int_{\nu} \Delta' \hat{\mathbf{L}}^{\alpha} \mathbf{B}^{T} \mathbf{D}^{\alpha} \mathbf{T} \mathbf{N}^{\alpha c} \Delta' \hat{\mathbf{E}}^{\alpha c} dV$$

$$- \frac{1}{2} \int_{\nu} \Delta' \hat{\mathbf{E}}^{\alpha c} \mathbf{N}^{c c} \mathbf{T} \mathbf{T}^{T} \mathbf{D}^{\alpha} \mathbf{B} \Delta' \mathbf{U} dV$$

$$+ \frac{1}{2} \int_{\nu} \Delta' \hat{\mathbf{E}}^{\alpha c} \mathbf{N}^{c c} \mathbf{T} \mathbf{T}^{T} \mathbf{D}^{\alpha} \mathbf{T} \mathbf{N}^{c c} \Delta' \hat{\mathbf{E}}^{c c} dV$$

$$+ \frac{1}{2} \int_{\nu} \Delta' \hat{\mathbf{E}}^{c c} \mathbf{N}^{c c} \mathbf{N}^{c c} \hat{\mathbf{D}}^{\alpha} \mathbf{N}^{c c} \Delta' \hat{\mathbf{E}}^{c c} dV$$

$$- \int_{\nu} \Delta' \mathbf{U}^{T} \mathbf{N}^{T} \Delta f dV - \int_{s} \Delta' \mathbf{U}^{T} \mathbf{N}^{T} \Delta t dS.$$
(14)

Applying the stationary condition to Eq. (14) and assuming that both D^{α} and D^{α} are symmetric, we get

$$\delta(\Delta\Pi) = \delta(\Delta'\mathbf{U}^T) \int_{\nu} \mathbf{B}^T \mathbf{D}^o \mathbf{B} dV \Delta \mathbf{U}$$

$$-\delta(\Delta'\mathbf{U}^T) \int_{\nu} \mathbf{B}^T \mathbf{D}^o \mathbf{T} \mathbf{N}^{cr} dV \Delta' \hat{\mathbf{E}}^{cr}$$

$$-\delta(\Delta' \hat{\mathbf{E}}^{cr}) \int_{\nu} \mathbf{N}^{cr} \mathbf{T}^T \mathbf{D}^o \mathbf{B} dV \Delta' \mathbf{U}$$

$$+\delta(\Delta' \hat{\mathbf{E}}^{cr}) \int_{\nu} \mathbf{N}^{cr} \mathbf{T}^T \mathbf{D}^o \mathbf{T} \mathbf{N}^{cr} dV \Delta' \hat{\mathbf{E}}^{cr}$$

$$+\delta(\Delta' \hat{\mathbf{E}}^{cr}) \int_{\nu} \mathbf{N}^{cr} \hat{\mathbf{D}}^{cr} \mathbf{N}^{cr} dV \Delta' \hat{\mathbf{E}}^{cr}$$

$$-\delta(\Delta' \mathbf{U}^T) \int_{\nu} \mathbf{N}^T \Delta f dV$$

$$-\delta(\Delta' \mathbf{U}^T) \int_{s} \mathbf{N}^T \Delta t dS$$

$$= 0.$$
(15)

Since $\delta(\Delta' \mathbf{U}^T)$ and $\delta(\Delta' \hat{\mathbf{E}}^{\sigma^T})$ are arbitrary, we obtain the element stiffness equation for the i^{th} element, i.e.,

$$\begin{bmatrix} \mathbf{k}_{11} & \mathbf{k}_{12} \\ \mathbf{k}_{21} & \mathbf{k}_{22} \end{bmatrix} \begin{bmatrix} \Delta' \mathbf{U} \\ \Delta' \hat{\mathbf{E}}^{cr} \end{bmatrix} = \begin{bmatrix} \Delta \mathbf{r} \\ 0 \end{bmatrix}$$
 (16)

where

$$\mathbf{k}_{11} = \int_{V} \mathbf{B}^{T} \mathbf{D}^{o} \mathbf{B} dV$$

$$\mathbf{k}_{12} = -\int_{V} \mathbf{B}^{T} \mathbf{D}^{o} \mathbf{T} \mathbf{N}^{cr} dV$$

$$\mathbf{k}_{21} = -\int_{V} \mathbf{N}^{cr} \mathbf{T} \mathbf{T}^{T} \mathbf{D}^{o} \mathbf{B} dV$$

$$\mathbf{k}_{22} = \int_{V} \mathbf{N}^{cr} \left(\hat{\mathbf{D}}^{cr} + \mathbf{T}^{T} \mathbf{D}^{o} \mathbf{T} \right) \mathbf{N}^{cr} dV$$

$$\Delta \mathbf{r} = \int_{V} \mathbf{N}^{T} \Delta \mathbf{f} dV + \int_{S} \mathbf{N}^{T} \Delta \mathbf{t} dS.$$
(17)

After assembling all element stiffness equations and applying prescribed displacements and forces, we arrange the system stiffness equation in the following form, i.e.,

$$\begin{bmatrix} \mathbf{K}_{11} & \mathbf{K}_{12} \\ \mathbf{K}_{21} & \mathbf{K}_{22} \end{bmatrix} \begin{bmatrix} \Delta \mathbf{U} \\ \Delta \hat{\mathbf{E}}^{cr} \end{bmatrix} = \begin{bmatrix} \Delta \mathbf{R}_{1} \\ \Delta \mathbf{R}_{2} \end{bmatrix}$$
(18)

where ΔU and $\Delta \hat{E}^{cr}$ represent, respectively, the nodal displacement increment and nodal local crack strain increment vectors for the system stiffness equation.

The static condensation is then used to remove the nodal displacement increment from the obtained system stiffness equation. Consequently, the equation can be written in the following form, i.e.,

$$\mathbf{K}^{cr} \Delta \hat{\mathbf{E}}^{cr} = \Delta \mathbf{R}^{cr} \tag{19}$$

where $K^{\prime\prime}$ and $\Delta R^{\prime\prime}$ are defined as

$$\mathbf{K}^{cr} = \mathbf{K}_{22} - \mathbf{K}_{21} \mathbf{K}_{11}^{-1} \mathbf{K}_{12}$$

$$\Delta \mathbf{R}^{cr} = \Delta \mathbf{R}_{2} - \mathbf{K}_{21} \mathbf{K}_{11}^{-1} \Delta \mathbf{R}_{1}.$$
 (20)

To investigate the stability of crack patterns, we compute the eigenvalues of \mathbf{K}^{cr} . If

all of the eigenvalues are positive, it means that the solution is stable with respect to the current crack pattern. Otherwise, the solution is unstable and bifurcation occurs [10, 11, 15]. This will finally result in the localization of the cracks. Note that the proposed scheme is not used to obtain the displacement solution. The scheme is used only for stability consideration. The displacement solution will be obtained from the original smeared crack model where the only basic unknowns are the nodal displacements.

3. Results

In order to illustrate the advantage of the proposed method in the analysis of the cracking localization, a simple one-dimensional uniaxial problem shown in Fig. 2 is considered. The bar has one fixed support at one end. At the other end, the controlled displacement \bar{u} is applied (see Fig. 2a). The length of the bar is 2L and the area is A. The material is assumed to be elastic with Young's modulus equal to E (see Fig. 2c). The bar is discretized into two elements, each of which has the length of L (see Fig. 2a). Each element can accommodate one crack. The characteristic length of each crack is equal to the length of the element. The conventional linear shape function is used for the displacement and local crack strain interpolations.

Assume no crack at the beginning. After that, the controlled displacement \bar{u} is increased until the stress in the bar reaches the tensile strength f_i . By the strength criterion, both elements are cracked (see Fig. 2b), and they are changed from the elastic elements into the smeared crack elements. Thereafter, the cracks follow the constitutive law for cracks (see Fig. 2d). For opening cracks, a linear relationship between the transmitted tensile stress and the crack opening displacement (COD) with the

slope
$$\frac{\Delta \sigma}{\Delta \text{COD}}$$
 equal to H is assumed. Since,

for ordinary cracks, softening behavior is always observed (H < 0), this relationship is called the tension-softening relationship. It can be seen from the tension-softening relationship (H < 0) that when a crack opens wider, the tensile stress transmitted across the crack decreases. This tension-softening relationship, which is used for all opening cracks, is also called the loading path.

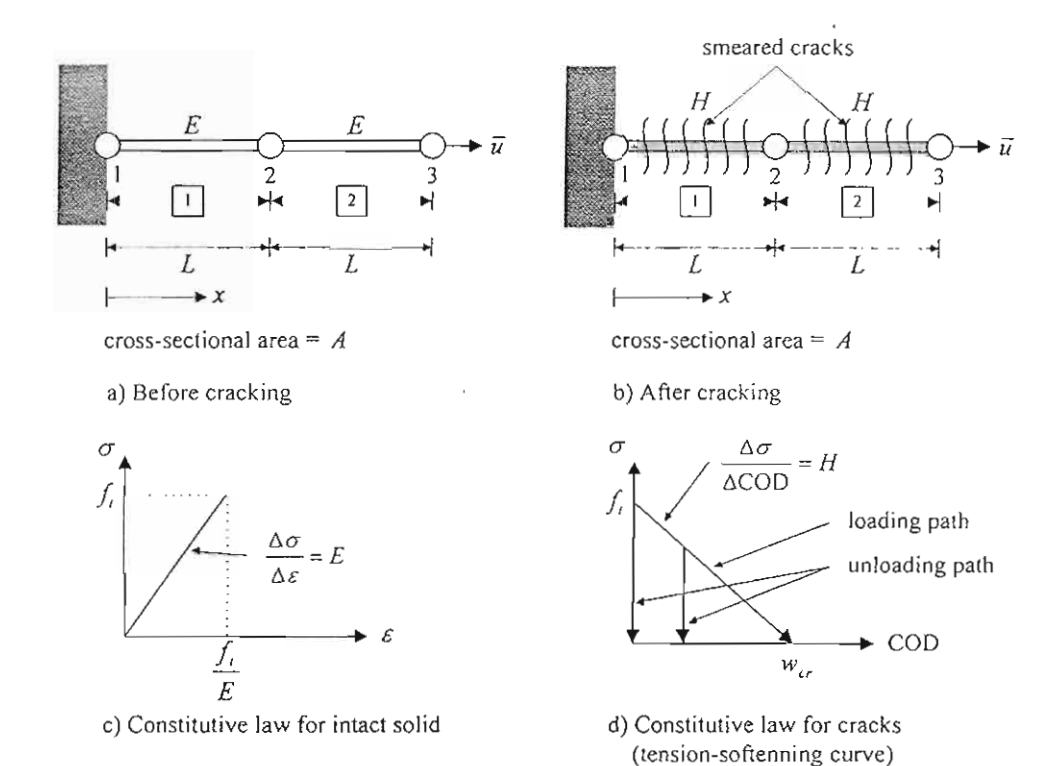


Fig. 2 Uniaxial problem using one-dimensional bar elements

Generally, during loading, there may be some cracks that stop opening. These cracks are the unloading cracks. When a crack stops opening, its COD stops increasing. In this study, cracking is assumed to be an irreversible process, which means that CODs will not decrease. Therefore, each of these cracks will follow a vertical unloading path with a constant COD equal to the current COD that the crack has just before the unloading occurs (see Fig. 2d). For cracks with different CODs when the unloading occurs, different vertical unloading paths will be used.

Consider an incremental step after the initiation of the cracks. Note that both elements are now the smeared crack elements. Assembling all element stiffness equations given by Eq. (16), we write the system stiffness equation as

$$\begin{bmatrix}
\frac{E}{L} - \frac{E}{L} & 0 & \frac{E}{2} & \frac{E}{2} & 0 & 0 \\
-\frac{E}{L} \frac{2E}{L} - \frac{E}{L} & -\frac{E}{2} & -\frac{E}{2} & \frac{E}{2} & \frac{E}{2} \\
0 - \frac{E}{L} \frac{E}{L} & 0 & 0 & -\frac{E}{2} - \frac{E}{2} \\
\frac{E}{2} - \frac{E}{2} & 0 & (E + \widetilde{H})L (E + \widetilde{H})L & 0 & 0 \\
\frac{E}{2} - \frac{E}{2} & 0 & (E + \widetilde{H})L (E + \widetilde{H})L & 0 & 0 \\
0 & \frac{E}{2} - \frac{E}{2} & 0 & 0 & (E + \widetilde{H})L (E + \widetilde{H})L \\
0 & \frac{E}{2} - \frac{E}{2} & 0 & 0 & (E + \widetilde{H})L (E + \widetilde{H})L \\
0 & \frac{E}{2} - \frac{E}{2} & 0 & 0 & (E + \widetilde{H})L (E + \widetilde{H})L \\
0 & \frac{E}{2} - \frac{E}{2} & 0 & 0 & (E + \widetilde{H})L (E + \widetilde{H})L \\
0 & \frac{E}{2} - \frac{E}{2} & 0 & 0 & (E + \widetilde{H})L (E + \widetilde{H})L \\
0 & \frac{E}{2} - \frac{E}{2} & 0 & 0 & (E + \widetilde{H})L (E + \widetilde{H})L \\
0 & \frac{E}{2} - \frac{E}{2} & 0 & 0 & (E + \widetilde{H})L (E + \widetilde{H})L \\
0 & 0 & 0 & (E + \widetilde{H})L (E + \widetilde{H})L \\
0 & 0 & 0 & 0 & (E + \widetilde{H})L (E + \widetilde{H})L \\
0 & 0 & 0 & 0 & (E + \widetilde{H})L (E + \widetilde{H})L \\
0 & 0 & 0 & 0 & (E + \widetilde{H})L (E + \widetilde{H})L \\
0 & 0 & 0 & 0 & (E + \widetilde{H})L (E + \widetilde{H})L \\
0 & 0 & 0 & 0 & (E + \widetilde{H})L (E + \widetilde{H})L \\
0 & 0 & 0 & 0 & (E + \widetilde{H})L (E + \widetilde{H})L \\
0 & 0 & 0 & 0 & (E + \widetilde{H})L (E + \widetilde{H})L \\
0 & 0 & 0 & 0 & (E + \widetilde{H})L (E + \widetilde{H})L \\
0 & 0 & 0 & 0 & (E + \widetilde{H})L (E + \widetilde{H})L \\
0 & 0 & 0 & 0 & (E + \widetilde{H})L (E + \widetilde{H})L \\
0 & 0 & 0 & 0 & (E + \widetilde{H})L (E + \widetilde{H})L (E + \widetilde{H})L \\
0 & 0 & 0 & 0 & (E + \widetilde{H})L (E + \widetilde{H})L (E + \widetilde{H})L \\
0 & 0 & 0 & 0 & 0 & (E + \widetilde{H})L (E + \widetilde{H})L (E + \widetilde{H})L \\
0 & 0 & 0 & 0 & 0 & (E + \widetilde{H})L \\
0 & 0 & 0 & 0 & 0 & (E + \widetilde{H})L (E + \widetilde$$

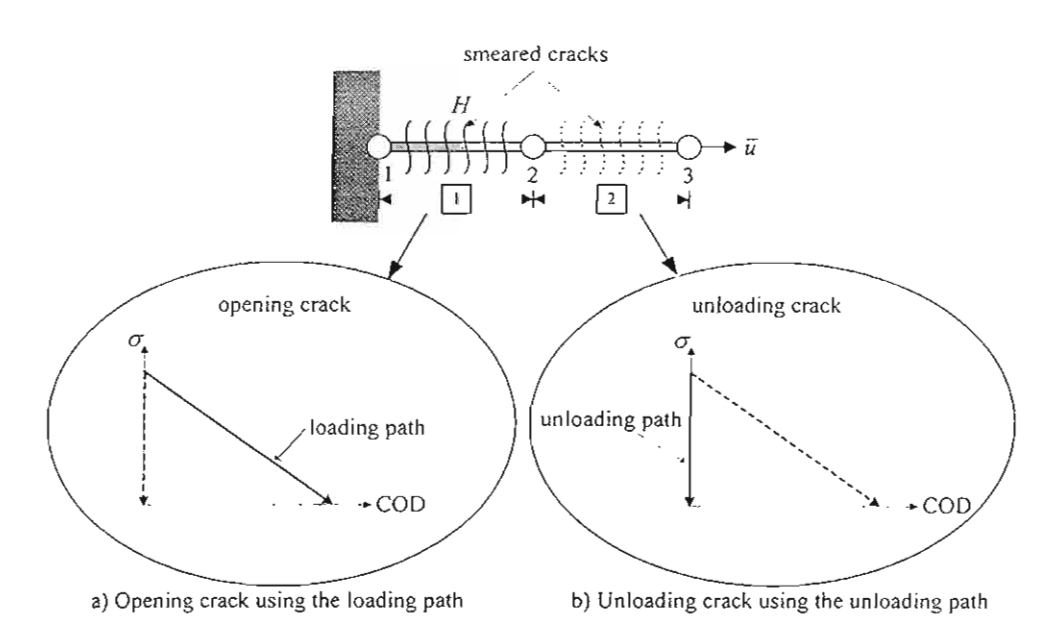


Fig. 3 Solution with one unloading crack

where
$$\widetilde{H} = \frac{\Delta \sigma}{\Delta \varepsilon''} = HL' = HL$$
. Here, L'

represents the characteristic length of the crack and is equal to L. In addition, ΔU_i , and ΔR_i represent the nodal displacement increment and the nodal force increment of the node i, respectively. Moreover, $\Delta' \hat{E}_j^{\alpha}$ represents the nodal local crack strain increment of the node j and, at the same time, of the element i.

Since ΔU_1 , ΔU_3 and ΔR_2 are prescribed, the equation can be reduced into

$$A = A \mathcal{E} \begin{cases} \frac{2\mathcal{E}}{L} - \frac{\mathcal{E}}{2} - \frac{\mathcal{E}}{2} - \frac{\mathcal{E}}{2} - \frac{\mathcal{E}}{2} - \frac{\mathcal{E}}{2} - \frac{\mathcal{E}}{2} \\ -\frac{\mathcal{E}}{2} \frac{(\mathcal{E} + \tilde{H})L}{3} \frac{(\mathcal{E} + \tilde{H})L}{6} - 0 & 0 \\ -\frac{\mathcal{E}}{2} \frac{(\mathcal{E} + \tilde{H})L}{6} \frac{(\mathcal{E} + \tilde{H})L}{3} - 0 & 0 \\ \frac{\mathcal{E}}{2} - 0 & 0 & \frac{(\mathcal{E} + \tilde{H})L}{3} \frac{(\mathcal{E} + \tilde{H})L}{6} \\ \frac{\mathcal{E}}{2} - 0 & 0 & \frac{(\mathcal{E} + \tilde{H})L}{6} \frac{(\mathcal{E} + \tilde{H})L}{3} \\ \frac{\mathcal{E}}{2} - 0 & 0 & \frac{\mathcal{E}}{2} - \frac{\mathcal{E}}{2$$

Using the static condensation to remove ΔU_2 , we get

$$\frac{AL}{24} \begin{bmatrix} \left(5E + 8\widetilde{H}\right) & \left(E + 4\widetilde{H}\right) & 3E & 3E \\ \left(E + 4\widetilde{H}\right) & \left(5E + 8\widetilde{H}\right) & 3E & 3E \\ 3E & 3E & \left(5E + 8\widetilde{H}\right) & \left(E + 4\widetilde{H}\right) \\ 3E & 3E & \left(E + 4\widetilde{H}\right) & \left(5E + 8\widetilde{H}\right) \end{bmatrix} \begin{bmatrix} \Delta' \hat{E}', \\ \Delta' \hat{E}',$$

The eigenvalues of the obtained stiffness matrix are $\frac{A\widetilde{H}L}{2}$, $\frac{A(E+\widetilde{H})L}{6}$, $\frac{A(E+\widetilde{H})L}{6}$ and $\frac{A(E+\widetilde{H})L}{2}$. All eigenvalues will be

positive only when $\widetilde{H}>0$. This means that the crack pattern having two cracks opening at the same time is unstable unless hardening behavior occurs at the cracks ($\widetilde{H}>0$). In reality, cracks will exhibit softening behavior. As a result, the two cracks cannot continue to open at the same time

If we assume that the crack in the element 2 undergoes the elastic unloading, this crack will follow the vertical unloading path

shown in Fig. 3b. The crack in the element 1, which still continues to open, will follow the loading path shown in Fig. 3a. Note, in Fig. 3b, that the unloading path for the crack in the element 2 has the COD equal to zero. This is because, at the current state, the cracks in both elements are just initiated and the CODs are still exactly equal to zero. Remember that an incremental step after the initiation of the cracks is being considered and the stable solution path for this incremental step is being searched. With the crack in the element 2 unloading, the system stiffness equation will contain only one crack element, i.e.,

$$\begin{bmatrix} \frac{E}{L} - \frac{E}{L} & 0 & \frac{E}{2} & \frac{E}{2} \\ -\frac{E}{L} \frac{2E}{L} - \frac{E}{L} & -\frac{E}{2} & -\frac{E}{2} \\ 0 - \frac{E}{L} \frac{E}{L} & 0 & 0 \\ \frac{E}{2} - \frac{E}{2} & 0 & \frac{\left(E + \widetilde{H}\right)L}{3} \left(E + \widetilde{H}\right)L} \begin{pmatrix} \Delta U_{i} \\ \Delta U_{i} \\ \Delta \tilde{E}_{i} \end{pmatrix} = \begin{bmatrix} \Delta R_{i} \\ \Delta R_{i} \\ \Delta R_{i} \\ 0 \\ 0 \end{bmatrix}$$

Employing the same process of applying the prescribed boundary conditions and using the static condensation, we obtain

$$\frac{AL}{24} \left[(5E + 8\widetilde{H}) (E + 4\widetilde{H}) \atop (E + 4\widetilde{H}) (5E + 8\widetilde{H}) \right] \left[\Delta' \hat{E}_{i}^{w} \right] = \frac{A}{4} \left\{ \underbrace{E \Delta \overline{u}}_{E \Delta \overline{u}} \right\}. \tag{25}$$

The eigenvalues of the stiffness matrix are
$$\frac{A(E+\widetilde{H})L}{6}$$
 and $\frac{A(E+2\widetilde{H})L}{4}$. Both will be

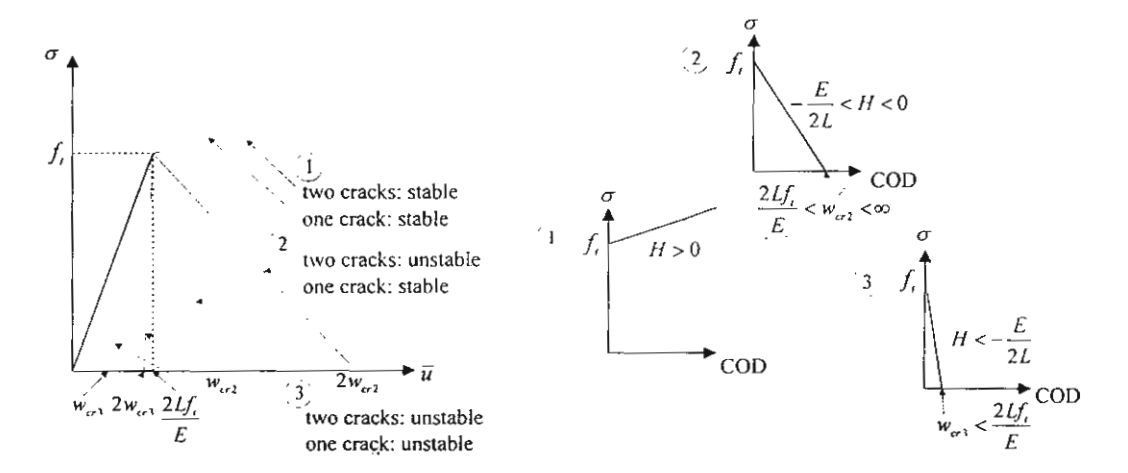
positive at the same time only when $\tilde{H} > -\frac{E}{2}$.

Assuming that the crack in the element 1 undergoes the elastic unloading will yield the same result.

In summary, immediately after the two elements are cracked due to the strength criterion employed, the equilibrium path with two opening cracks is unstable and bifurcation occurs unless the two cracks exhibit hardening behavior, i.e., when H>0. In reality, cracks will exhibit softening behavior. Therefore, the two cracks cannot continue to open at the same time. If one of the cracks undergoes the elastic unloading, the stable equilibrium path can be observed as long as $H>-\frac{E}{2L}$. In the case of

$$H < -\frac{E}{2L}$$
, even the equilibrium path with one

opening crack is not stable. Fig. 4 schematically shows the responses, obtained from the original smeared crack finite element model, for different cases of consideration. For this uniaxial problem, the responses obtained from the finite element model are exact since the linear shape function used in each element can exactly represent the exact displacement solutions, which are piecewise-linear functions of the axial coordinate. Note that the exact solutions mean

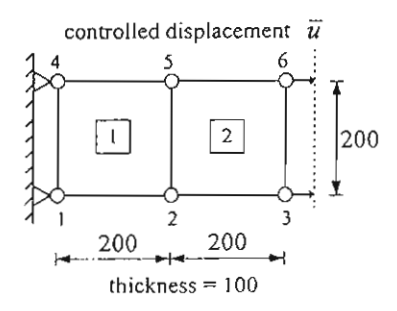


(24)

Fig. 4 Responses of the uniaxial problem using one-dimensional bar elements

the solutions that are obtained exactly from the equilibrium although they may not be stable. From Fig. 4, it can be seen that, when there is one opening crack and $H < -\frac{E}{2L}$, the obtained responses are the responses with snapback behavior. Under the displacement control, the snapback responses are always unstable.

Next, consider a uniaxial problem shown in Fig. 5. Same as the previous problem, the bar has a fixed support at one end and the displacement is controlled at the other end. However, this time, the two-dimensional elements will be used. The dimensions of the bar are as shown in the figure. The material is assumed to be elastic with Young's Modulus and Poisson's ratio equal to 25,000 and 0, respectively. The bar is discretized into two four-noded quadrilateral elements as also shown in the same figure. Each element can accommodate one crack. Since the alignment of each crack will be vertical and the elements are perfect rectangles, the characteristic length of each crack is equal to the horizontal dimension of the element. The conventional bilinear shape function is used for the displacement and local crack strain interpolations.



a) Before cracking

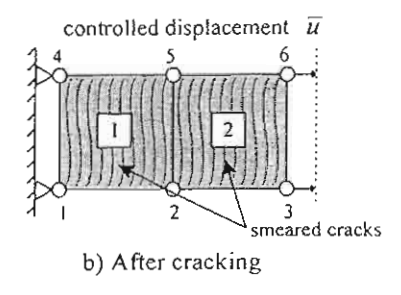


Fig. 5 Uniaxial problem using twodimensional elements

The controlled displacement \bar{u} is increased until the tensile stress in the bar reaches the tensile strength f_i , which initiates the cracks in both elements. After that, opening cracks are assumed to follow the constitutive law for cracks defined by Eq. (7). For this problem, the crack constitutive matrix $\hat{\mathbf{D}}^{e}$ is expressed as

$$\hat{\mathbf{D}}^{\mu} = \begin{bmatrix} \widetilde{H} & 0 \\ 0 & \widetilde{G} \end{bmatrix} \tag{26}$$

where \widetilde{H} and \widetilde{G} represent the mode I and mode II crack modulus, respectively.

Since the problem is purely uniaxial and there will be only mode I cracking, the parameter \widetilde{G} is irrelevant and a small value (0.00001) is used just to prevent spurious mode II instability. For mode I cracking, various linear tension-softening relationships shown in Fig. 6 are investigated. First, the tension-softening curve A, which has the critical crack opening displacement equal to 0.05, is used. Note that the critical crack opening displacement is the crack opening displacement at which the stress-free crack occurs. For this tension-softening

curve,
$$\widetilde{H} = \frac{\Delta \sigma_{mr}}{\Delta \hat{\varepsilon}_{mr}^{cr}}$$
 is equal to
 $HL' = \left(-\frac{2}{0.05}\right) 200$.

Again, consider an incremental step after the initiation of the cracks. After assembling all element stiffness equations and applying all prescribed boundary conditions, the static condensation is used to remove all nodal displacement degrees of freedom and the stiffness K^{α} in Eq. (19) is obtained. Since two

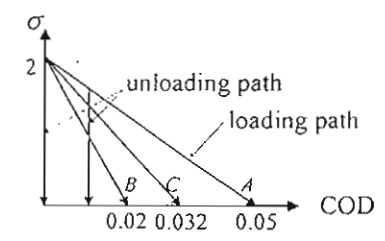


Fig. 6 Tension-softening curves for the problem using two-dimensional elements

opening cracks are being assumed, there will be totally 16 local crack strain increment degrees of freedom, eight from each of the two elements. Therefore, \mathbf{K}^{σ} is a 16×16 matrix. The eigenvalue analysis is performed on \mathbf{K}^{σ} and the eigenvalues are obtained as

Since not all eigenvalues are positive, the current crack pattern is not stable. Therefore, one of the cracks must undergo the elastic unloading. The element that undergoes the elastic unloading is incrementally considered as an elastic element without crack. In this problem, there are again two alternatives since either of the two elements can be selected as the unloading element. Both alternatives are investigated and the eigenvalues of the modified stiffness matrices \mathbf{K}^{α} for both cases are obtained as

Opening crack in the first element	Opening crack in the second element	
That element	second element	
4.5000×10 ⁹	1.8889×10^9	
1.8889×10 ⁹	4.5000×10 ⁹	
5.6667×10 ⁹	5.6667×10 ⁹	
4.5997×10 ⁹	1.7614×10 ⁹	
1.7614×10 ⁹	1.3889×10^9	
1.3889×10 ⁹	3.2680×10 ⁹	
3.9216×10 ⁹	4.5997×10 ⁹	
[10.000]	[000.01	

It can be seen that the solutions with only one opening crack are stable because all the eigenvalues are positive. It is interesting to check whether the solutions with one opening crack will be always stable even for different tension-softening curves. From the previous problem, it is found that steep tension-softening curves can lead to unstable one-opening-crack solutions. To investigate this matter, the tension-softening curves B and C in Fig. 6 are tried. In these B and C cases, \widetilde{H} is equal to $\left(-\frac{2}{0.02}\right)$ 200 and $\left(-\frac{2}{0.032}\right)$ 200, respectively.

From the eigenvalue analyses, the eigenvalues of the stiffness matrices K^{cr} for the case B are obtained as

Opening crack in the first element	Opening crack in the second element	
1.6667×10°	5.5556×10 ⁸	
5.5556×10 ⁸	1.6667×10°	
-7.5000×10°	-7.5000×10°	
1.3889×10°	1.3889×10°	
10.000	10.000	
3.8603×10°	3.2680×10°	
3.9216×10°	3.8603×10°	
-1.4991×10°	-1.4991×10°	

In addition, the eigenvalues for the case C are obtained as

Opening crack in the	Opening crack in the	
first element	second element	
1.3889×10 ⁹	1.3889×10 ⁹	
1.3889×10 ⁹	1.3889×10 ⁹	
-2.1458×10^{-6}	-1.9667×10^{-6}	
10.000	4.1667×10 ⁹	
4.1667×10 ⁹	10.000	
4.1667×10 ⁹	4.1667×10 ⁹	
6.9444×10 ⁸	6.9444×10 ⁸	
3.9216×10 ⁹	3.2680×10 ⁹	

From the result, it can be seen that the tension-softening curve B yields unstable solutions even when there is only one opening crack. As for the tension-softening curve C, one of the obtained eigenvalues in each of the two solutions is very small compared to the rest of

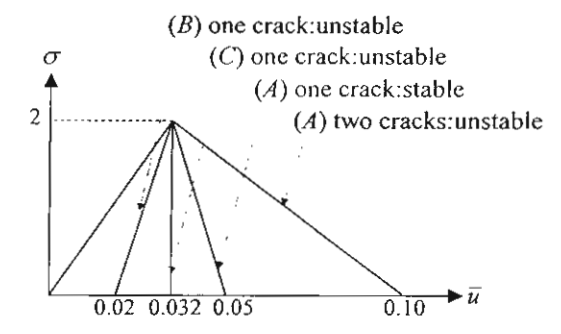


Fig. 7 Responses of the uniaxial problem for various tension-softening curves

the eigenvalues and must actually be considered as a zero. Therefore, the tension-softening curve C actually defines a boundary between stable and unstable one-opening-crack solutions. For those cases with tension-softening curves steeper than the curve C (e.g. the curve B), the solutions with one opening crack are not stable and they are in fact the snap-back responses. For those cases with tension-softening curves flatter than the curve C (e.g. the curve A), the solutions with one opening crack are stable. Note that the same tensile strength is assumed for all cases.

Fig. 7 shows the responses, obtained from the smeared crack finite element model, for all cases A, B and C. For the case A, the response without the localization is also plotted. Similar to the previous example, these results are also exact because the shape function used is capable of representing the exact solutions of this problem. From the results, it is clear that the localization judgment is necessary if the accurate solution is to be obtained.

4. Conclusion

The smeared crack approach can be used in the analysis of the cracking localization by employing the mixed formulation in the finite element method. In the formulation, the displacements and crack strains are both discretized. The discretization of the crack strains, which are the irreversible variables, allows the consideration of stability and bifurcation of equilibrium states with respect to the irreversible variables to be done easily. Therefore, the cracking localization can be subsequently discussed. The technique is tried with an axial bar problem employing both one-dimensional two-noded and two-dimensional four-noded elements. The obtained results show

promising capability of the method for the analysis of the cracking localization.

5. Acknowledgments

The authors are grateful to the Thailand Research Fund (TRF) for providing the financial support to this study.

6. References

- [1] Rots, J. G. and de Borst, R. Analysis of Mixed-Mode Fracture in Concrete, Journal of Engineering Mechanics, Vol.113, No.11, pp.1739-1758, 1987.
- [2] Rots, J. G., Stress Rotation and Stress Locking in Smeared Analysis Separation, Fracture Toughness and Fracture Energy: Test Methods Concrete and Rock, H. Takahashi, Folker H. Wittmann and H. Mihashi (Eds.), Balkema, Rotterdam, pp.367-382, 1989.
- [3] Dvorkin, E. N. and Assanelli, A. P., 2D Finite Elements with Displacement Interpolated Embedded Localization Lines: The Analysis of Fracture in Frictional Materials, Computer Methods in Applied Mechanics and Engineering, Vol.90, pp.829-844, 1991.
- [4] Jirasek, M. and Zimmermann, T., Rotating Crack Model with Transition to Scalar Damage, Journal of Engineering Mechanics, Vol.124, No.3, pp.277-284, 1998.
- [5] Shirai, N., JCI round robin analysis of size effect in concrete structures, Size Effect in Concrete Structures, H. Mihashi, H. Okamura and Z. P. Bazant (Eds.), E&FN Spon, London, pp.295-322, 1994.
- [6] Carpinteri, A., Softening and Snap-Back Instability in Cohesive Solids, International Journal for Numerical Methods in Engineering, Vol.28, pp.1521-1537, 1989.
- [7] Riks, E., An Incremental Approach to the Solution of Snapping and Buckling Problems, Int. J. Solids Structures, Vol.15, pp.529-551, 1979.
- [8] de Borst, R., Computation of Post-Bifurcation and Post-Failure Behavior of Strain-Softening Solids, Computers and Structures, Vol.25, No.2, pp.211-224, 1987.
- [9] Valente, S., Bifurcation Phenomena in Cohesive Crack Propagation, Computers

- and Structures, Vol.44, No.1/2, pp.55-62, 1992.
- [10] Nguyen, Q. S., Bifurcation and Post-Bifurcation Analysis in Plasticity and Brittle Fracture, J. Mech. Phys. Solids, Vol.35, No.3, pp.303-324, 1987.
- [11] Horii, H. and Okui, Y., Thermomechanics and Micromechanics-Based Continuum Theory for Localization Phenomena, Fracture of Brittle, Disordered Materials: Concrete, Rock, and Ceramics, G. Baker and B. L. Karihaloo (Eds.), E&FN Spon, London. pp.391-405, 1995.
- [12] Brocca, M., Analysis of Cracking Localization and Crack Growth Based on Thermomechanical Theory of Localization.

- Master of Engineering Thesis, The University of Tokyo, Tokyo, 1997.
- [13] Bazant, Z. P. and Oh, B. H., Crack Band Theory for Fracture of Concrete, Materiaux et Constructions, Vol.16, No.93, pp.155-177, 1983.
- [14] Shah, S. P., Swartz, S. E. and Ouyang, C., Fracture Mechanics of Concrete: Applications of Fracture Mechanics to Concrete, Rock, and Other Quasi-Brittle Materials, John Wiley & Sons, New York, 1995.
- [15] Bazant, Z. P. and Cedolin, L., Stability of Structures: Elastic, Inelastic, Fracture, and Damage Theories, Oxford University Press, New York, 1991.

Cracking Localization Analysis Using a Specially Treated Smeared Crack Finite Element Model with Energy Consideration

Pruettha Nanakorn and Vasan Thitawat
Sirindhorn International Institute of Technology, Thammasat University
PO Box 22, Thammasat-Rangsit Post Office
Pathumthani 12121, Thailand
Phone (66-2) 986-9011-13 Ext. 1906
Fax (66-2) 986-9011-13 Ext. 1900
E-Mail: nanakorn@siit.tu.ac.th

Abstract

In this paper, an analysis method to analyze problems involving cracking localization is proposed. The proposed analysis method employed the well-known smeared crack model. Nevertheless, in the finite element mixed formulation formulation. a discretizes not only displacements but also crack strains is used. This is to allow stability consideration of crack patterns to be done efficiently. Stability analysis of crack patterns is done by performing eigenvalue analysis of Hessian matrices obtained from the mixed finite element formulation. At each bifurcation point identified by the stability analysis, the actual equilibrium path is incrementally traced by searching for a crack pattern with the minimum total potential energy increment. Search algorithms employed include exhaustive search algorithm and a genetic algorithm. Finally, the proposed analysis method is used to analyze the four-point bending problem of plain concrete and the results are discussed.

1. Introduction

Tensile failure of quasi-brittle materials such as concrete is commonly known to start from formation of cracks, and propagation of the newly formed cracks or existing defects. After that, these cracks will localize into one or a few cracks. This will subsequently lead to the final failure. In order to capture the ultimate capacity of such materials in a structure, consideration of cracking localization cannot generally be neglected. However, the consideration of cracking localization needs a very expensive computation because solution

methods for solving localization problems involve checking stability and bifurcation of different equilibrium manv Consequently, many researchers avoid the consideration of cracking localization by either allowing many cracks to grow without the consideration of localization [1-3] or by assuming positions for localized cracks [4]. The first approach is not realistic and can generally lead to inaccurate results. Having many cracks without localization allows an incorrect amount of energy to dissipate from the domain. Thus, obtained results will also be inaccurate. However, in some cases where the gradient of stress is very high, it is possible that major cracks will finally prevail and other cracks will undergo elastic unloading even when cracking localization is not considered. The second approach, which assumes positions of localized cracks prior to analysis, may yield reasonable results in some cases. These include cases where assumed positions of localized cracks are reasonably or undoubtedly correct and cases where solutions are not sensitive to locations of localized cracks. Nevertheless, the approach is not appropriate for general cases since locations of localized cracks may not be easily predicted or solutions may be sensitive to locations of cracks.

Consideration of stability and bifurcation of equilibrium states is one of the major tasks to be done in the analysis of cracking localization. Many researchers have considered stability and bifurcation of equilibrium states by investigating definiteness of stiffness matrices [5-6]. When a stiffness matrix is positive-definite, an equilibrium state is considered stable. The same theory can be applied to the

analysis of cracking localization. However, cracking is an irreversible process. In this case, stability and bifurcation of equilibrium states can be determined by investigating definiteness stiffness matrices (Hessian matrices) with respect to irreversible constructed parameters [7]. These irreversible parameters can be crack opening displacements in the discrete crack approach or crack strains in the smeared crack approach. Investigating definiteness of Hessian matrices will provide information on stability of equilibrium paths. Consequently, bifurcation points can be located. Nevertheless, tracing the actual equilibrium path needs some more effort.

Employing Gibbs' statement of the second law of thermodynamics, Nemat-Nasser [8] pointed out that the equilibrium path that makes the total potential energy an absolute minimum would also render the elastic energy an absolute minimum. In addition, this path will also be the actual equilibrium path [9]. Employing the same concept, Brocca [10] used crack opening displacements in the discrete crack finite element analysis as irreversible analysis of cracking parameters in the localization. In his work, Hessian matrices constructed with respect to irreversible crack opening displacements are used to investigate stability and bifurcation of crack patterns. In addition, the equilibrium path is also traced by using the Simplex method to find the path with the minimum total potential energy. From his work, it is clear that Hessian matrices constructed with respect to irreversible parameters can easily be obtained when the discrete crack approach is employed because irreversible parameters are discrete. Nevertheless, the discrete crack approach is not suitable for problems with many cracks in the domain. Usually, in the cracking localization analysis, there will be many cracks occurring in the domain. As the number of cracks increases, the mesh topology may have to be changed to cope with the new crack patterns and this leads to more degrees of freedom. On the other hand, the smeared crack approach, which is more suitable for problems with many provide any discrete cracks, does not

irreversible parameters for construction of Hessian matrices. Another disadvantage of the smeared crack approach is that, with this approach, it is necessary to define the crackband width or the crack characteristic length. For fairly regular meshes, the characteristic length is frequently determined in an intuitive way which is difficult to generalize in a formal manner for irregular meshes and arbitrary crack However, for two-dimensional directions. domains, this problem can be overcome. Oliver [11] proposed a general approach for calculation of the characteristic length. In his study, a crack is modeled as a limiting case of two singular lines that coincide with the boundary of elements covering the crack path. The expression for the characteristic length is obtained by analyzing the energy dissipated from the band bounded by these two singular

To allow the consideration of cracking localization in the smeared crack model, Nanakorn and Soparat [12] proposed an analysis method that uses the smeared crack finite element model with a mixed formulation. In their work, the discretization is performed not only on the displacement field but also on the crack strain field. The newly introduced discrete nodal crack strain variables serve as the discrete irreversible variables needed for the localization analysis. However, their work is limited to stability analysis of crack patterns, and there is no attempt to trace the complete equilibrium path.

In this study, an analysis method cracking localization is proposed. In the proposed method, stability of crack patterns is investigated by employing the analysis method proposed by Nanakorn and Soparat [12]. When the current crack pattern becomes unstable, the stable crack pattern with the minimum total potential energy is searched for and selected as the solution path [8]. In the search for the stable crack pattern with the minimum total potential energy, an exhaustive algorithm and a genetic algorithm are used. The proposed analysis method is used to solve the cracking localization problem of a fourpoint bending beam of plain concrete. Finally, the obtained results are discussed.

2. Smeared Crack Model with a Mixed Finite Element Formulation

In the smeared crack model, the total strain increment $\Delta\epsilon$ is decomposed into the strain increment of the intact elastic solid $\Delta\epsilon''$ and the strain increment of the cracked solid $\Delta\epsilon''$, i.e.,

$$\Delta \varepsilon = \Delta \varepsilon^{o} + \Delta \varepsilon^{cr}. \tag{1}$$

The relationship between the global crack strain increment $\Delta \hat{\epsilon}^{cr}$ and the local crack strain increment $\Delta \hat{\epsilon}^{cr}$ is expressed as

$$\Delta \mathbf{\varepsilon}^{cr} = \mathbf{T} \Delta \hat{\mathbf{\varepsilon}}^{cr} \tag{2}$$

where T is the transformation matrix, which can be written as a function of the angle between the vector normal to the crack surfaces and the global x-axis.

By following Nanakorn and Soparat [12], the total potential energy increment of a cracked domain V is expressed as

$$\Delta\Pi = \Delta\Pi^{M} + \Delta\Pi^{D}$$

$$= \begin{bmatrix} \frac{1}{2} \int_{V} \Delta \varepsilon^{\sigma^{T}} \mathbf{D}^{\sigma} \Delta \varepsilon^{\sigma} dV \\ - \int_{V} \Delta \mathbf{u}^{T} \Delta \mathbf{f} dV - \int_{S} \Delta \mathbf{u}^{T} \Delta \mathbf{t} dS \end{bmatrix}$$

$$+ \begin{bmatrix} \frac{1}{2} \int_{V} \Delta \hat{\varepsilon}^{cr} \hat{\mathbf{D}}^{cr} \Delta \hat{\varepsilon}^{cr} dV \end{bmatrix}.$$
(3)

The total potential energy increment $\Delta\Pi$ shown above consists of two parts that are the mechanical potential energy increment $\Delta\Pi^M$ and the dissipated energy increment $\Delta\Pi^D$. Here, Δu denotes the displacement increment vector. In addition, \mathbf{D}^o and $\hat{\mathbf{D}}^{cr}$ denote the constitutive matrices for the intact elastic solid and the cracked solid, respectively. Finally, $\Delta \mathbf{f}$ and $\Delta \mathbf{t}$ represent the body force increment vector and the surface traction increment

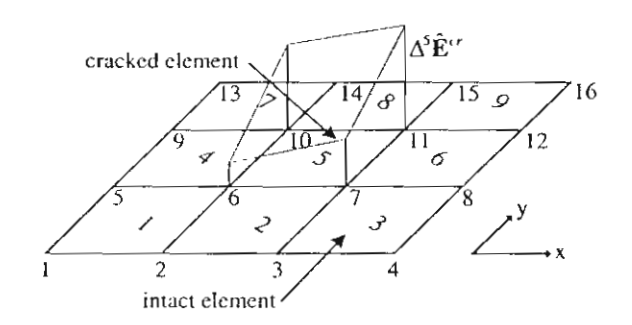


Fig. 1 A problem with one cracked element surrounded by intact elastic elements [12]

vector, respectively.

Discretizing both displacement and local crack strain increments, we have for the i^{th} element in the finite element analysis [12]

$$\Delta \mathbf{u} = \mathbf{N} \Delta^i \mathbf{U} \,, \tag{4a}$$

$$\Delta \hat{\mathbf{\epsilon}}^{cr} = \mathbf{N}^{cr} \Delta^i \hat{\mathbf{E}}^{cr} \tag{4b}$$

where N and N^{cr} represent the shape function matrices for the displacement increment and the local crack strain increment, respectively. In addition, $\Delta^i \mathbf{U}$ and $\Delta^i \hat{\mathbf{E}}^{cr}$ represent the nodal displacement increment and the nodal local crack strain increment, respectively. Note that the local crack strain increments are not continuous across elements and the nodal local crack strain increments of the same node for different elements can be different. One example is a problem with one cracked element surrounded by uncracked elements (see Fig. 1). In the cracked element including its boundary, non-zero crack strain increments can be expected. However, in the surrounding uncracked elements, the crack increments are expected to be zero because there is no crack in those elements. On the contrary, the total displacement increments must be continuous across all the elements.

From (2) and (4), the total strain increment and the global crack strain increment are expressed as

$$\Delta \mathbf{\varepsilon} = \mathbf{B} \Delta^i \mathbf{U} \,, \tag{5a}$$

$$\Delta \mathbf{\varepsilon}^{cr} = \mathbf{T} \mathbf{N}^{cr} \Delta^{i} \hat{\mathbf{E}}^{cr}. \tag{5b}$$

From (1), (3) and (5), the total potential energy increment can be expressed as

$$\Delta \Pi = \frac{1}{2} \int_{V} \Delta^{i} \mathbf{U}^{T} \mathbf{B}^{T} \mathbf{D}^{0} \mathbf{B} \Delta^{i} \mathbf{U} dV$$

$$- \frac{1}{2} \int_{V} \Delta^{i} \mathbf{U}^{T} \mathbf{B}^{T} \mathbf{D}^{0} \mathbf{T} \mathbf{N}^{cr} \Delta^{i} \hat{\mathbf{E}}^{cr} dV$$

$$- \frac{1}{2} \int_{V} \Delta^{i} \hat{\mathbf{E}}^{cr} \mathbf{N}^{cr} \mathbf{T}^{T} \mathbf{D}^{0} \mathbf{B} \Delta^{i} \mathbf{U} dV$$

$$+ \frac{1}{2} \int_{V} \Delta^{i} \hat{\mathbf{E}}^{cr} \mathbf{N}^{cr} \mathbf{T}^{T} \mathbf{D}^{0} \mathbf{T} \mathbf{N}^{cr} \Delta^{i} \hat{\mathbf{E}}^{cr} dV$$

$$+ \frac{1}{2} \int_{V} \Delta^{i} \hat{\mathbf{E}}^{cr} \mathbf{N}^{cr} \mathbf{N}^{cr} \mathbf{D}^{cr} \mathbf{N}^{cr} \Delta^{i} \hat{\mathbf{E}}^{cr} dV$$

$$- \int_{V} \Delta^{i} \mathbf{U}^{T} \mathbf{N}^{T} \Delta \mathbf{f} dV - \int_{S} \Delta^{i} \mathbf{U}^{T} \mathbf{N}^{T} \Delta \mathbf{t} dS.$$
(6)

Applying the stationary condition $\delta(\Delta\Pi)=0$, we obtain the element stiffness equation for the i^{th} element as

$$\begin{bmatrix} \mathbf{k}_{11} & \mathbf{k}_{12} \\ \mathbf{k}_{21} & \mathbf{k}_{22} \end{bmatrix} \begin{bmatrix} \mathbf{\Delta}^{i} \mathbf{U} \\ \mathbf{\Delta}^{i} \hat{\mathbf{E}}^{cr} \end{bmatrix} = \begin{bmatrix} \Delta \mathbf{r} \\ 0 \end{bmatrix}$$
 (7)

where
$$\mathbf{k}_{11} = \int_{V} \mathbf{B}^{T} \mathbf{D}^{o} \mathbf{B} dV$$
,
 $\mathbf{k}_{12} = -\int_{V} \mathbf{B}^{T} \mathbf{D}^{o} \mathbf{T} \mathbf{N}^{cr} dV$,
 $\mathbf{k}_{21} = -\int_{V} \mathbf{N}^{cr} \mathbf{T}^{T} \mathbf{D}^{o} \mathbf{B} dV$,
 $\mathbf{k}_{22} = \int_{V} \mathbf{N}^{cr} (\hat{\mathbf{D}}^{cr} + \mathbf{T}^{T} \mathbf{D}^{o} \mathbf{T}) \mathbf{N}^{cr} dV$,
 $\Delta \mathbf{r} = \int_{V} \mathbf{N}^{T} \Delta \mathbf{f} dV + \int_{S} \mathbf{N}^{T} \Delta \mathbf{f} dS$.

After assembling all element stiffness equations and applying prescribed displacements and forces, the system stiffness equation is arranged as

$$\begin{bmatrix} \mathbf{K}_{11} & \mathbf{K}_{12} \\ \mathbf{K}_{21} & \mathbf{K}_{22} \end{bmatrix} \begin{pmatrix} \Delta \mathbf{U} \\ \Delta \hat{\mathbf{E}}^{cr} \end{pmatrix} = \begin{bmatrix} \Delta \mathbf{R}_{1} \\ \Delta \mathbf{R}_{2} \end{bmatrix}$$
(8)

where ΔU and $\Delta \hat{E}^{cr}$ are the nodal displacement increment and the nodal local

crack strain increment of the system, respectively.

The static condensation is then used to remove the nodal displacement increment from the obtained system matrix equation. Consequently, the equation can be written in the following form, i.e.,

$$\mathbf{K}^{cr} \Delta \hat{\mathbf{E}}^{cr} = \Delta \mathbf{R}^{cr} \tag{9}$$

where \mathbf{K}^{cr} and $\Delta \mathbf{R}^{cr}$ are defined as

$$\mathbf{K}^{cr} = \mathbf{K}_{22} - \mathbf{K}_{21} \mathbf{K}_{11}^{-1} \mathbf{K}_{12}, \qquad (10a)$$

$$\Delta \mathbf{R}^{cr} = \Delta \mathbf{R}_2 - \mathbf{K}_{21} \mathbf{K}_{11}^{-1} \Delta \mathbf{R}_1.$$
 (10b)

In the consideration of stability of crack patterns, the eigenvalue analysis of K^{cr} is performed. If all the eigenvalues are positive, then it means that the stationary solution in (9) is stable with respect to the current crack pattern. Otherwise, the stationary solution is unstable and bifurcation occurs. Note that this scheme is only used for stability analysis of patterns, not for obtaining solution. The displacement displacement solution will be obtained from the original crack model where unknowns are the nodal displacement increments.

3. Equilibrium Path with The Minimum Total Potential Energy

When the equilibrium path reaches a bifurcation point, a fan of many possible equilibrium paths emanates from bifurcation point. In fact, if instability occurs in the real system, the actual equilibrium path is the path that contains the minimum total potential energy [9] or the minimum elastic strain energy [8]. These two conditions are actually the same [8], if one defines the total potential energy in the usual way. In this study, the minimum total potential energy criterion is employed. However, since the analysis is performed incrementally, and the potential energy is written in the incremental form [see (3)], the stable path with the minimum total potential energy increment is

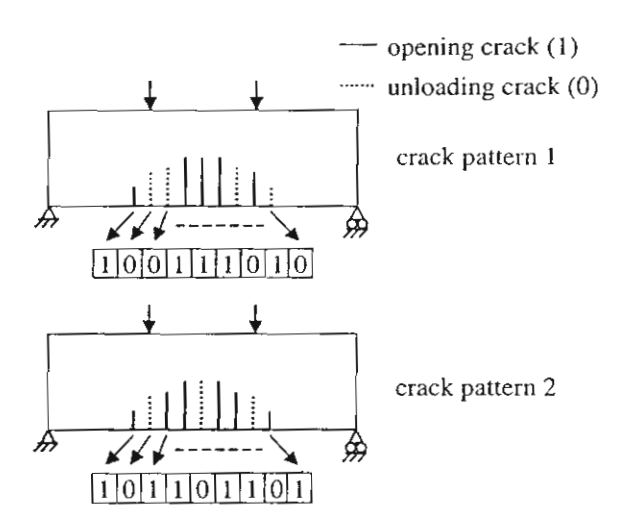


Fig. 2 Examples of coding of crack patterns

the desired solution path.

In order to obtain the solution path with the minimum total potential energy increment, energy increments of all possible equilibrium paths, which depend on their crack patterns, can be compared. This approach of comparing all possible solutions is essentially an exhaustive search. The algorithm for this search approach is simple and straightforward. Nevertheless, it is obvious that the technique is expensive and suitable only for small problems where the complete search is still possible. In the case of larger problems where many cracks occur in the domain and, as a result, many crack patterns are possible, the exhaustive search may not be practical and it is advisable employ appropriate optimization an technique to find the minimum energy path. In this study, a genetic algorithm (GA) [13] is used for this purpose because this optimization technique is suitable for problems with discrete variables. Variables in the minimization problem of the total potential energy increment are discrete statuses of cracks that can be either opening or unloading. Since GAs do not require the evaluation of the gradient of the function being minimized or maximized, the evaluation of the total potential energy increment is enough for the minimization process.

In this study, the simple GA is employed. It is composed of three different operators, i.e.,

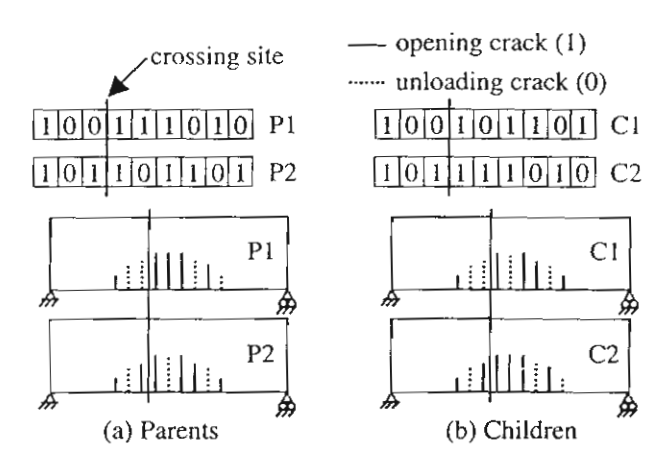


Fig. 3 One-point crossover

reproduction, crossover and mutation operators. These three operators are based on the same basic elements in the real natural genetics. The details of this technique can be found in the literature [13-14].

In general, GAs do not directly work with the parameters themselves. The algorithms start with coding of the parameter set. For coding, binary strings are most popular and convenient. Each point in a search space, often called "individual" in the GA terminology, is represented by a single string of number 0's and 1's. The optimization problem of this study is to minimize the total potential energy increment. The total potential energy increment to be minimized is a function of crack patterns. Therefore, each crack pattern will be coded as a binary string. The idea of the coding is to have each bit in a binary string represent the status of one particular crack. If the value of the bit is one (1), it indicates that its corresponding crack is opening. If the value of the bit is zero (0), the corresponding crack is unloading. Fig. 2 shows examples of the coding of two different crack patterns. The number of bits used in the string is equal to the number of the existing crack paths.

In GAs, the reproduction operator defines a process in which individuals are selected for mating based on their fitness values relative to that of the population. Fitness is defined as a figure of merit. Individuals with higher fitness values have higher probabilities of being selected for mating and subsequent genetic

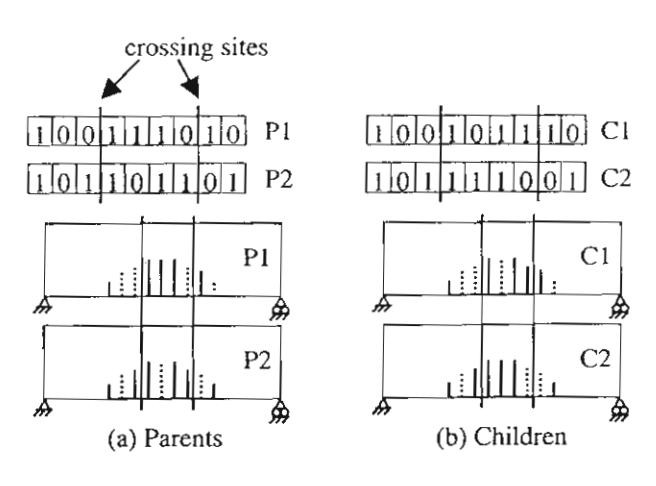


Fig. 4 Two-point crossover

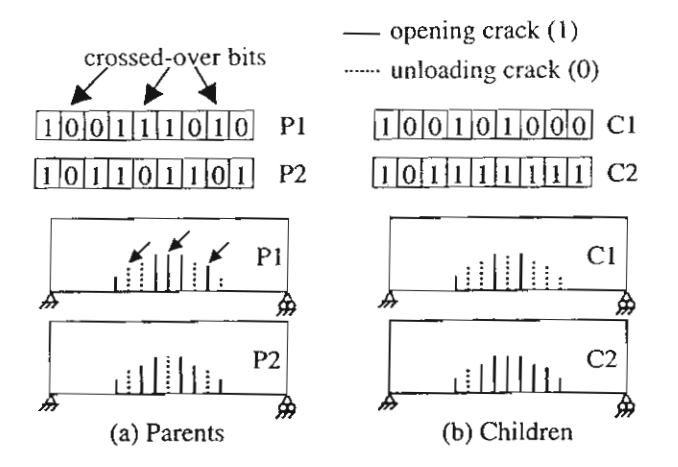


Fig. 5 Uniform crossover

actions. Consequently, highly fit individuals live and reproduce, and less fit individuals die. In this study, a crack pattern that results in a smaller total potential energy increment will be given a higher fitness value.

In the crossover operator, new strings are created by exchanging information among strings. Many crossover operators exist in the literature [13]. Generally, two strings are selected at random as a crossover pair and some portions of the two strings are exchanged. The two strings participating in the crossover are known as parent strings and the resulting strings are known as children strings. In this study, three types of crossover operator are employed, i.e., one-point, two-point and uniform crossover operators. Fig. 3 shows an example of the one-point crossover. In this

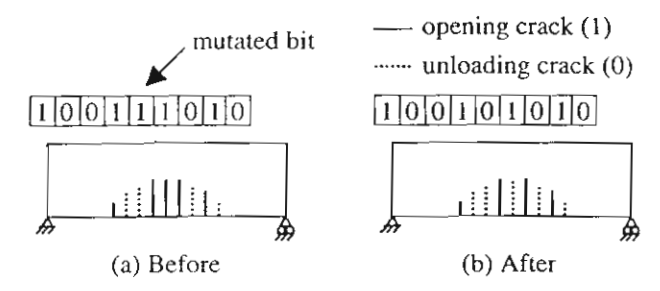


Fig. 6 Mutation

study, the one-point crossover is performed by randomly selecting a crossing site along the parent strings and by exchanging all bits on the right hand side of the selected crossing site. In the case of the two-point crossover, two crossing sites are randomly selected and all the bits between the two crossing sites of the two parent strings are exchanged as shown in Fig. 4. For the uniform crossover, the number of bits to be crossed over and their positions are randomly determined. Fig. 5 shows an example of this type of crossover in this study.

It is clear that the crossover operator may yield better or worse children strings. To be able to adjust the degree of the uncertainty of the crossover phase, it is not necessary to use all individuals in the mating pool in the operator. This is done by adjusting the probability that a crossover is performed (crossover probability).

The last genetic algorithm operator is the mutation operator. Fig. 6 shows an example of the mutation operator employed in this study. The mutation operator changes 1 to 0 and vice versa at a randomly chosen bit. The operator is used sparingly with a small probability (mutation probability).

4. Analysis Procedure

In the analysis, the specimen under consideration is analyzed by using the conventional smeared crack model. Cracks are initiated when the maximum tensile stress reaches the tensile strength of the material. After that, the cracks follow the tension-softening curve, which is treated as one of the material properties. The tension-softening curve is the relationship between the tensile

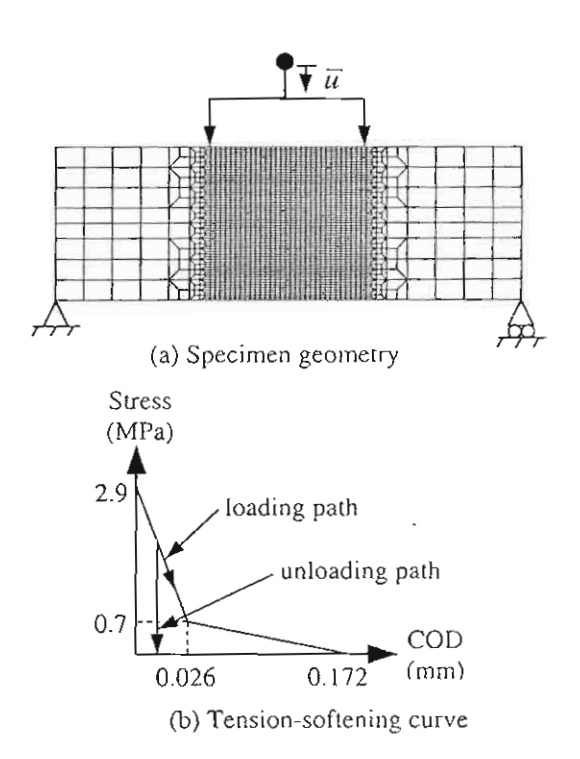


Fig. 7 Four-point bending problem

stress transferred across the crack surfaces and the crack opening displacement. Note that, in this study, shear retention of cracks is assumed negligible. As mentioned earlier, the analysis is done incrementally. In each step, the stability of the obtained crack pattern will be investigated by performing eigenvalue analysis of the matrix K^{cr} obtained from the mixed smeared crack finite element formulation [12]. If the crack pattern is found to be stable, the analysis is continued to the next step. However, if the crack pattern is unstable, the search for the crack pattern with the minimum total potential energy increment must be performed. Here, if the number of possible crack patterns is not very large, an exhaustive search can be employed; otherwise, a GA will be used, instead. It must be noted that, if a GA or another optimization technique is used, the obtained crack pattern may have a nearminimum total potential energy increment, not the true minimum one for the finite element discretization being currently used. In order to compare total potential energy increments of different crack patterns, the energy for cases with different crack patterns must be evaluated under the same controlled parameter. In this

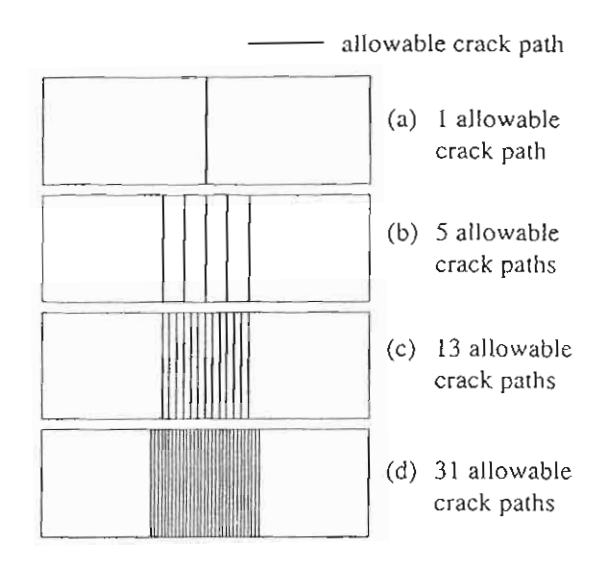


Fig. 8 Specimen with different numbers of allowable crack paths

study, the controlled displacement is used. After the crack pattern with the minimum or near-minimum total potential energy increment is obtained, the analysis is carried on to the next step. The same process is then repeated and the actual equilibrium path can be traced.

5. Results

Here, the classical four-point bending beam test of plain concrete shown in Fig. 7a is investigated. Specimen's dimension is $300\times100\times100$ mm. Controlled displacements are applied at the top of the beam, 100 mm from both ends. Young's modulus and Poison's ratio used are 27.5 GPa and 0.2, respectively. Unit weight of the material is 2,300 kg/m³. The tension-softening curve used is shown in Fig. 7b. In the analysis, four-noded quadrilateral elements are employed. The finite element mesh consists of 2,232 elements and 2,288 nodes (see Fig. 7a).

For this problem, it can be reasonably assumed that all crack paths are straight. To simplify the problem, cracks will be allowed to occur only on the pre-specified paths. The problem is solved both with and without the specimen's self-weight. When the self-weight is neglected, the problem is solved with various numbers of allowable crack paths as shown in Fig. 8, and, in all of these cases with different allowable crack paths, the equilibrium path

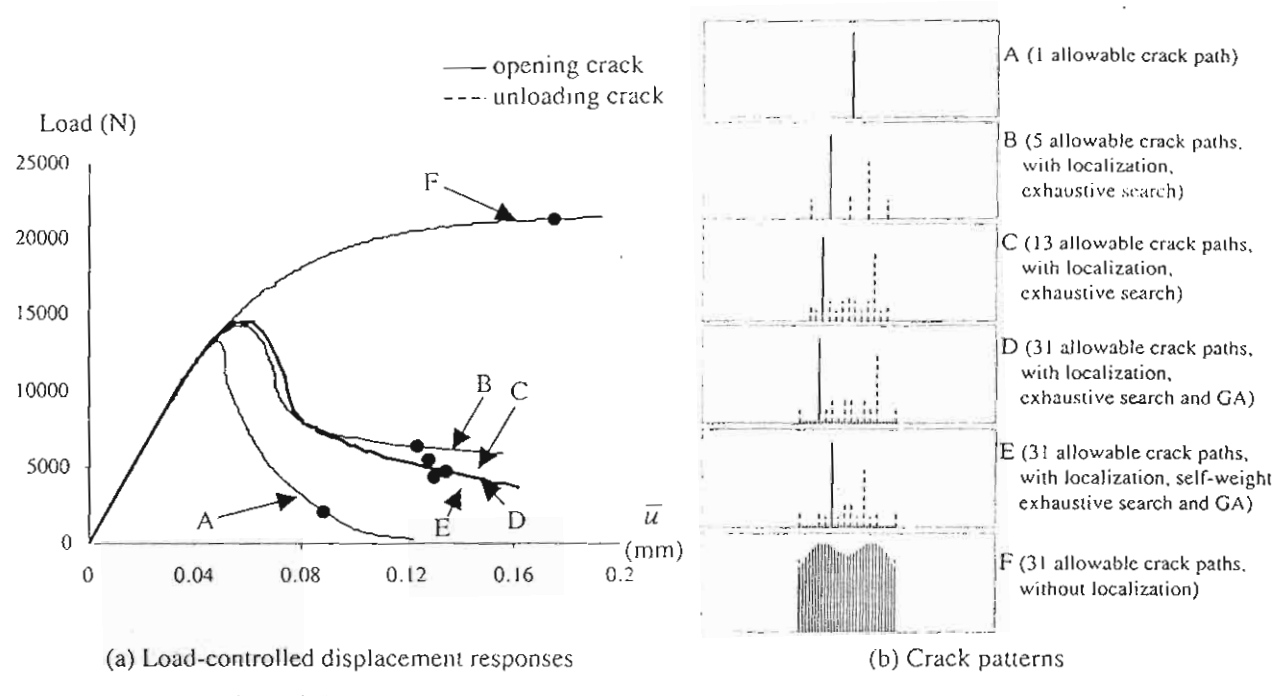


Fig. 9 Load-controlled displacement responses and crack patterns

with the minimum total potential energy increment is traced by employing an exhaustive search. In addition, only for the case with 31 allowable crack paths, a GA is also employed for the search. When the self-weight is considered, the analysis is done only for the case with 31 allowable crack paths, and the equilibrium path with the minimum total potential energy increment is traced by employing both exhaustive search and GA. GA parameters used in the analysis are shown in Table 1.

Fig. 9a shows load-controlled displacement responses for all of the calculations mentioned above. Moreover, it also includes the case with 31 allowable crack paths when the cracking localization is not considered. This additional case is performed without the self-weight and it will allow the importance of the localization analysis to be observed. Fig. 9b shows crack patterns obtained from these different cases at the loading points indicated by black circular

Table 1 GA parameters

Population size	40
Number of generations	40
Crossover probability	0.80
Mutation probability	0.05

markers on every response curve. At these loading points, the main cracks in all cases reach the length of 90 percent of the beam depth. For the case with 31 allowable crack paths with the localization consideration (the cases D and E), it can be seen that the results obtained from the exhaustive search and the GA are exactly the same. Therefore, it is shown that GAs can be used instead of the exhaustive search. It must be noted that the time used by the exhaustive search is very much longer than that used by the GA. For the cases B, C, and D where no self-weight is assumed, it can be seen that the obtained results, both crack patterns and response curves, are not much different. Therefore, for this problem, having only five allowable crack paths that are distributed properly is sufficient for obtaining the converged solution. Since it can be observed from the crack patterns of the cases B, C, and D that there are actually two long cracks in the beam, it may be understood that the response is actually governed by two main localized cracks which are not localized into one crack until at a much later loading stage. Also from the response curves, it is seen that the results of the case A, which assumes one localized crack at the center of the span, and the case F, which does not consider the

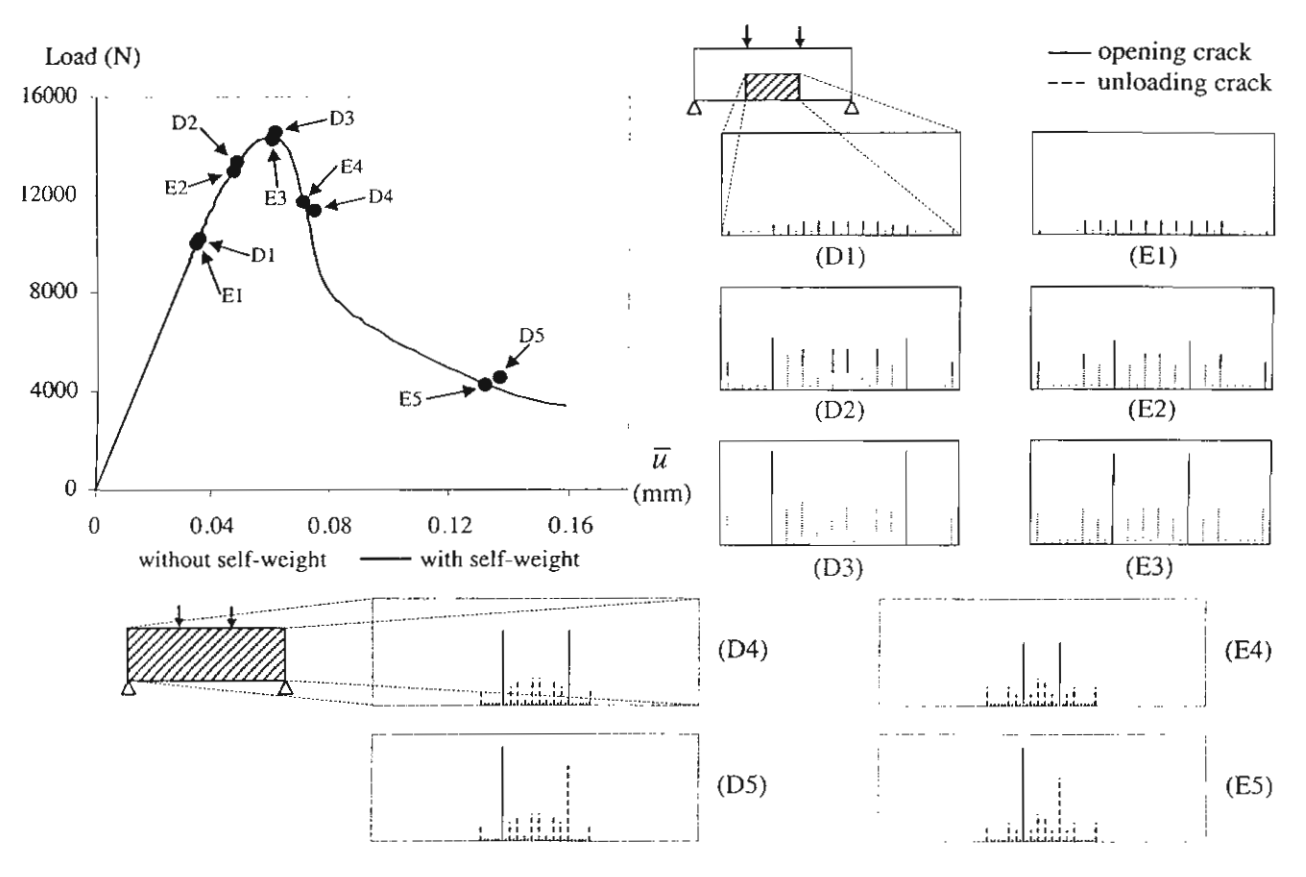


Fig. 10 Crack patterns of specimen with 31 allowable crack paths

localization, are very much different from those of the cases B, C, and D which properly consider the localization. Finally, from a comparison of the results of the cases D (without self-weight) and E (with self-weight), it can be seen that the load-displacement responses of both cases are very similar. Therefore. for this particular neglecting the self-weight does not have a significant effect. Nevertheless, it can also be observed from the obtained crack patterns that the two main cracks are closer to each other when the self-weight is considered. This is expected since the self-weight makes the stress higher at locations closer to the center of the span. Fig. 10 shows the crack patterns of the cases D and E at different loading stages.

6. Conclusions

In this study, an analysis method for cracking localization in quasi-brittle materials is presented. The analysis method employs the smeared crack finite elements with a mixed

formulation for the stability investigation of crack patterns. In the mixed formulation, the discretization is performed on not only the displacement field but also the crack strain field. The discretized crack strains will allow the stability analysis of crack patterns to be done more easily. At bifurcation points, the actual equilibrium path is traced incrementally by finding the path with the minimum total potential energy increment. The search for the minimum total potential energy increment is done by employing both the exhaustive and GA search algorithms, depending on the size of the problem being solved. It is found in this study that GAs can be efficiently used for this search. The results obtained from the fourpoint bending problem of plain concrete clearly show that the true localized solutions are very much different from the solution obtained by assuming one localized crack at the center of the span. Furthermore, the true localized solutions are also very much different from the solution obtained without the localization

consideration. It is also found that there are two major localized cracks that are not localized into one crack until at a much later loading stage. The behavior of the beam is therefore governed by these two cracks. This clearly illustrates that assuming only one localized crack from the beginning may lead to erroneous results. Finally, it is found that, for the four-point bending test of plain concrete, neglecting the self-weight does not have significant effect on the obtained results. With self-weight or without self-weight, there are two main localized cracks. Although these two cracks are slightly closer when the self-weight is considered, the difference between the obtained responses from both cases negligible.

7. Acknowledgements

Financial support from the Thailand Research Fund (TRF) for this research is gratefully acknowledged.

References

- [1] J. G. Rots and R. de Borst, "Analysis of Mixed-Mode Fracture in Concrete", Journal of Engineering Mechanics, Vol. 113, No. 11, 1987, pp. 1739-1758.
- [2] J. G. Rots, "Stress Rotation and Stress Locking Smeared in Analysis of Separation", Fracture Toughness and Fracture Energy: Test Methods for Concrete and Rock. H. Mihashi, Takahashi, and Folker H. Wittmann (Eds), Balkema, Rotterdam, 1989, pp. 367-382.
- [3] M. Jirasek and T. Zimmermann, "Rotating Crack Model with Transition to Scalar Damage", Journal of Engineering Mechanics, Vol. 124, No. 3, 1998, pp. 277-284.
- [4] N. Shirai, "JCI Round Robin Analysis of Size Effect in Concrete Structures", Size Effect in Concrete Structures, H. Mihashi, H. Okamura and Z. P. Bazant (Eds.), E&FN Spon, London, 1994, pp. 295-322.
- [5] E. Riks, "An Incremental Approach to the

- Solution of Snapping and Buckling Problems", Int. J. Solids Structures, Vol. 15, 1979, pp. 529-551.
- [6] S. Valente, "Bifurcation Phenomena in Cohesive Crack Propagation", Computers and Structures, Vol. 44, No.1/2, 1992, pp. 55-62.
- [7] Q. S. Nguyen, "Bifurcation and Post-Bifurcation Analysis in Plasticity and Brittle Fracture", J. Mech. Phys. Solids, Vol. 35, No. 3, 1987, pp. 303-324.
- [8] S. Nemat-Nasser, "The Second Law of Thermodynamics and Noncollinear Crack Growth", Proc. of the Third ASCE/EMD Specialty Conference, Austin, Texas, September, 1979, pp. 449-452.
- [9] Z. P. Bazant and L. Cedolin, Stability of Structures: Elastic, Inelastic, Fracture and Damage Theories, Oxford University Press, 1991.
- [10] M. Brocca, Analysis of Cracking Localization and Crack Growth Based on Thermomechanical Theory of Localization, Master of Engineering Thesis, The University of Tokyo, Tokyo, 1997.
- [11] J. Oliver, "A Consistent Characteristic Length for Smeared Cracking Models", International Journal for Numerical Methods in Engineering, Vol.28, 1989, pp. 461-474.
- [12] P. Nanakorn and P. Soparat, "A Mixed Finite Element Formulation for Analysis of Cracking Localization in Quasi-Brittle Materials", Proceedings of European Congress on Computational Methods in Applied Sciences and Engineering: ECCOMAS 2000, Barcelona, Spain, CD ROM: ISBN: 84-89925-70-4, 2000.
- [13] D. E. Goldberg, Genetic Algorithms in Search, Optimization, and Machine Learning, Addison-Wesley, 1989.
- [14] K. Deb, Optimization for Engineering Design: Algorithms and Examples, Prentice-Hall of India Private Limited, 1995.